SISSA

International School for Advanced Studies

PhD course in Statistical Physics

Academic Year 2015/2016

A study on non-equilibrium dynamics in isolated and open quantum systems

Thesis submitted for the degree of

Doctor Philosophiae

Candidate:

Alessio Chiocchetta

Supervisor:

Prof. Andrea Gambassi

Contents

List of publications

1. A. Chiocchetta, P.-É. Larré, and I. Carusotto,
Thermalization and Bose-Einstein condensation of quantum light in bulk nonlinear media
Europhys. Lett. **115**, 24002 (2016).

2. A. Chiocchetta, A. Gambassi, S. Diehl and J. Marino,
Universal short-time dynamics: boundary functional renormalization group for a temperature quench
arXiv:1606.06272.

3. A. Chiocchetta, M. Tavora, A. Gambassi and A. Mitra,
Short-time universal scaling and light-cone dynamics after a quench in an isolated quantum system in d spatial dimensions.
arXiv:1604.04614. Accepted for publication in Phys. Rev. B.

4. A. Chiocchetta, A. Gambassi and I. Carusotto,
Laser operation and Bose-Einstein condensation: analogies and differences.
arXiv:1503.02816 (contribution to the book *Universal Themes of Bose-Einstein Condensation*, edited by D. W. Snoke, N. P. Proukakis and P. B. Littlewood, Cambridge University Press).

5. L. M. Sieberer, A. Chiocchetta, A. Gambassi, U. C. Täuber and S. Diehl,
Thermodynamic Equilibrium as a Symmetry of the Schwinger-Keldysh Action.
Phys. Rev. B **92**, 134306 (2015).

6. A. Maraga, A. Chiocchetta, A. Mitra and A. Gambassi,
Aging and coarsening in isolated quantum systems after a quench: Exact results for the quantum $O(N)$ model with $N \to \infty$.
Phys. Rev. E **92**, 042151 (2015).

7. A. Chiocchetta, M. Tavora, A. Gambassi and A. Mitra,
Short-time universal scaling in an isolated quantum system after a quench.
Phys. Rev. B **91**, 220302(R) (2015).

8. A. Chiocchetta and I. Carusotto,
A quantum Langevin model for non-equilibrium condensation.
Phys. Rev. A **90**, 023633 (2014).

9. A. Chiocchetta and I. Carusotto,
Non-equilibrium quasi-condensates in reduced dimensions.
Europhys. Lett. **102**, 67007 (2013).

Motivation and plan of the thesis

The study of equilibrium macroscopic systems, i.e., *equilibrium statistical mechanics*, represents one of the most successful and powerful physical theories: it provides solid predictions about the macroscopic properties of many-body classical and quantum systems. This accomplishment is remarkable, given the huge number of degrees of freedom which constitute any macroscopic systems. Even more fascinating is the capability of this theory to describe complex physical phenomena as phase transitions, in which the macroscopic properties of a system change abruptly upon varying some control parameter, such as temperature, pressure, etc.

A fundamental requirement of this theory is the system to be at thermal equilibrium: while this condition applies to most of the ordinary matter and it is quite robust against modifications of the eternal conditions ("perturbations"), some physical systems escape this condition. As a result, non-equilibrium systems are characterized by a plethora of novel phenomena, which are absent in equilibrium ones. However, the study of these systems is not supported by a theory as well-understood as equilibrium statistical mechanics, and therefore it represents a challenging subject. In fact, there are several ways in which a system can be brought out of equilibrium and, correspondingly, different techniques are needed in order to approach the specific problem.

In this Thesis, I explored several different physical systems in which these effects occurs: even though non-equilibrium physics is a multi-faceted branch of physics, given the number of ways in which a system may be driven out of equilibrium, I found that separating the discussion on *isolated* and *open* quantum systems (part I and part II of this Thesis, respectively) could improve the readability of this work. However, this separation is not sharp, for the following reasons:

- The techniques and the concepts that are used to investigate these different systems are the same (e.g., the Keldysh formalism and the fluctuation-dissipation theorem).

- The phenomena which occurs in these systems results in similar physical features (e.g., aging dynamics occurs in both isolated and open systems, and non-equilibrium stationary states can be characterized by effective temperatures in both cases).

- The same experimental platform may be tuned to realize either an isolated or an open system (e.g., cold atom gases and quantum optical systems).

Therefore the work presented in this Thesis may be regarded as an attempt to extend ideas from one field to the one, with the hope that such cross-fertilization will provide new insight in unexplored areas of physics.

Plan of the thesis

The two main questions which the two parts of the Thesis will address are the following:

Q1: Is there universality in the non-equilibrium short-time dynamics of isolated quantum systems?

Q2: Can driven-dissipative quantum systems display thermal features?

More specifically, in Chapter 1, we provide an introduction to the physics of isolated quantum systems, summarizing the state of art of the experimental and theoretical understanding of these systems. In particular, the concept of dynamical phase transition is introduced. In Chapter 2 we show that a dynamical phase transition is predicted for the $O(N)$-symmetric ϕ^4 field theory, using simple mean-field and Gaussian approximations. In Chapter 3, based on Ref. [1], we study this model in the large N limit, in which it is exactly solvable: we characterize the phase transition and we found that, for quenches at and below the dynamical critical point, the correlation functions exhibit a universal dynamical scaling. The properties of the dynamical critical point are then characterized in Chapter 4 (based on Refs. [2, 3]) using a perturbative renormalization group approach, which allows to compute a novel non-equilibrium critical exponent θ characterizing the short-time dynamics of the correlation functions and the magnetization. In Chapter 5 (based on Ref. [4]) we develop a new approach to compute the critical exponent θ using the functional renormalization group scheme, and we benchmark our results with the relaxational model A.

The second part of the Thesis begins with an introduction (Chapter 6) to open quantum systems, in which their features are summarized. Part of it is devoted to the introduction to the quantum optical platforms in which the non-equilibrium Bose-Einstein condensation has been observed, and the features of this phenomenon are briefly reviewed, highlighting the open issues concerning the thermalization in these systems. In Chapter 7 (based on Ref. [5]) we present a quantum-Langevin formalism to model the non-equilibrium condensation. In Chapter 8 (based on Ref. [6]), we introduce the fluctuation-dissipation relation as an operative tool to experimentally and theoretically assess thermalization in quantum optical systems. In Chapter 9 (based on Ref. [7]), we identify the fluctuation-dissipation relations as a symmetry of the Keldysh functional, thus providing a powerful theoretical criterion to determine thermalization in open systems. Finally, in Chapter 10 (based on Ref. [8]) we discuss a recent proposal to use a quantum optical setting to simulate the dynamics of isolated quantum systems: we define a criterion to assess the quantumness of the light fluid in such experimental configuration, and we propose an experimental protocol to produce coherent light exploiting the analogy with equilibrium Bose-Einstein condensation.

Part I

Isolated quantum systems

Chapter 1

Introduction

1.1 Ultracold atoms

In the last decades, an intensive investigation has proved ultracold atomic gases to be one of the most powerful experimental platform for studying nonequilibrium quantum dynamics [9, 10]. The main reason of the success of these system lies on their wide tunability: interaction strength (via Feshbach resonances [11, 12]), density, temperature, and dimensionality can be tailored to realize many different physical scenarios. In particular, their weak coupling to the external environment and their low density suppresses dissipative and decoherence effects for times comparable or larger than the duration of the experiments, thus making them suitable to study the dynamics of isolated quantum systems. Accordingly, the real-time observation of their quantum coherent dynamics has become fully accessible, as demonstrated by the pioneering work of Greiner et al. [13], which succeeded in observing the long-lived coherent collapse and revival dynamics of the matter wave field of a Bose-Einstein condensate. Subsequently, a large number of non-equilibrium phenomena was experimentally observed: the Kibble-Zurek mechanism [14–16] in an elongated Bose gas [17], the dynamics of a charge-density wave in a strongly correlated one-dimensional Bose gas [18], the light-cone spreading of correlations [19], the dynamics of a mobile spin impurity [20] and of two-magnon bound states [21].

By trapping the ultracold gases in strong confining potentials it is possible to control their spatial dimensionality and to experimentally study their dynamics in reduced dimensions. In particular, the realization of such systems allows us to investigate the relation between thermalization and integrability. A groundbreaking experiment in this sense was performed in Ref. [22], in which a one-dimensional bosonic ultracold gas was prepared in a non-equilibrium configuration and let subsequently evolve, discovering that the system did not thermalize on experimental time scales. This was in clear contrast to the case of a three-dimensional gas, which immediately relaxes to a thermal distribution. This lack of thermalization can be understood as the consequence of the fact that this system is a very close experimental realization of the Lieb-Liniger gas with point-like interaction [23, 24], which is an integrable model. This remarkable result motivated the subsequent theoretical investigation on the interplay of integrability, quantum dynamics and thermalization in isolated systems.

Moreover, in subsequent experiments, the study of the relaxation dynamics of a coherently split one-dimensional Bose gas showed that the system retained memory of its initial state [25–29] and revealed that it did not relax to thermal equilibrium, but to a different steady state identified as a

long-lived prethermalized state (see Sec. 1.3 further below).

The theoretical framework for these phenomena, and in particular on the role of integrability, is outlined in the following Sections.

1.2 Stationary states: integrability, non-integrability

Let us consider a macroscopic quantum system which, after being prepared in some state, is left isolated from its environment. At $t = 0$ the system is let evolve in time and, as a consequence of its perfect isolation, this evolution is unitary and it is determined by the Hamiltonian $\hat{H}$ of the system. Then, it is natural to pose the following two questions:

1. *Does the system reach a stationary state?*
2. *If this is the case, which are the properties of this stationary state?*

The answer to the first question is, strictly speaking, "no". If the size of the system is finite, the dynamics of the system is expected to undergo *revivals* [30], i.e, it returns periodically in its initial configuration, as a consequence of the fact that its eigen-frequencies (viz. its energy levels) are discrete. On the other hand, in the thermodynamic limit, for which revivals are ruled out as the energy levels form a continuum, it is always possible to find observables which do not relax to a finite value (e.g., projectors onto eigenstates of the Hamiltonian). Nevertheless, averages of observables that are *local in space* are expected to relax to stationary values: in this sense, one says that the system reaches a stationary state when the averages of all local observables converge to some stationary values. Alternatively, one could consider just a small subsystem of the entire system: in this case, the rest of the system is expected to act as a bath for the subsystem, which therefore is allowed to relax to a stationary state [31, 32].

In order to present the properties of the stationary states, let us make a comparison with classical systems. In classical mechanics, the key property which determines the nature of the stationary state is ergodicity: if the dynamics of a system is ergodic, then the system will eventually relax to a thermal (microcanonical) state, otherwise it will relax to a non-thermal state. Classically, ergodicity is defined by requiring time averages of observables computed along trajectories in the phase space to be equal to averages over a suitable (microcanonical) probability distribution in phase-space. More precisely, given $X(t)$ a trajectory in the phase space with initial condition X_0 and total energy $H(X(t)) = E$, then the ergodicity condition can be formulated as

$$\lim_{T\to\infty} \frac{1}{T}\int_0^T \mathrm{d}t\, O(X(t))\delta(X - X(t)) = \frac{1}{\mathcal{N}}\int \mathrm{d}X\, O(X)\,\delta(E - H(X)) \equiv \int \mathrm{d}X\, O(X)\,\rho_{\mathrm{mc}}(E, X), \quad (1.1)$$

with $O(X)$ a generic observable and $\rho_{\mathrm{mc}}(E)$ the microcanonical probability distribution. The generalization of this notion of ergodicity to quantum systems is difficult: if $|\psi_0\rangle = \sum_\alpha c_\alpha |\alpha\rangle$ is the initial state, with $|\alpha\rangle$ the (non-degenerate) eigenstates of the Hamiltonian $\hat{H}$ with energy E_α, and $|\psi(t)\rangle = \mathrm{e}^{-i\hat{H}t}|\psi_0\rangle$ is the time evolution of the state, the time-averaged density matrix $\hat{\rho}_{\mathrm{diag}}$ (called diagonal ensemble) of the systems is given by:

$$\hat{\rho}_{\mathrm{diag}} \equiv \lim_{T\to\infty} \frac{1}{T}\int_0^T \mathrm{d}t\, |\psi(t)\rangle\langle\psi(t)| = \sum_\alpha |c_\alpha|^2 |\alpha\rangle\langle\alpha|. \quad (1.2)$$

Therefore, by defining

$$\hat{\rho}_{\rm mc} = \mathcal{N}^{-1} \sum_{E_\alpha \sim E} |\alpha\rangle\langle\alpha| \tag{1.3}$$

as the microcanonical density matrix, ergodicity requires that

$$\sum_\alpha |c_\alpha|^2 O_{\alpha\alpha} = \frac{1}{\mathcal{N}} \sum_{E_\alpha \sim E} O_{\alpha\alpha}. \tag{1.4}$$

It is clear that one cannot satisfy the previous equation in general by requiring $\hat{\rho}_{\rm diag} = \hat{\rho}_{\rm mc}$, because this would be true only for the special case $|c_\alpha|^2 = \mathcal{N}^{-1}$ [33–35]. The correct interpretation of Eq. (1.4) was first given in Refs. [36–38], which proposed the so-called eigenstate thermalization hypothesis (ETH), which can be formulated as the remarkably simple idea that the averages of observables are smooth functions of the energy of the eigenstates, i.e., $O_{\alpha\alpha} \sim O(E_\alpha)$. In fact, this condition implies that the l.h.s. of Eq. (1.4) does not depend on the values of $|c_\alpha|^2$, and, as a result, the value $O_{\alpha\alpha}$ corresponds to the thermal microcanonical average: in this sense, the information about thermalization is actually encoded in the structure of eigenstates. While there is no rigorous understanding of which observables satisfy ETH and which do not, ETH has been numerically verified for few-body observables [39]. The ETH has been numerically proven to work for *non-integrable* lattice models [40–57], while it does not apply to *integrable*.

In fact, also in classical statistical mechanics, ergodicity is broken for particular systems, i.e., integrable systems, which are characterized by having an extensive number of conserved quantities, which restrict the trajectories in phase space to a very small fraction of the manifold at constant energy, within which the various conserved quantities take the constant value set by the initial condition.

While the precise definition of integrability in quantum systems is a topic of debate (see, e.g., Refs. [58–60]), a rather standard definition is based on the existence of a large number of (quasi-) local operators $\hat{I}_\alpha$ which commute with the Hamiltonian $\hat{H}$ and with each other. The requirement that these conserved quantities are (quasi-) local excludes, e.g., projection operators on the eigenstates of the Hamiltonian or powers of the Hamiltonian itself, which are actually conserved by the dynamics in every quantum systems.

Analogously to classical systems, in which conserved quantities preclude the exploration of all phase space, the failure of integrable quantum systems to exhibit ETH can be traced back to these conserved quantities $\hat{I}_\alpha$. In this case, in fact, one expects, as a consequence of maximization of entropy [61], that the stationary value of observables may be described by a generalized Gibbs ensemble (GGE)

$$\hat{\rho}_{\rm GGE} \propto {\rm e}^{-\sum_\alpha \lambda_\alpha I_\alpha}, \tag{1.5}$$

as first conjectured in Ref. [62]. This conjecture has been verified by a large number of studies of integrable models [31, 62–89], and the GGE is now considered to be the final state of relaxation of generic quantum integrable systems [90, 91].

However, the question of which the relevant conserved quantities needed in the construction of the GGE are is not yet fully settled [92]. This issue has been discussed intensely [83, 84, 93–96], in particular with respect to the necessity to include quasi-local conserved operators [82, 90, 97–99].

1.3 Prethermalization

Understanding how extended isolated quantum systems relax to the eventual stationary state (thermal or not) is a challenging question, which originated a number of theoretical and experimental investigations. The phenomena occurring during the transient behavior of quantum systems relaxing from a far-from-equilibrium initial state are often collectively referred to as *prethermalization*. This term was originally introduced in Refs. [100, 101] in the context of models for early-universe dynamics, relativistic heavy-ion collision, and quantum gases. These works predicted that the dynamics of these system is characterized by two time-scales: (i) a first time scale, due to dephasing, after which global quantities, such as kinetic energy density and pressure, equilibrate to a value close to the eventual thermal one, and (ii) a second longer time scale after which also quantities such as the particle momentum distribution attain their thermal value. In fact, in between these time scales, the particle momentum distribution acquires a quasi-stationary non-thermal value. The interpretation of these two regimes is that in the initial one the interactions between quasiparticles are negligible, and therefore the dynamics is nearly integrable. This implies that the occupation numbers of quasi particles are approximately conserved quantities. The second time scale, instead, signals the onset of integrability-breaking interactions between quasi-particles, eventually leading to thermalization.

This ideas were soon shown to apply also to lattice models, where integrability-breaking terms were added to an integrable Hamiltonian: it emerged that near-integrable systems first relaxes to a "prethermalization plateau", i.e., to a metastable state described by a GGE, which is eventually destabilized towards a stable thermal state [102–116].

1.4 Universal non-equilibrium dynamics: non-thermal fixed points

The study of relaxation in isolated quantum systems leads to the fundamental question if any kind of *universality* may be displayed by the dynamics during the approach to the eventual stationary states. The idea of universality, originally developed in equilibrium statistical system, has been very successful in classifying and characterising matter near second-order phase transitions. In fact, at the onset of these phase transitions, observables and particularly correlations functions of the order parameter exhibit power-law algebraic and scaling behaviours, which are solely determined by mesoscopic features of the system (such as symmetries, conservation laws, and dimensionality), rather than by microscopic properties and structures. In this respect, it is possible to define *universality classes* which contains all the different physical systems which share these mesoscopic features and thus exhibit the same critical properties.

Universality in relaxional dynamics was firstly predicted in classical statistical systems such as relaxional models [117–121], driven-diffusive [122] and reaction-diffusion systems (both in the stationary and transient regime) [123–126], directed percolation [127–129], self-organized criticality [130], and roughening phenomena [131, 132]. This idea of non-equilibrium universal dynamics has been successively extended to isolated systems, leading to the notion of *non-thermal fixed point* (NTFP) (see Fig. 1.1), which encompass any physical situation in which the correlation of the order parameter $C(x,t) = \langle \phi(x,t)\phi(0,t) \rangle$ acquire, during the relaxation, a scaling form of the type $C(x,t) = t^{\alpha} f(t^{\beta} x)$. In the following Section we provide a more detailed discussion of what are the possible different mechanisms which originate NTFP.

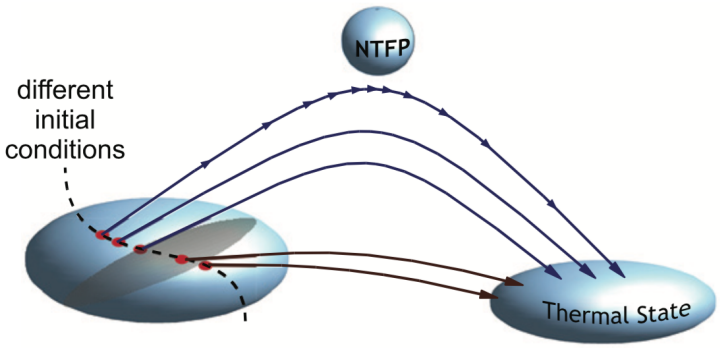

Figure 1.1: Sketch of a non-thermal fixed point, interpreted as a renormalization group flow (from Ref. [10]). While the system will always eventually approach the thermal state (which therefore acts as a stable fixed point), the intermediate dynamics is sensitive to initial conditions and it may result in different behaviours. In particular, for certain initial conditions, the system may evolve nearby a NTFP.

1.5 Physical origin of NTFPs

Several different physical mechanisms lie at the origin of the NTFPs, making evident that they are fixed points in a much broader sense than that understood for the usual ones related to phase transitions in equilibrium systems. This reflects the fact that non-equilibrium systems are characterized by a richer variety of phenomena then equilibrium ones. Among these several mechanisms, we recall:

1. **Turbulence.** Critical scaling phenomena in space and time are strongly reminiscent of turbulence in classical fluids [133, 134] and of superfluids [135, 136]. For example, according to the seminal theory of Kolmogorov, eddies created in a fluid break down into a cascade of smaller eddies until they become of the size set by dissipation of kinetic energy into heat. The associated energy cascade from macroscopic to microscopic scales builds up a non-equilibrium steady state. This was discussed in various contexts, including strong wave turbulence in low-energy Bose gases [137, 138], in relativistic scalar field theories [138–140], as well as abelian [141] and non-abelian gauge theories [142].

2. **Hydrodynamics.** Systems with conserved quantities (e.g., energy and particle number) possess the so-called *hydrodynamic* modes, which correspond to slow fluctuations of the conserved densities [143–145]. These modes give rise to long-time algebraic tails in the decay of generic correlation functions of such densities.

3. **Aging.** The non-equilibrium dynamics of a spatially extended classical system displays universality when the temperature of the system is quenched close to the critical one, a phenomenon

called *aging* [119,146]. While aging is known to occur in classical critical systems [119,146], only recently the same issue has been investigated after quenches in open [147–149] or isolated [2] quantum systems. However, while in the former case the critical point responsible for aging is the thermal one dictated by the presence of a thermal bath, in the latter the critical point has an intrinsic non-equilibrium nature.

4. **Coarsening.** The coarsening (or phase-ordering) dynamics occurs whenever the temperature of a system, prepared in the disordered phase, is quenched below its critical value, i.e., to values for which the system would display its ordered phase if it was at equilibrium [150–152]. As the global symmetry of the system cannot be globally broken by the (symmetric) dynamics, the system breaks the symmetry only locally and therefore it forms domains within which it reaches a local equilibrium. Inside each domain one of the possible (many) low-temperature values of the order parameter is displayed. The characteristic size of the domains grows algebraically in time, which results into peculiar scaling forms in the correlation functions.

1.6 Dynamical phase transitions

A topic which has attracted a certain amount of interest is the possible emergence of qualitatively different behaviours in the relaxational dynamics in isolated quantum system, upon changing the values of the parameters of the post-quench Hamiltonian, or upon changing its initial state. This kind of phenomena have been called *dynamical phase transitions* (DPT), as the different dynamical behaviours involved can be interpreted as "phases". In this sense, the first instance of DPT was found in the non-equilibrium dynamics of the BCS Hamiltonian after a quench of the interaction [153–161]: when the system is prepared with a finite superconductive gap, it was found that it subsequently relaxes to zero below a certain value of the post-quench interaction, while it approaches a finite (possibly oscillatory) value above such a critical value (see Fig. 1.2, left panel). Evidences of DPTs were later found in the mean field dynamics of the Hubbard model [162–167] and of the scalar ϕ^4 field theory [168]: also in these cases, the values of some time-averaged quantities was found to change dramatically upon varying a parameter of the post-quench Hamiltonian (see Fig. 1.2). All these studies relied on mean-field-like techniques, while only recently the effect of fluctuations was accounted for [1–3, 169–172]. This was crucial in order to understand the consequences of dephasing, and the effect of spatial dimensionality on these transitions. The investigation of DPTs is still in its infancy and many questions have still to be addressed, e.g., what is the universality class of these transitions, what is their relation with equilibrium phase transitions, and how their presence affect the relaxation towards thermal equilibrium.

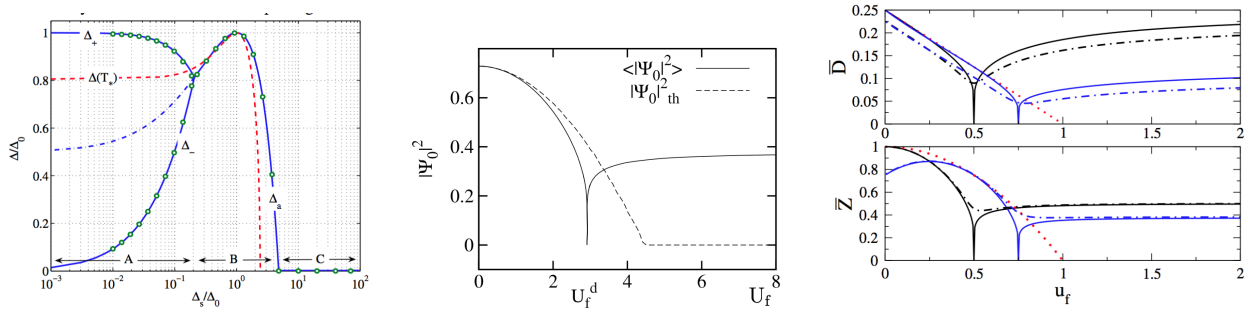

Figure 1.2: Left panel: asymptotic value of the superconductive gap as a function of the initial value of the gap, for a quench in the BCS model (from Ref. [155]). Middle panel: time-averaged condensate fraction as a function of the onsite interaction for a quench in the bosonic Hubbard model (from Ref. [163]). Right panel: time-averaged double occupation (top) and quasiparticle weight (bottom) as a function of the onsite interaction for a quench in the fermionic Hubbard model (from Ref. [165]).

Chapter 2

DPT of $O(N)$-model: mean field and Gaussian theory

Abstract

In this Chapter we introduce the $O(N)$ model, and we show that a DPT is predicted by a mean field analysis and from the Gaussian approximation. In the latter case, we compute correlation functions in momentum an real space, highlighting the emergence of a light-cone structure due to the quench. The Gaussian theory will provide the building block for more refined approaches, described in detail in Chapters 3 and 4.

2.1 Model and quench protocol

We consider a system described by the following $O(N)$-symmetric Hamiltonian in d spatial dimensions

$$H(r,u) = \int \mathrm{d}^d x \, \left[\frac{1}{2}\mathbf{\Pi}^2 + \frac{1}{2}(\nabla \boldsymbol{\phi})^2 + \frac{r}{2}\boldsymbol{\phi}^2 + \frac{u}{4!N}(\boldsymbol{\phi}^2)^2 \right], \tag{2.1}$$

where $\boldsymbol{\phi} = (\phi_1, \ldots, \phi_N)$ is a bosonic field with N components, while $\mathbf{\Pi}$ is the canonically conjugated momentum with $[\phi_a(\mathbf{x}), \Pi_b(\mathbf{x}')] = i\delta^{(d)}(\mathbf{x}-\mathbf{x}')\delta_{ab}$. Note that only the scalar products $\boldsymbol{\phi}^2 = \boldsymbol{\phi}\cdot\boldsymbol{\phi} = \sum_{i=1}^N \phi_i^2$ and $\mathbf{\Pi}^2$ enter Eq. (2.1), as a consequence of the symmetry. The coupling $u > 0$ controls the strength of the anharmonic interaction, while the parameter r control the distance from the critical point, as discussed further below. At time $t < 0$ the system is prepared in the disordered ground state $|\psi_0\rangle$ of the pre-quench non-interacting Hamiltonian $H(\Omega_0^2, 0)$, while the system is evolved with the post-quench Hamiltonian $H(r,u)$ for $t \geq 0$.

In the remainder of this Chapter, we discuss a very simple mean-field approximation of the model mentioned above, showing that a DPT emerges, and subsequently we discuss the Gaussian approximation. In Chapter 3 we study its exact solution in the limit $N \to \infty$, while in Chapter 4 we describe a renormalization group approach to the DPT.

2.2 Mean-field analysis

From Eq. (2.1) one can derive the Heisenberg equation for the field $\boldsymbol{\phi}$, which takes the form of a non-linear operatorial differential equation, i.e.,

$$\ddot{\boldsymbol{\phi}} - \nabla^2 \boldsymbol{\phi} + r\boldsymbol{\phi} + u(\boldsymbol{\phi}\cdot\boldsymbol{\phi})\boldsymbol{\phi} = 0, \tag{2.2}$$

where he initial conditions on the quantum field depends on the choice of the initial state. In order to provide some insight on the dynamics of this model, we present a simplified version of its mean-field theory, proposed in Ref. [168]. We assume Eq. (2.2) to be an equation for a single component classical field ($N = 1$), and the field ϕ to be spatially uniform, so that the Laplacian does not contribute to the dynamics. Then, Eq. (2.2) becomes :

$$\ddot{\phi} + r\phi + u\phi^3 = 0, \tag{2.3}$$

which is now an exactly solvable equation. In order to further simplify the discussion, we assume, without loss of generality, the initial conditions to be $\phi(t = 0) = \phi_0$ and $\dot{\phi}(t = 0) = 0$. Before discussing the solution of (2.3), let us recall what is expected at equilibrium. In this case, the mean-field of the Hamiltonian (2.1) is given by the so-called Landau-Ginzburg theory [173], i.e., the value of the order parameter is obtained by minimizing the free energy associated to H, i.e., the $\mathbb{Z}_2$ symmetric function

$$F(\phi) = \frac{r}{2}\phi^2 + \frac{u}{4}\phi^4. \tag{2.4}$$

Since $u > 0$, the minimum is given by $\bar{\phi} = 0$ if $r > 0$ and by $\bar{\phi} = \pm\phi_{\text{eq}} \equiv \pm\sqrt{r/u}$ if $r < 0$: in the latter case, the two minima are degenerate, and the system breaks the $\mathbb{Z}_2$ symmetry as it realizes only one of the two configurations. Accordingly, the simple Landau-Ginzburg theory predicts a change in the value of the order parameter, that is, a phase transition, at $r = 0$. We will now compare this result to what happens when the order parameter is equipped with the dynamics (2.3). To this end, it is important to notice that Eq. (2.3) conserves the total energy

$$E(\phi, \dot{\phi}) = \frac{1}{2}\dot{\phi}^2 + \frac{r}{2}\phi^2 + \frac{u}{4}\phi^4, \tag{2.5}$$

which is therefore fixed by the initial conditions. Given that we assumed $\dot{\phi}(t = 0) = 0$, the total energy is thus fixed by ϕ_0 as $E(\phi_0, 0) = F(\phi_0)$, with $F(\phi)$ defined in Eq. (2.4). In this respect, the Landau-Ginzburg free energy corresponds to the potential energy of the order parameter. Conservation of energy provides a simple way to visualize the behaviour of the solutions of Eq. (2.3), as depicted in Fig. 2.1. When $r > 0$ and $r = 0$ (upper and upper-middle figures) there is only a stationary solution, $\phi(t) = 0$, which corresponds to having the field at the bottom of the potential. When $\phi_0 \neq 0$, the order parameter oscillates indefinitely in time around the value $\bar{\phi} = 0$: these oscillations in time are expected to average to zero in an extended model, due to dephasing of different modes. When $r < 0$, the potential develops two wells, and consequently two new stationary solutions appears, i.e., $\phi(t) = \pm\phi_{\text{eq}}$, with ϕ_{eq} defined below Eq. (2.4). The behaviour of non-stationary solutions depend crucially on the total energy E: for $E < 0$ (lower-middle figure), the order parameter is trapped into one of the two wells, and it oscillates in time around a non-zero value $\bar{\phi} \neq 0$, which can be interpreted

as a breaking of the $\mathbb{Z}_2$ symmetry (the sign of $\bar{\phi}$ depends on the initial condition). On the other hand, for $E > 0$ (lower figure), the order parameters has enough energy to explore both wells, and correspondingly the order parameter oscillates in time around a zero value $\bar{\phi} = 0$.

The mean-field analysis thus shows the existence of a dynamical phase transition. In Ref. [168] the effect of fluctuations on the initial conditions was included, exploiting a formal analogy with phase transitions in a film geometry: it was shown that it does not modify qualitatively the phase diagram (reported in Fig. 2.2), except for a shift of the critical value of r_c at which the dynamical transition occurs.

2.3 Gaussian theory

In order to gain more insight on the DPT predicted by the mean-field theory summarized in the previous section, we consider now the full quantum case in absence of interaction ($u = 0$). In this way, it is possible to account for the Gaussian fluctuations and to have information about the spatial structure of the model. To this end, let us now consider the case in which the quench protocol described in Sec. 2.1 is modified to $H(\Omega_0^2, 0) \to H(r, 0)$, i.e., the quench is done between non-interacting models. In this case, the theory is exactly solvable and provides the starting point to approach the interacting theory. In particular, all the correlation functions can be computed exactly, both in momentum and real space. In the following, we discuss in detail their properties.

2.3.1 Correlation functions in momentum space

In this section we summarize the analysis of the quantum quench in a bosonic free field theory [174–176] which provides the basis for the analyses carried out in Chapters 3 and 4. Introducing the Fourier transform in momentum space of the fields $\boldsymbol{\phi}$ and $\boldsymbol{\Pi}$ as $\boldsymbol{\phi}(\mathbf{x}) = \int_{\mathbf{k}} \boldsymbol{\phi}_{\mathbf{k}}\, \mathrm{e}^{i\mathbf{k}\cdot\mathbf{x}}$ and $\boldsymbol{\Pi}(\mathbf{x}) = \int_{\mathbf{k}} \boldsymbol{\Pi}_{\mathbf{k}}\, \mathrm{e}^{i\mathbf{k}\cdot\mathbf{x}}$, respectively, where $\int_{\mathbf{k}} \equiv \int \mathrm{d}^d k/(2\pi)^d$, Eq. (2.1) for $u = 0$ can be written as

$$H(r, 0) = \frac{1}{2} \int_{\mathbf{k}} \left(|\boldsymbol{\Pi}_{\mathbf{k}}|^2 + \omega_k^2 \, |\boldsymbol{\phi}_{\mathbf{k}}|^2 \right), \tag{2.6}$$

where

$$\omega_k \equiv \sqrt{k^2 + r} \tag{2.7}$$

is the dispersion relation, while $|\boldsymbol{\Pi}_{\mathbf{k}}|^2 \equiv \boldsymbol{\Pi}_{\mathbf{k}} \cdot \boldsymbol{\Pi}_{\mathbf{k}}^\dagger = \boldsymbol{\Pi}_{\mathbf{k}} \cdot \boldsymbol{\Pi}_{-\mathbf{k}}$ and analogous for $\boldsymbol{\phi}$. The Heisenberg equations of motion for the operators after the quench $\Omega_0^2 \to r$, derived from $H(r, 0)$, is therefore $\ddot{\boldsymbol{\phi}}_{\mathbf{k}} + \omega_k^2 \boldsymbol{\phi}_{\mathbf{k}} = 0$, with solution

$$\boldsymbol{\phi}_{\mathbf{k}}(t) = \boldsymbol{\phi}_{\mathbf{k}}(0) \cos(\omega_k t) + \boldsymbol{\Pi}_{\mathbf{k}}(0) \frac{\sin(\omega_k t)}{\omega_k}. \tag{2.8}$$

In order to calculate the expectation values of the components $\phi_{j,\mathbf{k}}(0)$ and $\Pi_{j,\mathbf{k}}(0)$ (with $j = 1, \ldots, N$) on the initial state, it is convenient to introduce the standard bosonic annihilation and creation operators $b_{j,\mathbf{k}}$ and $b_{j,\mathbf{k}}^\dagger$, respectively, defined as

$$\phi_{j,\mathbf{k}} = \frac{1}{\sqrt{2\omega_k}} \left(b_{j,\mathbf{k}} + b_{j,-\mathbf{k}}^\dagger \right), \qquad \Pi_{j,\mathbf{k}} = -i \sqrt{\frac{\omega_k}{2}} \left(b_{j,\mathbf{k}} - b_{j,-\mathbf{k}}^\dagger \right). \tag{2.9}$$

Once expressed in terms of these operators, Eq. (2.6) becomes

$$H(r,0) = \sum_{j=1}^{N} \int_{\mathbf{k}} \omega_k \, b^{\dagger}_{j,\mathbf{k}} b_{j,\mathbf{k}}, \tag{2.10}$$

up to an inconsequential additive constant. Assuming the pre-quench state to be in equilibrium at a temperature $T = \beta^{-1}$, with Hamiltonian $H_0 = H(\Omega_0^2, 0)$, the density matrix of the system is given by $\rho_0 = \mathcal{Z}^{-1} \mathrm{e}^{-\beta H_0}$, where $\mathcal{Z} = \mathrm{tr}(\mathrm{e}^{-\beta H_0})$. Accordingly, one can evaluate the following statistical averages over ρ_0 by introducing the pre-quench operators $b^0_{j,\mathbf{k}}$ and $b^{0,\dagger}_{j,\mathbf{k}}$ as in Eq. (2.9):

$$\langle \phi_{i,\mathbf{k}}(0) \phi_{j,\mathbf{k}'}(0) \rangle = \delta_{\mathbf{k},-\mathbf{k}'} \delta_{ij} \frac{1}{2\omega_{0k}} \coth(\beta\omega_{0k}/2), \tag{2.11a}$$

$$\langle \Pi_{i,\mathbf{k}}(0) \Pi_{j,\mathbf{k}'}(0) \rangle = \delta_{\mathbf{k},-\mathbf{k}'} \delta_{ij} \frac{\omega_{0k}}{2} \coth(\beta\omega_{0k}/2), \tag{2.11b}$$

$$\langle \phi_{i,\mathbf{k}}(0) \Pi_{j,\mathbf{k}'}(0) \rangle = 0, \tag{2.11c}$$

where $\delta_{\mathbf{k},-\mathbf{k}'} \equiv (2\pi)^d \, \delta^{(d)}(\mathbf{k} + \mathbf{k}')$, and

$$\omega_{0k} = \sqrt{k^2 + \Omega_0^2} \tag{2.12}$$

is the pre-quench dispersion relation. Since the initial state does not break the $O(N)$ symmetry one has $\langle \phi_{j,\mathbf{k}}(0) \rangle = \langle \Pi_{j,\mathbf{k}}(0) \rangle = 0$ and therefore Eq. (2.8) implies that $\langle \phi_{j,\mathbf{k}}(t) \rangle = 0$ at all times t. The correlation functions of the field $\boldsymbol{\phi}$ during the evolution can be easily determined on the basis of Eqs. (2.8), (2.11a), and (2.11b). Hereafter, we focus on the retarded and Keldysh Green's functions, defined respectively as

$$iG_{jl,R}(|\mathbf{x} - \mathbf{x}'|, t, t') = \vartheta(t - t') \langle \big[\phi_j(\mathbf{x}, t), \phi_l(\mathbf{x}', t') \big] \rangle, \tag{2.13a}$$

$$iG_{jl,K}(|\mathbf{x} - \mathbf{x}'|, t, t') = \langle \big\{ \phi_j(\mathbf{x}, t), \phi_l(\mathbf{x}', t') \big\} \rangle, \tag{2.13b}$$

where $\vartheta(t < 0) = 0$ and $\vartheta(t \geq 0) = 1$. Note that, as a consequence of the invariance of the Hamiltonian under spatial translations and rotations, $G_{R/K}$ depend only on the distance $|\mathbf{x} - \mathbf{x}'|$ between the points $\mathbf{x}$ and $\mathbf{x}'$ at which the fields are evaluated. Accordingly, it is convenient to consider their Fourier transforms which are related to the Fourier components of the field $\boldsymbol{\phi}_{\mathbf{k}}$ via

$$\delta_{\mathbf{k},-\mathbf{k}'} \, iG_{jl,R}(k, t, t') = \vartheta(t - t') \langle \big[\phi_{j,\mathbf{k}}(t), \phi_{l,\mathbf{k}'}(t') \big] \rangle, \tag{2.14a}$$

$$\delta_{\mathbf{k},-\mathbf{k}'} \, iG_{jl,K}(k, t, t') = \langle \big\{ \phi_{j,\mathbf{k}}(t), \phi_{l,\mathbf{k}'}(t') \big\} \rangle. \tag{2.14b}$$

In the absence of symmetry breaking, the $O(N)$ symmetry implies that these functions do not vanish only for $j = l$, i.e., $G_{jl,R/K} = \delta_{jl} G_{R/K}$. Accordingly, in what follows, their dependence on the field components is no longer indicated. The Gaussian Green's functions (henceforth denoted by a subscript 0) in momentum space can be immediately determined by using the expression of the time evolution of the field $\phi_{j,\mathbf{k}}$ in Eq. (2.8) and the averages over the initial condition in Eqs. (2.11a) and (2.11b), which yield

$$G_{0R}(k, t, t') = -\vartheta(t - t') \frac{\sin(\omega_k (t - t'))}{\omega_k}, \tag{2.15a}$$

$$G_{0K}(k, t, t') = -i \frac{\coth(\beta\omega_{0k}/2)}{\omega_k} [K_+ \cos(\omega_k (t - t')) + K_- \cos(\omega_k (t + t'))], \tag{2.15b}$$

where

$$K_{\pm} = \frac{1}{2}\left(\frac{\omega_k}{\omega_{0k}} \pm \frac{\omega_{0k}}{\omega_k}\right), \tag{2.16}$$

with ω_k and ω_{0k} given in Eqs. (2.7) and (2.12), respectively. While the retarded Green's function G_{0R}, within this Gaussian approximation, does not depend on the initial state and it is therefore time-translation invariant (TTI), the Keldysh Green's function G_{0K} acquires a non-TTI contribution as a consequence of the quantum quench. Note that, in the absence of a quench, $\omega_k = \omega_{0k}$ and therefore $K_+ = 1$ and $K_- = 0$: correspondingly, the G_{0K} in Eq. (2.15b) recovers its equilibrium TTI expression. In addition, if the temperature T of the initial state vanishes $T = 0$, i.e., the system is in the ground state of the pre-quench Hamiltonian H_0, the $G_{R/K}$ in Eqs. (2.15a) and (2.15b) at small wavevectors $k \ll \Omega_0$ and at $r = 0$ read

$$G_{0R}(k,t,t') = -\vartheta(t-t')\frac{\sin(k(t-t'))}{k}, \tag{2.17a}$$

$$G_{0K}(k,t,t') = -i\frac{\Omega_0}{2k^2}[\cos(k(t-t')) - \cos(k(t+t'))], \tag{2.17b}$$

which can be expressed therefore as scaling forms. These scalings are related, in terms of renormalization group, to a Gaussian fixed point. In fact, one recognizes from Eqs. (2.15a) and (2.15b) that, for momenta $k \ll \Omega_0$, the correlation length is simply given by $\xi = r^{-1/2}$, due to the dependence of this expression on the combination $k^2 + r$. Accordingly, for $r \to r_c = 0$, this correlation length ξ diverges, thus signalling the onset of a transition and, correspondingly, the emergence of scale invariance into the correlation functions. Moreover, recalling the definition of the critical exponent ν, i.e., $\xi \sim |r - r_c|^{-\nu}$, one immediately realizes that in the present case $\nu = 1/2$, which is also the value expected at the Gaussian fixed point for the corresponding equilibrium model [177–179].

2.3.2 Particle distribution

A relevant quantity we consider below is the number $n_{\mathbf{k}}$ of particles with momentum $\mathbf{k}$ after the quench, defined as $n_{\mathbf{k}} = b^\dagger_{\mathbf{k}} b_{\mathbf{k}}$ in terms of the operators introduced in Eq. (2.9), where the index of the field component has been omitted for clarity. The operator $n_{\mathbf{k}}$ can be conveniently expressed in terms of the field $\phi_{\mathbf{k}}$ and its conjugate momentum $\Pi_{\mathbf{k}}$ as

$$n_{\mathbf{k}} + \frac{1}{2}\delta_{\mathbf{k},\mathbf{k}} = \frac{1}{4\omega_k}(\{\Pi_{\mathbf{k}}, \Pi_{-\mathbf{k}}\} + \omega_k^2\{\phi_{\mathbf{k}}, \phi_{-\mathbf{k}}\}). \tag{2.18}$$

Since each term in this expression is proportional to the (infinite) volume $V = \int \mathrm{d}^d x$ of the system, we consider the associated finite *momentum density* $\mathcal{N}_{\mathbf{k}} \equiv \langle n_{\mathbf{k}}\rangle / V$, which can be expressed in terms of the Green's functions in momentum space as

$$\mathcal{N}_{\mathbf{k}} + \frac{1}{2} = \frac{i}{4\omega_k}[G^{\Pi}_K(k,t,t) + \omega_k^2 G_K(k,t,t)], \tag{2.19}$$

where we introduced $i\delta_{\mathbf{k},-\mathbf{k}'} G^{\Pi}_K(t,t') = \langle\{\Pi_{\mathbf{k}}(t), \Pi_{\mathbf{k}'}(t')\}\rangle$ in analogy with G_K in Eq. (2.13b). Taking into account the Heisenberg equations of motion $\dot{\phi}_{\mathbf{k}} = \Pi_{\mathbf{k}}$, the equal-time G^{Π}_K can be expressed as

$$G^{\Pi}_K(k,t,t) = \partial_t \partial_{t'} G_K(k,t,t')\Big|_{t=t'} \equiv \ddot{G}_K(k,t,t), \tag{2.20}$$

from which it follows that the momentum density $\mathcal{N}_{\mathbf{k}}$ can be expressed in terms of G_K only:

$$\mathcal{N}_{\mathbf{k}} + \frac{1}{2} = \frac{i}{4\omega_k}[\ddot{G}_K(k,t,t) + \omega_k^2 G_K(k,t,t)]. \tag{2.21}$$

The r.h.s. of this equation can be calculated within the Gaussian approximation (hence the subscript 0) by using Eq. (2.15b), which yields

$$\mathcal{N}_{0\mathbf{k}} + \frac{1}{2} = \frac{1}{2} K_+ \coth(\beta\omega_{0k}/2). \tag{2.22}$$

Note that $\mathcal{N}_{0\mathbf{k}}$ does not depend on time, because the post-quench Hamiltonian $H(r,0)$ can be written as in Eq. (2.10), i.e., as a linear combination of the momentum densities which are therefore conserved quantities. In addition, the number of excitations after the quench is finite even at $T = 0$ as a consequence of the energy injected into the system upon quenching. In the absence of a quench, instead, $K_+ = 1$ and Eq. (2.22) renders the Bose equilibrium distribution $\mathcal{N}_{0\mathbf{k}} = 1/[\exp(\beta\omega_{0k}) - 1]$.

2.3.3 Deep quenches limit and effective temperature

In the rest of the discussion, we mostly focus on the limit of *deep quench* $\Omega_0^2 \gg \Lambda$, where Λ is some ultra-violet cut-off inherent the microscopic structure of the system, the deep-quench limit can be equivalently expressed as $\Omega_0 \gg \Lambda$. Interpreting Λ as being related to the inverse of the lattice spacing of the underlying microscopic lattice, the condition $\Omega_0 \gg \Lambda$ implies that the correlation length $\simeq \Omega_0^{-1}$ of fluctuations in the pre-quench state is smaller than the lattice spacing, i.e., the system is in a highly disordered state. In turn, as was realized in Refs. [174–176, 180], this disordered initial state resembles a high-temperature state and, in fact, the momentum density in Eq. (2.22) takes the form

$$\mathcal{N}_{0\mathbf{k}} \simeq \frac{T_{\text{eff}}}{\omega_k} \tag{2.23}$$

of a thermal one in the deep-quench limit, with an effective temperature given by

$$T_{\text{eff}} = \Omega_0/4. \tag{2.24}$$

This similarity is made even more apparent by considering the fluctuation-dissipation theorem (FDT) [181] which relates in frequency-momentum space the Keldysh and retarded Green's functions of a system in thermal equilibrium at temperature β^{-1} as

$$G_K(\omega,k) = \coth(\beta\omega/2)[G_R(k,\omega) - G_R(k,-\omega)]. \tag{2.25}$$

Out of equilibrium, one can *define* an effective temperature $T_{\text{eff}} = \beta_{\text{eff}}^{-1}$ such that $G_{K/R}$ satisfy the FDT [182–185], which generically depends on both frequency ω and momentum k as a consequence of the lack of thermalization. In the present case, considering only the stationary part of Eq. (2.15b), the Fourier transform of G_{0K} is related to the one of G_{0R} in Eq. (2.15a) via

$$G_{0K}(k,\omega) = \frac{\Omega_0}{2\omega}[G_{0R}(k,\omega) - G_{0R}(k,-\omega)], \tag{2.26}$$

which takes the form of the FDT in Eq. (2.25) with the same (high) temperature $T = T_{\rm eff}$ as defined above in Eq. (2.24) from the behavior of $\mathcal{N}_{0\mathbf{k}}$. As shown in Chapter 4 the fact that the system appears to be "thermal" in the deep-quench limit has important consequences on its critical properties. Indeed, it behaves effectively as a d-dimensional classical system rather than a $d+1$-dimensional one, the latter expected for a closed quantum system at zero temperature. Accordingly, the effect of a deep quench on a DPT is heuristically the same as that of a non-vanishing temperature on a quantum phase transition, where the temperature is so high that the system falls out of the so-called quantum-critical regime [179, 186, 187]. However, as discussed in Chapters 3 and 4, this DPT is characterized by novel universal non-equilibrium properties, absent in the transition at equilibrium.

2.3.4 Correlation functions in real space and light-cone dynamics

In this section we discuss the properties of the Green's functions in real space $G_{R/K}(x,t,t')$, with $x = |\mathbf{x}_1 - \mathbf{x}_2|$, highlighting the emergence of a light cone in the dynamics in both correlation [174] and response [185, 188] functions, which has been observed experimentally [19, 189] in the correlation function of a one-dimensional quantum gas. The emergence of a light cone is due [174, 185, 188] to the fact that the entangled quasi-particle pairs generated by the quench propagate ballistically with a velocity v, causing a qualitative crossover in the behavior of the Green's functions from short times, at which they behave as in the initial state, to long times at which the effect of the quench dominate; this is accompanied by an enhancement of these functions right on the light cone.

Since $G_{R/K}(x,t,t')$ depend separately on the two times t and t', there are two kind of light cones emerging in their structure: one for $x = t+t'$ and one for $x = t-t'$. For the Keldysh Green's function $G_K(x,t,t)$ at equal times , the enhancement at the light cone can be physically interpreted as due to the simultaneous arrival at positions $\mathbf{x}_1$ and $\mathbf{x}_2$ of highly entangled excitations generated by the quench [174]. For the specific Hamiltonian in Eq. (2.1), the present normalization sets the velocity of propagation to $v = 1$. While in principle the value of v is affected by the presence of the interaction, this is not the case up to one loop in perturbation theory, as shown in the rest of this section. For the retarded Green's function $G_R(x,t,t')$ the enhancement at the light cone can also be again understood from the ballistic propagation of excitations with velocity $v = 1$: a perturbation created at $x = 0$ at time t' cannot be felt at position x until the condition $x = |t - t'|$ is obeyed. After this time, the effect of the initial perturbation decreases upon increasing t for a fixed value of x, and so the response function approaches zero.

Exploiting the spatial isotropy and translational invariance, $G_{R/K}(x,t,t')$ in d spatial dimensions can be calculated from their Fourier transforms $G_{R/K}(k,t,t')$ in Eqs. (2.15a) and (2.15b) as

$$G_{R,K}(x,t,t') = \frac{1}{x^{d/2-1}\,(2\pi)^{d/2}} \int_0^\Lambda \mathrm{d}k\, k^{d/2} J_{d/2-1}(kx) G_{R,K}(k,t,t'), \tag{2.27}$$

where we included a sharp ultra-violet cut-off Λ in the integral over $\mathbf{k}$ and J_α indicates the Bessel function of the first kind. This expression is obtained by exploiting the fact the functions $G_{R,K}$ depend only on the modulus k of the wavevector $\mathbf{k}$: one can then perform a change of variables using hyperspherical coordinates and then integrate over the angular variables [190].

In this section we focus on the case of a critical quench, corresponding to a vanishing post-quench value of the parameter $r = 0$. Correspondingly, the correlation length $\xi = r^{-1/2}$ diverges, causing

the emergence of universal scaling forms and algebraic decays also in the light-cone structure of the Green's functions. Let us first consider spatial dimension $d = 4$. The Gaussian retarded Green's function $G_{0R}^{d=4}(x,t,t')$ follows from Eqs. (2.27) and (2.15a):

$$G_{0R}^{d=4}(x,t,t') = -\frac{1}{4\pi^2 x^3}\int_0^{\Lambda x} \mathrm{d}y\, y J_1(y)\sin(y(t-t')/x), \tag{2.28}$$

where we assume, for simplicity, $t > t'$. Denoting by $\tau = t - t'$ the difference between the two times, for $\Lambda x \gg 1$ and $\Lambda\tau \gg 1$ we find that G_{0R} exhibits a light cone, similarly to what was observed in other models [183, 185, 188]:

$$G_{0R}^{d=4}(x \gg \tau) = \frac{\Lambda^3}{4\pi^{5/2}\,(\Lambda x)^{5/2}}\sin(\Lambda\tau)\,[\sin(\Lambda x) + \cos(\Lambda x)] \simeq 0, \tag{2.29a}$$

$$G_{0R}^{d=4}(x = \tau) = -\frac{\Lambda^3}{12\pi^{5/2}\,(\Lambda\tau)^{3/2}}, \tag{2.29b}$$

$$G_{0R}^{d=4}(x \ll \tau) = -\frac{\Lambda^2}{4\pi^{5/2}\tau\,(\Lambda x)^{3/2}}\cos(\Lambda\tau) \simeq 0. \tag{2.29c}$$

Inside ($x \ll \tau$) and outside ($x \gg \tau$) the light cone, G_{0R} vanishes on average due to the rapidly oscillating terms, while exactly on the light cone $x = \tau = t - t'$ it does not, and actually is characterized by an algebraic temporal decay $\propto \tau^{-3/2}$. Accordingly $G_{0R}(x,\tau)$ is peaked at $x = \tau$ and vanishes away from this point in a manner which depends on the ultraviolet (UV) physics.

In Sec. 4.2.3 we show that this basic behavior is preserved even in presence of interactions, provided that the dynamics is in the collisionless prethermal regime. However, the algebraic decay at $x = |t - t'|$ will be modified in two ways: first, it will depend on whether the initial perturbation occurs at a short time or at a long time relative to a microscopic time scale Λ^{-1}, which is not captured by the Gaussian quench discussed here. Second, the algebraic decay will acquire corrections described by the anomalous exponent θ_N for t' at short times.

The Gaussian Keldysh Green's function $G_{0K}^{d=4}(x,t,t)$ at equal times, in real space, and in the deep-quench limit follows from Eqs. (2.27) and (2.17b):

$$iG_{0K}^{d=4}(x,t,t) = \frac{\Omega_0}{8\pi^2 x}\int_0^{\Lambda} \mathrm{d}k\,[1 - \cos(2kt)]J_1(kx). \tag{2.30}$$

Evaluating the integral, the light cone is observed to emerge for $\Lambda x \gg 1$ and $\Lambda t \gg 1$, upon crossing the line $x = 2t$,

$$iG_{0K}^{d=4}(x \gg 2t) \simeq \mathcal{O}\left(\frac{J_0(\Lambda x)}{x^2}\right) \simeq 0, \tag{2.31a}$$

$$iG_{0K}^{d=4}(x = 2t) \simeq \frac{\Omega_0}{8\pi^{5/2}}\frac{\Lambda^2}{(\Lambda x)^{3/2}}, \tag{2.31b}$$

$$iG_{0K}^{d=4}(x \ll 2t) \simeq \frac{\Omega_0}{8\pi^2}\frac{\Lambda^2}{(\Lambda x)^2}. \tag{2.31c}$$

Outside the light cone, i.e., for $x \gg 2t$, the behavior of G_{0K} is primarily determined by the initial state as the effect of the quench has not yet set in. Since the initial state is gapped, with two-point correlations decaying rapidly upon increasing their distance, G_{0K} vanishes outside the light cone for $\Lambda x \gg 1$. Inside the light cone ($x \ll 2t$), instead, a time-independent value is obtained, which is characterized by an algebraic spatial decay $\propto x^{-2}$. Finally, right on the light cone $x = 2t$, the correlator G_{0K} is enhanced, showing a slower algebraic decay $\propto x^{-3/2}$.

While above we focused on the case $d = 4$, it is interesting to study the behavior of G_{0K} in generic spatial dimensionality d, which we compare in Sec. 4.2.3 with the results of the perturbative dimensional expansion in the presence of interactions. Note that G_{0K} outside the light cone vanishes for the reason indicated above; thus we discuss here its behavior at and inside the light cone. Instead of regularizing the momentum integrals via a sharp cut-off as we did in Eq. (2.27), we consider below a generic cut-off function $f(k/\Lambda)$ such that $f(x \ll 1) = 1$, with an exponential decay as $x \gg 1$. In view of the asymptotic form of Bessel functions [191], and noting that they oscillate in phase with $G_{0K}(k, t, t)$ on the light cone, we find (see Eq. (2.27))

$$\begin{aligned} iG_{0K}(x = 2t) &\simeq \frac{\Omega_0}{x^{d/2-1}\,(2\pi)^{d/2}} \int_0^\infty \mathrm{d}k\, k^{d/2} \frac{f(k/\Lambda)}{k^2\sqrt{kx}} \\ &\propto \frac{1}{x^{d-2}} \int_0^\infty \mathrm{d}y\, y^{(d-5)/2} f\left(\frac{y}{\Lambda x}\right) \\ &\simeq \frac{1}{x^{d-2}} \int_0^{\Lambda x} \mathrm{d}y\, y^{(d-5)/2} \\ &\propto \frac{1}{x^{(d-1)/2}}. \end{aligned} \tag{2.32}$$

Inside the light cone $x \ll 2t$ we find, instead,

$$\begin{aligned} iG_{0K}(x \ll 2t) &\simeq \frac{\Omega_0}{x^{d/2-1}\,(2\pi)^{d/2}} \int_0^\infty \mathrm{d}k\, k^{d/2} f(k/\Lambda) J_{d/2-1}(kx) \frac{1}{k^2} \\ &\propto \frac{1}{x^{d-2}} \int_0^\infty \mathrm{d}y\, y^{-2+d/2} J_{d/2-1}(y) f\left(\frac{y}{\Lambda x}\right) \\ &\propto \frac{1}{x^{d-2}}, \end{aligned} \tag{2.33}$$

where we replaced $\sin^2(kt)$ appearing in $G_{0K}(k, t, t)$ (see Eq. (2.17b)) with its temporal mean value $1/2$ and in the last line the cut-off function f has been replaced by 1 because the rapidly oscillating Bessel function suppresses the integral at large arguments. In summary, for a deep quench to the critical point of the Gaussian theory in d spatial dimensions one finds

$$iG_{0K}(x \gg 2t) \simeq 0, \tag{2.34a}$$

$$iG_{0K}(x = 2t) \propto \frac{1}{x^{(d-1)/2}}, \tag{2.34b}$$

$$iG_{0K}(x \ll 2t) \propto \frac{1}{x^{d-2}}. \tag{2.34c}$$

The response function on the other hand can be simply derived by using Eqs. (2.17a) and (2.27),

$$G_{0R}(x = t - t') \propto \frac{1}{x^{(d-1)/2}} \tag{2.35}$$

and vanishes away from $x = t - t'$ as discussed above.

As anticipated above and shown in Sec. 4.2.3, these expressions acquire sizeable corrections when a finite value of the post-quench interaction u is included, with corrections taking the form of an anomalous scaling which modifies the exponents appearing in Eqs. (2.34) and (2.35).

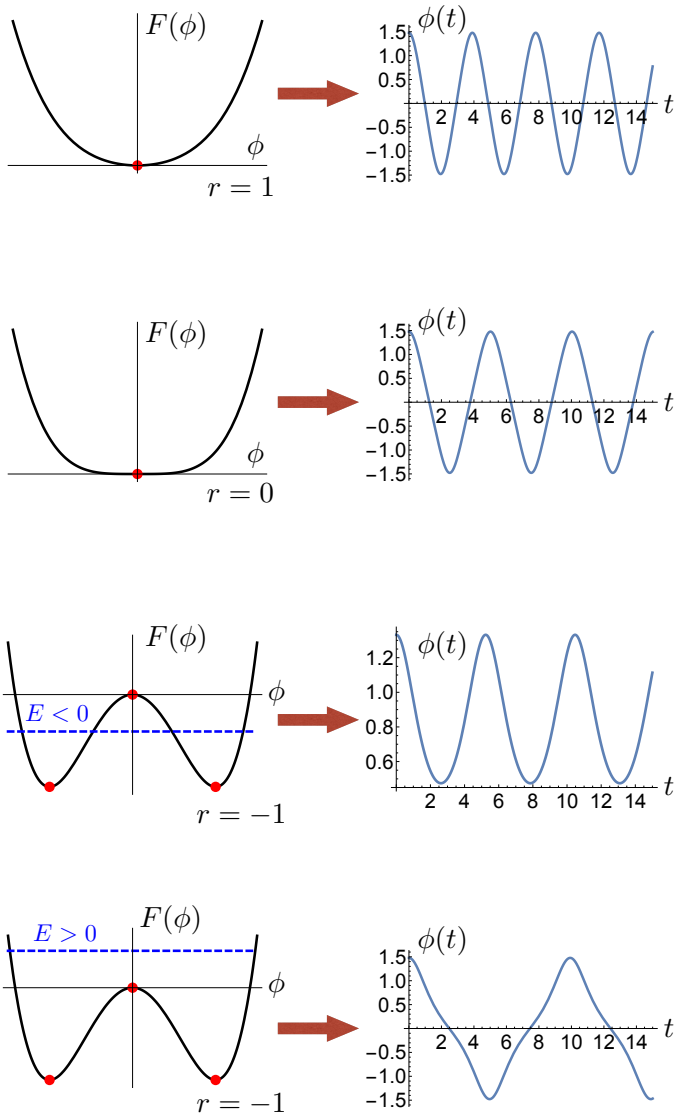

Figure 2.1: Potentials and corresponding time evolution of the order parameter $\phi(t)$ for different values of r and E and $u = 1$. Upper and upper-middle figures: potentials for $r = 1$ and $r = 0$ have one absolute minimum (red dots), and the corresponding evolution oscillates around zero. Lower and lower-middle figures: potentials for $r = -1$ have two degenerate minima and a relative maximum (red dots); the corresponding evolutions oscillates around a finite value if $E < 0$ (lower-middle figure) and around zero if $E > 0$.

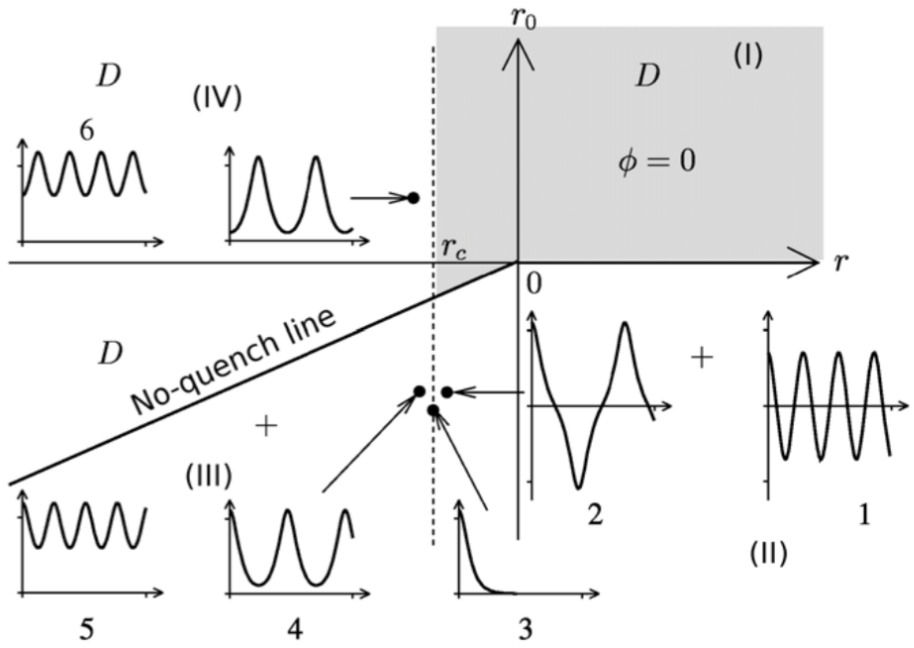

Figure 2.2: Mean-field non-equilibrium phase diagram (from Ref [168]). Four "phases" are identified: (I) for $r > r_c$ and $r_0 > 0$, the order parameter $\phi(t)$ vanishes identically; (II) $r > r_c$ and $r_0 < 0$, where $\phi(t)$ shows oscillations around zero; (III) and (IV) where $\phi(t)$ shows oscillations with a non-zero average.

Chapter 3

DPT of $O(N)$-model: large-N limit

Abstract

The non-equilibrium dynamics of an isolated quantum system after a sudden quench to a dynamical critical point is expected to be characterized by scaling and universal exponents due to the absence of time scales. We explore these features for a quench of the parameters of a Hamiltonian with $O(N)$ symmetry, starting from a ground state in the disordered phase. In the limit of infinite N, the exponents and scaling forms of the relevant two-time correlation functions can be calculated exactly. Our analytical predictions are confirmed by the numerical solution of the corresponding equations. Moreover, we find that the same scaling functions, yet with different exponents, also describe the coarsening dynamics for quenches below the dynamical critical point.

In this chapter we will study the quench protocol described in Section 2.1 in the limit $N \to \infty$. In the following we will exploit the fact that, if the $O(N)$ symmetry in the initial state is not broken, the average $\langle \phi_a \phi_b \rangle$ (where $\langle \dots \rangle \equiv \langle \psi_0 | \dots | \psi_0 \rangle$) vanishes unless $a = b$, with its non-vanishing value independent of a, and equal to the fluctuation $\langle \phi^2 \rangle$ of a generic component ϕ of the field. In the limit $N \to \infty$, the model (2.1) can be solved by taking into account that, at the leading order, the quartic interaction in Eq. (2.1) decouples as [169–171, 180]

$$(\boldsymbol{\phi}^2)^2 \to 2(N+2)\langle \phi^2 \rangle \boldsymbol{\phi}^2 - N(N+2)\langle \phi^2 \rangle^2; \tag{3.1}$$

as shown in Ref. [192], this decoupling corresponds to the Hartree-Fock approximation, which becomes exact for $N \to \infty$. Once inserted into Eq. (2.1), the dynamics of the various components of the fields decouples and each of them is ruled (up to an inconsequential additive constant) by the effective time-dependent quadratic Hamiltonian

$$H_{\rm eff}(t) = \frac{1}{2} \int \mathrm{d}^d x \, \left[\Pi^2 + (\nabla \phi)^2 + r_{\rm eff}(t) \phi^2 \right], \tag{3.2}$$

where $r_{\rm eff}(t)$ is determined by the condition

$$r_{\rm eff}(t) = r + \frac{u}{6} \langle \phi^2(\mathbf{x}, t) \rangle. \tag{3.3}$$

In a field-theoretical language, $r_{\rm eff}(t)$ plays the role of a renormalized square effective mass of the field ϕ. Due to the quadratic nature of $H_{\rm eff}$, it is convenient to decompose the field ϕ into its Fourier components $\phi_{\mathbf{k}}$, according to $\phi(\mathbf{x},t)=\int \mathrm{d}^d k\, \phi_{\mathbf{k}}(t)\mathrm{e}^{i\mathbf{k}\cdot\mathbf{x}}/(2\pi)^d$, with an analogous decomposition for Π. Each of these components can be written in terms of the annihilation and creation operators [170,171] $a_{\mathbf{k}}$ and $a^\dagger_{\mathbf{k}}$, respectively, diagonalizing the initial Hamiltonian:

$$\phi_{\mathbf{k}}(t)=f_{\mathbf{k}}(t)a_{\mathbf{k}}+f^*_{\mathbf{k}}(t)a^\dagger_{-\mathbf{k}}, \tag{3.4}$$

where $f_{\mathbf{k}}(t)=f_{-\mathbf{k}}(t)$ is a complex function depending on both time t and momentum $\mathbf{k}$. Note that the canonical commutation relations between ϕ and Π imply [170]

$$2\,\mathrm{Im}[f_{\mathbf{k}}(t)\dot{f}^*_{\mathbf{k}}(t)]=1. \tag{3.5}$$

The Heisenberg equation of motion for $\phi_{\mathbf{k}}$ derived from the Hamiltonian (3.2) yields the following evolution equation for $f_{\mathbf{k}}(t)$:

$$\ddot{f}_{\mathbf{k}}+[k^2+r_{\rm eff}(t)]f_{\mathbf{k}}=0, \tag{3.6}$$

with $k=|\mathbf{k}|$. This equation is supplemented by the initial conditions

$$f_{\mathbf{k}}(0)=1/\sqrt{2\omega_{0k}}\quad\text{and}\quad \dot{f}_{\mathbf{k}}(0)=-i\sqrt{\omega_{0k}/2}, \tag{3.7}$$

where $\omega^2_{0k}=k^2+\Omega_0^2$, which can be obtained by diagonalizing the quadratic pre-quench Hamiltonian and by imposing the continuity [174,175] of $\phi_{\mathbf{k}}(t)$ at $t=0$.

Since the Hamiltonian is quadratic, all the information on the dynamics is encoded in its two-time functions, such as the retarded (G_R) and Keldysh (G_K) Green's functions, which are defined in Eqs. (2.14). Accordingly, $r_{\rm eff}$ in Eq. (3.3) can be expressed in terms of G_K as

$$r_{\rm eff}(t)=r+\frac{u}{12}\int\frac{\mathrm{d}^d k}{(2\pi)^d}\,iG_K(k,t,t)h(k/\Lambda), \tag{3.8}$$

where the function

$$h(x)=\begin{cases}0 & \text{for}\quad x\gg 1,\\ 1 & \text{for}\quad x\ll 1,\end{cases} \tag{3.9}$$

implements a large-$\mathbf{k}$ cut-off at the scale Λ in order to make the theory well-defined at short distances, while it does not affect it for $k\ll\Lambda$. By using Eq. (3.4) in Eqs. (2.14b) and (2.14a), we find that $G_{K,R}$ can be written in terms of the function $f_{\mathbf{k}}$ as:

$$iG_K(k,t,t')=2\mathrm{Re}\left[f_{\mathbf{k}}(t)f^*_{\mathbf{k}}(t')\right], \tag{3.10}$$

$$G_R(k,t,t')=2\theta(t-t')\mathrm{Im}\left[f_{\mathbf{k}}(t)f^*_{\mathbf{k}}(t')\right]. \tag{3.11}$$

The dynamics of the system can be determined by solving the set of self-consistency equations given by Eqs. (3.6), (3.8) and (3.10). Generically, these equations do not admit an analytic solution and therefore one has to resort to numerical integration. Nevertheless, in the following section, we show that some quantities can be analytically calculated when the post-quench Hamiltonian is close to the dynamical critical point.

3.1 Dynamical phase transition and scaling equations

In Refs. [169–171] it was shown that, after the quench, the system approaches a stationary state, in which the effective Hamiltonian becomes time-independent. Such a stationary state was then argued to be non-thermal as a consequence of the integrability of the model. In particular, in Ref. [171], it was demonstrated that when r in Eq. (2.1) is tuned to a critical value r_c, the long-time limit r^* of the corresponding effective parameter $r_{\text{eff}}(t)$ in Eq. (3.2) vanishes and therefore the fluctuations of the order parameter become critical, signalling the occurrence of a dynamical phase transition. More precisely, as a consequence of the divergence of the spatial correlation length $\xi \equiv (r^*)^{-1/2}$, the correlation functions at long times acquire scaling forms characterized by universal critical exponents.

Similarly to the case of classical systems after a quench of the temperature [119], the correlation functions exhibit dynamical scaling forms not only in the steady state, but also while approaching it [2]: in particular, relying on dimensional analysis and on the lack of additional time- and length-scales at $r = r_c$, one expects the effective value $r_{\text{eff}}(t)$ to scale as:

$$r_{\text{eff}}(t) = \frac{a}{t^2}\sigma(\Lambda t), \tag{3.12}$$

where the function σ is normalized by requiring $\sigma(\infty) = 1$, such that $r_{\text{eff}}(t)$ vanishes at long times as

$$r_{\text{eff}}(t) = \frac{a}{t^2} \quad \text{for} \quad \Lambda t \gg 1, \tag{3.13}$$

while a is a dimensionless quantity. The non-universal corrections introduced by $\sigma(\Lambda t) - 1$ to this long-time limit are negligible for $\Lambda t \gg 1$. On the contrary, for $\Lambda t \lesssim 1$, they become dominant and non-universal behavior is displayed. Accordingly, one can identify a *microscopic time* [2] $t_\Lambda \simeq \Lambda^{-1}$ which separates these two regimes: for $0 \leq t \lesssim t_\Lambda$ the dynamics is dominated by non-universal microscopic details; for $t \gtrsim t_\Lambda$, instead, the dynamics becomes universal. This discussion assumes that the function $\sigma(\tau)$ has a well-defined limit as $\tau \to \infty$, which might not be the case in the presence of oscillatory terms. In fact, as shown in the numerical analysis presented in Sec. 3.2, the non-universal function σ depends on how the cut-off Λ is implemented in the model, i.e., on the choice of the function $h(x)$ in Eq. (3.8). In particular, the choice of a sharp cut-off turns out to make $\sigma(\tau)$ oscillate, masking the universal long-time behavior $r_{\text{eff}}(t) \sim t^{-2}$.

As a consequence of the universal form of Eq. (3.13) for $t \gtrsim t_\Lambda$, the correlation functions are expected to exhibit scaling properties. In order to show this, it is convenient to rescale time and write the function $f_{\mathbf{k}}(t)$ as $f_{\mathbf{k}}(t) = g_{\mathbf{k}}(kt)$. Inserting Eq. (3.13) into Eq. (3.6), one finds the equation for $g_{\mathbf{k}}(x)$:

$$g''_{\mathbf{k}}(x) + \left(1 + \frac{a}{x^2}\right) g_{\mathbf{k}}(x) = 0, \tag{3.14}$$

valid for $x \equiv kt \gtrsim kt_\Lambda$, whose solution is:

$$g_{\mathbf{k}}(x) = \sqrt{x}[A_{\mathbf{k}} J_\alpha(x) + B_{\mathbf{k}} J_{-\alpha}(x)], \tag{3.15}$$

where $J_\alpha(x)$ is the Bessel function of the first kind and

$$\alpha = \sqrt{\frac{1}{4} - a}. \tag{3.16}$$

Below we show that it is consistent to assume $a < 1/4$ and therefore α to be real. The constants $A_{\mathbf{k}}$ and $B_{\mathbf{k}}$ in Eq. (3.15) are fixed by the initial condition of the evolution, as discussed below. For later reference, we recall that

$$J_\alpha(x) \simeq \begin{cases} (x/2)^\alpha/\Gamma(1+\alpha), & x \ll 1, \\ \cos(x - \alpha\pi/2 - \pi/4)\sqrt{2/(\pi x)}, & x \gg 1, \end{cases} \tag{3.17}$$

where $\Gamma(x)$ is the Euler gamma function [191]. Note that Eq. (3.15) encodes the complete dependence of $f_{\mathbf{k}}(t)$ on time t for $t \gtrsim t_\Lambda$, whereas its dependence on the wave vector $\mathbf{k}$ is encoded in the yet unknown functions $A_{\mathbf{k}}$ and $B_{\mathbf{k}}$. By using the following identity for the Wronskian of Bessel functions [191]

$$J_\alpha(x)J'_{-\alpha}(x) - J_{-\alpha}(x)J'_\alpha(x) = -\frac{2\sin(\alpha\pi)}{\pi x}, \tag{3.18}$$

one can show that Eq. (3.5) requires the coefficients $A_{\mathbf{k}}$, $B_{\mathbf{k}}$ to satisfy the relation:

$$\mathrm{Im}[A_{\mathbf{k}}B^*_{\mathbf{k}}] = -\frac{\pi}{4\sin(\alpha\pi)}\frac{1}{k}. \tag{3.19}$$

This relation is not sufficient in order to determine completely $A_{\mathbf{k}}$ and $B_{\mathbf{k}}$ unless the full functional form of $r_{\mathrm{eff}}(t)$ is taken into account, including its non-universal behavior for $t \lesssim t_\Lambda$; this would allow us to fix $A_{\mathbf{k}}$ and $B_{\mathbf{k}}$ on the basis of the initial conditions for the evolution, which at present cannot be reached from Eq. (3.15), it being valid only for $t \gtrsim t_\Lambda$. However, for a deep quench — such as that one investigated in Ref. [2] — with $\Omega_0 \gg \Lambda$, the initial conditions (3.7) for the evolution of $f_{\mathbf{k}}$ become essentially independent of $\mathbf{k}$ and read:

$$f_{\mathbf{k}}(0) \simeq 1/\sqrt{2\Omega_0}, \quad \dot{f}_{\mathbf{k}}(0) \simeq -i\sqrt{\Omega_0/2}. \tag{3.20}$$

At time $t \simeq t_\Lambda \simeq \Lambda^{-1}$, $f_{\mathbf{k}}(t_\Lambda)$ can be calculated from a series expansion $f_{\mathbf{k}}(t_\Lambda) = f_{\mathbf{k}}(0) + t_\Lambda\dot{f}_{\mathbf{k}}(0) + t_\Lambda^2\ddot{f}_{\mathbf{k}}(0) + \mathcal{O}(t_\Lambda^3)$ and by using Eqs. (3.6) and (3.20) one may readily conclude that its dependence on k comes about via $(k/\Lambda)^2$ and $k/(\Omega_0\Lambda)$; accordingly, at the leading order, it can be neglected for $k \ll \Lambda$. On the other hand, $f_{\mathbf{k}}$ at t_Λ can be evaluated from Eq. (3.15) and, since $kt_\Lambda \simeq k/\Lambda \ll 1$, we can use the asymptotic form of the Bessel functions for small arguments, finding:

$$f_{\mathbf{k}}(t_\Lambda) \propto A_{\mathbf{k}}(kt_\Lambda)^{1/2+\alpha} + B_{\mathbf{k}}(kt_\Lambda)^{1/2-\alpha}. \tag{3.21}$$

In order to have $f_{\mathbf{k}}(t_\Lambda)$ independent of $\mathbf{k}$ at the leading order, it is then necessary that:

$$A_{\mathbf{k}} \simeq A(k/\Lambda)^{-1/2-\alpha}, \quad B_{\mathbf{k}} \simeq B(k/\Lambda)^{-1/2+\alpha}, \tag{3.22}$$

where A and B are yet unknown complex numbers. While this scaling is expected to be true for $k \ll \Lambda$, non-universal corrections may appear for $k \simeq \Lambda$. Note that Eq. (3.22) is consistent with (3.19), provided that:

$$\mathrm{Im}[AB^*] = -\frac{\pi\Lambda^{-1}}{4\sin(\alpha\pi)}. \tag{3.23}$$

The numerical analysis discussed in Sec. 3.2 actually shows that $A_{\mathbf{k}}$ turns out to be purely imaginary, while $B_{\mathbf{k}}$ real. Combining Eqs. (3.22) with (3.15), (3.10), and (3.11), one finds a simple form for the retarded Green's function

$$\begin{aligned} G_R(k,t,t') = -\theta(t-t')\frac{\pi}{2\sin\alpha\pi}(tt')^{1/2}\times \\ \left[J_\alpha(kt)J_{-\alpha}(kt') - J_{-\alpha}(kt)J_\alpha(kt')\right], \end{aligned} \tag{3.24}$$

while the one for $iG_K(k,t,t')$ is somewhat lengthy and thus we do not report it here explicitly. In order to determine a and therefore α from the self-consistent condition in Eq. (3.8), it is actually sufficient to know $iG_K(k,t,t')$ for $t=t'$, which is given by

$$\begin{aligned} iG_K(k,t,t) = 2\Lambda t\left\{|A|^2(k/\Lambda)^{-2\alpha}J_\alpha^2(kt)\right. \\ \left. + |B|^2(k/\Lambda)^{2\alpha}J_{-\alpha}^2(kt) + 2\mathrm{Re}[AB^*]J_\alpha(kt)J_{-\alpha}(kt)\right\}. \end{aligned} \tag{3.25}$$

Accordingly, while Eq. (3.19) is sufficient in order to determine the complete form of G_R, the one of G_K still contains unknown coefficients A and B which are eventually determined by the initial conditions; nevertheless, the scaling properties of both of these functions are already apparent. In fact, their dynamics is characterized by two temporal regimes, which we refer to as *short* ($kt \ll 1$) and *long* ($kt \gg 1$) *times*. Stated differently, the temporal evolution of each mode $\mathbf{k}$ has a typical time scale $\sim k^{-1}$ determined by the value of the momentum itself and the corresponding short-time regime extends to macroscopically long times for vanishing momenta.

Let us focus on G_R in Eq. (3.24): at short times $t' < t \ll k^{-1}$ it becomes independent of k

$$G_R(k,t,t') \simeq -\frac{t}{2\alpha}\left(\frac{t'}{t}\right)^{1/2-\alpha}\left[1-\left(\frac{t'}{t}\right)^{2\alpha}\right], \tag{3.26}$$

where we used the asymptotic expansion in Eq. (3.17). For well-separated times $t \gg t'$, the second terms in brackets is negligible and $G_R(k, t\gg t', t')$ displays an algebraic dependence on the ratio t'/t. At long times $k^{-1} \ll t', t$, instead, G_R becomes time-translational invariant and by keeping the leading order of the asymptotic expansion of the Bessel functions in Eq. (3.17), it reads

$$G_R(k,t,t') \simeq -\theta(t-t')\frac{\sin k(t-t')}{k}, \tag{3.27}$$

which is nothing but the G_R of a critical Gaussian Hamiltonian after a deep quench [2]. Similarly, at short times $t \ll k^{-1}$ and to leading order in Λt, $G_K(k,t,t)$ reads (see Eqs. (3.25) and (3.17))

$$iG_K(k,t,t) \simeq \frac{2^{1-2\alpha}\,|A|^2}{\Gamma^2(1+\alpha)}(\Lambda t)^{1+2\alpha}, \tag{3.28}$$

which is independent of the momentum k, as it is the case for G_R within the same temporal regime. At long times $t \gg k^{-1}$, instead, one finds

$$iG_K(k,t,t) \simeq \frac{2|A|^2}{\pi}\left(\frac{\Lambda}{k}\right)^{1+2\alpha}, \tag{3.29}$$

to leading order in k/Λ, where the possible oscillating terms have been neglected, as they are supposed to average to zero when an integration over momenta is performed. The resulting expression turns out to be time-independent and, contrary to what happens with G_R, it *does not* correspond to the G_K of a critical Gaussian theory after a deep quench [2], reported further below in Eq. (3.30). This fact should be regarded as a consequence of the non-thermal nature of the stationary state which is eventually reached by the system and which retains memory of the initial state. Since the effective Hamiltonian (3.2) is Gaussian, it is tempting to interpret the anomalous momentum dependence $\sim k^{-1-2\alpha}$ in Eq. (3.29) in terms of a quench in a truly Gaussian theory. In the latter case, it was shown [174–176] that, for deep quenches,

$$iG_K(k,t,t) \simeq \frac{\Omega_0}{2k^2}, \tag{3.30}$$

which is similar to an equilibrium distribution with an effective temperature $T_{\rm eff} \simeq \Omega_0$. Accordingly, Eq. (3.29) can be regarded as resulting from a quench of a Gaussian theory with a momentum-dependent initial "temperature" $\Omega_0(k) \sim k^{1-2\alpha}$.

Equations (3.28) and (3.29) show that the term proportional to $|A|^2$ in the expression (3.25) of $G_K(k,t,t)$ is dominant at both long and short times: accordingly, we can neglect the remaining ones and the Keldysh Green's function with two different times t, t' acquires the scaling form

$$iG_K(k,t,t') = 2|A|^2 \left(\frac{\Lambda}{k}\right)^{1+2\alpha} \sqrt{k^2tt'}J_\alpha(kt)J_\alpha(kt'), \tag{3.31}$$

which can be derived from Eqs. (3.15), (3.22), and (3.10). This expression can now be used in order to derive from the self-consistency equation (3.8) the value of the constant a and therefore of the exponent α (see Eq. (3.16)) which characterizes the scaling forms (3.24) and (3.31). For $\Lambda t \gg 1$ one can approximate $r_{\rm eff}(t)$ with Eq. (3.13) and, by assuming a sharp cut-off

$$h(x) = \theta(1-x), \tag{3.32}$$

Eq. (3.8) becomes

$$\frac{a}{t^2} = r_c + \frac{a_d}{6}|A|^2\, u\Lambda^d R_{d,\alpha}(\Lambda t) \tag{3.33}$$

at the critical value r_c of r. In this expression we introduced the function

$$R_{d,\alpha}(x) = x\int_0^1 {\rm d}y\, y^{d-1-2\alpha}J_\alpha^2(xy), \tag{3.34}$$

while $a_d = \Omega_d/(2\pi)^d$ with $\Omega_d = 2\pi^{d/2}/\Gamma(d/2)$ the d-dimensional solid angle. Expanding $R_{d,\alpha}(x)$ for large argument $x \gg 1$, one finds that

$$R_{d,\alpha}(x) = W_{d,\alpha}(x) + c_{d,\alpha}^{(0)} + \frac{c_{d,\alpha}^{(1)}}{x^{d-1-2\alpha}} + \frac{c_{d,\alpha}^{(2)}}{x^2} + \mathcal{O}\left(\frac{1}{x^4}\right), \tag{3.35}$$

where $W_{d,\alpha}(x)$ is a fast oscillating function which is a consequence of the sharp cut-off considered in the integral over momenta and $c_{d,\alpha}^{(i)}$ are certain coefficients, the relevant values of which are provided further below. Once the expansion (3.35) is plugged into Eq. (3.33), the r.h.s. of the latter can be

expanded in decreasing powers of Λt which have to match the term on its l.h.s., resulting in a set of conditions fixing the values of r_c, α, and u. Notice that the oscillations contained in $W_{d,\alpha}(x)$ would be compensated by sub-leading terms in the l.h.s. of Eq. (3.33) (which are not reported, see the discussion after Eq. (3.13)), thus confirming the non-universal nature of $W_{d,\alpha}(x)$. The value of r_c is determined such as to cancel the constant contribution $\propto c^{(0)}_{d,\alpha}$ on the r.h.s., while α has to be fixed such that $c^{(1)}_{d,\alpha} = 0$ in order to cancel the term $\propto (\Lambda t)^{1+2\alpha-d}$ which cannot be matched by the l.h.s. of Eq. (3.33) [1]. This procedure — typically used for solving this kind of self-consistency equations [146, 193–195] — can be regarded as a systematic way of canceling terms which result from corrections to scaling and, therefore, it allows a comparison with the results obtained within a renormalization group approach (with some exceptions, see Ref. [195]). For our purposes, it is sufficient to focus on the condition

$$c^{(1)}_{d,\alpha} = \frac{1}{2\sqrt{\pi}} \frac{\Gamma\left(\frac{1}{2} - \frac{d}{2} + \alpha\right) \Gamma\left(\frac{d}{2}\right)}{\Gamma\left(1 - \frac{d}{2} + \alpha\right) \Gamma\left(1 - \frac{d}{2} + 2\alpha\right)} = 0, \tag{3.36}$$

which is solved by requiring the argument of one of the two Γ functions in the denominator to equal a non-positive integer. The two corresponding infinite sets of solutions $\mathcal{S}'$ and $\mathcal{S}$ for α are given by

$$\mathcal{S}' = \left\{ \frac{d-2}{2} - n \right\}_{n \geq 0}, \quad \mathcal{S} = \left\{ \frac{d-2}{4} - \frac{n}{2} \right\}_{n \geq 0}, \tag{3.37}$$

with integer n. The physically relevant solution can be selected by requiring a to match its Gaussian value $a = 0$ (or, equivalently, $\alpha = 1/2$, see Eq. (3.16)) at the upper critical dimensionality $d_c = 4$ of the model [2, 171]. Note that this Gaussian value of a can be easily inferred by inspecting the scaling behavior of $G_{R,K}$ for the quench towards a non-interacting theory (compare, e.g., Eqs. (3.29) and (3.30)). Accordingly, one finds a single possible solution from $\mathcal{S}$, i.e.,

$$\alpha = \frac{d-2}{4} \qquad \text{and} \qquad a = \frac{d}{4}\left(1 - \frac{d}{4}\right), \tag{3.38}$$

with $a > 0$ for all values of d between $d_l = 2$ and $d_c = 4$, while for $d > 4$ the Gaussian theory applies and therefore

$$\alpha = \frac{1}{2} \qquad \text{and} \qquad a = 0. \tag{3.39}$$

For $d \geq d_c$, $c^{(2)}_{d,\alpha} \propto a$ vanishes and the leading temporal dependence of the r.h.s. of Eq. (3.33) at long times is $\propto c^{(1)}_{d,\alpha=1/2} (\Lambda t)^{-(d-2)}$ and therefore

$$r_{\text{eff}}(t) \propto (\Lambda t)^{-(d-2)}, \tag{3.40}$$

up to oscillating terms, instead of the behavior $\propto t^{-2}$ in Eq. (3.13). Equations (3.38) and (3.39) together with Eqs. (3.24) and (3.31) completely characterize the scaling behavior of $G_{K,R}$ after a deep

[1] In passing we mention that, alternatively, one might require the exponent of this term to equal the one on the l.h.s. of Eq. (3.33), i.e., $1 + 2\alpha - d = -2$. Correspondingly, the divergence of $c^{(2)}_{d,\alpha} \propto a/[2\pi(3 + 2\alpha - d)]$ cancels the one of $c^{(1)}_{d,\alpha}$ reported in Eq. (3.36): the eventual contribution $\propto t^{-2}$ on the r.h.s. of Eq. (3.33) is finite but negative and it would therefore require an unphysical negative value of the coupling constant u in order to match the term on the l.h.s. of the same equation.

quench to the critical point. These results can be compared with the predictions of Ref. [2], formulated with a dimensional expansion around the upper critical dimensionality d_c of the $O(N)$ model, which is expected to reduce to the present one for $N \to \infty$. There, the time dependence of $G_{K,R}$ for $kt, kt' \ll 1$ and $t' \ll t$ was parametrized in terms of the exponent θ as

$$G_R(k,t,t') \propto -t(t'/t)^\theta \quad \text{and} \quad G_K \propto (tt')^{1-\theta}, \tag{3.41}$$

from which it follows that θ is related to the exponent α introduced in Eqs. (3.24) and (3.31) by $\theta = 1/2 - \alpha$. Moreover, it was found in Ref. [2] (see Chapter 4) that $\theta = \epsilon/4 + \mathcal{O}(\epsilon^2)$ with $\epsilon \equiv 4 - d$, in agreement with Eq. (3.38), which yields $\theta = 1 - d/4$ for $d < 4$.

We note here that among the remaining solutions of Eq. (3.36) in $\mathcal{S}$ and $\mathcal{S}'$ which do not match the Gaussian value at $d = d_c$, only one turns out to be compatible with having a positive value of the coupling constant u in Eq. (3.33). This solution belongs to $\mathcal{S}'$, and is given by

$$\alpha_{\rm co} = \frac{d-2}{2} \qquad \text{with} \qquad a_{\rm co} = \frac{(3-d)(d-1)}{4}; \tag{3.42}$$

remarkably, it turns out to be related to the coarsening occurring after a quench to $r < r_c$, as we argue and demonstrate further below.

3.2 Numerical results

In order to test the quality of the analytical predictions of the previous section, we studied in detail the numerical solution of the evolution equations (3.6) for $f_{\mathbf{k}}(t)$, under the constraint provided by Eq. (3.8), with G_K given by Eq. (3.10). The numerical integration of these equations has been performed using an algorithm based on the Bulirsch-Stoer method [196], while the integrals over momentum k have been computed using the extended Simpson's rule [196] with a mesh of 7.5×10^4 points.

In Sec. 3.2.1 we consider the case of a quench to the critical point, comparing the numerical results for the relevant correlation functions with the analytical predictions derived in Sec. 3.1. In Sec. 3.2.2 we present, instead, results for a quench below the critical point, and show some numerical evidence of the emergence of scaling properties during coarsening.

3.2.1 Quench to the critical point

In order to determine the critical value r_c of the parameter r in Eq. (2.1) one can conveniently use the ansatz proposed in Ref. [171, 180], i.e.,

$$r_c = -\frac{u}{4!} \int \frac{d^d k}{(2\pi)^d} \frac{2k^2 + \Omega_0^2}{k^2 \sqrt{k^2 + \Omega_0^2}} \, h(k/\Lambda), \tag{3.43}$$

which turns out to correctly predict r_c also beyond the case of a deep quench. The rationale behind this ansatz relies on the assumption that $G_K(k,t,t)$ at $t \to \infty$ has approximately the same form as for the case of a quench to $r = 0$ in the non-interacting case $u = 0$ [180]. Although the validity of this assumption for a quench to the critical point is questionable because, as shown in Sec. 3.1, G_K

differs significantly from the non-interacting case $u = 0$ (see, e.g., Ref. [2]), Eq. (3.43) anyhow provides accurate predictions for the value of r_c.

The accuracy of the ansatz (3.13) for the long-time behavior of $r_{\rm eff}(t)$ can be tested by calculating $r_{\rm eff}(t)$ according to Eqs. (3.8) and (3.10), based on the numerical solution of the evolution equation (3.6) for $f_{\mathbf{k}}(t)$.

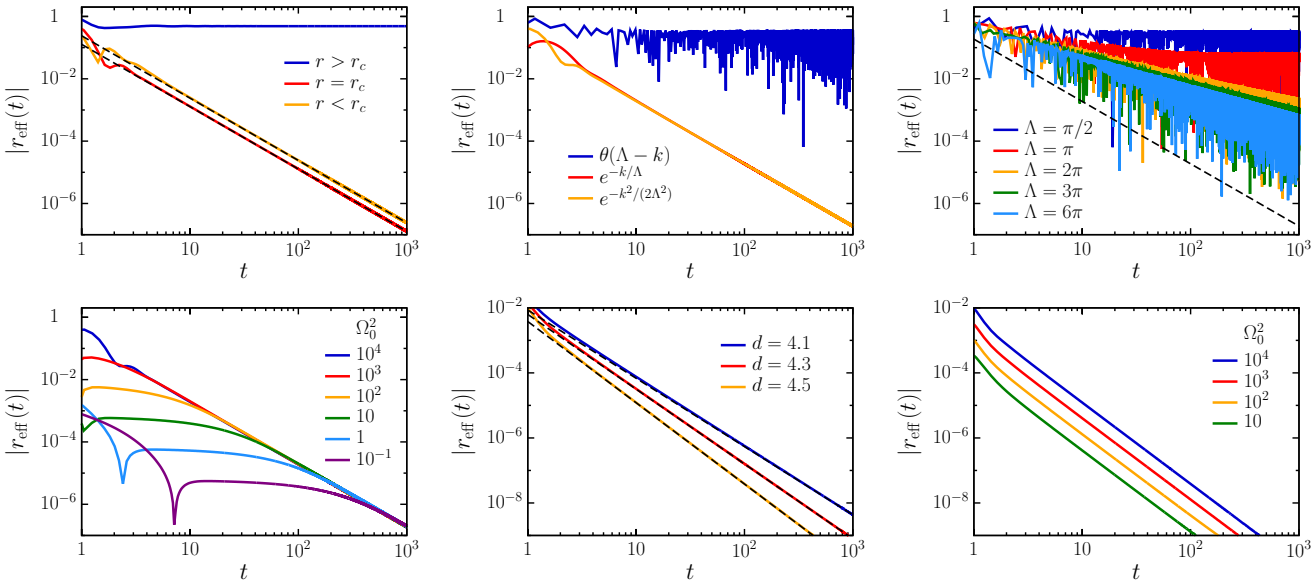

Figure 3.1: Effective parameter $r_{\rm eff}$ as a function of time t. Upper left panel: $r_{\rm eff}$ for a quench above (uppermost curve), at (lowermost curve), and below (intermediate curve) the critical point r_c with $d = 3.4$, $\Omega_0^2 = 10^2$, $u \simeq 80$, and a Gaussian cut-off function $h(k/\Lambda) = \exp[-k^2/(2\Lambda^2)]$ with $\Lambda = \pi/2$. The black dashed lines indicate an algebraic decay $\sim t^{-2}$. Upper central panel: $r_{\rm eff}$ at $r = r_c$ for sharp (uppermost curve) and smooth (lowermost curves) cut-off functions $h(k/\Lambda)$ indicated in the legend (see also the main text) with $d = 3$, $\Omega_0^2 = 10^2$, $u \simeq 47$, and $\Lambda = \pi/2$. Upper right panel: $r_{\rm eff}$ at $r = r_c$ for various values of the sharp cut-off Λ,increasing from top to bottom, with $d = 3$, $\Omega_0^2 = 10^4$, and $u \simeq 4.74$, compared with the expected algebraic decay $\sim t^{-2}$ (dashed line). Lower left panel: $r_{\rm eff}$ at $r = r_c$ for various values of the initial parameter Ω_0^2, decreasing from top to bottom, with $d = 3$, $u \simeq 4.74$, and a Gaussian cut-off function h with $\Lambda = \pi/2$. Lower central panel: $r_{\rm eff}$ at $r = r_c$ for several values of $d > d_c = 4$, $u = 1$, $\Omega_0^2 = 10^4$ and a Gaussian cut-off function h with $\Lambda = \pi/2$; the dashed lines superimposed on the curves are proportional to $t^{-2.1}$ (uppermost curve), $t^{-2.3}$ (intermediate curve) and $t^{-2.5}$ (lowermost curve). Lower right panel: $r_{\rm eff}$ at $r = r_c$ for several values of Ω_0,decreasing from top to bottom, with fixed $d = 4.5$, $u = 1$ and a Gaussian cut-off function h with $\Lambda = \pi/2$.

In Fig. 3.1 we show the time dependence of $r_{\rm eff}(t)$ after a deep quench. In particular, the upper left panel demonstrates, in spatial dimension $d = 3.4$, that while $r_{\rm eff}(t)$ at long times approaches a finite value for $r > r_c$, it generically vanishes for both $r = r_c$ and $r < r_c$. In particular, the corresponding decay turns out to be $\sim t^{-2}$ in both cases, as indicated by the dashed lines, in agreement with the

ansatz (3.13) at criticality. Such an algebraic behavior actually sets in after some time $t_\Lambda \sim \mathcal{O}(\Lambda^{-1})$, where Λ is the cut-off employed in the algorithm. As expected, the actual possibility of detecting this algebraic decay depends on the way the model is regularized, i.e., on the specific function $h(x)$ used in Eq. (3.8) in order to introduce the cut-off Λ. This is illustrated by the upper central panel of Fig. 3.1 for a quench at criticality $r = r_c$ in $d = 3$, in which the momentum integral in Eq. (3.8) is regularized with a sharp cut-off as in Eq. (3.32) (uppermost curve) or with a smooth exponential $h(x) = \mathrm{e}^{-x}$ or Gaussian $h(x) = \mathrm{e}^{-x^2/2}$ functions (lower curves), with characteristic scale Λ. (Note that the value of r_c is also affected by this choice, according to Eq. (3.43).) While the sharp cut-off causes persistent oscillations in $|r_{\mathrm{eff}}(t)|$, which mask the expected behavior $\sim t^{-2}$, the smooth ones are qualitatively similar and they reveal this algebraic decay after some time t_Λ. The persistent oscillations displayed for a sharp cut-off function are expected to be sub-leading compared to the Λ-independent decay $\sim t^{-2}$ in a formal expansion in decreasing powers of Λ: accordingly, their amplitude is expected to decrease as Λ increases. This is clearly demonstrated by the curves in the upper right panel of Fig. 3.1, which, from top to bottom, slowly approach the expected algebraic behavior (dashed line) upon increasing the value of Λ. Accordingly, in order to detect the universal behavior $\sim t^{-2}$ in the presence of a sharp cut-off, very large values of Λ have to be used, resulting in a longer computational time with respect to that required by an exponential or Gaussian cut-off function h. The onset of a scaling regime for $r_{\mathrm{eff}}(t)$ for a quench at criticality is also expected to be influenced by the value of the pre-quench parameter Ω_0^2, as discussed in Sec. 3.1 and in Ref. [2]. In particular, while the analytic investigation in Sec. 3.1 assumes a deep quench, i.e., $\Omega_0 \gg \Lambda$, it is instructive to check numerically how the actual value of Ω_0 influences the time t_Λ after which the expected universal algebraic behavior $\sim t^{-2}$ sets in. The curves in the lower left panel of Fig. 3.1 show, from top to bottom, that t_Λ increases significantly upon decreasing the value of Ω_0^2, until the eventual algebraic behavior is completely masked by the initial non-universal transient occurring at $t < t_\Lambda$ when $\Omega_0 \ll \Lambda$. If the spatial dimensionality d of the model is larger than the upper critical dimensionality $d_c = 4$, the leading-order temporal decay of $r_{\mathrm{eff}}(t)$ is no longer proportional to t^{-2}, because the corresponding proportionality constant a vanishes (see Eq. (3.13)). In this case, $r_{\mathrm{eff}}(t)$ still vanishes at long times with the algebraic law $\sim t^{-(d-2)}$ given in Eq. (3.40). This dependence is shown in the lower central panel for $d = 4.1$, 4.3 and 4.5. The theoretical prediction for the exponent of this decay is indicated by the corresponding dashed lines, while its prefactor is a non-universal constant which depends — in contrast to the case $d < 4$ — on the actual values of the parameters of the system, e.g., Ω_0, as shown in the lower right panel for $d = 4.5$.

As discussed in Sec. 3.1, the scaling behavior of $r_{\mathrm{eff}}(t)$ implies the emergence of algebraic dependences on time in $G_{R,K}$, numerical evidences for which are presented in Fig. 3.2 for a deep quench occurring at $d = 3$. In particular, $G_K(k, t, t)$ at criticality is expected to display the short-time scaling in Eq. (3.28) for $t \ll k^{-1}$ (which actually extends to long times for $k = 0$), while in the long-time limit $t \gg k^{-1}$, G_K displays (up to oscillating terms) the scaling in Eq. (3.29) as a function of k. In order to corroborate these predictions, the left and right upper panels of Fig. 3.2 show the dependence on time t and momentum k, respectively, of G_K within these two regimes, for quenches occurring at $r > r_c$ (lowermost curves), $r = r_c$ (intermediate curves), and $r < r_c$ (uppermost curves). The upper left panel demonstrates that $G_K(k = 0, t, t)$, after a quench to criticality, grows in time as $\sim t^{3/2}$ (intermediate dashed line) in agreement with Eqs. (3.28) and (3.38) for $d = 3$. If the quench occurs above criticality, instead, G_K displays oscillations with an asymptotic period $\propto \xi = (r^*)^{-1/2}$ where $r^* = r_{\mathrm{eff}}(t \to \infty)$ as expected on general grounds [2] and as suggested by the lowermost curve. Remarkably, an algebraic

behavior $\sim t^2$ (uppermost dashed line) emerges for quenches occurring below the critical point (i.e., with $r < r_c$), which signals that the corresponding coarsening occurs on a dynamical length scale which grows in time [150]. Further below (see Fig. 3.4), we discuss the dependence of the power of this algebraic decay on the spatial dimensionality d. We anticipate here that the present law $\sim t^2$ agrees with what one would obtain by extending the scaling prediction in Eq. (3.28) to quenches below r_c and by using the value $\alpha_{\rm co} = 1/2$ from Eq. (3.42) instead of α. The upper right panel, instead, reports the dependence on k of the value eventually reached by $G_K(k,t,t)$ at a fixed but long time $t \gg k^{-1}$. In particular, at criticality $r = r_c$ (intermediate curve), G_K approaches, up to oscillatory terms, the algebraic behavior $\sim k^{-3/2}$ (lower dashed line) in agreement with Eqs. (3.29) and (3.38) in $d = 3$. For $r < r_c$ (uppermost curve), G_K still displays, up to oscillatory terms, an algebraic dependence on k, but with a different power $\sim k^{-2}$ (upper dashed line) which again agrees with the extension of the critical scaling form (3.29) below r_c with α replaced by $\alpha_{\rm co}$. When the quench occurs, instead, above the critical point, G_K tends to a constant, up to oscillations. In all the cases illustrated in Fig. 3.2, non-universal contributions affect the various curves for $k \gtrsim \Lambda = \pi/2$, due to the effects of the regularizing function h. As far as $G_R(k,t,t')$ is concerned, Eq. (3.24) provides its complete expression within the scaling regime at criticality $r = r_c$. In particular, $G_R(k = 0, t, t')$ acquires the scaling form (3.26), while $G_R(k,t,t')$ becomes time-translationally invariant at long times $k^{-1} \ll t' < t$ as in Eq. (3.27). The lower left panel of Fig. 3.2 shows that $G_R(k = 0, t, t')/t$ with $t' < t$ becomes indeed a function of the ratio t'/t only. At criticality (lowermost curve) this agrees with what is expected on the basis of Eqs. (3.26) and (3.38) in $d = 3$ (which renders $\alpha = 1/4$), with $|G_R(k = 0, t, t')/t| \propto \Phi_{1/4}(t'/t)$ (dashed line), where we define

$$\Phi_\alpha(x) \equiv x^{1/2-\alpha} - x^{1/2+\alpha}. \tag{3.44}$$

For a quench below r_c, instead, the same quantity becomes $|G_R(k = 0, t, t')/t| \propto 1 - (t'/t)$ (dashed line); this agrees with $\Phi_{1/2}(t'/t)$, i.e., with what one would infer by extending the critical scaling function (3.26) below r_c and by using the value $\alpha_{\rm co} = 1/2$ in Eq. (3.42) for the exponent α. The inset shows, instead, the numerical data for $G_R(k = 0, t, t')$ after a quench to $r > r_c$, as a function of t' and fixed $t > t'$, which is characterized by persistent oscillations. As mentioned above, for this kind of quench, $r_{\rm eff}(t)$ approaches a finite asymptotic value r^* at large times and, up to the leading order, the system behaves as a Gaussian model quenched at r^*, for which the response function is given by [2] Eq. (3.27) with

$$k \to \sqrt{k^2 + r^*}. \tag{3.45}$$

The dashed line reported in the inset of the figure, which is actually indistinguishable from the numerical data, corresponds to this theoretical prediction with $k = 0$ (see also next panel), confirming its accuracy. The lower right panel of Fig. 3.2 shows $G_R(k, t > t', t')$ as a function of $k(t - t')$ for two fixed long times t and $t' < t$ and upon varying k. The main plot shows the corresponding numerical curves both for $r = r_c$ and $r < r_c$, which are however perfectly superimposed and practically indistinguishable from the theoretical prediction in Eq. (3.27) (dashed line), the latter being independent of the actual value of α. The inset, instead, shows G_R for $r > r_c$: also in this case, the numerical data are indistinguishable from the corresponding theoretical prediction obtained on the basis of Eqs. (3.27) and (3.45), as explained above while illustrating the previous panel.

The numerical results presented in Figs. 3.1 and 3.2 refer to a quench of the model in a certain spatial dimensionality d. In order to test both the predictions in Eq. (3.38) and some of the features

of the scaling functions at criticality we repeated the analysis of the previous figures for a variety of values of d, the results of which are reported in Fig. 3.3. In particular, the long-time behavior of $r_{\rm eff}(t)$ after a quench at $r = r_c$ (such as the one displayed for $d = 3.4$ in the upper left panel of Fig. 3.1) can be fitted with the expected algebraic law at^{-2} in order to extract the value of a as a function of d. The resulting numerical estimates are indicated by the dots in the upper left panel of the figure, where they are compared with the theoretical prediction in Eq. (3.38) (dashed line). While the agreement between the latter and the numerical data is very good for $d \lesssim 3.6$, slight deviations appear upon approaching the upper critical dimensionality $d_c = 4$ of the model, due to the expected corrections to scaling which are known to become increasingly relevant as $d \to d_c$ [195].

Analogously, by fitting the time dependence of the critical $iG_K(k = 0, t, t)$ with the algebraic law $\sim t^\gamma$, one can estimate the numerical value of γ as a function of d. These estimates, reported in the upper right panel of Fig. 3.3 (symbols), can then be compared with the analytical prediction $\gamma \equiv 1 + 2\alpha = d/2$ for $d < 4$ and $\gamma = 2$ for $d \geq 4$ (dashed line) which follows from Eqs. (3.28), (3.38), and (3.39). Also in this case the agreement between the data and the analytical prediction is very good apart from a region around d_c, where corrections to scaling make the extraction of the exponent from the data more difficult. While both of the previous evidences in favor of the theoretical predictions of Sec. 3.1 are based on the scaling properties of G_K and of $r_{\rm eff}(t)$, an independent and more stringent test is provided by the analysis of the response function G_R, whose analytical form in Eqs. (3.24) and (3.26) does not involve unknown parameters (such as those which fix, instead, the amplitude of $G_K(k = 0, t, t)$ in Eq. (3.28)). In particular, another estimate of α can be obtained by fitting $|G_R(k = 0, t, t')/t|$ with $C\,\Phi_\alpha(t'/t)$ (see Eq. (3.44)) as predicted by Eq. (3.26). The resulting values of α are reported in the lower left panel of Fig. 3.3 together with the analytical prediction (dashed line) of Eqs. (3.38) and (3.39). Alternatively, one can estimate the value of the proportionality constant C by fitting $|G_R(k = 0, t, t')/t|$ with $C\Phi_\alpha(t'/t)$ where α is now fixed to the theoretically expected value reported in Eqs. (3.38) and (3.39). The resulting numerical estimates are indicated by the symbols in the lower right panel of Fig. 3.3 together with the analytical prediction (dashed line) $C = 1/(2\alpha)$ which follows from Eq. (3.26) and from the theoretical values of α of Eqs. (3.38) and (3.39). Also for the lower left panel, the agreement with theoretical predictions is good, except for values close to d_c, while it is remarkably good for the lower right panel.

Further below we argue that the exponent $\gamma = 1 + 2\alpha$ which describes the algebraic behavior of $G_K(k, t, t)$ both at short and long times (see Eqs. (3.28) and (3.29)) is the same as the one introduced in Ref. [171] in order to characterize the small-momentum behavior $\sim k^{-\gamma}$ of $\rho_k(t)$ up to a cut-off $k^* \sim t^{-1}$. The quantity $\rho_k(t)$ corresponds to the average number of excitations with momentum k of the pre-quench Hamiltonian which are produced after a so-called double quench, i.e., when the parameters of the post-quench Hamiltonian are restored suddenly to their initial values after a time t has elapsed from the first quench occurring at $t = 0$. The values of γ which were numerically determined in Ref. [171] for a quench to the critical point in $d = 3$ and 4, i.e., $\gamma = 3/2$ and 2 are in perfect agreement with our numerical estimates and analytical predictions reported in the upper right panel of Fig. 3.3.

3.2.2 Quench below the critical point

The Keldysh (Fig. 3.2, upper panels) and the retarded (Fig 3.2, lower panels) Green's functions G_K and G_R, respectively, for $r > r_c$ are characterized by an oscillatory behavior, which denotes the presence of a finite length scale ξ in the model, set by the asymptotic value r^* of $r_{\rm eff}(t)$. On the contrary, for $r < r_c$, the effective parameter $r_{\rm eff}(t)$ turns out to decay to zero as $\simeq a_{\rm co} t^{-2}$ (see the upper left panel of Fig. 3.1), i.e., with the same power law as at criticality $r = r_c$: correspondingly, $G_{R,K}$ exhibit algebraic behaviors, which however differ from the critical ones. In fact, it is rather related to the phenomenon of *coarsening* which we discuss further below in Sec. 3.2.3. As we discussed in Sec. 3.1, the value of $a_{\rm co}$ — as well as of a for $r = r_c$ — can in principle be determined in such a way as to satisfy the self-consistent equations (3.33) and (3.36), which indeed admit two different solutions, reported in Eqs. (3.38) and (3.42). While the former correctly describes the observed behavior at criticality (see the evidence presented in Fig. 3.3), it is quite natural to expect the latter to describe the other possible scaling behavior, i.e., the one associated with coarsening. Numerical evidence of this fact is presented in Fig. 3.4. In particular, the upper left panel shows the value of $a_{\rm co}$ (symbols) for various values of d, as inferred by fitting the corresponding numerical data of $r_{\rm eff}(t)$ for $r < r_c$ with $a_{\rm co} t^{-2}$. The dashed line corresponds to the theoretical prediction reported in Eq. (3.42). Although the numerical data reported in Fig. 3.4 refer to a quench with $r = -3 < r_c$, we have verified that these numerical estimates are not affected by the choice of $r < r_c$. Note that while a at $r = r_c$ as a function of the dimensionality d shows a marked change in behavior upon crossing the upper critical dimensionality d_c (see the upper left panel of Fig. 3.3), being zero above it, this is not the case for $a_{\rm co}$. Analogous consideration holds for the other quantities discussed further below, when compared with the corresponding ones at criticality. Heuristically this might be expected based on the fact that — as in the case of classical systems [150, 197] — coarsening for $r < r_c$ is generally driven by a different mechanism compared to the one controlling the behavior at $r = r_c$, which is related to critical fluctuations and which is therefore affected upon crossing d_c (see Sec. 3.2.3). As a peculiar feature of $a_{\rm co}$, we note that it vanishes for $d = 3$.

As argued above and demonstrated by the curves in the upper left panel of Fig. 3.2, $G_K(k = 0, t, t)$ grows algebraically both at $r = r_c$ and for $r < r_c$, in the latter case as $\sim t^{\gamma_{\rm co}}$. The upper right panel of Fig. 3.4 shows the estimates of $\gamma_{\rm co}$ obtained by fitting the numerical data for $G_K(k = 0, t, t)$, as a function of the dimensionality d. The dashed line corresponds to the theoretical prediction $\gamma_{\rm co} = 1 + 2\alpha_{\rm co}$ with $\alpha_{\rm co}$ given by Eq. (3.42). As it was done in Fig. 3.3 for $r = r_c$, the lower panels of Fig. 3.4 consider $G_R(k, t, t')$ at $k = 0$. By assuming that the scaling behavior in Eq. (3.26) carries over to $r < r_c$, $|G_R(k, t, t')/t|$ is fitted by $C_{\rm co}\Phi_{\alpha_{\rm co}}(t'/t)$ (with Φ_α given in Eq. (3.44)) in order to extract $\alpha_{\rm co}$ (lower left panel) or to estimate $C_{\rm co}$ once $\alpha_{\rm co}$ has been fixed to its theoretical value in Eq. (3.42). In both panels the corresponding theoretical predictions are reported as dashed lines and, as in the case of the upper panels, the agreement with the numerical data is excellent, with a hint of slight deviations upon approaching the lower critical dimensionality $d = 2$ of this model.

As we mentioned at the end of Sec. 3.2.1, the exponent $\gamma_{\rm co} = 1 + 2\alpha_{\rm co}$ discussed here in connection to the scaling of $G_K(k, t, t)$ (see Eqs. (3.28) and (3.29)) is the same as the exponent γ introduced in Ref. [171] in order to characterize the scaling behavior of $\rho_k(t)$. The values of γ which was numerically determined in Ref. [171] for a quench below the critical point in $d = 3$ and 4, i.e., $\gamma = 2$ and 3 are in perfect agreement with our numerical estimates and analytical predictions reported in the upper right

panel of Fig. 3.4.

3.2.3 Coarsening

The numerical data presented in Sec. 3.2.2 clearly show that the non-equilibrium dynamics of the system after a quench to $r < r_c$ features an emerging scaling behavior which we partly rationalized in Sec. 3.1 and which is characterized by scaling exponents depending on the spatial dimensionality d. As anticipated, these scaling forms are expected to be related to the coarsening dynamics [169, 170], analogously to what happens in classical systems after a quench below the critical temperature [150, 151, 197]. In fact, when a classical system prepared in a disordered state is quenched below the critical temperature, the global symmetry cannot be dynamically broken and, consequently, the order parameter remains zero in average. Nevertheless, symmetry is broken locally by the creation of domains within which the order parameter φ takes the value characterizing one of the possible different and competing phases. The average linear extension $L(t)$ of the ordered domains increases with time t, until a specific domain possibly prevails over the others, establishing the equilibrium state. However, because of such competition, $L(t)$ grows algebraically as $L(t) \propto t^{1/z_c}$, where $z_c > 0$ is an exponent depending on the universal properties of the model, and equilibrium is reached only in an infinite time. Consequently, this lack of an intrinsic length scale in the system affects the equal-time two-point correlation function

$$C(\mathbf{r}, t) = \langle \varphi(\mathbf{x} + \mathbf{r}, t)\varphi(\mathbf{x}, t)\rangle, \tag{3.46}$$

and its spatial Fourier transform $C(k, t)$, which, according to the scaling hypothesis [150], are expected to display the scaling forms

$$C(\mathbf{r}, t) = f(r/L(t)) \text{ and } C(k, t) = [L(t)]^d \widetilde{f}(kL(t)), \tag{3.47}$$

where d is the spatial dimensionality and $\widetilde{f}(x)$ the Fourier transform of $f(x)$.

The scaling forms for a quench below r_c highlighted in Sec. 3.2.2 *do not* satisfy the scaling hypothesis (3.47), as it was noticed for $d = 3$ in Refs. [169, 170]. In fact, the Keldysh Green's function at equal times $G_K(k, t, t)$ — which corresponds to the correlation function $C(k, t)$ mentioned above — can be written as a scaling form by using Eqs. (3.31) and (3.42), which reads:

$$G_K(k, t, t) = [L(t)]^{\gamma_{co}} \mathcal{G}_d(kL(t)), \tag{3.48}$$

where $\mathcal{G}_d(x)$ is the scaling function, $L(t) \propto t$ (i.e., the coarsening exponent z_c takes the value $z_c = 1$) and $\gamma_{co} = d - 1$. As this γ_{co} differs from d, Eq. (3.48) violates the scaling form (3.47) in all spatial dimensions.

3.3 Concluding remarks

In this Chapter we provided a complete characterization of the dynamical scaling which emerges after a deep quench of an *isolated* quantum vector model with $O(N)$ symmetry at or below the point of its dynamical phase transition. The lack of intrinsic time and length scales is responsible for the occurrence of *aging* phenomena similar to the ones observed in non-equilibrium classical systems [119, 146] or, more recently, in isolated [2] quantum many body systems. While previous investigations

of this phenomenon were based on a perturbative, dimensional expansion around the upper critical dimensionality $d_c = 4$ of the model [2], here we carry out our analysis within the exactly solvable (non-perturbative) limit $N \to \infty$, which allows us to obtain exact results for scaling exponents and scaling functions of the relevant dynamical correlations, depending on the dimensionality d of the model. We find that the value of the pre-quench spatial correlation length (assumed to be small) controls the microscopic time t_Λ after which the aging behavior emerges: in addition, it acts as an effective temperature for the dynamics after the quench, which, inter alia, determines a shift of the upper critical dimensionality d_c of the model, as it occurs in equilibrium quantum systems at finite temperature [179,186]. Moreover, we provide evidence of the emergence of a dynamic scaling behavior for quenches below r_c, associated with coarsening, which we characterized numerically and analytically by studying the dependence of the relevant exponents on the spatial dimensionality d of the system.

The exactly solvable model considered here provides a prototypical example of a dynamical phase transition (DPT) and of the associated aging occurring in a non-thermal stationary state. This state is expected to become unstable in systems with finite N, when the non-integrable terms of the Hamiltonian become relevant, causing thermalization. Nonetheless, this DPT might be still realized in the prethermal stage of the relaxation of actual quantum systems evolving in isolation from the surrounding environment [25, 101–103, 105–108, 189, 198–200]. The latter are nowadays rather easily realized in trapped ultracold atoms, the behavior of which can be analyzed with remarkable spatial and temporal resolution [19,20,201–206]. In general, physical systems which can be described by some effective Hamiltonian with $O(N)$ symmetry include experimental realizations with ultra-cold atoms of the Bose-Hubbard model [201–203] (corresponding to $N = 2$) and one-dimensional tunnel-coupled condensates [189,207] ($N = 1$). In passing, we mention that an alternative and promising experimental realization of these models currently under investigation [208] is based on fluids of light propagating in non-linear optical media (see Chapter 10), which is expected to be ready for testing in the near future.

At least in principle, the universal dynamic scaling behavior emerging after a sudden quench which is highlighted in the present Chapter can be experimentally studied by determining directly the two-time linear response and correlation functions of the system. Alternatively, one can exploit the statistics of excitations produced after a (double) quench, as proposed in Ref. [171]. In fact, the n-th cumulant $C_n(t)$ of the corresponding distribution was shown to grow as a function of the time t elapsed since the quench, with a behavior which may saturate, grow logarithmically or algebraically, depending on n, d and on whether the quench occurs above, at, or below criticality. In particular, it was shown [171] that the increase in time of $C_n(t)$ is proportional to the integral over $\mathbf{k}$ of the n-th power of the quantity $\rho_k(t)$ related to the number of excitations, which we briefly discussed in the last paragraph of Sec. 3.2.1. In turn, at long times, the leading growth of $\rho_k(t)$ is the same as the one of $|f_{\mathbf{k}}(t)|^2$ (see the definition of $\rho_k(t)$ in Ref. [171]), i.e., of $iG_K(k,t,t)$ (see Eq. (3.10) here). As a result, a simple comparison with Eqs. (3.28) and (3.29) yields

$$C_n(t) \propto \int \mathrm{d}^d k \, [iG_K(k,t,t)]^n \propto t^{n(1+2\alpha)-d}, \tag{3.49}$$

for a quench to the critical point; for a quench below it, instead, one finds the same expression with α replaced by α_{co}, i.e.,

$$C_n(t) \propto \int \mathrm{d}^d k \, [iG_K(k,t,t)]^n \propto t^{n(1+2\alpha_{\mathrm{co}})-d}, \tag{3.50}$$

where the values of the exponents α and $\alpha_{\rm co}$ are given in Eqs. (3.38), (3.39), and (3.42). As a result, a measure of the statistics of the number of excitations for a quench would provide direct information on the aging and coarsening properties of the system.

The quantum aging and coarsening discussed in this Chapter enrich the list of mechanisms underlying the scale-invariant non-thermal fixed points (NTFP) [137, 209, 210], which have been so far interpreted in terms of quantum turbulence [138,139,211] and dynamics of topological defects [212,213]. The extent to which these mechanisms are interconnected and combined in the dynamics of physical systems represents an intriguing yet challenging question for future investigations.

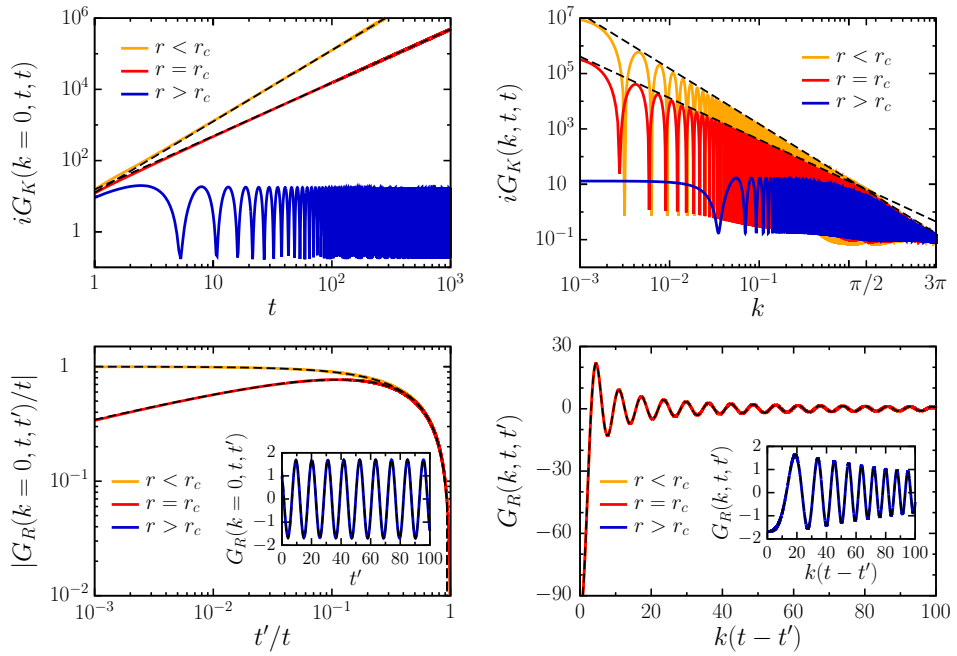

Figure 3.2: Keldysh and retarded Green's functions G_K and G_R, respectively. Upper left panel: $G_K(k,t,t)$ at $k = 0$ and equal times as a function of time t, for r below (uppermost curve), at (intermediate curve), and above (lowermost curve) the critical value r_c. The dashed lines superimposed to the curves for $r = r_c$ and $r < r_c$ are proportional to $t^{3/2}$ and t^2, respectively. Upper right panel: $G_K(k,t,t)$ at fixed equal times $t = 10^3$ as a function of momentum k after a quench with r below (yellow, uppermost line), at (red, intermediate line) and above (blue, lowermost line) the critical value r_c. The dashed lines superimposed on the curves for $r = r_c$ and $r < r_c$ are proportional to $k^{-3/2}$ and k^{-2}, respectively. Lower left panel, main plot: retarded Green's function $|G_R(k,t,t')/t|$ for $k = 0$ and $t = 2 \times 10^3$ as a function of t'/t for quenches of r at (lower curve) and below (upper curve) the critical value r_c. The black dashed lines superimposed on the curves for $r = r_c$ and $r < r_c$ correspond to the theoretical predictions $2\Phi_{1/4}(t'/t)$ (see Eq. (3.44)) and $\Phi_{1/2}(t'/t)$, respectively. Inset: retarded Green's function $G_R(k,t,t')$ for $k = 0$ and $t = 2 \times 10^3$ as a function of t' for quenches of r above the critical value r_c. The black dashed line corresponds to the prediction in Eq. (3.27) with $k \to \sqrt{r^*}$ (see the main text) and $r^* \simeq 0.34$. Lower right panel: retarded Green's function $G_R(k,t,t')$ as a function of $k(t-t')$ for $t = 2 \times 10^3$, $t' = 1.9 \times 10^3$ and r below (main plot, yellow, superimposed on the red one), at (main plot, red, superimposed on the yellow one) and above (inset, blue, solid curve) the critical value r_c. In the main plot, the two curves are indistinguishable from the superimposed dashed line, which corresponds to the theoretical prediction in Eq. (3.27). In the inset, the curve is indistinguishable from the superimposed dashed line which corresponds to Eqs. (3.27) and (3.45) with $r^* \simeq 0.34$. In all the panels of this figure, the spatial dimensionality is fixed to $d = 3$, $\Omega_0^2 = 10^2$, $u \simeq 47$, and a Gaussian cut-off is used with $\Lambda = \pi/2$.

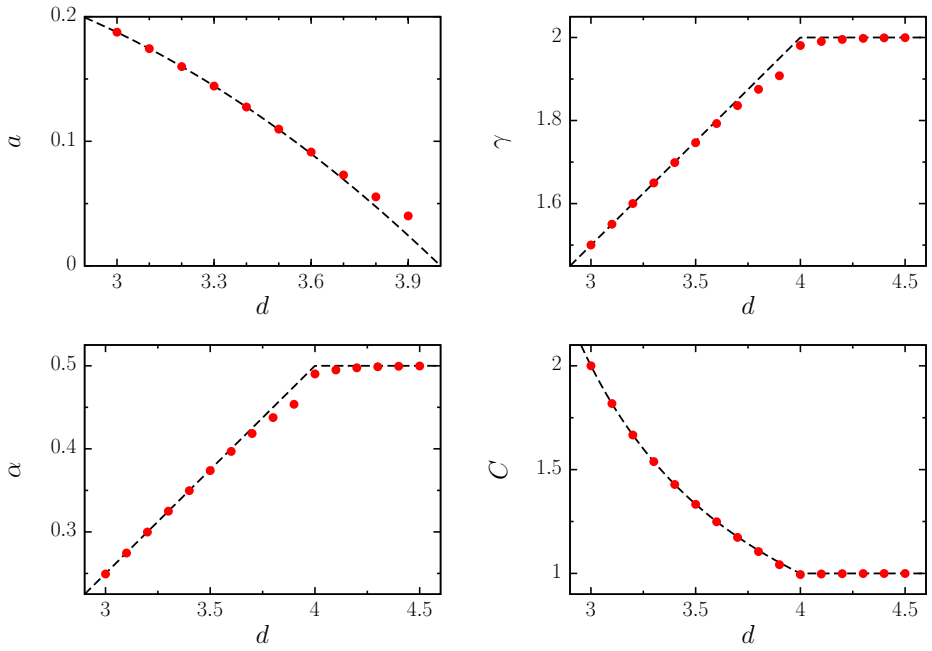

Figure 3.3: Numerical values (symbols) of the exponents γ, and α and prefactors a and C as functions of the spatial dimensionality d for a quench at the critical point. Upper left panel: coefficient a of the effective parameter $r_{\rm eff}(t)$ computed numerically compared with the theoretical value $a = d(1-d/4)/4$ (dashed line). Upper right panel: exponent γ obtained by fitting $iG_K(k=0,t,t)$ with an algebraic law $\propto t^{\gamma}$; the dashed line indicates the analytical value $\gamma = d/2$ for $d < 4$ and $\gamma = 2$ for $d > 4$. Lower left panel: exponent α obtained by fitting $|G_R(k=0, t=2\times 10^3, t')/t|$ with $C\,\Phi_\alpha(t'/t)$, see Eq. (3.44); the dashed line represents the theoretical value $\alpha = (d-2)/4$ for $d < 4$ and $\alpha = 1/2$ for $d > 4$. Lower right panel: prefactor C of $G_R(k=0,t,t')$ as a function of the dimension d, obtained by fitting $|G_R(k=0, t=2\times 10^3, t')/t|$ with $C\Phi_\alpha(t'/t)$, with α given by the theoretical values reported above; the dashed line represents the theoretical prediction for $C = 2/(d-2)$ for $d < 4$ and $C = 1$ for $d \geq 4$ (see Eq. (3.26)). The numerical data presented in this figure have been obtained with a Gaussian cut-off function with $\Lambda = \pi/2$ and $\Omega_0^2 = 10^4$, while for each point a different (inconsequential) value of u has been used. The statistical error bars on the numerical points are smaller than the symbol size.

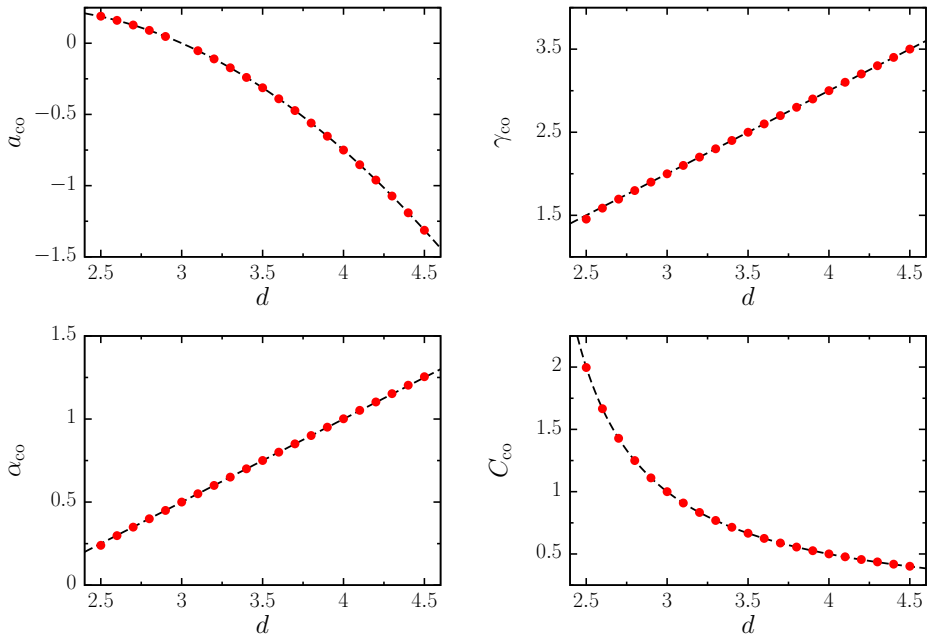

Figure 3.4: Numerical values (symbols) of exponents $\gamma_{\rm co}$, and $\alpha_{\rm co}$ and prefactors $a_{\rm co}$ and $C_{\rm co}$ as functions of dimension d for a quench below the critical point. Upper left panel: numerical estimates for the coefficient $a_{\rm co}$ of the algebraic decay of the effective parameter $r_{\rm eff}(t) \simeq a_{\rm co} t^{-2}$ as a function of dimension d, compared with the theoretical value $a_{\rm co} = (3-d)(d-1)/4$ (dashed line) . Upper right panel: numerical estimates of the exponent $\gamma_{\rm co}$ obtained by fitting $iG_K(k=0,t,t)$ with $t^{\gamma_{\rm co}}$; the dashed line represents the analytical prediction $\gamma_{\rm co} = d-1$. Lower left panel: exponent $\alpha_{\rm co}$ obtained by fitting $|G_R(k=0, t=2\times 10^3, t')/t|$ as $C_{\rm co}\,\Phi_{\alpha_{\rm co}}(t'/t)$ (with $\Phi_\alpha(x)$ given in Eq. (3.44)); the dashed line represents the theoretical value $\alpha_{\rm co} = (d-2)/2$. Lower right panel: prefactor $C_{\rm co}$ of $G_R(k,t,t')$ as a function of the dimension d, obtained by fitting $|G_R(k=0, t=2\times 10^3, t')/t|$ as $C_{\rm co}\Phi_{\alpha_{\rm c0}}(t'/t)$, with $\alpha_{\rm co}$ fixed to its corresponding theoretical value (see Eq. (3.42)); the dashed line represents the theoretical value $C_{\rm co} = 1/(d-2)$. The numerical data presented in this figure refer to a system with $\Omega_0^2 = 10^4$, $r=-3$, and a Gaussian cut-off function with $\Lambda = \pi/2$; for each point a different (inconsequential) value of u has been used. The statistical error bars on the numerical points are smaller than the symbol size.

Chapter 4

DPT of $O(N)$-model: Renormalization group

Abstract

We investigate the effects of fluctuations on the dynamics of an isolated quantum system represented by a ϕ^4 field theory with $O(N)$ symmetry after a quench in $d > 2$ spatial dimensions. A perturbative renormalization-group approach involving a dimensional expansion in $\epsilon = 4-d$ is employed in order to study the evolution within a prethermal regime controlled by elastic dephasing. In particular, we focus on a quench from a disordered initial state to the critical point, which introduces an effective temporal boundary in the evolution. At this boundary, the relevant fields acquire an anomalous scaling dimension, while the evolution of both the order parameter and its correlation and response functions display universal aging. Since the relevant excitations propagate ballistically, a light cone in real space emerges. At longer times, the onset of inelastic scattering appears as secularly growing self-generated dissipation in the effective Keldysh field theory, with the strength of the dissipative vertices providing an estimate for the time needed to leave the prethermal regime.

4.1 Keldysh action for a quench

In this chapter we show how the interaction modifies the dynamics after a quench compared to those of the Gaussian model discussed in Chapter 2, for general values of N (while in Chapter 3 only the specific value $N \to \infty$ was considered). To this end, we use perturbation theory and renormalization-group techniques, the formulation of which is particularly simple within the Keldysh functional formalism [214, 215]. For later convenience, in this section we briefly recall how a quench can be describe within it.

For simplicity, we assume that the system is prepared in a thermal state described by the density matrix ρ_0 introduced after Eq. (2.10), where now H_0 is a generic pre-quench Hamiltonian, not necessarily quadratic. After the quench, the dynamics of the system is ruled by the post-quench Hamiltonian

H obtained from H_0 by changing some parameters at time $t = 0$. Accordingly, the expectation value of any operator $\mathcal{O}$ can be expressed in the following functional form [215]:

$$\langle \mathcal{O}(t) \rangle = \int \mathcal{D}\boldsymbol{\phi}\, \mathcal{O}[\boldsymbol{\phi}_f(t)]\, \mathrm{e}^{iS_K}, \tag{4.1}$$

where $S_K = S_K[\boldsymbol{\phi}_I, \boldsymbol{\phi}_f, \boldsymbol{\phi}_b]$ is the Keldysh action, which is a functional of the fields $\boldsymbol{\phi}_f$, $\boldsymbol{\phi}_b$ and $\boldsymbol{\phi}_I$, referred to, respectively, as *forward*, *backward* and *initial* fields; $\mathcal{D}\boldsymbol{\phi} \equiv D[\boldsymbol{\phi}_f, \boldsymbol{\phi}_b, \boldsymbol{\phi}_I]$ is the functional measure. Note that the r.h.s. of Eq. (4.1) involves N-component vector fields $\boldsymbol{\phi}_{f,b,I}$, with $\boldsymbol{\phi}_f$ replacing the original operator field $\boldsymbol{\phi}$ in the formal expression $\mathcal{O}[\boldsymbol{\phi}]$ of $\mathcal{O}$. The action $S_K = S_s + S_b$ consists of the two parts S_s and S_b corresponding, respectively, to the initial state and the post-quench dynamics, where

$$S_s = i \int_0^\beta \mathrm{d}\tau\, \mathcal{L}_0^E(\boldsymbol{\phi}_I), \tag{4.2a}$$

$$S_b = \int_0^\infty \mathrm{d}\tau \left[\mathcal{L}(\boldsymbol{\phi}_f) - \mathcal{L}(\boldsymbol{\phi}_b)\right], \tag{4.2b}$$

where $\mathcal{L}(\boldsymbol{\phi})$ is the Lagrangian associated with the Hamiltonian (2.1), i.e.,

$$\mathcal{L}(\boldsymbol{\phi}) = \int_{\mathbf{x}} \left[\frac{1}{2}\dot{\boldsymbol{\phi}}^2 - \frac{1}{2}(\nabla\boldsymbol{\phi})^2 - \frac{r}{2}\boldsymbol{\phi}^2 - \frac{u}{4!N}\left(\boldsymbol{\phi}^2\right)^2\right], \tag{4.3}$$

while $\mathcal{L}_0^E(\boldsymbol{\phi})$ is the Euclidean Lagrangian associated with the pre-quench Hamiltonian, namely

$$\mathcal{L}_0^E(\boldsymbol{\phi}) = \int_{\mathbf{x}} \left[\frac{1}{2}\dot{\boldsymbol{\phi}}^2 + \frac{1}{2}(\nabla\boldsymbol{\phi})^2 + \frac{\Omega_0^2}{2}\boldsymbol{\phi}^2\right]. \tag{4.4}$$

In order to simplify the notation, hereafter the spatial and temporal dependence of the fields is not explicitly indicated. The fields $\boldsymbol{\phi}_f$, $\boldsymbol{\phi}_b$ and $\boldsymbol{\phi}_I$ in Eq. (4.1) are not actually independent but are related by the boundary conditions

$$\begin{cases} \boldsymbol{\phi}_f(t) = \boldsymbol{\phi}_b(t), \\ \boldsymbol{\phi}_b(0) = \boldsymbol{\phi}_I(0), \\ \boldsymbol{\phi}_f(0) = \boldsymbol{\phi}_I(\beta). \end{cases} \tag{4.5}$$

Note that if the observable $\mathcal{O}$ in Eq. (4.1) is calculated at $t = 0^-$, then these boundary conditions reduce to the periodic one $\boldsymbol{\phi}_I(0) = \boldsymbol{\phi}_I(\beta)$ usually encountered in a Matsubara path-integral [214]. The functional representation in Eqs. (4.1), (4.2a), and (4.2b) correspond to the Schwinger-Keldysh contour [215]: the usual forward-backward branches of the contour of integration are supplemented by an initial branch in imaginary time which appears as a consequence of the initial density matrix ρ_0 represented by S_s in Eq. (4.2a). The actions S_s and S_b are referred to as *surface* and *bulk* action, respectively, for a reason which will become clear further below. It is convenient to express the forward and backward fields $\boldsymbol{\phi}_f$ and $\boldsymbol{\phi}_b$, respectively, in the so-called retarded-advanced-Keldysh basis [215] via $\boldsymbol{\phi}_f = (\boldsymbol{\phi}_c + \boldsymbol{\phi}_q)/\sqrt{2}$ and $\boldsymbol{\phi}_b = (\boldsymbol{\phi}_c - \boldsymbol{\phi}_q)/\sqrt{2}$, where the fields $\boldsymbol{\phi}_c$ and $\boldsymbol{\phi}_q$ are referred to as

classical and *quantum* fields, respectively. In these terms, the retarded and Keldysh Green's functions in Eqs. (2.13a) and (2.13b) read [215]

$$iG_R(|\mathbf{x}-\mathbf{x}'|,t,t') = \langle \phi_c(\mathbf{x},t)\phi_q(\mathbf{x}',t')\rangle, \tag{4.6}$$

$$iG_K(|\mathbf{x}-\mathbf{x}'|,t,t') = \langle \phi_c(\mathbf{x},t)\phi_c(\mathbf{x}',t')\rangle, \tag{4.7}$$

where, as before, we do not indicate the indices of the field components of $\boldsymbol{\phi}_{c,q}$ because the $O(N)$ symmetry forces them to be equal for the fields inside the expectation values. The expression of $G_{R/K}$ given in Eqs. (2.15b) and (2.15a) can alternatively be calculated within the functional formalism introduced above, as we discuss in App. 4.A. For the quench protocol described in Sec. 2.1, S_s and S_b can be written as

$$S_s = i\int_{\mathbf{x}}\int_0^{\beta} \mathrm{d}\tau\, \left[\frac{1}{2}(\dot{\boldsymbol{\phi}}_I)^2 + \frac{1}{2}(\nabla\boldsymbol{\phi}_I)^2 + \frac{\Omega_0^2}{2}\boldsymbol{\phi}_I^2\right], \tag{4.8}$$

$$S_b = \int_{\mathbf{x}}\int_0^{+\infty} \mathrm{d}t\, \left[\dot{\boldsymbol{\phi}}_q\cdot\dot{\boldsymbol{\phi}}_c - (\nabla\boldsymbol{\phi}_q)\cdot(\nabla\boldsymbol{\phi}_c) - r\,\boldsymbol{\phi}_q\cdot\boldsymbol{\phi}_c - \frac{u_c}{12N}(\boldsymbol{\phi}_q\cdot\boldsymbol{\phi}_c)\boldsymbol{\phi}_c^2 - \frac{u_q}{12N}(\boldsymbol{\phi}_c\cdot\boldsymbol{\phi}_q)\boldsymbol{\phi}_q^2\right]. \tag{4.9}$$

Note that the coupling constant u in Eq. (2.1) is indicated in Eq. (4.9) as $u_{c,q}$: although, in principle, $u_c = u_q = u$, the couplings of the terms $(\boldsymbol{\phi}_q\cdot\boldsymbol{\phi}_c)\boldsymbol{\phi}_c^2$ and $(\boldsymbol{\phi}_c\cdot\boldsymbol{\phi}_q)\boldsymbol{\phi}_q^2$ deriving from $\left(\boldsymbol{\phi}^2\right)^2$ may behave differently under RG and therefore we denote them with different symbols. Given that S_s is Gaussian, the functional integral in Eq. (4.1) with an observable $\mathcal{O}(t)$ at time $t \neq 0$ can be simplified [216] by calculating the integral over $\boldsymbol{\phi}_I$. For convenience, we first rewrite Eq. (4.8) in momentum space, where it reads

$$S_s = \frac{i}{2}\int_{\mathbf{k}}\int_0^{\beta} \mathrm{d}\tau\, \left(\dot{\boldsymbol{\phi}}_I^2 + \omega_{0k}^2\boldsymbol{\phi}_I^2\right), \tag{4.10}$$

with ω_{0k} given in Eq. (2.12). In order to integrate out $\boldsymbol{\phi}_I$, we solve the saddle-point equation with the boundary conditions $\boldsymbol{\phi}_I(\beta) = \boldsymbol{\phi}_f(0)$ and $\boldsymbol{\phi}_I(0) = \boldsymbol{\phi}_b(0)$, we insert the solution back in S_s and then we perform the integral in τ. The resulting action is

$$S_s = i\int_{\mathbf{k}} \frac{\omega_{0k}}{2}\left[\boldsymbol{\phi}_{0c}^2\tanh(\beta\omega_{0k}/2) + \boldsymbol{\phi}_{0q}^2\coth(\beta\omega_{0k}/2)\right], \tag{4.11}$$

where $\boldsymbol{\phi}_{0c} \equiv \boldsymbol{\phi}_c(t=0)$ and $\boldsymbol{\phi}_{0q} \equiv \boldsymbol{\phi}_q(t=0)$. Accordingly, the initial action S_s can be regarded as a functional which weights the value of $\boldsymbol{\phi}_{c,q}$ at $t=0$, and therefore it determines the initial conditions for the subsequent evolution. In order to show this, e.g., for $T=0$, one can consider the saddle-point equations for the action $S_K = S_b + S_s$, with S_b and S_s given in Eqs. (4.9) and (4.11), respectively, finding

$$i\,\omega_{0k}\boldsymbol{\phi}_c(0) = \dot{\boldsymbol{\phi}}_q(0) \quad \text{and} \quad i\,\omega_{0k}\boldsymbol{\phi}_q(0) = \dot{\boldsymbol{\phi}}_c(0), \tag{4.12}$$

where the time derivatives on the r.h.s. of these equations come from the integration by parts in the bulk action S_b. Note that in the generalized boundary conditions (4.12), classical and quantum fields are coupled. In addition, for $\omega_{0k} \to +\infty$, Dirichlet boundary conditions are effectively recovered. Since the quench induces a breaking of time-translational invariance, the Keldysh action in Eq. (4.1) can be formally regarded as the action of a semi-infinite system [193, 194, 217, 218] in $d+1$ dimensions in which the bulk is described by S_b, the d-dimensional surface by S_s, while t measures the distance from that boundary.

4.1.1 Keldysh Green's function as a propagation of the initial state

In the absence of an initial condition (e.g., assuming the quench to occur at $t = -\infty$), the bulk action S_b in Eq. (4.9) is characterized by having only the retarded Green's function G_{0R} as the Gaussian propagator. This can be readily seen from the absence of a term $\boldsymbol{\phi}_q^2$ in the bulk action (4.9) when $u_{q,c} = 0$. (In passing we note that this is the reason why an infinitesimally small term $\propto \boldsymbol{\phi}_q^2$ which satisfies the fluctuation-dissipation theorem [215] has to be added to this action in order to recover the equilibrium Keldysh Green's function G_K.) In the presence of the quench at $t = 0$, instead, correlations appear already in the Gaussian theory because of the "forward propagation" of those which are present in the initial state. In fact, the Keldysh Green's function can be generically written as

$$iG_K(1,2) = \langle \phi_c(1)\phi_c(2)\, \mathrm{e}^{-\frac{1}{2}\int_{\mathbf{k}}\left(\omega_{0k}\phi_{0q}^2 - \dot{\phi}_{0q}^2/\omega_{0k}\right)} \rangle_b, \tag{4.13}$$

where $n \equiv (\mathbf{k}_n, t_n)$ and $\langle \dots \rangle_b$ denotes the average taken on the bulk action only, i.e., without the quench. This expression follows from Eq. (4.1), while the argument of the exponential from Eqs. (4.11) and (4.12), where, for the purpose of illustration, we assumed an initial state with $\beta^{-1} = 0$. Within the Gaussian approximation $u_{c,q} = 0$ and in the deep-quench limit the second term in the exponential of Eq. (4.13) is negligible compared to the first one, such that this relation takes the simpler form

$$iG_K(k,t,t') = \Omega_0 G_R(k,t,0) G_R(k,t',0), \tag{4.14}$$

which follows from applying Wick's theorem and which suggests that, indeed, G_K can be simply regarded as the forward propagation in time via G_R of the correlations in the initial state. Actually, one can show from the Dyson equations [215] of the theory (see App. 4.B) that Eq. (4.14) holds beyond the Gaussian approximation, provided that the Keldysh component of the self-energy vanishes. In the present case, however, such a component is generated in the perturbative expansion at two loops via the sunset diagram and therefore Eq. (4.14) applies only up to one loop. The physical interpretation of this fact is that, from the RG point of view, the non-vanishing diagrams contributing to the Keldysh Green's function G_K also generate an interaction vertex $\propto \boldsymbol{\phi}_q^2$ in the bulk action S_b, which are then responsible for the emergence of a G_K within the bulk. More generally, such a vertex in the bulk is also expected to destabilize the pre-thermal state and eventually induce thermalization within the system [184, 219, 220]: in this sense, the validity of Eq. (4.14) can be regarded as the hallmark of the pre-thermal regime. Note that in the limit $N \to \infty$ of the present model, the Keldysh component of the self-energy vanishes to all orders in perturbation theory, which renders the previous relation an exact identity [1].

4.2 Perturbation theory

In this Section we consider the perturbative effect of the quenched interaction on the Gaussian theory described in Chapter. 2. The interaction $\propto (\boldsymbol{\phi}^2)^2$ in the post-quench Hamiltonian (2.1) generates the two vertices $u_c(\boldsymbol{\phi}_q \cdot \boldsymbol{\phi}_c)\boldsymbol{\phi}_c^2$ and $u_q(\boldsymbol{\phi}_c \cdot \boldsymbol{\phi}_q)\boldsymbol{\phi}_q^2$ in the action (4.9) of the Keldysh formalism, which we refer to as *classical* and *quantum vertices*, respectively. Though, in principle, $u_{c,q} = u$ we allow $u_c \neq u_q$ in view of the possibility that these two couplings flow differently under RG, see Sec. 4.4. At one loop, these two vertices cause: (a) a renormalization of the post-quench parameter r, which, compared

to the Gaussian approximation, shifts its critical value to $r_c \neq 0$; (b) a logarithmic dependence of $G_{R/K}(k,t,t')$ on times t, t' and momenta k, suggesting the emergence of a corresponding algebraic behavior once the perturbative series is resummed. These effects are found in the deep-quench limit for $d = 4$, which is recognized to be the upper critical dimensionality of the system in Sec. 4.4. Although Eq. (4.14) applies to the one-loop calculation considered here, it is anyhow instructive to determine separately the correction to both G_R and G_K, which is done in Sec. 4.2.1. Based on these results, we analyze in Sec. 4.2.2 the momentum distribution, while in Sec. 4.2.3 we investigate the Green's functions in real space, highlighting the effects on the light cone which we discussed in Sec. 2.3.4 within the Gaussian approximation.

4.2.1 Green's function in momentum space

The one-loop corrections to $iG_{R/K}$ are due to the tadpole diagrams associated with the two interaction vertices. However, the absence of a Gaussian propagator of the form $\langle \phi_q \phi_q \rangle$ prevents the quantum vertex from contributing and therefore the only contribution is due to the classical vertex $2u_c(\boldsymbol{\phi}_q \cdot \boldsymbol{\phi}_c)\boldsymbol{\phi}_c^2/(4!N)$ via the tadpole:

$\mathcal{T}(t) =$ 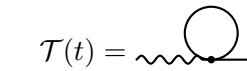 . (4.15)

Here and in the diagrams which follow, a wiggly line is associated to the field ϕ_q, while a normal one to the field ϕ_c. Accordingly, a Gaussian retarded Green's function corresponds to a line which starts normal and and becomes wiggly, and vice versa, while the Gaussian Keldysh Green's function is represented by a normal line. This tadpole involves the integral of $iG_{0K}(k,t,t)$ over the momentum k (corresponding to the closed normal line in the diagram), which has to be calculated with a suitable large-k cutoff Λ. In the case of a deep quench, the time-dependent tadpole $\mathcal{T}(t)$ can be written as

$$\mathcal{T}(t) = -i\frac{u_c(N+2)}{12N}\int \frac{\mathrm{d}^4k}{(2\pi)^4}\, f(\omega_k/\Lambda) iG_{0K}(k,t,t) \equiv -i[B_0 + B(t)], \tag{4.16}$$

where, by using Eq. (2.17b),

$$B_0 \equiv \frac{u_c(N+2)\Omega_0}{24N}\int \frac{\mathrm{d}^4k}{(2\pi)^4}\frac{1}{\omega_k^2} f(\omega_k/\Lambda) \tag{4.17}$$

and

$$B(t) \equiv -\frac{u_c(N+2)\Omega_0}{24N}\int \frac{\mathrm{d}^4k}{(2\pi)^4}\frac{\cos(2\omega_k t)}{\omega_k^2} f(\omega_k/\Lambda), \tag{4.18}$$

while the function $f(x)$ implements the ultra-violet cut-off as discussed in Sec. 2.3.4. In the following, we assume the convenient smooth function $f(x) = \mathrm{e}^{-x}$, which is preferable to a sharp cut-off $f(x) = \vartheta(1-x)$ as the former, contrary to the latter, does not produce spurious sub-leading oscillatory factors, which can mask the truly universal behaviour [1]. For simplicity, we focus below on the case in which the post-quench parameter r is tuned at the value $r = r_c$, such that any macroscopic length-scale is removed from the correlation functions, which therefore becomes self-similar. In this sense, r_c corresponds to a critical point where the system becomes scale invariant. As we expect r_c to be perturbatively small in the coupling constant u_c (at least within the dimensional expansion), one

can actually set $r = 0$ in the perturbative expression for the one-loop correction. Accordingly, from Eqs. (4.17) and (4.18), one finds

$$B_0 = 4\theta_N \Lambda^2, \qquad B(t) = \theta_N (2\Lambda)^2 \frac{(2\Lambda t)^2 - 1}{[1 + (2\Lambda t)^2]^2}, \tag{4.19}$$

where we introduced, for later convenience, the constant

$$\theta_N = \frac{1}{8\pi^2} \frac{N+2}{96N} \Omega_0 u_c. \tag{4.20}$$

While B_0 in Eq. (4.19) has no finite limit for $\Lambda \to \infty$ and therefore its specific value depends on the specific form of the cut-off function f in Eq. (4.17), $B(t)$ becomes independent of it for $\Lambda t \gg 1$, with

$$B(t \gg \Lambda^{-1}) \simeq \frac{\theta_N}{t^2}. \tag{4.21}$$

In order to determine the one-loop correction δG_R to G_R, the tadpole $\mathcal{T}(t)$ in Eq. (4.16) has to be integrated with two Gaussian retarded functions G_{0R}, i.e.,

$$\delta G_R(q,t,t') = \quad t \quad t'$$
$$= \int_0^\infty \mathrm{d}\tau \, G_{0R}(q,t,\tau) i\mathcal{T}(\tau) G_{0R}(q,\tau,t'). \tag{4.22}$$

Let us first discuss the contribution to δG_R due to the time-independent part B_0 of the tadpole $\mathcal{T}$, which generates an effective shift of the parameter r. In fact, this can be seen by reverting the argument, i.e., by considering the effect that a perturbatively small shift δr of the parameter r has on $G_R(q,t,t')$ for $t > t'$. Since δr couples to $-i\boldsymbol{\phi}_c \cdot \boldsymbol{\phi}_q$ in the exponential factor appearing in Eq. (4.1) (see also Eq. (4.9)) one has, up to first order in δr,

$$G_R(q,t,t')\big|_{r+\delta r} = G_R(q,t,t')\big|_r + \delta r \int_0^\infty \mathrm{d}\tau \; G_R(q,t,\tau)\big|_r \, G_R(q,\tau,t')\big|_r, \tag{4.23}$$

where G_R has been expressed as the expectation value in Eq. (4.6). Comparing Eq. (4.22) with Eq. (4.23) one can see that the contribution of B_0 is the same as that one of a shift δr of the parameter r, i.e.,

$$r \mapsto r + B_0 + \mathcal{O}(u^2). \tag{4.24}$$

Accordingly, the resulting critical value r_c of r becomes $r_c = -B_0 + \mathcal{O}(u^2)$.

We consider next the term containing the time-dependent part $B(\tau)$ of the tadpole $\mathcal{T}(\tau)$ in Eq. (4.22). Because of the causality of the retarded Green's functions G_{0R} in the integrand of this equation, the integration domain in τ runs from t' to t, where henceforth we assume $t > t'$. Within this domain, $B(\tau)$ is well approximated by Eq. (4.21) as soon as t, $t' \gg \Lambda^{-1}$ and, correspondingly, the integral can be easily calculated. Focussing on a quench to the critical point $r = r_c$, the correction δG_R to the retarded Green's function G_R beyond its Gaussian expression can be written as

$$\delta G_R(q,t,t') = -G_{0R}(q,t,t') \theta_N F_R(qt, qt'), \tag{4.25}$$

with the scaling function

$$F_R(x,y) = \frac{\sin(x+y)}{\sin(x-y)}[\mathrm{Ci}(2x) - \mathrm{Ci}(2y)] - \frac{\cos(x+y)}{\sin(x-y)}[\mathrm{Si}(2x) - \mathrm{Si}(2y)], \tag{4.26}$$

where the sine integral $\mathrm{Si}(x)$ and cosine integral $\mathrm{Ci}(x)$ are defined, respectively, as

$$\mathrm{Si}(x) = \int_0^x \mathrm{d}t\, \frac{\sin t}{t}, \quad \mathrm{Ci}(x) = -\int_x^\infty \mathrm{d}t\, \frac{\cos t}{t}. \tag{4.27}$$

The scaling function $F_R(x,y)$ is a consequence of the absence of length- and time-scales at the critical point $r = r_c$. At short times t, $t' \ll q^{-1}$, the expansion of the cosine integral $\mathrm{Ci}(x) \simeq \ln x$ renders a logarithmic term and, correspondingly, the leading order of Eq. (4.25) reads:

$$\delta G_R(q, t > t') = \theta_N\,(t + t')\ln(t/t'). \tag{4.28}$$

When these two times are well separated, i.e., $t' \ll t \ll q^{-1}$, the total retarded Green's function $G_R = G_{0R} + \delta G_R$ reads, to leading order,

$$G_R(q,t,t') = -t\left[1 - \theta_N\,\ln(t/t') + \mathcal{O}(u^2)\right], \tag{4.29}$$

where we used the fact that, at criticality, $G_{0R}(q,t,t') \simeq (t - t')$ for $t' < t \ll q^{-1}$, see Eq. (2.17a). Equation (4.29) suggests that the perturbative series can be resummed such that these logarithms result into an algebraic time dependence

$$G_R(q = 0, t \gg t') \simeq -t\left(t'/t\right)^{\theta_N}, \tag{4.30}$$

as is actually proven in Sec. 4.5.3 with the aid of the RG approach. In the analysis above we have assumed that both times t and t' involved in G_R are much longer than the microscopic time scale $\simeq \Lambda^{-1}$. In the opposite case in which the shorter time t' is at the "temporal boundary", i.e., $t' \ll \Lambda^{-1} \ll t$ or, equivalently, $t' = 0$, it turns out that G_R up to one loop (see App. 4.C)

$$G_R(q,t,0) \propto -t\left[1 - \theta_N\,\ln(\Lambda t)\right], \tag{4.31}$$

has a logarithmic dependence on Λt and therefore shows a formal divergence as Λ grows. This divergence can be regularized only by means of a renormalization, i.e., of a redefinition of the fields appearing in the surface action (see Sec. 4.5) which is responsible for the emergence of the algebraic scaling at small times suggested by Eq. (4.29).

Consider now the Keldysh Green's function G_K: the one-loop contributions to this function can be expressed in terms of the same tadpole $\mathcal{T}(t)$ as the one in Eq. (4.15) contributing to the retarded Green's function G_R, the only difference being in the final integrations. In particular, iG_K receives two contributions

$$\delta iG_K(q,t,t') = \quad$$

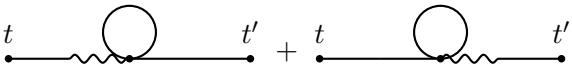

$$= \int_0^\infty \mathrm{d}\tau\, iG_{0R}(q,t,\tau)\mathcal{T}(\tau)iG_{0K}(q,\tau,t') + (t \leftrightarrow t'), \tag{4.32}$$

accordingly to the notation explained after Eq. (4.15). Taking into account the decomposition of $\mathcal{T}$ in Eq. (4.16) one recognizes, as in the case of G_R, that the term in $\delta i G_K$ which is proportional to B_0 is similar to the one which would be generated by a shift δr of the parameter r in G_{0K} and therefore it can be absorbed in a redefinition of this parameter as in Eq. (4.24).

The explicit calculation (reported in App. 4.D) of the most singular correction $\delta i G_K$ in Eq. (4.32) renders, to leading order in $q/\Lambda \ll 1$ and for t, $t' \gg \Lambda^{-1}$,

$$\delta i G_K(q,t,t') = i G_{0K}(q,t,t')\, \theta_N \left[2\ln(q/\Lambda) - F_K(qt, qt')\right], \tag{4.33}$$

where θ_N is given in Eq. (4.20), while $F_K(x,y)$ is a scaling function defined as

$$F_K(x,y) = \mathrm{Ci}(2x) + \mathrm{Ci}(2y). \tag{4.34}$$

Note that the first contribution on the r.h.s. of Eq. (4.33) contains a term which grows logarithmically as Λ increases. Differently from the case of the retarded Green's function [see Eq. (4.31)], the divergence for $\Lambda \to \infty$ occurs even for finite values of t and t'. This is not surprising, because G_K is proportional to a product of two retarded functions $G_R(t,0)$ with one vanishing time argument [see Eq. (4.14)], each of them carrying a logarithmic divergence, see Eq. (4.31). At short times t, $t' \ll q^{-1}$, the scaling function F_K in Eq. (4.33) reads $F_K(x \ll 1, y \ll 1) \simeq \ln(xy)$, with the logarithm coming from the series expansion of the cosine integral Ci for small arguments [see Eq. (4.27)]. Accordingly, the leading behaviour of the total Keldysh Green's function $G_K = G_{0K} + \delta G_K$ at short times is given by

$$i G_K(q,t,t') = i G_{0K}(q,t,t') \left[1 - \theta_N \ln(\Lambda^2 t t')\right]. \tag{4.35}$$

As for the retarded Green's function in Eq. (4.31), this expression suggests that the dependence on time beyond perturbation theory is actually algebraic, of the form

$$i G_K(q=0,t,t') \sim \left(tt'\right)^{1-\theta_N}, \tag{4.36}$$

where $G_{0K}(q,t,t')$ at criticality and for t, $t' \ll q^{-1}$ is given by Eq. (2.17b). The re-summation of the logarithms emerging in perturbation theory will be justified in Secs. 4.4 and 4.5 on the basis of the renormalization-group approach. In the opposite regime of long times $t \gg q^{-1}$ (or, alternatively, large wavevectors $t^{-1} \ll q \ll \Lambda$), the equal-time Keldysh Green's function $G_K(q,t,t)$ (and, consequently, the momentum density in Eq. (2.21)) acquires an anomalous dependence on the momentum q, as can be seen from the re-summation of the logarithm in Eq. (4.33):

$$i G_K(q \gg t^{-1}, t, t) \propto q^{-2+2\theta_N}, \tag{4.37}$$

where we took into account that $F_K(x \gg 1, y \gg 1) \simeq \sin(2x)/(2x) + \sin(2y)/(2y)$. Accordingly, at long times, the stationary part of the Keldysh Green's function acquires the anomalous scaling (4.37): however, this anomalous scaling is not related to the anomalous dimension of the field $\phi_c(t)$, as it happens in equilibrium systems where the renormalization of $\phi_c(t)$ induces the anomalous dimension η [121]. Instead, the reason for the scaling observed here turns out to be the renormalization of the initial quantum field ϕ_{0q}: this becomes clear by comparing Eq. (4.14) with Eq. (4.31). The initial-slip exponent θ_N thus characterizes not only the short-time critical behaviour of the Green's functions, but also their long-time form, in contrast to what happens in classical diffusive systems [119]. This fact can be regarded as a peculiarity of the prethermal state, which retains memory of the initial state as a consequence of the fact that the dynamics induced by the post-quench Hamiltonian is analytically solvable.

4.2.2 Momentum distribution

The one-loop correction to the Gaussian momentum density $\mathcal{N}_{0\mathbf{k}}$ in Eq. (2.22) can be straightforwardly calculated on the basis of the definition (2.21), taking into account the perturbative correction δG_K to the Keldysh Green's function G_K in Eq. (4.33). Accordingly, the total momentum density $\mathcal{N}_{\mathbf{k}} = \mathcal{N}_{0\mathbf{k}} + \delta\mathcal{N}_{\mathbf{k}}$ at small momenta $k \ll \Lambda$ and microscopically long times $t \gg \Lambda^{-1}$ reads

$$\mathcal{N}_{\mathbf{k}}(t) + \frac{1}{2} = \frac{\Omega_0}{4k}\left\{1 + 2\theta_N[\ln(k/\Lambda) - F_{\mathcal{N}}(kt)]\right\}, \tag{4.38}$$

where the scaling function $F_{\mathcal{N}}(x)$ is defined as

$$F_{\mathcal{N}}(x) = \mathrm{Ci}(2x) - \frac{\sin(2x)}{2x}, \tag{4.39}$$

with $F_{\mathcal{N}}(x \ll 1) \simeq \ln x$, while $F_{\mathcal{N}}(x \gg 1) \simeq -\cos(2x)/(2x)^2$. As discussed above in Sec. 4.2.1, the presence of logarithmic corrections suggests that the exact momentum density exhibits an algebraic dependence on momentum and/or time. In fact, after a resummation of the leading logarithms — motivated by the RG approach presented in Secs. 4.4 and 4.5 — the momentum density reads

$$\mathcal{N}_{\mathbf{k}}(t) + \frac{1}{2} \simeq \frac{\Omega_0}{4}\frac{1}{\Lambda}\left(\frac{\Lambda}{k}\right)^{1-2\theta_N}\mathcal{F}(kt), \tag{4.40}$$

where, consistently with the perturbative expansion, $\mathcal{F}(x) \equiv \exp[-2\theta_N F_{\mathcal{N}}(x)]$ is a scaling function such that (see Eq. (4.39))

$$\mathcal{F}(x) = \begin{cases} x^{-2\theta_N} & \text{for} \quad x \ll 1, \\ 1 & \text{for} \quad x \gg 1. \end{cases} \tag{4.41}$$

Accordingly, at a certain time t, the momentum distribution $\mathcal{N}_{\mathbf{k}}(t) + 1/2$ displays different algebraic behaviors as a function of k, i.e., the unperturbed one $\sim k^{-1}$ for $k \ll t^{-1}$ and the anomalous one $\sim k^{-1+2\theta_N}$ for $k \gg t^{-1}$, with the crossover occurring at $k \sim t^{-1}$ (see Fig. 4.1).

4.2.3 Green's functions in real space: light-cone dynamics

Based on the perturbative expressions reported in the previous section, we focus here on the Green's functions $G_{R,K}$ in real space and determine the corrections to their Gaussian expressions $G^0_{R,K}$ reported in Sec. 2.3.4. Up to the first order in the perturbative and dimensional expansion they can be written as,

$$G_{R,K} = G_{0R,K} + \delta G^{\delta r}_{R,K} + \delta G^{u}_{R,K} + \delta G^{\epsilon}_{R,K} + \mathcal{O}(u_c^2, \epsilon u_c, \epsilon^2) \tag{4.42}$$

where $\delta G^{\delta r}_{R,K}$ is the correction from the renormalization of the parameter r, i.e., from the constant part B_0 of the tadpole in Eq. (4.16), $\delta G^{u}_{R,K}$ contains the universal part coming from the time-dependent part $B(t)$ of the tadpole, while $\delta G^{\epsilon}_{R,K}$ comes from expanding $G_{0R,K}$ in Eq. (2.27) up to the first order in the dimensional expansion, with $\epsilon = 4 - d$. Some details of the calculation are given in App. 4.E. In what follows we assume that the systems is poised at the critical value $r = r_c$ discussed after Eq. (4.24), which cancels exactly the term $\delta G^{\delta r}_{R,K}$ in Eq. (4.42), therefore neglected below.

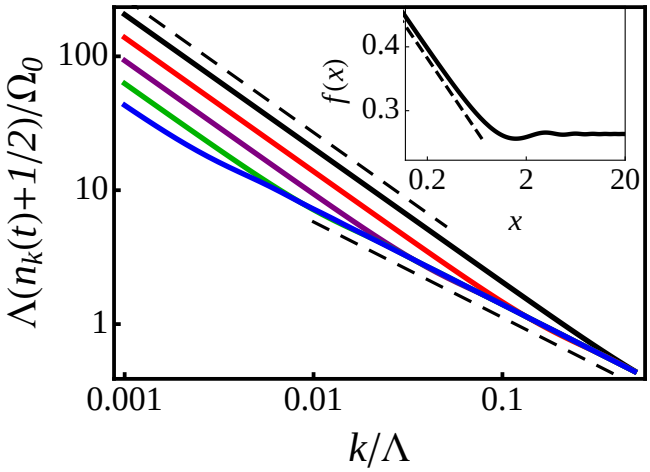

Figure 4.1: Momentum distribution n_k after the quench, as a function of $k/\Lambda \ll 1$ for $\Lambda t = 2$, 8, 32, 128, 512 (solid lines, from top to bottom). The algebraic short- and long-time behaviors of n_k are highlighted by the upper $\sim k^{-1}$ and lower $\sim k^{-1+2\theta}$ dashed lines, respectively. The inset shows a log-log plot of the scaling function $f(x)$, which approaches $\sim x^{-2\theta}$ for $x \lesssim 1$ (dashed line). With the purpose of highlighting the crossover, we set $\epsilon = 2$ in the perturbative expressions of these curves.

For the retarded Green's function we find, from Eq. (2.27), that corrections arise only on the light cone, namely (see App. 4.E)

$$\delta G_R^{\epsilon}(x = t - t', t, t') = G_{0R}(x = t - t', t, t') \frac{\epsilon}{2} \ln x \tag{4.43}$$

while, from the Fourier transform of Eq. (4.25) in hyperspherical coordinates, one finds

$$\delta G_R^{u}(x, t, t') = \frac{\theta_N}{4\pi^2 x^3} \int_0^{\Lambda x} \mathrm{d}y \, y J_1(y) \\ \times \left\{ \sin\left(\frac{y(t+t')}{x}\right) \left[\mathrm{Ci}\left(\frac{2ty}{x}\right) - \mathrm{Ci}\left(\frac{2t'y}{x}\right) \right] - \cos\left(\frac{y(t+t')}{x}\right) \left[\mathrm{Si}\left(\frac{2ty}{x}\right) - \mathrm{Si}\left(\frac{2t'y}{x}\right) \right] \right\}, \tag{4.44}$$

where θ_N is given by Eq. (4.20). For $t' \to 0$, a logarithmic singularity emerges in the previous expression due to $\mathrm{Ci}(2t'y/x)$ (while $\mathrm{Si}(2t'y/x)$ vanishes), which may be rewritten as:

$$G_R(x, t \gg t') \simeq G_{0R}(x, t \gg t') \left[1 + \theta_N \ln\left(\Lambda t'\right)\right]. \tag{4.45}$$

Combined with Eq. (4.43), Eq. (4.45) and the expression of G_{0R} given in Eq. (2.29b), this implies

$$G_R(x = t - t', \Lambda t' \gg 1) \propto t^{-3/2+\epsilon/2}, \tag{4.46a}$$

$$G_R(x = t - t', \Lambda t' \ll 1) \propto t^{-3/2+\epsilon/2} t'^{\theta_N}. \tag{4.46b}$$

Accordingly, the presence of interaction affects only the behaviour of G_R on the light cone $x = t - t'$, provided the initial perturbation was applied at a very short time t', modifying the Gaussian

scaling (2.29b) through an anomalous scaling with respect to t'. Note, however, that the scaling law $\propto t'^{\theta_N}$ is visible only for $t' \ll \Lambda^{-1}$, i.e., only before a non-universal microscopic time controlled by lattice effects, and therefore its presence is expected to be masked by non-universal contributions which dominate at such short time scales.

Turning to $G_K(x,t,t')$, for simplicity we focus here only on its behavior at equal times $t'=t$: this allows us to study the structure of G_K as far as the light cone at $x=t+t'=2t$ is concerned. Outside this light cone, i.e., for $2t \ll x$, iG_K vanishes as it is essentially determined by the pre-quench state which is characterized by very short-range correlation. Accordingly, we consider the expression of iG_K only on and inside the light cone. In particular, on the light cone we find (see App. 4.E for details)

$$\delta G_K^{\epsilon}(x=2t,t,t) = G_{0K}(x=2t,t,t)\frac{\epsilon}{2}\ln x, \tag{4.47}$$

while inside it (see App. 4.E),

$$\delta G_K^{\epsilon}(x \ll 2t,t,t) = G_{0K}(x \ll 2t,t,t)\,\epsilon \ln x. \tag{4.48}$$

The loop correction δG_K^u to $G_K(x,t,t)$ follows from the Fourier transform in hyperspherical coordinates of Eqs. (4.33) and (4.34), and takes the form

$$i\delta G_K^u(x,t,t) = 2\theta_N \frac{\Omega_0}{8\pi^2 x}\int_0^{\Lambda} \mathrm{d}q\, J_1(qx)\Big\{[1-\cos(2qt)]\,[-\mathrm{Ci}(2qt)+\ln(q/\Lambda)] + \sin(2qt)\mathrm{Si}(2qt)\Big\}. \tag{4.49}$$

From this expression it is straightforward to see that at long times, inside the light cone (see App. 4.E)

$$i\delta G_K^u(x \ll 2t,t,t) = -2\theta_N G_{0K}(x \ll 2t,t,t). \tag{4.50}$$

On the light cone $x=2t$, instead, there are no logarithmic corrections to δG_K^u, as shown in App. 4.E. Combining Eqs. (4.48) and Eq. (4.50) with G_{0K} in Eqs. (2.31c) we obtain the expression of the scaling behavior of G_K inside the light cone, while combining Eq. (4.47) with Eq. (2.31b), we obtain that one for the scaling on the light cone. The corresponding final expressions are (see also Eq. (2.31a)):

$$iG_K(x \gg 2t) \simeq 0, \tag{4.51a}$$

$$iG_K(x=2t) \simeq t^{-3/2+\epsilon/2}, \tag{4.51b}$$

$$iG_K(x \ll 2t) \simeq x^{-2+\epsilon-2\theta_N}. \tag{4.51c}$$

In summary, interactions modify the correlation function $G_K(x,t,t)$ as follows: on the light cone $x=2t$, G_K still decays $\propto 1/x^{(d-1)/2}$ upon increasing x, as in the Gaussian case (see Eq. (2.34b)), while inside the light cone, i.e., for $x \ll 2t$, this decay changes qualitatively compared to that case (see Eq. (2.34c)) and becomes faster $\propto 1/x^{d-2+2\theta_N}$. The latter is consistent with the slower decay [2] of the momentum distribution $iG_K(q \gg t^{-1})$ upon increasing q, compared to its Gaussian expression, found in the previous section, see Eq. (4.37). It is also interesting to note that while in quenches of one-dimensional systems ($d=1$), which belong to the Luttinger liquid universality class, interactions do modify the scaling of G_K on the light cone [200], this is not the case for the present system, at least up to the first order in perturbation theory.

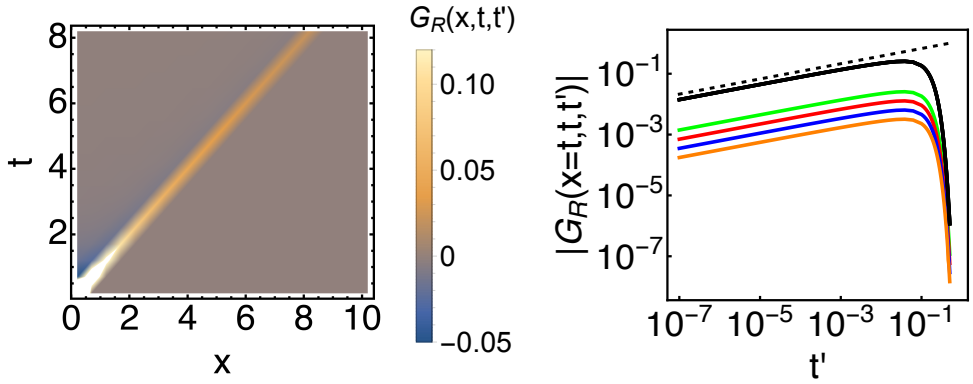

Figure 4.2: $G_R(x,t,t')$ after a quench to the dynamical critical point for the $O(N)$ model with $N \to \infty$ and spatial dimension $d = 3$, with an UV cut-off $\Lambda = \pi/2$. Left panel: $G_R(x,t,t')$ as a function of x and t for $t' = 0.1$. The numerical value of G_R is expressed as indicated by the color code in the legend. Right panel: plot of $G_R(x,t,t')$ on a double logarithmic scale as a function of t' for various values of $x = t$. The coloured solid lines correspond to sections with $t = 80$ (lower, orange line), $t = 40$ (lower-middle, blue line), $t = 20$ (upper-middle, red line), and $t = 10$ (upper, green line), respectively. The solid black line corresponds to a rescaling of the solid coloured line with t, i.e., to $tG_R(x,t,t')$, over which the coloured solid lines collapse. For small values of t', $G_R(x,t,t')$ displays an algebraic growth $\propto t'^{0.25}$, as indicated by the corresponding dashed line, which is in agreement with Eq. (4.46b).

In order to test the validity of the scaling behavior summarized above (see Eqs. (4.46) and (4.51)) beyond perturbation theory, we consider the $O(N)$ model in the exactly solvable limit $N \to \infty$ which has been considered, e.g., in Chapter 3. In particular, after a deep quench to the critical point, $G_R(x,t,t')$ and $iG_K(x,t,t)$ can be calculated, respectively, via a Fourier transform of $2\mathrm{Im}\,[f_{\mathbf{k}}(t)f^*_{\mathbf{k}}(t')]$ and $2|f_{\mathbf{k}}(t)|^2$, where the evolution of the complex coefficients $f_{\mathbf{k}}$ is determined numerically, according to Eqs. (13), (7) and (11) of Ref. [1].

In Fig. 4.2 we report the resulting $G_R(x,t,t')$ in spatial dimension $d = 3$, as a function of x and t (with fixed $t' \ll t$) on the left panel, and as a function of t' on the lightcone $x = t - t' \simeq t$ on the right one. The light cone of $G_R(x,t,t')$ is clearly visible in the left panel: in fact, upon varying x for fixed $t, t' \ll t$, $G_R(x,t,t')$ vanishes for $x \ll t$ and $x \gg t$, while it grows as it approaches the light cone. The colored solid curves on the right panel, instead, show that $G_R(x = t,t,t')$ grows algebraically as $G_R(x = t,t,t') \propto t'^{\theta_N}$ for small values of t' and various values of t, in agreement with Eq. (4.46b), with the proper value $\epsilon = 1$ and $\theta_N \to \theta_\infty = 1/4$ (see, c.f., Eq. (4.71)) in $d = 3$. Moreover, by rescaling the colored solid curves by t, i.e., by plotting $tG_R(x = t,t,t')$ as a function of t' with fixed t, all the curves collapse on the master curve indicated by the solid black line, in agreement with the algebraic dependence on t predicted by Eq. (4.46b). Analogous agreement with the scaling behaviors in Eq. (4.46) is found for $d \neq 3$, showing that these relations hold beyond perturbation theory.

In Fig. 4.3 we report $G_K(x,t,t)$ for the same model in spatial dimensionality $d = 3$, as a function of x and t on the left panel, while on the right panel iG_K is shown as a function of x along the cuts in the (x,t)-plane indicated by the corresponding dashed lines on the left panel. The light cone of $iG_K(x,t,t)$ is clearly visible in the left panel: in fact, $iG_K(x,t,t)$ vanishes for $x > 2t$, while it grows

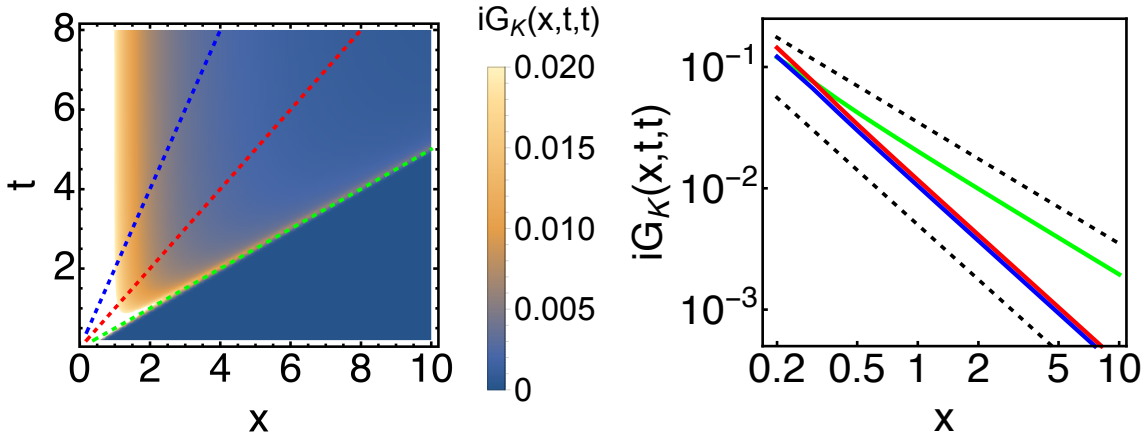

Figure 4.3: $G_K(x,t,t)$ after a quench to the dynamical critical point for the $O(N)$ model with $N \to \infty$ and spatial dimension $d = 3$, with an UV cut-off $\Lambda = \pi/2$. Left panel: $G_K(x,t,t)$ as a function of x and t. The numerical value of G_K is expressed as indicated by the color code in the legend. The dashed lines correspond to the sections $x = t/2$ (upper, blue line), $x = t$ (middle, red line) and $x = 2t$ (lower, green line), respectively, which are highlighted in the right panel. Right panel: plot of $G_K(x,t,t)$ on a double logarithmic scale as a function of x along the sections of the (x,t)-plane highlighted in the left panel, i.e., the dashed lines correspond to the sections $x = t/2$ (lower, blue line), $x = t$ (middle, red line) and $x = 2t$ (upper, green line), respectively. Along the first two and the last sections, $G_K(x,t,t)$ displays an algebraic decay $\propto x^{-3/2}$ and $\propto x^{-1}$, respectively, as indicated by the corresponding lower and upper dashed lines. This behaviour is in agreement with Eqs. (4.51b) and (4.51c).

as it approaches either this light cone or the line $x = 0$ (where the white color indicates large values compared to those displayed in the rest of the plot and indicated by the color code) from within the region with $x < 2t$, and it vanishes upon increasing x and t. The curves on the right panel, instead, show that $G_K(x,t,t) \propto x^{-3/2}$ (lowermost and intermediate solid lines) as x grows within the light cone, i.e., with $x = t/2$ and $x = t$, while $G_K(x,t,t) \propto x^{-1}$ (uppermost line) exactly on the light cone $x = 2t$, in agreement with Eqs. (4.51b) and (4.51c), respectively, with the proper value $\epsilon = 1$ and $\theta_N \to \theta_\infty = 1/4$ (see, c.f., Eq. (4.71)) in $d = 3$. Analogous agreement with the scaling behaviors in Eq. (4.51) is found for $d \neq 3$, showing that these relations hold beyond perturbation theory.

4.3 Magnetization dynamics

In the previous sections we focused on the temporal evolution of two-time quantities after a quench, assuming that the $O(N)$ symmetry of the initial state is not broken by the dynamics. However, as it happens in classical systems (see, e.g., Ref. [119]), universal features are expected to emerge also in the evolution of one-time quantities such as the order parameter, when the symmetry of the initial state is broken by a suitable small external field $\mathbf{h}(\mathbf{x})$, which is then switched off at $t > 0$. As we show below, the short-time behavior of the mean order parameter $\mathbf{M}(\mathbf{x}, t)$ (henceforth referred to as the magnetization) actually provides one additional direct measure of the short-time exponent θ_N encountered in the previous sections. In Secs. 4.3.1 and 4.3.2 below, we study the evolution of $\mathbf{M}$ in perturbation theory and by solving the Hartree-Fock equations (which are exact in the limit $N \to \infty$), respectively.

4.3.1 Magnetization dynamics from perturbation theory

The inclusion of a symmetry-breaking field in the pre-quench Hamiltonian H_0 induces a non-vanishing value of the order parameter $\mathbf{M}(\mathbf{x}, t) \equiv \langle \boldsymbol{\phi}(\mathbf{x}, t) \rangle$, which evolves after the quench. If the post-quench Hamiltonian H is tuned to its critical point, one expects this evolution to be characterized by universal exponents. More precisely, in this section we investigate the effect of modifying $H_0 = H(\Omega_0^2, 0)$ in Eq. (2.1) as:

$$H_0 = \int_{\mathbf{x}} \left[\frac{1}{2}\boldsymbol{\Pi}^2 + \frac{1}{2}(\nabla\boldsymbol{\phi})^2 + \frac{\Omega_0^2}{2}\boldsymbol{\phi}^2 - \mathbf{h}\cdot\boldsymbol{\phi} \right], \tag{4.52}$$

where $\mathbf{h} \equiv \mathbf{h}(\mathbf{x})$ is the external field which breaks explicitly the $O(N)$ symmetry of H_0 and therefore of the initial state. Within the Keldysh formalism, this corresponds to a change in the initial action (4.11), which now reads, in momentum space:

$$S_s = i \int_{\mathbf{k}} \frac{\omega_{0k}}{2} \left[\left(\boldsymbol{\phi}_{0c,\mathbf{k}} - \sqrt{2}\frac{\mathbf{h}_\mathbf{k}}{\omega_{0k}^2} \right)^2 \tanh(\beta\omega_{0k}/2) + \boldsymbol{\phi}_{0q,\mathbf{k}}^2 \coth(\beta\omega_{0k}/2) - 2\beta\frac{|\mathbf{h}_\mathbf{k}|^2}{\omega_{0k}^3} \right], \tag{4.53}$$

where $\mathbf{h}_\mathbf{k}$ indicates the Fourier transform of $\mathbf{h}(\mathbf{x})$ and ω_{0k} is given in Eq. (2.12). Recalling that the integration by parts of $\dot{\boldsymbol{\phi}}_q \cdot \dot{\boldsymbol{\phi}}_c$ in the bulk action (4.9) generates a term proportional to $\dot{\boldsymbol{\phi}}_{0q} \cdot \boldsymbol{\phi}_{0c}$ in the initial action S_s, one can easily see from the change of variables $\boldsymbol{\phi}_{0c,\mathbf{k}} \to \boldsymbol{\phi}_{0c,\mathbf{k}} + \sqrt{2}\mathbf{h}_\mathbf{k}/\omega_{0k}^2$ that taking the functional average $\langle \dots \rangle_\mathbf{h}$ with $\mathbf{h} \neq \mathbf{0}$ is equivalent to calculating it with $\mathbf{h} = \mathbf{0}$, but with a

modified weight, i.e.,

$$\langle \dots \rangle_{\mathbf{h}} = \langle \dots \mathrm{e}^{-i\sqrt{2}\int_{\mathbf{k}} \mathbf{h}_{\mathbf{k}}\cdot\dot{\boldsymbol{\phi}}_{0q,\mathbf{k}}/\omega_{0k}^2}\rangle_{\mathbf{h}=0}. \tag{4.54}$$

This means that any average in the presence of the field $\mathbf{h}$ can be calculated as in its absence by considering the insertion of the operator shown in the r.h.s. of Eq. (4.54). Let us first consider the Gaussian approximation, i.e., set $u = 0$. Using either Eq. (4.54) or by repeating the calculations of Chapter 2 with the pre-quench Hamiltonian (4.52), one finds that

$$\langle \boldsymbol{\phi}_{\mathbf{k}}(t)\rangle = \frac{\mathbf{h}_{\mathbf{k}}}{\omega_{0k}^2}\cos(\omega_k t). \tag{4.55}$$

Moreover, while G_R is not affected by $\mathbf{h} \neq \mathbf{0}$, the Keldysh Green's function is modified because of the presence of a non-vanishing $\langle \boldsymbol{\phi}_{\mathbf{k}}(t)\rangle$ as:

$$\langle\{\phi_{i,\mathbf{k}}(t), \phi_{j,\mathbf{k}'}(t')\}\rangle = \delta_{i,j}\,\delta_{\mathbf{k},-\mathbf{k}'} iG_K(k,t,t') + 2\langle\phi_{i,\mathbf{k}}(t)\rangle\langle\phi_{j,\mathbf{k}'}(t')\rangle, \tag{4.56}$$

where $G_K(k,t,t')$ is the same as in Eq. (2.15b), i.e., the Keldysh Green's function corresponding to $\langle \boldsymbol{\phi}_{\mathbf{k}}(t)\rangle = \mathbf{0}$. In the following, we assume the initial external field $\mathbf{h}$ to be spatially homogeneous and aligned with the first component of the field, i.e.,

$$h_i(\mathbf{x}) = \delta_{i,1} M_0 \Omega_0^2. \tag{4.57}$$

Note that the residual symmetry of the initial state under $O(N-1)$ transformations involving the components $i = 2, \dots, N$ of the field which are transverse to $\mathbf{h}$ (collectively indicated by $\perp$) implies that the only non-vanishing post-quench component of the magnetization is the one along $i = 1$ (referred to as longitudinal and indicated by $\parallel$), i.e.,

$$M_i(\mathbf{x}, t) = \delta_{i,1} M(t). \tag{4.58}$$

Accordingly, from Eq. (4.55), one finds

$$M(t) = M_0 \cos(\sqrt{r}t), \tag{4.59}$$

which shows that the order parameter M oscillates indefinitely with angular frequency $\sqrt{r}$ and that at the Gaussian critical point $r = 0$ it does not evolve.

Beyond the Gaussian approximation $u = 0$ considered above, one has to take into account the presence of interaction in the post-quench Hamiltonian, which affects the temporal evolution of M in Eq. (4.58). Focussing, for concreteness, on the critical point $r = r_c$ (with $r_c \neq 0$ due to the presence of interaction, see Sec. 4.2.1, in particular Eq. (4.24)) and on a deep quench, the same perturbative expansion illustrated in Sec. 4.2 renders, at one loop, a correction $M(t) = M_0 + \delta M(t)$ with

$$\delta M(t) = \int_0^t \mathrm{d}t'\, G_{0R}(k=0,t,t') \left[B(t') M_0 + \frac{2u_c}{4!N} M_0^3 \right], \tag{4.60}$$

where only the time-dependent part $B(t')$ of the tadpole $i\mathcal{T}(t')$ in Eq. (4.16) contributes to Eq. (4.60) because the time-independent contribution B_0 is cancelled by assuming $r = r_c$, as explained for the correlation functions in Sec. 4.2.1. Taking into account the explicit expression of $B(t)$ in Eq. (4.19)

and of G_{0R} in Eq. (2.17a) it is easy to find that δM exhibits a logarithmic dependence on t for $\Lambda t \gg 1$, and a quadratic growth in time:

$$\delta M(t) \simeq M_0 \theta_N \ln(\Lambda t) - M_0 \frac{u_c}{4!N} (M_0 t)^2, \tag{4.61}$$

where θ_N is given in Eq. (4.20). This expression indicates that the dynamics of the magnetization $M(t)$ is characterized by two regimes: for $t \ll t_i \simeq 1/(M_0\sqrt{u_c})$ the term proportional to t^2 is negligible, and therefore δM is dominated by the logarithmic term. This suggest that, after a proper resummation of the logarithms, the magnetization grows algebraically as a function of time as $M(t) \propto M_0(\Lambda t)^{\theta_N}$. On the other hand, when $t \gtrsim t_i$ the second term in the r.h.s. of Eq. (4.61) becomes dominant, signalling a crossover to a different dynamical regime. Notice that, for these two regimes to be distinguishable, one must require that $\Lambda t_i \gg 1$, i.e., $\Lambda \gg M_0\sqrt{u_c}$. In Sec. 4.5.4, we assess the existence of these two dynamical regimes by showing that a general scaling form can be derived for the magnetization M after a quench to the critical point, which involves the scaling variable associated with M_0 as in Eq. (4.136).

4.3.2 Magnetization dynamics from a self-consistent Hartree-Fock approximation

In the previous subsection, the post-quench dynamics of the model in Eq. (4.53) has been studied via a perturbative dimensional expansion around the upper critical dimensionality $d = d_c$. However, as in the case with $\mathbf{h} = \mathbf{0}$ discussed in detail in Ref. [1], the temporal evolution of $\mathbf{M}(\mathbf{x}, t)$ for $N \to \infty$ can be determined beyond perturbation theory, i.e., for a generic value of the spatial dimensionality d. In fact, in this limit, the Hartree-Fock or self-consistent approximation where the $(\boldsymbol{\phi}^2)^2$ interaction is approximated by a quadratic "mean-field" term $\propto \boldsymbol{\phi}^2\langle\boldsymbol{\phi}^2\rangle$ becomes exact. The latter corresponds to an effective, time-dependent square "mass" $r(t)$ which is calculated self-consistently, see, e.g., Refs. [1, 169–171]. As in Sec. 4.3.1, the initial magnetic field $\mathbf{h}$ is taken along the direction of the first component of the field, see Eq. (4.57), and therefore the post-quench order parameter is given by Eq. (4.58) with $M(0) = \sqrt{N}M_0$, where the multiplicative factor $\sqrt{N}$ is needed in order to have a well-defined limit $N \to \infty$, as discussed below.

The one-loop equations governing the time evolution of the system are [169]:

$$\left[\partial_t^2 + r(t) - \frac{u}{3}M^2(t)\right] M(t) = 0, \tag{4.62a}$$

$$\left[\partial_t^2 + q^2 + r(t) - \frac{u}{6N} i G_K^{\parallel}(x=0,t,t)\right] G_K^{\parallel}(q,t,t') = 0, \tag{4.62b}$$

$$\left[\partial_t^2 + q^2 + r(t) - \frac{u}{3}M^2(t)\right] G_K^{\perp}(q,t,t') = 0, \tag{4.62c}$$

$$r(t) = r + \frac{u}{2}\left[M^2(t) + \frac{1}{2N} i G_K^{\parallel}(x=0,t,t) + \frac{N-1}{6N} i G_K^{\perp}(x=0,t,t)\right], \tag{4.62d}$$

where $G_K^{\parallel}$ and $G_K^{\perp}$ are the Keldysh Green's functions of the longitudinal and of a generic transverse component of the field, respectively, while $r(t)$ is the time-dependent effective parameter self-consistently determined from Eq. (4.62d)

To solve this system of equations we need to specify initial conditions for the magnetization and the Green's functions. Since, from the Heisenberg equations of motion $\dot{\phi} = \Pi$, with ϕ and Π the

components of the fields and its conjugate momentum along $\mathbf{h}$, and since in the initial state $\langle \Pi(t=0)\rangle = 0$, one concludes that $\dot{M}(t)|_{t=0} = 0$. The initial conditions for the $G_K^{\parallel,\perp}(q,t,t')$, $\partial_t G_K^{\parallel,\perp}(q,t,t')$ and $\partial_t\partial_{t'} G_K^{\perp}(q,t,t')$ are [169]:

$$G_K^{\parallel,\perp}(q,t=0,t'=0) = \frac{1}{\sqrt{q^2 + r_{\parallel,\perp}(0)}}, \tag{4.63a}$$

$$\partial_t G_K^{\parallel,\perp}(q,t=0,t'=0) = 0, \tag{4.63b}$$

$$\partial_t\partial_{t'} G_K^{\parallel,\perp}(q,t=0,t'=0) = \sqrt{q^2 + r_{\parallel,\perp}(0)}, \tag{4.63c}$$

where we introduced

$$r_\parallel(0) = r(0), \tag{4.64a}$$

$$r_\perp(0) = r(0) - \frac{u}{3}M_0^2. \tag{4.64b}$$

The set of Eqs. (4.62) is not analytically solvable and in general one has to resort to approximations or to a numerical evaluation. However, in the limit $N \to \infty$, one can see from Eqs. (4.62) that the quadratic term $\propto M^2(t)$ can be neglected for times $t \ll t_i$, with t_i defined by the condition

$$r + \frac{u}{12} i G_K^{\perp}(x=0,t_i,t_i) \simeq \frac{u}{3} M^2(t_i); \tag{4.65}$$

with these assumptions, Eqs. (4.62) simplify to:

$$\left[\partial_t^2 + r(t)\right] M(t) = 0, \tag{4.66a}$$

$$\left[\partial_t^2 + q^2 + r(t)\right] G_K^{\parallel,\perp}(q,t,t') = 0, \tag{4.66b}$$

$$r(t) = r + \frac{u}{12} i G_K^{\perp}(x=0,t,t). \tag{4.66c}$$

The critical value r_c of the parameter r can be obtained via the ansatz suggested in Ref. [171], namely:

$$r_c = -\frac{u}{4!}\int_q \mathrm{e}^{-q/\Lambda} \frac{2q^2 + \Omega_0}{q^2\sqrt{q^2+\Omega_0}}, \tag{4.67}$$

where the integral is regularized through the smooth cut-off function $\exp(-q/\Lambda)$. This regularization is used to evaluate all the integrals over momentum in the self-consistent Eqs. (4.66): the choice of a smooth cutoff is crucial in order to avoid spurious non-universal oscillations which would mask the real universal behaviour of the dynamical quantities [1]. For $r = r_c$, the effective parameter $r(t)$ at long times $\Lambda t \gg 1$ has (up to rapidly oscillatory terms) the following universal behavior [1]

$$r(t) = \frac{a}{t^2}, \tag{4.68}$$

in which the value of a can be obtained analytically and for $2 < d < 4$ is given by [1]

$$a = \frac{d}{4}\left(1 - \frac{d}{4}\right). \tag{4.69}$$

By inserting this expression into Eq. (4.66a), we then obtain

$$M(t \gg \Lambda^{-1}) \propto (\Lambda t)^{\theta_\infty}, \tag{4.70}$$

where [1]

$$\theta_\infty = 1 - \frac{d}{4}, \tag{4.71}$$

which agrees with Eq. (4.20) in the limit $N \to \infty$ and up to the first order in $\epsilon = 4 - d$ after the fixed-point value of the coupling constant u_c is introduced in that expression, according to what we discuss further below in Sec. 4.4.2 (see, in particular, Eq. (4.91)). Accordingly, for times smaller than t_i estimated below (but much longer than the microscopic scale Λ^{-1}), the order parameter increase is controlled by the universal exponent θ_∞. The time dependence of $M(t)$ obtained from the numerical solution of Eqs. (4.66a), (4.66b), and (4.66c) with $r = r_c$ and various values of the spatial dimensionality d are shown in Fig. 4.4, where they are also compared with the analytical prediction in Eq. (4.70).

In order to estimate the timescale t_i beyond which Eqs. (4.66) are no longer valid, we analyse Eq. (4.65). First, note that, as $d \to 4$, $M(t) \simeq \mathcal{A}(\Lambda t)^{\theta_\infty}$ becomes almost independent of t and equal to M_0 (see Fig. 4.4) and therefore $\mathcal{A} \simeq M_0$. Hence, for d sufficiently close to 4 we may safely approximate $M(t) \simeq M_0(\Lambda t)^{\theta_\infty}$. Using this approximation in Eq. (4.65) and solving for t_i with the aid of Eq. (4.68), we obtain, to leading order in θ_∞, the following expression for t_i:

$$\Lambda t_i \simeq \frac{\sqrt{3}\Lambda}{M_0}\sqrt{\frac{a}{u}} \propto \frac{1}{M_0}. \tag{4.72}$$

This estimate of t_i is compatible for $d \to 4$ with the scaling derived from the RG analysis in Sec. 4.5.4, see Eq. (4.136) .

4.4 Renormalization group: Wilson approach

In the previous sections we discussed the emergence of scaling behaviors on the basis of the results of perturbative calculations at the lowest order in the interaction strength, with the sole exception of the exact results presented in Sec. 4.3.2. Here and in Sec. 4.5, instead, we demonstrate that such scaling behaviors follow from the existence of a fixed point in the renormalization-group (RG) flow which we determine within the Wilson and Callan-Symanzik approach, respectively. In particular, this allows us to determine the fixed-point value of u_c on which θ_N in Eq. (4.20) depends and which is not fixed by the perturbative calculations above.

4.4.1 Canonical dimensions

In order to determine the canonical dimensions of the relevant coupling constants and parameters in the Keldysh actions (4.8) and (4.9) which describe the non-equilibrium dynamics of the model, we consider the scaling of the corresponding Gaussian theory in the case of a deep quench $\Omega_0 \gg \Lambda$, with

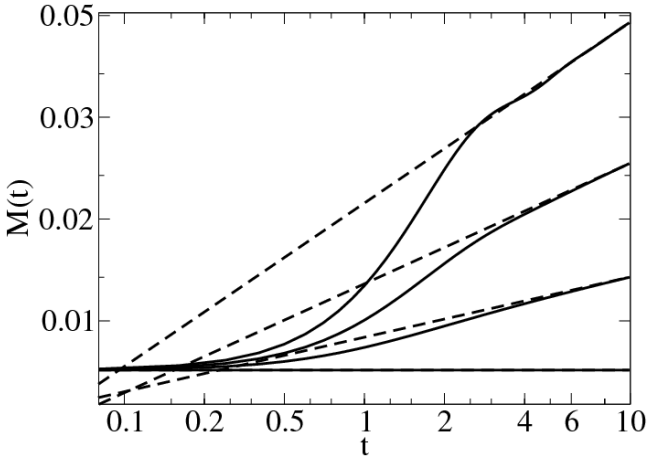

Figure 4.4: Magnetization $M(t)$ as a function of time t (on a double logarithmic scale) for various values of the spatial dimensionality $d = 2.5$, 3, 3.5, and 4, from top to bottom. The solid lines indicate the numerical solution of the self-consistent equations (4.66) with $r = r_c$ and $M_0 = 0.005$. The dashed lines, instead, indicate the corresponding algebraic increase $\propto t^{\theta_\infty}$ (see Eq. (4.70)) with θ_∞ reported in Eq. (4.71). These numerical solutions correspond to the case $\Omega_0 = 25$, $\Lambda = 1$ and to an exponential cutoff function e^{-q} introduced for the regularization of the integrals as in Eq. (4.67) (see also the discussion in Ref. [1]).

a vanishing temperature $T = 0$ of the initial state. Accordingly, the only operators appearing in the initial action S_s in Eq. (4.11) are:

$$\omega_{0k}\, \boldsymbol{\phi}^2_{c,q} = \left[\Omega_0 + \frac{k^2}{2\Omega_0} + O(k^4/\Omega_0^3)\right] \boldsymbol{\phi}^2_{c,q}. \tag{4.73}$$

Since we consider $\Omega_0 \gg \Lambda$ and the leading term in the expansion of ω_{0k} (see Eq. (2.12)) is the most relevant in the RG sense, we can approximate $\omega_{0k} \simeq \Omega_0$. However, as the classical and quantum fields $\boldsymbol{\phi}_{c,q}$ can in principle have different flows under RG, we allow the coefficients of the corresponding terms $\boldsymbol{\phi}_c^2$ and $\boldsymbol{\phi}_q^2$ in the initial action to be different, denoting them by Ω_{0c} and Ω_{0q}, respectively.

In order to study the canonical scaling of the model, we introduce an arbitrary momentum scale μ, such that space and time coordinates scale as $\mathbf{x} \sim \mu^{-1}$ and $t \sim \mu^{-z}$, where z is the dynamical critical exponent with $z = 1$ within the Gaussian approximation. While in thermal equilibrium, the canonical dimensions of the fields and of the couplings follow immediately from requiring the action to be dimensionless, this requirement is no longer sufficient in the present case, given the large number of fields involved in the total Keldysh action $S_s + S_b$. Accordingly, in order to fix these dimensions we impose the following two conditions: (i) the canonical dimensions of the fields at the surface $t = 0$ are the same as in the bulk $t > 0$ and (ii) Ω_{0q} is dimensionless. Condition (i) — which do not necessarily hold beyond the Gaussian approximation — basically amounts at requiring the continuity of the fields during the quench and, in fact, it is the functional translation of the operatorial conditions $\boldsymbol{\phi}(0^-) = \boldsymbol{\phi}(0^+)$ and $\boldsymbol{\Pi}(0^-) = \boldsymbol{\Pi}(0^+)$ [1,174,175]. Condition (ii), instead, is based on the fact that Ω_{0q}

plays the role of an effective temperature — see the discussion in Sec. 2.3.3 — and temperatures are known to be scale-invariant in equilibrium quantum systems outside the quantum critical regime [187]. Using these conditions, from Eqs. (4.9) and (4.8) one finds the scaling of the fields

$$\boldsymbol{\phi}_c(x) \sim \mu^{(d-2)/2}, \qquad \boldsymbol{\phi}_q(x) \sim \mu^{d/2}, \tag{4.74}$$

and of the couplings

$$\Omega_{0c} \sim \mu^2, \quad r \sim \mu^2, \quad u_c \sim \mu^{4-d}, \quad u_q \sim \mu^{2-d}, \tag{4.75}$$

from which it follows that the upper critical dimensionality is $d = d_c = 4$. Notice that the quantum vertex u_q is irrelevant for $d > 2$. This conclusion is consistent with the dimensional crossover presented and discussed in Sec. 2.3.3: the upper critical dimensionality, which is 3 for a quantum system in equilibrium at $T = 0$, is increased to 4 by the effect of a deep quench. Note, in addition, that the positive canonical dimension of the classical initial "mass" Ω_{0c} implies that it grows indefinitely under RG and therefore its stable fixed-point value is $\Omega_{0c} = +\infty$.

4.4.2 One-loop corrections

In order to account for the effects of the interaction, in this subsection we derive the RG equations in perturbation theory up to one loop, based on a momentum-shell integration [221]. It turns out that this is sufficient to highlight the emergence of an initial-slip exponent, while additional effects, such as the emergence of dissipative terms and thermalization, can be captured only by including contributions at two or more loops, which account for inelastic processes [184, 219, 220, 222].

We assume that the actions in Eqs. (4.8) and (4.9) are defined in momentum space with momenta of modulus $k < \Lambda$, where Λ is a cutoff set by the inverse of some microscopic length scale, e.g., a possible lattice spacing. In order to implement the RG transformation in momentum space [177, 178] we decompose each field $\phi(k) \in \{\boldsymbol{\phi}_c, \boldsymbol{\phi}_q\}$ as a sum of a "slow" and a "fast" component $\phi_<(k)$ and $\phi_>(k)$, respectively, i.e., as $\phi = \phi_< + \phi_>$, where $\phi_<(k)$ involves only modes with $0 \le k < \Lambda - \mathrm{d}\Lambda$, while $\phi_>(k)$ involves the remaining ones within the momentum shell $\Lambda - \mathrm{d}\Lambda \le k \le \Lambda$ of small thickness $\mathrm{d}\Lambda = \delta\ell\,\Lambda$, with $0 < \delta\ell \ll 1$. Then, the fast fields are integrated out from the action: this generates new terms which renormalize the bare couplings of the action of the remaining slow fields. Here we do this integration perturbatively in the coupling constant and therefore the exponential factor in Eq. (4.1) is first split into the Gaussian and interaction parts $S_\mathrm{G} + S_\mathrm{int}$, then expanded up to second order in the interaction terms, with the remaining expectation values of the fast fields calculated with respect to their Gaussian action S_G. Finally, the result is re-exponentiated using a cumulant expansion:

$$\begin{aligned}\int \mathcal{D}[\phi_>, \phi_<]\, \mathrm{e}^{i(S_\mathrm{G}+S_\mathrm{int})} &\simeq \int \mathcal{D}[\phi_>, \phi_<]\, \mathrm{e}^{iS_\mathrm{G}} \left[1 + i\, S_\mathrm{int} - \frac{1}{2} S_\mathrm{int}^2\right] \\ &\simeq \int \mathcal{D}\phi_<\ \exp\left\{ i S_\mathrm{G}^< + i\, \langle S_\mathrm{int}\rangle_> - \frac{1}{2}\langle S_\mathrm{int}^2\rangle_>^c \right\},\end{aligned} \tag{4.76}$$

where $S_\mathrm{G}^< = S_\mathrm{G}[\phi_<]$ is the Gaussian action calculated on the slow fields, $\langle \dots \rangle_>$ denotes the functional integration with respect to $S_\mathrm{G}[\phi_>]$, while the superscript c indicate the connected average. For the

case we are interested in,

$$S_{\rm int} = -\frac{2u_c}{4!N}\int_{\mathbf{x},t>0}(\boldsymbol{\phi}_q\cdot\boldsymbol{\phi}_c)|\boldsymbol{\phi}_c|^2 - \frac{2u_q}{4!N}\int_{\mathbf{x},t>0}(\boldsymbol{\phi}_q\cdot\boldsymbol{\phi}_c)|\boldsymbol{\phi}_q|^2. \tag{4.77}$$

After the integration, coordinates and fields are rescaled in order to restore the initial value of the cutoff:

$$x \to bx, \quad t \to b^z t, \quad \phi_i \to b^{\zeta_i}\phi_i, \quad \phi_{0,i} \to b^{\zeta_{0,i}}\phi_{0,i}, \tag{4.78}$$

where $i = c, q$ and $b = \Lambda/(\Lambda - {\rm d}\Lambda) \simeq 1 + \delta\ell$. The field scaling dimensions ζ_i and $\zeta_{0,i}$ — the Gaussian values of which can be read directly from Eq. (4.74) — generically acquire an anomalous contribution due to the interactions. The resulting action for the slow fields (which, after rescaling are renamed as the original fields ϕ) then acquires contributions from both integration and rescaling and the expression of the new effective parameters (denoted below by $'$) in the action in terms of the original ones constitute the so-called RG recursion relations.

In passing, we mention that, strictly speaking, the functional integral on the l.h.s. of Eq. (4.76) is actually equal to one and therefore the renormalization procedure outlined above — which in equilibrium is typically implemented on the partition function of the statistical system under study — would look unnecessary. However, this is no longer the case if one either adds externals sources for the field (as done, e.g., in App. 4.A) or, equivalently, implements integration and rescaling directly on correlation functions.

Assuming, for the sake of clarity, a vanishing temperature $T = 0$ in the initial state, we find the following RG recursion relations (see App. 4.F for details) at the lowest order in perturbation theory

$$r' = b^2\,(r + u_c I_1)\,, \tag{4.79a}$$
$$u_c' = b^{2-2\zeta_c}\,u_c\,(1 - u_c I_2)\,, \tag{4.79b}$$
$$u_q' = b^{2-2\zeta_q}\,u_q\,(1 - u_q I_2)\,, \tag{4.79c}$$

where the integrals $I_{1,2}$ can be decomposed in time-independent and time-dependent parts as $I_{1,2}(t) = I_{1,2}^{\rm b} + I_{1,2}^{\rm s}(t)$, with the time-independent terms

$$I_1^{\rm b} = \delta\ell\, c_{1,N}\frac{\Lambda^d}{\omega_\Lambda}K_+, \tag{4.80a}$$
$$I_2^{\rm b} = \delta\ell\, c_{2,N}\frac{\Lambda^d}{\omega_\Lambda^4}\omega_{0\Lambda}, \tag{4.80b}$$

while the time-dependent ones are

$$I_1^{\rm s}(t) = \delta\ell\, c_{1,N}\frac{\Lambda^d}{\omega_\Lambda}K_-\cos(2\omega_\Lambda t), \tag{4.81a}$$
$$I_2^{\rm s}(t) = \delta\ell\, c_{2,N}\frac{\Lambda^d}{\omega_\Lambda^3}\Big[K_-\,2\omega_\Lambda\, t\,\sin(2\omega_\Lambda t) - \frac{\omega_{0\Lambda}}{\omega_\Lambda}\cos(2\omega_\Lambda t)\Big], \tag{4.81b}$$

where $K_\pm$, $\omega_\Lambda = \omega_{k=\Lambda}$ and $\omega_{0\Lambda} = \omega_{0,k=\Lambda}$, with ω_k and ω_{0k} given in Eqs. (2.7) and (2.12), respectively. Notice that, in terms of Ω_{0q} and Ω_{0c}, the functions $K_\pm$ now reads (see also App. 4.A)

$$K_\pm(k) = \frac{1}{2}\left(\sqrt{\frac{k^2+r}{k^2+\Omega_{0c}^2}} \pm \sqrt{\frac{k^2+\Omega_{0q}^2}{k^2+r}}\right). \tag{4.82}$$

In the expressions above we introduced the coefficients

$$c_{1,N} = \frac{N+2}{12N}a_d \quad \text{and} \quad c_{2,N} = \frac{N+8}{24N}a_d, \tag{4.83}$$

where $a_d = \Omega_d/(2\pi)^d$, with $\Omega_d = 2\pi^{d/2}/\Gamma(d/2)$ is the d-dimensional solid angle, $\Gamma(x)$ being the gamma function. Note that $I_{1,2}$ are time-dependent quantities as a consequence of the non-TTI term of G_{0K} in Eq. (2.15b).

In order to cast the RG equations in a convenient differential form, we take into account that $b \simeq 1+\delta\ell$, with $\delta\ell \ll 1$ and we keep from Eq. (4.79) only the first order in $\delta\ell$. Neglecting for the time being the time-dependent terms $I_1^{\rm s}$ and $I_2^{\rm s}$ (see further below for a discussion), we find the differential equations:

$$\frac{\mathrm{d}r}{\mathrm{d}\ell} = 2r + u_c\frac{c_{1,N}}{2}\frac{\Lambda^d}{\omega_\Lambda}\left[\sqrt{\frac{\Lambda^2+r}{\Lambda^2+\Omega_{0c}^2}} + \sqrt{\frac{\Lambda^2+\Omega_{0q}^2}{\Lambda^2+r}}\right], \tag{4.84a}$$

$$\frac{\mathrm{d}u_c}{\mathrm{d}\ell} = u_c\left[(d_c-d) - c_{2,N}\,u_c\frac{\Lambda^d}{\omega_\Lambda^4}\sqrt{\Lambda^2+\Omega_{0q}^2}\right], \tag{4.84b}$$

$$\frac{\mathrm{d}u_q}{\mathrm{d}\ell} = u_q\left[(d_q-d) - c_{2,N}\,u_c\frac{\Lambda^d}{\omega_\Lambda^4}\sqrt{\Lambda^2+\Omega_{0q}^2}\right]. \tag{4.84c}$$

For later convenience, we defined here the classical and quantum "upper critical dimensions" d_c and d_q, respectively, as $d_{c,q} = 2 + d - 2\zeta_{c,q}$.

While Eqs. (4.84) are valid in the generic case, henceforth we focus on a deep quench. As noted in Sec. 4.4.1, Ω_{0c} has a stable fixed point at $\Omega_{0,c}^* = +\infty$ for a deep quench and, correspondingly, the first term in brackets in Eq. (4.84a) vanishes. Moreover, from the Gaussian scaling we find $d_c = 4$, $d_q = 2$, and therefore the quantum vertex is irrelevant for $d > 2$ and can be neglected. Finally, using the fact that $\Omega_{0q} \gg \Lambda$, Eqs. (4.84a) and (4.84b) become

$$\frac{\mathrm{d}r}{\mathrm{d}\ell} = 2r + u_c\Omega_{0q}\frac{c_{1,N}}{2}\frac{\Lambda^{4-\epsilon}}{\Lambda^2+r}, \tag{4.85a}$$

$$\frac{\mathrm{d}u_c}{\mathrm{d}\ell} = u_c\left[\epsilon - u_c\Omega_{0q}c_{2,N}\Lambda^{-\epsilon}\right], \tag{4.85b}$$

where $\epsilon = 4-d$, while $c_{1,N}$ and $c_{2,N}$ can be calculated here for $d = 4$. These flow equations admit a non-trivial fixed point $Q_{\rm dy}(\Omega_{0q})$ in the (r, u_c)-plane, which, at the lowest order in the dimensional expansion, is given by

$$Q_{\rm dy}(\Omega_0) = \left(-\epsilon\Lambda^2\frac{c_{1,N}}{4c_{2,N}}, \frac{\epsilon}{\Omega_{0q}c_{2,N}}\right) = \left(-\frac{\epsilon\Lambda^2(N+2)}{2(N+8)}, \epsilon\frac{192\pi^2N}{\Omega_{0q}(N+8)}\right), \tag{4.86}$$

which corresponds to the dynamical transition. This point turns out to be stable for $\epsilon > 0$, while it becomes unstable for $\epsilon < 0$, i.e, $d > d_c$ such that, as it happens in equilibrium, the resulting theory is effectively Gaussian. Right before Eqs. (4.84) we mentioned that these equations have been determined by neglecting the time-dependent parts $I^{\rm s}_{1,2}$ of the integrals $I_{1,2}$ in Eqs. (4.79). These parts are responsible for rapid oscillations on the temporal scale $\sim \omega_\Lambda^{-1} \simeq \Lambda^{-1}$ set by the microscopic structure of the model, which however do not contribute to time averages of the slow fields on much longer time scales. We emphasize that these terms are not universal as they strongly depend on the regularization. For instance, if a soft cut-off was used instead of a sharp one, these fast-oscillating terms would be replaced by functions which decay smoothly to zero on a temporal scale $\simeq \Lambda^{-1}$ (cf. Ref [1]), and therefore they would clearly not contribute to Eqs. (4.84).

Equations (4.84a) and (4.84b) are remarkably similar to those for the same model *in equilibrium* at a finite temperature $T = \beta^{-1}$ (see, e.g., Ref. [187]) which, in turn, admit a non-trivial fixed point $Q_{\rm eq}(T)$ [179,186]. In fact, both of them can be cast in the form

$$\frac{{\rm d}r}{{\rm d}\ell} = 2r + \frac{c_{1,N}}{2}\, u\, F(r), \tag{4.87a}$$

$$\frac{{\rm d}u}{{\rm d}\ell} = u\left[(d_c - d) + c_{2,N}\, u\, F'(0)\right], \tag{4.87b}$$

where u indicates, in equilibrium, the coupling constant of the model in Eq. (2.1), while out of equilibrium, it stands for u_c. For a quench, $F(r)$ reads

$$F^{\rm neq}(r) = \frac{\Lambda^d}{\sqrt{\Lambda^2 + r}}\left(\sqrt{\frac{\Lambda^2 + r}{\Lambda^2 + \Omega_{0c}^2}} + \sqrt{\frac{\Lambda^2 + \Omega_{0q}^2}{\Lambda^2 + r}}\right), \tag{4.88}$$

while in equilibrium,

$$F^{\rm eq}(r) = \frac{\Lambda^d}{\sqrt{\Lambda^2 + r}} 2 \coth\left(\beta\sqrt{\Lambda^2 + r}/2\right). \tag{4.89}$$

The relationship between the thermal and the dynamical fixed points $Q_{\rm eq}$ and $Q_{\rm dy}$ has been extensively discussed in Ref. [2]. Note that the upper critical dimension is $d_c = 3$ both in the case of a vanishing initial mass (i.e., $\Omega_{0q}^2 = \Omega_{0c}^2 = r$) and of the equilibrium theory at temperature $T = 0$; instead, the upper critical dimension is $d_c = 4$ for both the case of a deep quench and of equilibrium at a finite temperature. These similarities provide further support to the observations made in Sec. 2.3.3 that the stationary state after the quench resembles an equilibrium state, with the initial value Ω_{0q} of the parameter r in the former case playing the role of an effective temperature in the latter. Accordingly, the deep quench is responsible for a change of the upper critical dimensionality of the dynamical transition, in the very same way as a finite temperature modifies the upper critical dimensionality for an equilibrium quantum phase transition.

Although the analysis here reported only applies in dimensions above the lower critical one d_l, this "dimensional crossover" induced by the quench appears to be a generic feature of non-equilibrium isolated quantum systems. In fact, the same effect was shown to appear for a quench in the integrable one-dimensional Ising chain in transverse field [71,72,223], where the eventual (non-thermal) stationary state does not display any critical behaviour. Correspondingly, the equilibrium Ising chain in a

transverse field [179] displays a quantum phase transition at $T = 0$ (as it can be mapped on a classical Ising model in two spatial dimensions), while no phase transition occurs for $T > 0$ (as the corresponding classical Ising model would be in one spatial dimension). In addition, a recent experiment [224] on a one-dimensional Bose gas with two components suggested the absence of scaling behaviour in the long-time dynamics of the system. In this case, the dynamics was shown to be captured by the effective Hamiltonian (2.1) with $N = 1$, which, at equilibrium, is characterized by a quantum phase transition at $T = 0$ which however disappears for $T > 0$. Accordingly, we do not expect any DPT in this case.

A remarkable consequence of the structure of RG equations (4.87) is that the value of the critical exponent ν — which can be obtained as the eigenvalue of the linearized RG flow around the fixed point [177, 178] $u = u^* = -\epsilon/[c_{2,N}F'(0)] + \mathcal{O}(\epsilon^2)$ — is independent of the specific form of $F(r)$ and it is given by $\nu^{-1} = 2 - c_{1,N}\epsilon/(2c_{2,N}) + \mathcal{O}(\epsilon^2)$, i.e., by

$$\nu = \frac{1}{2} + \frac{N+2}{N+8}\frac{\epsilon}{4} + \mathcal{O}(\epsilon^2), \tag{4.90}$$

with $\epsilon = d_c - d$. Accordingly, both the dynamical and the equilibrium transitions are characterized by the same exponent ν, a fact which was already noticed in Ref. [171] for the $O(N)$ model in the limit $N \to \infty$. However, one may wonder if also the other independent critical exponent of the equilibrium theory, i.e., the anomalous dimension η, is the same as the one of the dynamical phase transition. The answer to this question is far from being trivial, since the computation of η requires a two-loop calculation which would also generate dissipative terms, responsible also for the destabilization of the prethermal state.

The analysis presented above reveals the existence of the fixed point $Q_{\rm dy}$ (see Eq. (4.86)) of the RG flow, which is approached upon considering increasingly long-distance properties whenever the value of the parameter r in Eq. (2.1) equals a certain critical value r_c, which depends, inter alia, on u_c and which corresponds to the stable manifold of the fixed point $Q_{\rm dy}$. Accordingly, the coupling constant u_c which appears in the perturbative calculations discussed in Sec. 4.2 with an unknown value can be substituted with its fixed-point value u_c^* corresponding to $Q_{\rm dy}$. In particular, inserting Eq. (4.86) into Eq. (4.20), and noting that $\Omega_{0q} = \Omega_0$, the initial-slip exponent eventually reads:

$$\theta_N = \frac{\epsilon}{4}\frac{N+2}{N+8} + \mathcal{O}(\epsilon^2). \tag{4.91}$$

The value of θ_N in the limit $N \to \infty$ agrees with the exact results presented in Chapter 3 and reported here in Eq. (4.71).

4.4.3 Dissipative and secular terms

The integration procedure outlined in Sec. 4.4.2 generates a number of terms in addition to those which are present in the action before integration. Physically, as the system evolves in time, inelastic collisions induce a thermalization process, and the system starts acting as a bath for itself. It is then natural to wonder whether dissipative terms might emerge [219]. In particular, they would be encoded of the form $ig_1\boldsymbol{\phi}_q^2$, $ig_2^A(\boldsymbol{\phi}_q \cdot \boldsymbol{\phi}_c)^2$ and $ig_2^B\boldsymbol{\phi}_q^2\boldsymbol{\phi}_c^2$ in the bulk action, which indeed correspond to having, respectively, additive (g_1) and multiplicative ($g_2^{A,B}$) Gaussian noise acting on the system [215]. Based

on the canonical power counting associated with the deep quench (see Sec. 4.4.2, with $d_c = 4$), these couplings turn out to scale as

$$g_1 \sim \mu, \qquad g_2^A \sim g_2^B \sim \mu^{3-d}; \tag{4.92}$$

accordingly g_1 is expected to be relevant in all spatial dimensions while $g_2^{A,B}$ are relevant only for $d < 3$. If these terms are generated under RG, their effect is to change significantly the properties of the resulting action and to induce a crossover towards a different fixed point, with a different canonical scaling. However, in order for g_1 to be generated one needs to consider at least a two-loop contribution and therefore one is allowed to neglect it in our one-loop analysis. On the other hand, corrections to $g_2^{A,B}$ are generated at one loop (see App. 4.F) as

$$\delta S^{(2)}_{(\mathrm{diss})} = i \int_{\mathbf{x},t} \left[\delta g_2^A(t) \left(\boldsymbol{\phi}_c^< \cdot \boldsymbol{\phi}_q^< \right)^2 + \delta g_2^B(t) (\boldsymbol{\phi}_c^<)^2 (\boldsymbol{\phi}_q^<)^2 \right], \tag{4.93}$$

with

$$\delta g_2^A(t) = \delta\ell \, \frac{a_d}{144} \frac{N+6}{N^2} \frac{\Lambda^d}{\omega_\Lambda^2} \left[u_c^2 \left(K_+^2 + K_-^2 \right) - u_c u_q \right] t, \tag{4.94a}$$

$$\delta g_2^B(t) = \delta\ell \, \frac{a_d}{72} \frac{1}{N^2} \frac{\Lambda^d}{\omega_\Lambda^2} \left[u_c^2 \left(K_+^2 + K_-^2 \right) - u_c u_q \right] t, \tag{4.94b}$$

with $K_\pm$ given in Eq. (4.82) and a_d after Eq. (4.83). In the absence of a quench of the parameter r, i.e., with $r = \Omega_0^2$ one has $K_+ = 1$, $K_- = 0$ and $u_c = u_q$; accordingly, the dissipative vertices $\delta g_2^{A,B}(t)$ vanish at this order in perturbation theory, because the quench of the coupling constant u (occurring from a vanishing to a non-vanishing value) does not affect the Gaussian propagators and has consequences only at higher-order terms in perturbation theory. The dissipation is also absent in the limit $N \to \infty$, as it can be seen from the scaling $\propto N^{-1}$ of the terms in Eq. (4.94): this implies that the prethermal state is actually the true steady-state of the model after the quench, in agreement with the fact that the Hamiltonian H becomes solvable in this limit [1]. In all the other cases, the dissipative correction increases upon increasing the time t and accordingly, though formally irrelevant for $d > 3$, $\delta g_2^{A,B}(t)$ grows indefinitely, spoiling the perturbative expansion. This kind of divergence is due to the presence of the so-called secular terms in the simple perturbative expansion which has been done here. Although several techniques exist to avoid these terms [102, 225–227], we emphasize that they affect significantly only the long-time dynamics, while being essentially inconsequential as far as the short-time behaviour we are considering here is concerned. An estimate of the time at which the contributions of Eq. (4.94) become important can be obtained by requiring them to be of the same order as the other couplings present in the action. Considering, for simplicity, the values of r, u_c and u_q at their fixed points in the deep-quench limit (4.86), one can readily derive the RG equations for $g_2^{A,B}$ from Eq. (4.94). Then, by identifying the dimensionless RG flow parameter ℓ with the time t elapsed since the quench, i.e., by setting $\ell = \ln(\Lambda t)$, one finds

$$\Lambda^{d-3} \frac{\mathrm{d} g_2^A}{\mathrm{d}(\Lambda t)} = \epsilon^2 \frac{N+6}{(N+8)^2} \frac{2}{a_d}, \tag{4.95}$$

$$\Lambda^{d-3} \frac{\mathrm{d} g_2^B}{\mathrm{d}(\Lambda t)} = \epsilon^2 \frac{1}{(N+8)^2} \frac{1}{a_d}. \tag{4.96}$$

Accordingly, for large N, the dissipative couplings $g_2^{A,B}(t)$ become of order one at time scales $\Lambda t_A^* \sim N/\epsilon^2$ and $\Lambda t_B^* \sim N^2/\epsilon^2$, respectively. Note, however, that corrections to $g_2^{A,B}$ are generated also for $d > 4$ (i.e., $\epsilon < 0$), when the coupling u_c is irrelevant: in fact, u_c still generates anyhow terms which are responsible for thermalization, providing thus an instance of a sort of *dangerously irrelevant* operator [219]. In this case, the time scales t_A^* and t_B^* are modified to $\Lambda t_A^* \sim N/(u_c^0)^2$ and $\Lambda t_B^* \sim N^2/(u_c^0)^2$, where u_c^0 indicates the microscopic value of the coupling constant u_c. Accordingly, for large values of N or small values of $\max\{\epsilon, u_c^0\}$, the dissipative vertices can be disregarded for quite long times after the quench.

4.5 Renormalization group: Callan-Symanzik approach

In spite of its transparent physical interpretation, the Wilson RG discussed in the previous section is not very practical for carrying out actual calculations. In fact, as we showed in Section 4.4, it still leaves a certain degree of arbitrariness in fixing the dimensions of all the fields and therefore one has to supplement the analysis with additional physical arguments, as we did in order to fix the upper critical dimensionality to $d_c = 4$. More severely, Wilson RG is limited in providing predictions of some critical exponents beyond one loop [228] and therefore different techniques have been developed for extending the RG analysis. In view of these difficulties, in this section we discuss the issue of the emergence of the short-time universal scaling within an alternative renormalization scheme, inspired by the well-established field-theoretical approach (see, e.g., Ref. [121]). The idea is to regularize the correlation functions of the relevant fields by redefining the couplings and the fields so as to remove the terms in perturbation theory which would be divergent upon increasing the ultraviolet cutoff Λ, suitably introduced into the original (bare) action. As a result, the effective action as well as all the correlation functions generated by it, once expressed in terms of these renormalized couplings and fields, is free of divergences. This renormalized action depends on the arbitrary scale μ which defines the momentum scale of the effective theory. Using the fact that the original correlation functions — determined by the bare action — are actually independent of μ, one can derive a Callan-Symanzik flow equation for the correlation functions which involves also the RG equations for the relevant couplings of the theory. Note that, because of the breaking of TTI induced by the quench, it is no longer viable to define a Fourier transform of the correlation functions and consequently the Callan-Symanzik equations discussed below will be derived for the correlation functions rather than the vertex functions which are usually introduced when TTI is not broken.

4.5.1 Renormalization of the initial fields

As anticipated above, the divergences upon increasing the cutoff Λ which emerge in perturbation theory, can be cancelled by a suitable renormalization of coupling constants and fields: in practice, this is achieved by calculating the relevant correlation functions at particular values of the times and momenta — the so-called normalization point (NP) — of the involved fields and by absorbing the resulting divergences in a redefinition of coupling and fields. In particular, we define the NP as times $t = \mu^{-1}$ and vanishing momenta $q = 0$ for all fields involved in the correlation function. For simplicity, we focus below on the critical point $r = r_c$, which, as shown in Sec. 4.2, is shifted away from its Gaussian value $r_c = 0$ because of the interaction.

We consider first the retarded Green's function $G_R(k,t,t') = \langle \phi_c(t)\phi_q(t')\rangle$, where, for the sake of simplicity, the indices of the field components have been suppressed and the fields inside the correlators are consequently assumed to refer to the same component For simplicity, the dependence on k is understood on the l.h.s. of the previous equality. As shown in App. 4.C, G_R is finite in the formal limit $\Lambda \to \infty$ as long as both times $t > t'$ do not vanish, while it grows $\propto \ln(\Lambda t)$ when the earlier time t' vanishes, i.e., when the involved quantum field is the one at the boundary $\boldsymbol{\phi}_{0q}$. In fact, at the normalization point,

$$\langle \phi_c(t)\phi_{0q}\rangle\big|_{\rm NP} = [1 - \theta_N \ln(\Lambda/\mu)] \times \text{finite terms}, \tag{4.97}$$

where by "finite terms" we mean an expression which is finite as $\Lambda \to \infty$. In order to reabsorb the logarithmic divergence in Eq. (4.97), we redefine the initial quantum field as $\boldsymbol{\phi}_{q0} = Z_0^{1/2}\boldsymbol{\phi}^R_{0q}$, where $\boldsymbol{\phi}^R_{q0}$ is the corresponding renormalized field and the renormalization constant Z_0 is determined such that the renormalized retarded Green's function $G^R_R(t,0) \equiv \langle \phi_c(t)\phi^R_{0q}\rangle = Z_0^{-1/2}G_R(t,0)$, remains finite as $\Lambda \to \infty$. This requires

$$Z_0^{1/2} = 1 - \theta_N \ln(\Lambda/\mu), \tag{4.98}$$

up to the lowest order in perturbation theory considered in this Chapter. Since Eq. (4.14) holds up to the same order, the renormalized Keldysh Green's function G^R_K can be simply defined as:

$$G^R_K(k,t,t') = \Omega_{0q}G^R_R(k,t,0)G^R_R(k,t',0) = Z_0^{-1}G_K(k,t,t'). \tag{4.99}$$

As shown in Sec. 4.2.1, the perturbative correction to $G_K(k,t,t')$ generates a term $\propto \ln(\Lambda/\mu)$ for generic values of the times t and t'. After the introduction of the renormalization constant as in Eq. (4.99), this logarithmic dependence is actually removed from G^R_K.

4.5.2 Renormalization of the coupling constant

In addition to the renormalizations introduced above, which render finite $G^R_{K,R}$, one has also to consider that the coupling constant u_c is renormalized by the interactions and that this renormalization is essential for determining the RG flow of the whole system. In order to determine it, we study the perturbative corrections to the four-point function $\langle \phi_{cj}(1)\phi_{ql}(2)\phi_{qm}(3)\phi_{qn}(4)\rangle$ to second order in u_c, where, with a more convenient notation, $\phi_{cj,qj}(n)$ denotes the j-component of the N-component field $\boldsymbol{\phi}_{c,q}$ calculated at the space-time point $n \equiv (\mathbf{x}_n, t_n)$. Taking into account the possible diagrams, one finds:

$\langle \phi_{cj}(1)\phi_{ql}(2)\phi_{qm}(3)\phi_{qn}(4)\rangle =$ 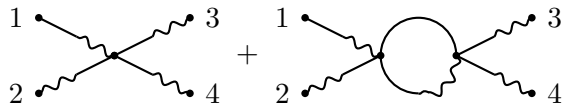

$$= \langle \phi_{cj}(1)\phi_{ql}(2)\phi_{qm}(3)\phi_{qn}(4)\left[1 - i\frac{2u_c}{4!N}\int_{1'}(\boldsymbol{\phi}_q\cdot\boldsymbol{\phi}_c)\boldsymbol{\phi}_c^2 - \frac{1}{2}\left(\frac{2u_c}{4!N}\right)^2\int_{1'}(\boldsymbol{\phi}_q\cdot\boldsymbol{\phi}_c)\boldsymbol{\phi}_c^2\int_{2'}(\boldsymbol{\phi}_q\cdot\boldsymbol{\phi}_c)\boldsymbol{\phi}_c^2\right]\rangle_0$$

$$\equiv I_0 + I_1 + I_2, \tag{4.100}$$

where the integrations run on the points indicated as $1'$ and $2'$ at which the arguments of the corresponding integrands are calculated, while I_m indicates the contribution of order u_c^m to that expansion.

Note that I_0 vanishes because, as a consequence of Wick's theorem, it is proportional to a two-point correlation of quantum fields $\langle\phi_q\phi_q\rangle_0 = 0$. The first order term I_1, instead, can be written as

$$\begin{aligned} I_1 &= -i\frac{2u_c}{4!N}\int_{1'}\langle\phi_{cj}(1)\phi_{ql}(2)\phi_{qm}(3)\phi_{qn}(4)(\boldsymbol{\phi}_q\cdot\boldsymbol{\phi}_c)\boldsymbol{\phi}_c^2(1')\rangle_0 \\ &= -i\frac{u_c}{6N}F_{jlmn}\int_{1'}G_{0R}(1,1')G_{0R}(1',2)G_{0R}(1',3)G_{0R}(1',4), \end{aligned} \tag{4.101}$$

where $F_{jlmn} = \delta_{jl}\delta_{mn} + \delta_{jm}\delta_{ln} + \delta_{jn}\delta_{lm}$. The calculation of I_2 is slightly more involved and it is reported in App. 4.G (see Eq. (4.191)). Among the many terms generated by the repeated use of Wick's theorem, we need to retain only those which renormalize the local vertex. After discarding the terms which do not fulfil this requirement, one finds (see Eq. (4.197))

$$I_2 = \frac{N+8}{36N}F_{jlmn}\,u_c^2\int_{1'}G_{0R}(1,1')G_{0R}(1',2)G_{0R}(1',3)G_{0R}(1',4)\int_{2'}G_{0K}(1',2')G_{0R}(1',2'). \tag{4.102}$$

Accordingly, adding I_1 to I_2, the four-point correlation function reads:

$$\langle\phi_{cj}(1)\phi_{ql}(2)\phi_{qm}(3)\phi_{qn}(4)\rangle = -i\frac{u_c}{6N}F_{jlmn}\int_{1'}G_{0R}(1,1')G_{0R}(1',2)G_{0R}(1',3)G_{0R}(1',4)(1+J), \tag{4.103}$$

where the integral J, for $d = 4$ and $\Lambda t \gg 1$ (see App. 4.G), is given by (see Eqs. (4.198) and (4.199))

$$J = \frac{N+8}{6N}u_c\int_{\mathbf{x}}\int_0^t \mathrm{d}t'\, iG_{0K}(\mathbf{x},t,t')G_{0R}(\mathbf{x},t-t') = -\frac{N+8}{24N}a_4u_c\Omega_{0q}\ln(\Lambda t). \tag{4.104}$$

Accordingly, by evaluating the four-point function in Eq. (4.100) at the normalization point, one finds

$$\langle\phi_c\phi_q\phi_q\phi_q\rangle\Big|_{\mathrm{NP}} = u_c\left[1 - u_c\Omega_{0q}\frac{N+8}{24N}a_4\ln(\Lambda/\mu)\right]\times\text{finite terms}. \tag{4.105}$$

In order to render this correlation function finite as $\Lambda\to\infty$, one introduces the dimensionless renormalized coupling constant g_R as

$$\frac{a_4}{16}\Omega_{0q}u_c = \mu^{4-d}Z_g g_R, \tag{4.106}$$

where the factor $a_4\Omega_{0q}/16$ (with $a_4 \equiv a_{d=4}$, as defined below Eq. (4.83)) is introduced for later convenience. Note that up to this order in perturbation theory, it is not necessary to introduce a renormalization of the bulk classical and quantum fields. Accordingly, one concludes that Z_g has to be chosen in such a way as to cancel the logarithmic dependence in Eq. (4.105) and therefore

$$Z_g = 1 + u_c\Omega_{0q}\frac{N+8}{24N}a_4\ln(\Lambda/\mu). \tag{4.107}$$

4.5.3 Renormalization-group (Callan-Symanzik) equations

Within the renormalization scheme discussed above, one can infer the renormalization-group equations by exploiting the arbitrariness of the scale μ which was introduced in order to renormalize the critical model. In fact, the original (bare) action is actually independent of the (infrared) scale μ and

therefore the logarithmic derivative with respect to μ of the corresponding bare coupling constants and correlation functions, once expressed in terms of the renormalized ones, has to vanish when taken with fixed bare coupling constants and cutoff Λ. By taking the logarithmic derivative $\mu\,\partial/\partial\mu$ of Eq. (4.106) one finds

$$\mu\frac{\partial g_R}{\partial\mu} \equiv \beta(g_R) = -\epsilon\, g_R + \frac{2}{3}\frac{N+8}{N}\, g_R^2, \tag{4.108}$$

where we used the fact that, from Eq. (4.106), $a_4\Omega_{0q}u_c\mu^{d-4}/16 = g_R + O(g_R^2)$, and we introduced $\epsilon \equiv 4-d$. Henceforth, the derivative with respect to μ is always understood as taken with fixed bare parameters. This β-function determines the flow of the coupling constant as the critical theory is approached for $\mu \to 0$ and it is characterized by a fixed-point value g_R^* such that $\beta(g_R^*) = 0$, with

$$g_R^* = \frac{3}{2}\frac{N}{N+8}\epsilon + O(\epsilon^2), \tag{4.109}$$

which is infrared (IR) stable for $d < 4$, while the Gaussian fixed point $g_R^* = 0$ becomes stable for $d > 4$.

In order to highlight the consequences of the existence of this fixed point on the correlation functions, we consider one which involves N_c and N_q classical and quantum fields in the bulk (i.e., with non-vanishing times), respectively, and N_0 initial quantum fields, which we schematically indicate as

$$G_{\{N\}} \equiv \langle [\phi_c]^{N_c}[\phi_q]^{N_q}[\phi_{0q}]^{N_0}\rangle = Z_c^{N_c/2}Z_q^{N_q/2}Z_0^{N_0/2}G^R_{\{N\}}. \tag{4.110}$$

Here $\{N\} = (N_c, N_q, N_0)$, $G^R_{\{N\}}$ indicates the same quantity $G_{\{N\}}$ expressed in terms of the renormalized fields, while $Z_{c,q}$ are the renormalization constants of the bulk fields with $Z_{c,q} = 1$ up to the order in perturbation theory which we are presently interested in. Note that any correlation function which involves a classical field taken at the boundary $t = 0$ vanishes in a deep quench because of the effective initial conditions on the classical field, see Eq. (4.12). By requiring that the logarithmic derivative of the l.h.s. of Eq. (4.110) with respect to the renormalization scale μ vanishes when taken at fixed bare parameters, and by expressing the r.h.s. in terms of renormalized quantities, one finds the Callan-Symanzik equation [195]

$$\left\{\mu\partial_\mu + \frac{N_c}{2}\gamma_c + \frac{N_q}{2}\gamma_q + \frac{N_0}{2}\gamma_0 + \beta\partial_g\right\} G^R_{\{N\}} = 0, \tag{4.111}$$

where we introduced the functions

$$\gamma_{c,q,0} \equiv \mu\,\partial_\mu \ln Z_{c,q,0}|_{\rm bare}. \tag{4.112}$$

At the lowest order in perturbation theory one has $\gamma_{c,q} = 0$, while

$$\gamma_0 = \frac{N+2}{3N}g_R + O(g_R^2), \tag{4.113}$$

which follows from Eq. (4.98). Equation (4.111) can be solved in full generality by employing the method of characteristics and, in conjunction with dimensional analysis, renders the scaling behaviour of the renormalized correlation function $G^R_{\{N\}}$. Note that, in principle, $G^R_{\{N\}}$ still depends on the

cut-off Λ. However, dimensional analysis done by using μ as the reference scale implies that $G^R_{\{N\}}$ actually depends on Λ/μ, which diverges as one explores the long-time and large-scale properties of the theory by letting $\mu \to 0$. However, the renormalizations introduced above in Secs. 4.5.1 and 4.5.2 were in fact determined such that this limit (formally $\Lambda \to \infty$) renders finite quantities. Accordingly, the leading scaling behaviour of the renormalized quantities can actually be obtained by removing their dependence on Λ, i.e., by assuming $\Lambda \gg \mu$ For simplicity, we focus here on the scaling behaviour emerging at the fixed point g^*_R (see Eq. (4.109)) of the coupling constant. Accordingly, Eq. (4.111) simplifies as

$$\left\{\mu\partial_\mu + \frac{N_0}{2}\gamma_0^*\right\} G^R_{\{N\}}(\{k,t\};\mu) = 0, \tag{4.114}$$

where

$$\gamma_0^* = \frac{\epsilon}{2}\frac{N+2}{N+8} + O(\epsilon^2) \tag{4.115}$$

indicates the value of γ_0 calculated at the fixed point. In order to exploit the consequences of dimensional analysis, we define the dimensionless renormalized Green's functions $\hat{G}^R_{\{N\}}$ in the momentum-time representation

$$G^R_{\{N\}}(\{k,t\};\mu) = \mu^{d^{\mathbf{k}}_{\{N\}}} \hat{G}^R_{\{N\}}\left(\{k/\mu, \mu t\}\right), \tag{4.116}$$

where $\{k,t\}$ indicates the set of times and momenta at which the various fields are calculated, while $d^{\mathbf{k}}_{\{N\}}$ takes into account the canonical scaling of the fields in momentum space and of the delta functions which ensure momentum conservation, i.e.,

$$d^{\mathbf{k}}_{\{N\}} = d + N_c\zeta^{\mathbf{k}}_c + N_q\zeta^{\mathbf{k}}_q + N_0\zeta^{\mathbf{k}}_{q0} + \dots. \tag{4.117}$$

Note that the r.h.s. of Eq. (4.116) is calculated with the dimensionless parameters corresponding to those appearing on the l.h.s. The factors $\zeta^{\mathbf{k}}_c, \zeta^{\mathbf{k}}_q$ and $\zeta^{\mathbf{k}}_{q0}$ denote the canonical scaling of the classical, quantum in the bulk and quantum at the surface fields in momentum space and, from Sec. 4.4.1, they read

$$\zeta^{\mathbf{k}}_c = -\frac{d+2}{2}, \qquad \zeta^{\mathbf{k}}_q = \zeta^{\mathbf{k}}_{q0} = -\frac{d}{2}. \tag{4.118}$$

The dots in Eq. (4.117) account for the possibility of including derivatives of the fields into the correlation functions (4.110): they scale differently from the fields and therefore they would add new contributions to $d^{\mathbf{k}}_{\{N\}}$. Accordingly, by inserting Eq. (4.116) in Eq. (4.114), one finds

$$\left\{\mu\partial_\mu + d^{\mathbf{k}}_{\{N\}} + \frac{N_0}{2}\gamma_0^*\right\} \hat{G}^R_{\{N\}}\left(\{k/\mu, \mu t\}\right) = 0. \tag{4.119}$$

Using the method of characteristics it is possible to transform this partial differential equation into an ordinary one in terms of an arbitrary dimensionless parameter l:

$$\left\{l\frac{\mathrm{d}}{\mathrm{d}l} + d^{\mathbf{k}}_{\{N\}} + \frac{N_0}{2}\gamma_0^*\right\} \hat{G}^R_{\{N\}}\left(\{k/(\mu l), \mu l\, t\}\right) = 0, \tag{4.120}$$

the solution of which is simply given by

$$l^{N_0\gamma_0^*/2 + d^{\mathbf{k}}_{\{N\}}} \hat{G}^R_{\{N\}}\left(\left\{\frac{k}{\mu l}, \mu l t\right\}\right) = \hat{G}^R_{\{N\}}\left(\left\{\frac{k}{\mu}, \mu t\right\}\right), \tag{4.121}$$

which expresses nothing but the fact that the correlation function is a homogeneous (i.e., scale-invariant) function of its argument, as expected at the critical point. Specializing this general expression to the case of the retarded function G_R^R with two fields in the bulk (i.e., $G_{\{N\}}^R$ with $N_0 = 0$, $N_c = N_q = 1$) one finds, at sufficiently long times:

$$G_R^R(k,t,t') = l^{-1} G_R^R\left(k/l, lt, lt'\right). \tag{4.122}$$

When, instead, one of the fields is at the boundary ($N_q = 0$ and $N_c = N_0 = 1$) one finds

$$G_R^R(k,t,0) = l^{-1+\gamma_0^*/2} G_R^R\left(k/l, lt, 0\right). \tag{4.123}$$

The scaling of G_K can be thus inferred on the basis of Eq. (4.99) with the aid of Eq. (5.7a), which yield

$$G_K^R(k,t,t') = l^{-2+\gamma_0^*} G_K^R\left(k/l, lt, lt'\right). \tag{4.124}$$

The scaling forms in Eqs. (4.122), (4.123), and (4.124) are consistent with those inferred from the perturbation theory in Sec. 4.2.1, with the identification

$$\theta_N = \frac{\gamma_0^*}{2} = \frac{\epsilon}{4}\frac{N+2}{N+8} + O(\epsilon^2). \tag{4.125}$$

For example, by choosing $l \sim (\Lambda t)^{-1} \ll 1$ in Eq. (4.123), one finds $G_R^R(k,t,0) = t^{1-\gamma_0^*/2} G_R^R(kt,1,0)$, which is nothing but the resummed version of the perturbative result reported in Eq. (4.31).

The Callan-Symanzik equation (4.111) alone does not provide information on the two-time scaling suggested in Eq. (4.29), which actually emerges as a consequence of the fact that the smaller time t' approaches the "surface" $t' = 0$ at which the anomalous dimension of the field $\boldsymbol{\phi}_{0q}$ differs from the one of the quantum field $\boldsymbol{\phi}_q$ in the bulk. In order to work out the consequences of this fact, we consider here the equivalent of the standard short-distance expansion of quantum field theory [195,229] adapted to $\phi_q(t')$ at short times [146], which we assume to be valid for $t' \to 0$:

$$\phi_q(t') = \sum_{i \geq 0} \sigma_{i,q}(t') O_i, \tag{4.126}$$

where O_i indicates operators located at the surface, ordered such that their scaling dimension increases upon increasing i, while $\sigma_{i,q}(t')$ are functions of t'. In the limit $t' \to 0$, this sum is dominated by the most relevant term O_0, which is ϕ_{0q}, and therefore we can simply write Eq. (4.126) as $\phi_q(t') \simeq \sigma_q(t')\phi_{0q}$, where we dropped the terms of the expansion which are less singular as $t' \to 0$. The scaling form of $\sigma_q(t')$ can be derived by inserting this expansion in Eq. (4.121) and by reading out the scaling behavior, which turns out to be

$$\sigma_q(t') = l^{-\gamma_0^*/2} \sigma_q(lt'), \tag{4.127}$$

at the critical point. Finally, by using Eqs. (4.123) and (4.127), one finds:

$$G_R(k,t,t' \to 0) \simeq \sigma_q(t') G_R(k,t,0) = t \left(\frac{t'}{t}\right)^{\gamma_0^*/2} G_R(kt,1,0), \tag{4.128}$$

which is the resummed version of Eq. (4.29), taking into account the relationship between γ_0^* and θ_N in Eq. (4.125). Equations (4.123), (4.124) and (4.128) demonstrate that the resummation of the leading logarithms which emerge in perturbation theory and which we did somewhat arbitrarily in Sec. 4.2, is fully justified by the existence of an IR-stable fixed point for the flow of the coupling constant.

4.5.4 Scaling of magnetization

The approach developed above can be conveniently used in order to determine the scaling form of the magnetization $M(t) \equiv M_1(t) = \langle \boldsymbol{\phi}_1(\mathbf{x}, t) \rangle$ in the presence of a symmetry-breaking term in the pre-quench Hamiltonian H_0, which was discussed in Sec. 4.3 either within perturbation theory or in the exactly solvable limit $N \to \infty$. In fact, Eq. (4.54) (which is valid beyond perturbation theory) can be expanded in powers of M_0, assuming a homogeneous external field $\mathbf{h}$ with the components given in Eq. (4.57); focussing on the components of the fields along direction 1 of the initial field $\mathbf{h}$, this yields

$$M(t) = \sum_{n=1}^{+\infty} \frac{(-i\sqrt{2}M_0)^n}{n!} \int \mathrm{d}^d x_1 \cdots \mathrm{d}^d x_n \langle \phi_c(\mathbf{x}, t) \dot{\phi}_{0q}(\mathbf{x}_1) \cdots \dot{\phi}_{0q}(\mathbf{x}_n) \rangle_{h=0}, \tag{4.129}$$

(the term with $n = 0$ in the previous expansion vanishes due to the choice of the initial condition) from which it follows that the scaling of $M(t)$ is related to that one of correlation functions containing the initial field $\dot{\phi}_{0q} \equiv \dot{\phi}_q(t = 0)$. Note that due to spatial translational invariance, the r.h.s. of Eq. (4.129) is actually independent of $\mathbf{x}$. In fact, the logarithmic dependence on Λ of the one-loop correction to the magnetization pointed out in Sec. 4.3 (see, in particular, Eq. (4.61)) can be suitably cancelled (according to the approach discussed in this section) with a renormalization of $\dot{\phi}_{0q} = Z_{\dot{0}}^{1/2} \dot{\phi}_{0q}^R$, where a simple calculation gives

$$Z_{\dot{0}} = 1 + 2\theta_N \ln(\Lambda/\mu). \tag{4.130}$$

Note that $Z_{\dot{0}}$ differs from Z_0 in Eq. (4.98), which means that the anomalous dimension (defined as in Eq. (4.112))

$$\gamma_{\dot{0}} \equiv \mu \partial_\mu \ln Z_{\dot{0}}|_{\mathrm{bare}} = -\frac{N+2}{3N} g_R + O(g_R^2) \tag{4.131}$$

of $\dot{\phi}_{0q}$ is different from that one of ϕ_{0q}, i.e., from γ_0 in Eq. (4.113). Accordingly, when $\gamma_{\dot{0}}$ is evaluated at the fixed point g_R^* reported in Eq. (4.109), it renders:

$$\gamma_{\dot{0}}^* = -\frac{\epsilon}{2} \frac{N+2}{N+8} + O(\epsilon^2) = -2\theta_N. \tag{4.132}$$

Following the same line of argument as in Sec. 4.5.3, one can easily derive a Callan-Symanzik equations for the correlations functions appearing on the r.h.s. of Eq. (4.129), which are of the form of Eq. (4.110) but with the fields ϕ_{0q} replaced by $\dot{\phi}_{0q}$ and, correspondingly, γ_0 by $\gamma_{\dot{0}}$ in the equations which follow. At the critical point, one eventually finds the scaling equation

$$l^{d^{\mathbf{x}}_{\{N\}} - n\theta_N} \langle \phi_c(lt, l\mathbf{x}) \dot{\phi}_{0q}(l\mathbf{x}_1) \cdots \dot{\phi}_{0q}(l\mathbf{x}_n) \rangle = \langle \phi_c(t, \mathbf{x}) \dot{\phi}_{0q}(\mathbf{x}_1) \cdots \dot{\phi}_{0q}(\mathbf{x}_n) \rangle, \tag{4.133}$$

where $d^{\mathbf{x}}_{\{N\}}$ accounts for the canonical scaling dimension of the fields in real space and reads:

$$d^{\mathbf{x}}_{\{N\}} = N_c \zeta_c^{\mathbf{x}} + N_{\dot{0}} \zeta_{\dot{0}}^{\mathbf{x}} = [d - 2 + n(d+2)]/2, \tag{4.134}$$

for $N_c = 1$ and $N_{\dot{0}} = n$, while $\zeta_c^{\mathbf{x}} = (d-2)/2$ and $\zeta_{\dot{0}}^{\mathbf{x}} = (d+2)/2$ are, respectively, the canonical scaling dimensions of the fields ϕ_c and $\dot{\phi}_q$ in real space, which can easily be determined from Sec. 4.4.1 by noticing that $\dot{\phi}_{0q}$ has the same dimension as $\mu\phi_{0q}$, where μ is an arbitrary momentum scale, see

Eq. (4.74). Substituting Eq. (4.133) into Eq. (4.129) one obtains, after a change of variables in the spatial integrals:

$$M(t) = l^{d/2-1} \sum_{n=1}^{+\infty} \frac{(-i\sqrt{2})^n}{n!} \left(l^{-d/2+1-\theta_N} M_0 \right)^n \times \int \mathrm{d}^d x_1 \cdots \mathrm{d}x_n \langle \phi_c(lt, l\mathbf{x}) \dot{\phi}_{0q}(l\mathbf{x}_1) \cdots \dot{\phi}_{0q}(l\mathbf{x}_n) \rangle_{h=0} \tag{4.135}$$

from which, by choosing $l = (\Lambda t)^{-1}$ at long times $t \gg \Lambda^{-1}$, we find a scaling form for the magnetization:

$$M(t) = M_0 \, t^{\theta_N} \, \mathcal{M} \left(t^{d/2-1+\theta_N} M_0 \right). \tag{4.136}$$

This results entails the existence of a time scale $t_i \sim M_0^{1/(d/2-1+\theta_N)}$ at which the increasing of the magnetization $M(t) \propto t^{\theta_N}$ switches to a different behaviour. For $d \to 4$, this result is in agreement with the t_i estimated in Sec. 4.3 for the critical quench of the $O(N)$ model for $N \to \infty$ (see Eq. (4.72)).

4.6 Concluding remarks

In this Chapter we investigated the effects of fluctuations on the dynamical transition beyond mean-field theory which is observed after a quench of the parameters of an isolated quantum many-body system with $O(N)$ symmetry. In particular, we accounted for fluctuations at the lowest order in the post-quench coupling constant, extending the analysis of Ref. [2] to the spatio-temporal structure of response and correlation functions and to the dynamics of the order parameter, while providing the details of the results anticipated therein. We found that, before thermalization eventually occurs as a consequence of the interaction which is switched on upon quenching, the system approaches a pre-thermal state within which it undergoes a dynamical transition. We have characterized this transition within a Wilson's renormalization-group approach, showing that it is associated with a stable fixed point of the RG flow of the relevant control parameters and that it displays remarkable analogies with the corresponding equilibrium phase transition at finite temperature. Nevertheless, the breaking of the invariance of the dynamics under time translations caused by the quench induces a novel algebraic and universal behavior at short times with new features compared to the classical case. This universal short-time behavior is characterized by a new critical exponent θ_N calculated here to the leading order in a dimensional expansion [see Sec. 4.4, Eq. (4.91)]. This result is found in agreement with the expression of the one for a critical quench of the $O(N)$ model in the limit $N \to \infty$ [see Sec. 4.3, Eq. (4.71)], in which the model is exactly solvable. The correlation functions after the quench are characterized by scaling forms which depend on the exponent θ_N and which we determined by using Callan-Symanzik equations [see Sec. 4.5.3, Eq. (4.120)]. Moreover, when an external field breaks the $O(N)$ symmetry of the initial state (restored after the quench), the dynamics of the order parameter exhibits an algebraic growth, controlled by the initial-slip exponent θ_N, up to a certain macroscopic time t_i [see Sec. 4.5.4, Eq. (4.136)].

This slow dynamics, which is referred to as aging, is very similar to the one occurring in both classical dissipative systems and open quantum system, though it belongs to a different universality class and is characterized by different scaling forms (see Appendix of Ref. [1]). Among these differences,

the most marked ones concern the spatio-temporal dependence of the correlation functions, since they exhibit here a light cone due to ballistically propagating excitations in the prethermal state [see Sec. 4.2.3 and Figs. 4.2 and 4.3].

Another difference between the open and closed quantum system is that for the latter, entanglement entropy of the unitarily evolving state is a good measure of quantum correlations, and a recent study showed how the aging exponent entering here, also controls the scaling of the entanglement spectrum [230].

As a future perspective, the study of the destabilization of the prethermal regime and the resulting crossover towards the full thermalization represents an interesting question as well as a technical challenge. In fact, as discussed in Sec. 4.4.3, the inclusion of the effect of two-loop diagrams becomes intractable within the usual perturbative techniques because of the appearance of secular terms, and therefore more elaborate resummation schemes are required. Moreover, the study of aging in fermionic systems represents an important issue, also because the classical limit of these systems is far from trivial, and therefore their genuinely quantum nature is expected to bear completely new features.

Appendix

4.A Functional derivation of Green's functions

In this Appendix we show how to derive the Green's functions $G_{0K,0R}$ in Eqs. (2.15a) and (2.15b) from the Gaussian part of the action (4.8), (4.9) considered in Sec. 4.1. In order to do this, one introduces additional terms in the Keldysh action, in which the various fields are coupled linearly to some external sources $\mathbf{j}_{c,q}$ and $\mathbf{j}_{0c,0q}$. Accordingly, any correlation function can be obtained by differentiating the generating function

$$\mathcal{Z}_K[\{\mathbf{j}\}] = \int D[\boldsymbol{\phi}_c, \boldsymbol{\phi}_q, \boldsymbol{\phi}_{0c}, \boldsymbol{\phi}_{0q}]\, \mathrm{e}^{iS} = \mathrm{e}^{W[\{\mathbf{j}\}]}. \tag{4.137}$$

where $\{\mathbf{j}\} \equiv (\mathbf{j}_c, \mathbf{j}_q, \mathbf{j}_{0c}, \mathbf{j}_{0q})$. If one were interested in calculating correlation functions which involve $\dot{\boldsymbol{\phi}}_{0c}$ or $\dot{\boldsymbol{\phi}}_{0q}$, additional sources should be coupled to these fields. It turns out that the intermediate results of the actual calculation of W do depend on whether one integrates out first $\boldsymbol{\phi}_c$ or $\boldsymbol{\phi}_q$, as shown below; however, the final result is the same. First let us integrate out $\boldsymbol{\phi}_q$: in order to do this, we integrate by parts the time derivatives in the bulk action in Eq. (4.9), as

$$\begin{aligned} S_K = {} & i \int_{\mathbf{k}} \frac{\omega_{0k}}{2} \left[\boldsymbol{\phi}_{0c}^2 \, \tanh\left(\beta\omega_{0k}/2\right) + \boldsymbol{\phi}_{0q}^2 \, \coth\left(\beta\omega_{0k}/2\right) \right] \\ & - i \int_{\mathbf{k}} \left[\mathbf{j}_{0c} \, \boldsymbol{\phi}_{0q} + \mathbf{j}_{0q} \, \boldsymbol{\phi}_{0c} - i \boldsymbol{\phi}_{0q} \, \dot{\boldsymbol{\phi}}_{0c} \right] + \int_{\mathbf{k}} \int_0^\infty \mathrm{d}t \, \left[-\boldsymbol{\phi}_q \left(\ddot{\boldsymbol{\phi}}_c + \epsilon \dot{\boldsymbol{\phi}}_c + \omega_k^2 \boldsymbol{\phi}_c - \mathbf{j}_c \right) + \mathbf{j}_q \, \boldsymbol{\phi}_c \right]. \end{aligned} \tag{4.138}$$

where we set $\Omega_{0c} = \Omega_{0q} = \Omega_0$ for the sake of simplicity and we defined $\mathbf{j}_{0c} \, \boldsymbol{\phi}_{0q} = \mathbf{j}_{0c} \cdot \boldsymbol{\phi}_{0q}$. Note that the integration by parts generates an additional term $-i\boldsymbol{\phi}_{0q}\dot{\boldsymbol{\phi}}_{0c}$ in the part of the action located at $t = 0$ and that we added to S_K an infinitesimal term proportional to $\epsilon > 0$. This term contains the operator $\boldsymbol{\phi}_q\dot{\boldsymbol{\phi}}_c$, and therefore it can be regarded as an infinitesimal dissipation [215]. The reason for including it is twofold, as it regularizes the Keldysh functional while ensuring causality. Notice also that such a term breaks the exchange symmetry $\boldsymbol{\phi}_c \leftrightarrow \boldsymbol{\phi}_q$ of the bulk action, which holds for $\mathbf{j}_c = \mathbf{j}_q = 0$. The integration of $\boldsymbol{\phi}_q$ generates a functional delta function the support of which is on the solution $\bar{\boldsymbol{\phi}}_c$ of the equation

$$\left(\partial_t^2 + \epsilon \, \partial_t + \omega_k^2\right) \bar{\boldsymbol{\phi}}_c = \mathbf{j}_c, \tag{4.139}$$

i.e., on

$$\bar{\boldsymbol{\phi}}_c(t) = \boldsymbol{\phi}_{0c} \, \mathrm{e}^{-\epsilon t} \cos(\omega_k t) + \mathrm{e}^{-\epsilon t} \dot{\boldsymbol{\phi}}_{0c} \, \frac{\sin(\omega_k t)}{\omega_k} + \int_0^t \mathrm{d}t' \, \frac{\mathrm{e}^{-\epsilon t} \sin[\omega_k (t - t')]}{\omega_k} \mathbf{j}_c(t'), \tag{4.140}$$

where $\boldsymbol{\phi}_{0c} \equiv \boldsymbol{\phi}_c(t=0)$ and $\dot{\boldsymbol{\phi}}_{0c} \equiv \dot{\boldsymbol{\phi}}_c(t=0)$. Note that in Eq. (4.140) one can safely take the limit $\epsilon \to 0$. Then, we expand $\boldsymbol{\phi}_c$ around $\bar{\boldsymbol{\phi}}_c$ and we integrate out the Gaussian fluctuations of $(\boldsymbol{\phi}_c - \bar{\boldsymbol{\phi}}_c)$. Finally, we integrate out the remaining fields $\boldsymbol{\phi}_{0c}$, $\boldsymbol{\phi}_{0q}$ and $\dot{\boldsymbol{\phi}}_c$, finding

$$W[\{\mathbf{j}\}] = \int_{\mathbf{k}} \left\{ \frac{1}{2}\,\mathbf{j}_{0q}^2\, iG_{0K}(k,0,0) - \int_t \left[\mathbf{j}_{0q}\,\mathbf{j}_q(t)\,G_{0K}(k,t,0) + \mathbf{j}_{0c}\,\mathbf{j}_q(t)\,G_{0R}(k,t,0)\right] \right.$$
$$\left. - \int_{t,t'} \left[\mathbf{j}_q(t)\,\mathbf{j}_c(t')\,iG_{0R}(k,t,t') + \frac{1}{2}\,\mathbf{j}_q(t)\mathbf{j}_q(t')iG_{0K}(k,t,t')\right]\right\}, \tag{4.141}$$

where $\int_t = \int_0^\infty \mathrm{d}t$ and G_{0R}, G_{0K} are those defined in Eqs. (2.15a) and (2.15b) and indeed they can be obtained by taking suitable functional derivatives of this $W[\{\mathbf{j}\}]$, which establish the connection between these functions $G_{0K,0R}$ and the correlation functions of the fields. Consider now the case in which $\boldsymbol{\phi}_c$ and $\boldsymbol{\phi}_q$ are integrated in the reversed order: we rewrite S_K as

$$S_K = i\int_{\mathbf{k}} \frac{\omega_{0k}}{2}\left[\boldsymbol{\phi}_{0c}^2\,\tanh\left(\beta\omega_{0k}/2\right) + \boldsymbol{\phi}_{0q}^2\,\coth\left(\beta\omega_{0k}/2\right)\right]$$
$$- i\int_{\mathbf{k}} \left[\mathbf{j}_{0c}\,\boldsymbol{\phi}_{0q} + \mathbf{j}_{0q}\,\boldsymbol{\phi}_{0c} - i\boldsymbol{\phi}_{0c}\,\dot{\boldsymbol{\phi}}_{0q}\right] + \int_{\mathbf{k}}\int_0^\infty \mathrm{d}t\,\left[-\boldsymbol{\phi}_c\left(\ddot{\boldsymbol{\phi}}_q - \epsilon\dot{\boldsymbol{\phi}}_q + \omega_k^2\boldsymbol{\phi}_q - \mathbf{j}_q\right) + \mathbf{j}_c\,\boldsymbol{\phi}_q\right], \tag{4.142}$$

where the additional term generated in the action located at $t = 0$ is different from the one in Eq. (4.138). Note that, as in Eq. (4.138) we introduced an infinitesimal term with $\epsilon > 0$. The integration of $\boldsymbol{\phi}_c$ generates a delta function the support of which is on the solution of the equation:

$$(\partial_t^2 - \epsilon\,\partial_t + \omega_k^2)\bar{\boldsymbol{\phi}}_q = \mathbf{j}_q, \tag{4.143}$$

i.e., on

$$\bar{\boldsymbol{\phi}}_q(t) = \boldsymbol{\phi}_{0q}\,\mathrm{e}^{\epsilon t}\,\cos(\omega_k t) + \dot{\boldsymbol{\phi}}_{0q}\,\mathrm{e}^{\epsilon t}\,\frac{\sin(\omega_k t)}{\omega_k} + \int_0^t \mathrm{d}t'\,\frac{\sin[\omega_k(t-t')]}{\omega_k}\mathbf{j}_q(t'), \tag{4.144}$$

Note that, differently from Eq. (4.140), the infinitesimal term $\propto \epsilon$ generates an exponential factor which makes $\bar{\boldsymbol{\phi}}_q$ grow exponentially in time. In order to avoid this unphysical divergence, we have to impose $\bar{\boldsymbol{\phi}}_q(t \to +\infty) = 0$, which fixes the value of $\boldsymbol{\phi}_{0q}$ and $\dot{\boldsymbol{\phi}}_{0q}$ to

$$\boldsymbol{\phi}_{0q} = \int_0^{+\infty} \mathrm{d}t\,\frac{\sin(\omega_k t)}{\omega_k}\,\mathrm{e}^{-\epsilon t}\,\mathbf{j}_q(t), \tag{4.145}$$

$$\dot{\boldsymbol{\phi}}_{0q} = -\int_0^{+\infty} \mathrm{d}t\,\cos(\omega_k t)\,\mathrm{e}^{-\epsilon t}\,\mathbf{j}_q(t), \tag{4.146}$$

from which Eq. (4.144) can be rewritten as

$$\bar{\boldsymbol{\phi}}_q(t) = -\int_t^{+\infty} \mathrm{d}t'\,\frac{\sin[\omega_k(t-t')]}{\omega_k}\,\mathrm{e}^{\epsilon(t-t')}\,\mathbf{j}_q(t'). \tag{4.147}$$

Due to the fact that $t' > t$, the limit $\epsilon \to 0$ can now be safely taken in this last expression. Finally, we expand $\boldsymbol{\phi}_q$ around $\bar{\boldsymbol{\phi}}_q$ and integrate out the Gaussian fluctuations, we replace the values of $\boldsymbol{\phi}_{0q}$ and $\dot{\boldsymbol{\phi}}_{0q}$ with Eqs. (4.145) and (4.146) in the surface action and we eventually integrate out $\boldsymbol{\phi}_{0c}$. The final result is the same W as the one given in Eq. (4.141).

4.B Relationship between G_K and G_R in a deep quench

In this Appendix we show that Eq. (4.14), which connect G_K and G_R for a deep quench, is valid to all orders in perturbation theory if the Keldysh self-energy Σ_K defined below vanishes. This is the case, e.g., in the limit $N \to \infty$ of the present model, discussed in Ref. [1].

To show this, we recall that the Dyson equation [215] for the post-quench propagator G of a theory in the presence of interaction can be written symbolically as

$$\left(G_0^{-1} - \Sigma\right) G = 1, \tag{4.148}$$

in terms of the post-quench Gaussian propagator G_0 and of the self-energy Σ of the system after the quench. In turn, G and Σ for a Keldysh action have the structure

$$G = \begin{pmatrix} G_K & G_R \\ G_A & 0 \end{pmatrix}, \quad \Sigma = \begin{pmatrix} 0 & \Sigma_A \\ \Sigma_R & \Sigma_K \end{pmatrix}, \tag{4.149}$$

and analogous for the Gaussian propagator. The functions Σ_K and Σ_R are, respectively, the Keldysh and retarded self-energies, which fully encode the effect of the interaction $u_{c,q}$. Equation (4.148) is actually a shorthand notation for a set of integral equations of the form (we drop the dependence on the momentum variables $\mathbf{k}$ since the equations are local in $\mathbf{k}$)

$$\begin{aligned} G_K(t,t') = G_{0K}(t,t') &+ \int_{t_1,t_2} G_{0R}(t,t_1)\Sigma_K(t_1,t_2)G_R(t',t_2) \\ &+ \int_{t_1,t_2} G_{0R}(t,t_1)\Sigma_R(t_2,t_1)G_K(t_2,t') + \int_{t_1,t_2} G_{0K}(t,t_1)\Sigma_R(t_1,t_2)G_R(t',t_2), \end{aligned} \tag{4.150}$$

and

$$\begin{aligned} G_R(t,t') &= G_{0R}(t,t') + \int_{t_1 t_2} G_{0R}(t_1,t')\Sigma_R(t_1,t_2)G_R(t,t_2) \\ &= G_{0R}(t,t') + \int_{t_1 t_2} G_R(t_1,t')\Sigma_R(t_1,t_2)G_{0R}(t,t_2). \end{aligned} \tag{4.151}$$

In the last equality we have expressed the equation in an equivalent form in which G_R and G_{0R} are interchanged, which corresponds to a different order in the resummation of the one-particle irreducible diagrams contributing to Σ. In order to simplify the notation, we do not indicate here the two indices of the components of the fields involved in these $G_{R,K}$, $G_{0R,0K}$ and Σ_R, as they are all diagonal in component space. In order to prove Eq. (4.14), we assume that $\Sigma_K = 0$ and that, within the Gaussian approximation, G_{0K} and G_{0R} are related via

$$iG_{0K}(t,t') = \Omega_0 G_{0R}(t,0)G_{0R}(t',0), \tag{4.152}$$

which holds for the case we are interested in, see Eqs. (2.15a) and (2.15b). Then, we prove that the function $iG_K^T(t,t') \equiv \Omega_0 G_R(t,0)G_R(t',0)$ satisfies the same equation as G_K, and therefore they have

to be equal, i.e., $iG_K(t,t') = iG_K^T(t,t') = \Omega_0 G_R(t,0)G_R(t',0)$, since the Dyson equation is linear. In fact, by using Eq. (4.151), one can rewrite $G_K^T(t,t')$ as:

$$iG_K^T(t,t') = \Omega_0 G_{0R}(t,0)G_{0R}(t',0) + \Omega_0 \int_{t_1 t_2} G_{0R}(t,0)G_{0R}(t_1,0)\Sigma_R(t_1,t_2)G_R(t',t_2) + \Omega_0 \int_{t_1 t_2} G_R(t',0)G_R(t_1,0)\Sigma_R(t_1,t_2)G_{0R}(t,t_2). \quad (4.153)$$

The relation (4.152) between G_{0K} and G_{0R} implies, after an exchange of the integration variables t_1 and t_2 in the last integral of the previous equation, that

$$G_K^T(t,t') = G_{0K}(t,t') + \int_{t_1 t_2} G_{0K}(t,t_1)\Sigma_R(t_1,t_2)G_R(t',t_2) + \int_{t_1 t_2} G_{0R}(t,t_1)\Sigma_R(t_2,t_1)G_K^T(t',t_2), \quad (4.154)$$

which is exactly Eq. (4.150) satisfied by G_K under the assumption that $\Sigma_K = 0$.

An alternative derivation of the same result is the following: Thinking of Ω_0 as a perturbative parameter, one can now include perturbatively its effects in Σ. In particular, Σ_K then accounts for the Gaussian term $\propto \Omega_0$ while G_0 includes only G_{0R}, which is not proportional to Ω_0, while $G_{0K} = 0$ — see Eqs. (2.15a) and (2.15b). Accordingly, Eq. (4.148) implies the integral equation

$$G_K(t,t') = \int_{t_1,t_2} G_R(t,t_1)G_R(t',t_2)\Sigma_K(t_1,t_2), \quad (4.155)$$

which holds regardless of whether interactions are present or not. Note that, in the absence of interactions, Eq. (4.155) implies

$$\Sigma_K^0(t,t') = -i\Omega_0 \delta(t-t')\delta(t), \quad (4.156)$$

because of Eq. (4.152), where Σ_K^0 can be thought of as a Keldysh "self-energy" at the zeroth order in the interactions, but which, in fact, simply accounts for the initial distribution after the quench, and it emerges naturally from discretizing the Keldysh action in time and from accounting for the initial density matrix [215]. Under the assumption that the interaction introduced by $u_c \neq 0$ does not affect Σ_K (a condition which we expressed in the derivation above as $\Sigma_K = 0$) — which therefore equals its Gaussian value Σ_K^0 — one obtains immediately Eq. (4.14).

4.C Renormalization of G_R in momentum space at initial times

In this section we show how a logarithmic dependence on the large cutoff Λ appears in the retarded Green's function $G_R(q,t,t')$ in perturbation theory at one-loop when the earlier time t' is set at the temporal boundary, i.e., with $t' = 0$. Let us focus on Eq. (4.22), which expresses the perturbative correction δG_R to G_R, and assume that the time-independent part B_0 of the tadpole $i\mathcal{T}$ (see Eq. (4.16)) has been reabsorbed in a proper redefinition of the parameter r, according to Eq. (4.24). Due to the causal structure of G_R, the domain of integration in Eq. (4.22) is effectively restricted to the interval $t' \leq \tau \leq t$ and therefore the integral is finite for $\Lambda \to +\infty$ as long as $t' \neq 0$, because the only possible

source of singularity associated with $B(\tau) \sim \tau^{-2}$ in Eq. (4.19) is located at $\tau = 0$, see Eq. (4.21). On the other hand, if $t' = 0$, Eq. (4.22) renders, at the critical point $r = r_c$,

$$\delta G_R(t,0) = \int_0^{t_2} \mathrm{d}t\, G_{0R}(q,t_2,t) B(t) G_{0R}(q,t,0) \equiv I_R(t), \tag{4.157}$$

in which one cannot take $\Lambda \to +\infty$ in $B(\tau)$ from the outset, but this can be done only after a convenient subtraction of the singular term $\sim 1/\tau^2$ has been introduced in the integral $I_R(t)$. Since $G_{0R}(q,\tau,0) = -\tau + O(\tau^2)$ and $G_{0R}(q,t,\tau) = G_R(q,t,0) + O(\tau)$, a convenient way of writing $I_R(t)$ and of introducing the subtraction is

$$I_R(t) = \int_0^t \mathrm{d}\tau \left[G_{0R}(q,t,\tau) G_{0R}(q,\tau,0) + G_{0R}(q,t,0)\ \tau \right] B(\tau) - G_{0R}(q,t,0) \int_0^t \mathrm{d}\tau\, \tau B(\tau), \tag{4.158}$$

where the first integral on the r.h.s. is finite for $\Lambda \to +\infty$, given that the term within square brackets vanishes $\sim \tau^2$ as $\tau \to 0$ and therefore regularizes the singularity that $B(\tau)$ develops as Λ grows. The second integral, instead, can be explicitly calculated by using the explicit expression of $B(t)$ in Eq. (4.19) and it gives

$$\int_0^t \mathrm{d}\tau\, \tau B(\tau) = -\theta_N \int_0^{\Lambda t} \mathrm{d}\tau\, \tau \frac{1-\tau^2}{(\tau^2+1)^2} = \theta_N \ln(\Lambda t) + \text{finite terms}, \tag{4.159}$$

where θ_N is given in Eq. (4.20) and the terms which have been omitted are finite as Λt increases. Accordingly, a logarithmic divergence proportional to $G_R(q,t,0)$ occurs in $I_R(t)$ in the limit $\Lambda \to +\infty$.

4.D Renormalization of G_K in momentum space

In this section we provide some details of the calculation of the one-loop correction $\delta i G_K$ to the Keldysh Green's function iG_K of the model after a deep quench, reported in Eq. (4.32). As in App. 4.C, the correction involves the tadpole $i\mathcal{T}$, the time-independent part of which can be reabsorbed in a redefinition of the parameter r as in Eq. (4.24). As a result, Eq. (4.32) can be rewritten, at the critical point $r = r_c$ (see after Eq. (4.24)), as

$$\delta i G_K(q,t,t') = -\frac{\Omega_0}{q^2} [I_K(t) \sin(qt') + I_K(t') \sin(qt)], \tag{4.160}$$

where the integral I_K is given by

$$\begin{aligned} I_K(t) &= \frac{1}{q} \int_0^t \mathrm{d}\tau \sin(q(t-\tau)) B(\tau) \sin(q\tau) \\ &= \frac{1}{q} \int_0^{+\infty} \mathrm{d}\tau \sin(q(t-\tau)) B(\tau) \sin(q\tau) - \frac{1}{q} \int_t^{+\infty} \mathrm{d}\tau \sin(q(t-\tau)) B(\tau) \sin(q\tau) \\ &\equiv I_{K1}(t) + I_{K2}(t), \end{aligned} \tag{4.161}$$

where, for later convenience, we introduced the two integrals $I_{K1,2}$, which we calculate separately. Given the expression of $B(t)$ in Eq. (4.19), I_{K1} can be calculated analytically and it reads:

$$I_{K1}(t) = \theta_N \left\{ -\frac{\pi}{2} \mathrm{e}^{-q/\Lambda} \cos(qt) - \sin(qt) \left[\cosh\left(\frac{q}{\Lambda}\right) \mathrm{Chi}\left(\frac{q}{\Lambda}\right) - \sinh\left(\frac{q}{\Lambda}\right) \mathrm{Shi}\left(\frac{q}{\Lambda}\right) \right] \right\}, \tag{4.162}$$

where we introduced the hyperbolic cosine and sine integral, defined as

$$\mathrm{Chi}(x) = \gamma + \ln x + \int_0^x \mathrm{d}t\, \frac{\cosh t - 1}{t}, \qquad \mathrm{Shi}(x) = \int_0^x \mathrm{d}t\, \frac{\sinh t}{t}, \tag{4.163}$$

respectively, where $\gamma \simeq 0.577$ is the Euler-Mascheroni constant. The integral $I_{K2}(t)$ in Eq. (4.161) can be easily calculated for $t \gg \Lambda^{-1}$, in which case the function $B(t)$ is approximated as in Eq. (4.21) and yields

$$I_{K2}(t) = \theta_N \left\{ \sin(qt)\, \mathrm{Ci}(2qt) + \cos(qt) \left[\frac{\pi}{2} - \mathrm{Si}(2qt) \right] \right\}, \tag{4.164}$$

where Ci and Si were introduced in Eq. (4.27). Summing Eqs. (4.162) and (4.164) one eventually finds for $I_K(t)$ in Eq. (4.161), at the leading order for $q/\Lambda \ll 1$,

$$I_K(t) = -\theta_N \left\{ \sin(qt) \left[\ln(q/\Lambda) - \mathrm{Ci}(2qt) \right] + \cos(qt)\, \mathrm{Si}(2qt) \right\}. \tag{4.165}$$

This expression can be inserted into Eq. (4.160) which, taking into account Eq. (2.17a) for the Gaussian Keldysh Green's function, gives the explicit form of the correction

$$\delta i G_K(q,t,t') = i G_{0K}(q,t,t')\, \theta_N \left[2 \ln(q/\Lambda) - F_K(qt, qt') \right] + \delta g_K(q,t,t'), \tag{4.166}$$

where $F_K(x,y)$ is a scaling function defined as:

$$F_K(x,y) = \mathrm{Ci}(2x) + \mathrm{Ci}(2y), \tag{4.167}$$

while $\delta g_K(q,t,t')$ contains only oscillating and finite corrections:

$$\delta g_K(q,t,t') = \theta_N \frac{\Omega_0}{q^2} \left[\sin(qt)\cos(qt')\mathrm{Si}(2qt') + \sin(qt')\cos(qt)\mathrm{Si}(2qt) \right]. \tag{4.168}$$

4.E Corrections to Green's functions in real space

In this Appendix we analyze the one-loop perturbative corrections to $G_{R,K}$ in real space and time, in order to investigate how their structure is modified by fluctuations. The starting point is Eq. (2.27) which we rewrite for convenience

$$G_{R,K}(x,t,t') = \frac{1}{x^{1-\epsilon/2}\, (2\pi)^{2-\epsilon/2}} \int_0^\infty \mathrm{d}q\, q^{2-\epsilon/2} J_{1-\epsilon/2}(qx) f\left(q/\Lambda\right) G_{R,K}(q,t,t'), \tag{4.169}$$

in which we introduced the cut-off function $f(x)$, as specified above Eq. (2.32). The first correction $\delta G^{\epsilon}_{R,K}$ to the Gaussian $G_{0R,0K}$ comes from the first-order expansion of this expression in powers of ϵ, which involves an expansion of $J_{1-\epsilon/2}$, given by [231]

$$\partial_\nu J_\nu(y)|_{\nu=1} = \frac{\pi}{2} Y_1(y) + \frac{J_0(y)}{y}, \tag{4.170}$$

where $Y_1(y)$ is the Bessel function of the second kind. The above expansion does not produce any logarithmic divergence. For the response function, using the Gaussian retarded Green's function G_{0R} in Eq. (2.17a), we may write,

$$\delta G_R^\epsilon(x,t,t') = -\frac{1}{x^{1-\epsilon/2}\,(2\pi)^2}\int_0^\infty \mathrm{d}q q^{1-\epsilon/2} J_1(qx)\sin(q(t-t'))f\left(q/\Lambda\right) + \frac{1}{x\,(2\pi)^2}\int_0^\infty \mathrm{d}q q J_1(qx)\sin(q(t-t'))f(q/\Lambda). \quad (4.171)$$

Due to the oscillatory nature of the integrands, the two integrals above provide a non-vanishing contribution only if the oscillations from the asymptotic form of the Bessel function $J_1(qx)$ as a function of q are in phase with the oscillations of $\sin(q(t-t'))$, i.e., only for $x = t - t'$, in which case one finds

$$\delta G_R^\epsilon(x = t-t') \simeq -\frac{1}{x^{3-\epsilon}\,(2\pi)^2}\int_0^{\Lambda x}\mathrm{d}y\frac{y^{1-\epsilon/2}}{\sqrt{y}} + \frac{1}{x^3\,(2\pi)^2}\int_0^{\Lambda x}\mathrm{d}y\frac{y}{\sqrt{y}} \propto \frac{x^{\epsilon/2}-1}{x^{3/2}}, \quad (4.172)$$

where we used the fact that $f(y)$ sharply drops to zero for $y \gtrsim 1$. Expanding this expression in ϵ, we obtain $\delta G_R^\epsilon = (\epsilon/2)\,(\ln x) G_{0R}$.

Concerning the correction δG_K^ϵ to G_K, we use again the argument that the term coming from the expansion of $J_{1-\epsilon/2}$ does not generate any logarithmic divergence, and therefore we focus on the remaining terms; for simplicity, as in Sec. 2.3.4, we consider on the case of equal times, i.e., of $G_K(x,t,t)$ for which Eqs. (4.169) and (2.17b) give

$$i\delta G_K^\epsilon(x,t,t) = \frac{\Omega_0}{2x^{1-\epsilon/2}\,(2\pi)^2}\int_0^\infty \mathrm{d}q q^{-\epsilon/2} J_1(qx)\left[1-\cos(2qt)\right] f\left(q/\Lambda\right) - \frac{\Omega_0}{2x\,(2\pi)^2}\int_0^\infty \mathrm{d}q J_1(qx)\left[1-\cos(2qt)\right] f(q/\Lambda). \quad (4.173)$$

On the light cone $x = 2t$, the oscillations of $J_1(qx)$ in the integrand as a function of q are in phase with those of $1-\cos(2qt)$ and therefore, after the change of variable $y = qx$,

$$i\delta G_K^\epsilon(x = 2t, t, t) \simeq \frac{\Omega_0}{2x^{2-\epsilon}\,(2\pi)^2}\int_0^{\Lambda x}\mathrm{d}y\frac{y^{-\epsilon/2}}{\sqrt{y}} - \frac{\Omega_0}{2x^2\,(2\pi)^2}\int_0^{\Lambda x}\mathrm{d}y\frac{1}{\sqrt{y}} \propto \frac{x^{\epsilon/2}-1}{x^{3/2}}. \quad (4.174)$$

Accordingly, on the light cone,

$$\delta G_K^\epsilon(x = 2t, t, t) = (\epsilon/2)\,(\ln x) G_{0K}. \quad (4.175)$$

Inside the light cone, i.e., for $x \ll 2t$, $\cos(2qt)$ may be neglected as it is out of phase with the asymptotic oscillations of J_1, which actually provides an UV cutoff to the remaining integral:

$$i\delta G_K^\epsilon(x \ll 2t, t, t) \simeq \frac{\Omega_0}{2x^{2-\epsilon}\,(2\pi)^2}\int_0^\infty \mathrm{d}y y^{-\epsilon/2} J_1(y) - \frac{\Omega_0}{2x^2\,(2\pi)^2}\int_0^\infty \mathrm{d}y J_1(y) \propto \frac{x^\epsilon - 1}{x^2}. \quad (4.176)$$

Accordingly, inside the light cone,

$$\delta G_K^{\epsilon}(x \ll 2t, t, t) = \epsilon(\ln x) G_{0K}. \tag{4.177}$$

Concerning, instead, the interaction corrections $\delta G^u_{R,K}$ at one-loop (see Eq. (4.42)), one essentially needs to Fourier transform the corresponding expressions of $\delta G_{R,K}$ obtained in Sec. 4.2.1, which can be calculated directly for $d = 4$:

$$\delta G^u_{R,K}(x, t, t') = \frac{1}{4\pi^2 x} \int_0^{\Lambda} \mathrm{d}q q^2 J_1(qx) \delta G_{R,K}(q, t, t'). \tag{4.178}$$

Using Eq. (4.25) for δG_R, we obtain Eq. (4.44) in the main text. Similarly, using the one-loop interaction correction to G_K given in Eq. (4.33), we obtain Eq. (4.49). Extracting logarithmic corrections from δG^u_R in Eq. (4.44) is straightforward and this is discussed in the main text, see Sec. 4.2.3. Here, instead, we focus on δG^u_K and outline how to extract such corrections from the corresponding expression in Eq. (4.49). At long times $x \ll 2t$,

$$\begin{aligned} i\delta G^u_K(x \ll 2t, t, t) &\simeq 2\theta_N \frac{\Omega_0}{8\pi^2 x^2} \int_0^{\infty} \mathrm{d}y J_1(y) \ln\left(\frac{y}{\Lambda x}\right) \\ &\simeq -2\theta_N \ln(\Lambda x) G_{0K} + 2\theta_N \frac{\Omega_0}{8\pi^2 x^2}(-\gamma + \ln 2), \end{aligned} \tag{4.179}$$

where we have used the identity [231] $\int_0^{\infty} \mathrm{d}y J_1(y) \ln(y) = -\gamma + \ln 2$, where $\gamma \simeq 0.577$ is the Euler-Mascheroni constant. On the light cone $x = 2t$, instead, it is convenient to rewrite Eq. (4.49) as

$$i\delta G^u_K(x = 2t) = -2\theta_N \ln(\Lambda x) G_{0K} + 2\theta_N \frac{\Omega_0}{8\pi^2 x^2} k(\Lambda x) \tag{4.180}$$

with

$$k(x) = \int_0^x \mathrm{d}y J_1(y) (1 - \cos y) [-\mathrm{Ci}(y) + \ln y], \tag{4.181}$$

where we have dropped the $\sin(x)\mathrm{Si}(x)$ term, as it does not provide a logarithmic correction. Now integrating Eq. (4.181) by parts, one finds

$$k(x) = [-\mathrm{Ci}(x) + \ln x] \int_0^x \mathrm{d}y J_1(y) (1 - \cos y) - \int_0^x \mathrm{d}y \frac{1 - \cos y}{y} \int_0^y \mathrm{d}y' J_1(y') \left(1 - \cos y'\right). \tag{4.182}$$

Moreover, since $\int_0^y \mathrm{d}y' J_1(y')(1 - \cos y') \sim \sqrt{y}$ for $y \to \infty$, the last term does not give logarithmic corrections. Accordingly, the logarithmic correction comes only from the first term on the r.h.s. of Eq. (4.182), which is actually proportional to G_{0K} in real space (see Eq. (2.30)) and therefore the logarithmic contribution of the second term $\Omega_0 k(\Lambda x \gg 1)/(8\pi^2 x^2) \simeq \ln(\Lambda x) G_{0K}$ on the r.h.s. of Eq. (4.180) cancels the one coming from the first term. This means that the interaction term, up to this order in perturbation theory, does not affect the leading algebraic behavior of G_K on the light cone.

4.F Wilson's RG: one-loop corrections

As discussed in Sec. 4.4, in the Wilson's RG the effective action for the slow fields can be obtained by integrating out the fast fields. After a rescaling of space and time coordinates and fields, one obtains the recursion relations for the parameters of the (effective) action, as summarized in Eqs. (4.79). In order to highlight the emergence of a non-trivial fixed point, we will consider the ϵ-expansion around $d_c = 4$, with $\epsilon = d_c - d$. The first-order correction to the original (bare) action of the slow fields is

$$\delta S^{(1)} = -u_c \int_{\mathbf{x},t} \boldsymbol{\phi}_c \cdot \boldsymbol{\phi}_q \, I_1(t), \tag{4.183}$$

where, exploiting the spatial translational invariance of the Keldysh Green's function,

$$I_1(t) = \frac{N+2}{12N} i G^{>}_{0K}(\mathbf{x} = 0, t, t). \tag{4.184}$$

The second-order correction, instead, is given by:

$$\delta S^{(2)} = i \frac{1}{2} \langle S^2_{\rm int} \rangle^c_> \tag{4.185}$$

where $S_{\rm int}$ is given in Eq. (4.77), while the superscript c indicates that only connected diagrams have to be considered. $\delta S^{(2)}$ contains corrections $\delta S^{(2)}_{\rm coh}$ and $\delta S^{(2)}_{\rm diss}$ to both the coherent and dissipative vertices, respectively, and is non-local both in time and space. Let us focus first on the coherent vertices; denoting, for simplicity, $n \equiv (\mathbf{x}_n, t_n)$, the corrections read:

$$\begin{aligned}
\delta S^{(2)}_{\rm coh} = & -u_c^2 \frac{N+8}{N^2} \left(\frac{2}{4!}\right)^2 \sum_{j,l=1}^{N} \int_{1,2} \left\{ \phi^2_{cl}(1) \phi_{cj}(2) \phi_{qj}(2) i G_{0K}(1,2) G_{0R}(2,1) + \phi^2_{cl}(2) \phi_{cj}(1) \phi_{qj}(1) i G_{0K}(1,2) G_{0R}(1,2) \right\} \\
& - u_q u_c \left(\frac{2}{4!}\right)^2 \frac{N+8}{N^2} \sum_{j,l=1}^{N} \int_{1,2} \left\{ \phi^2_{ql}(1) \phi_{cj}(2) \phi_{qj}(2) i G_{0K}(1,2) G_{0R}(2,1) + \phi^2_{ql}(2) \phi_{cj}(1) \phi_{qj}(1) i G_{0K}(1,2) G_{0R}(1,2) \right\} \\
& = -u_c 2 \left(\frac{2}{4}\right)^2 \frac{N+8}{N^2} \sum_{j,l=1}^{N} \int_{1,2} \left\{ u_c \, \phi^2_{cl}(1) \phi_{cj}(2) \phi_{qj}(2) + u_q \, \phi^2_{ql}(1) \phi_{cj}(2) \phi_{qj}(2) \right\} i G_{0K}(1,2) G_{0R}(2,1),
\end{aligned} \tag{4.186}$$

where in the last equality we simply relabelled the variables in the second integral. In order to retain only the local part of the resulting interaction, we expand the field $\phi_{c,q}(1)$ around point 2 as

$$\boldsymbol{\phi}_{c,q}(\mathbf{z}_1) \simeq \boldsymbol{\phi}_{c,q}(\mathbf{z}_2) + (\mathbf{z}_1 - \mathbf{z}_2) \cdot \frac{\partial \boldsymbol{\phi}_{c,q}(\mathbf{z}_2)}{\partial \mathbf{z}_2} + \dots \tag{4.187}$$

with $\mathbf{z}_i \equiv (\mathbf{x}_i, t_i)$, and we retain only the first term of the expansion $\boldsymbol{\phi}_{c,q}(2) \equiv \boldsymbol{\phi}_{c,q}(\mathbf{z}_2)$, as derivatives of higher order are expected to be irrelevant. Accordingly, the correction to the local vertices is

$$\delta S^{(2)}_{\rm coh} = -\frac{2u_c}{4!N} \int_{x,t} \left[u_c \, (\boldsymbol{\phi}_q \cdot \boldsymbol{\phi}_c) \boldsymbol{\phi}_c^2 + u_q \, (\boldsymbol{\phi}_c \cdot \boldsymbol{\phi}_q) \boldsymbol{\phi}_q^2 \right] I_2(t), \tag{4.188}$$

where

$$I_2(t) = \frac{N+8}{6N}\int_{\mathbf{x}',t'} iG_{0K}(\mathbf{x}',t,t')G_{0R}(\mathbf{x}',t-t'), \tag{4.189}$$

where the spatial translational invariance of $G_{R,K}$ has been used. Finally, assuming for simplicity $T=0$ in the initial state, by using Eqs. (2.15a) and (2.15b), the integrals I_1 and I_2 read:

$$I_1 = \frac{N+2}{12N}\int_{>}\frac{\mathrm{d}^d k}{(2\pi)^d} iG_{0K}(k,t,t) \simeq \frac{N+2}{12N}a_d\frac{\mathrm{d}\Lambda}{\Lambda}\Lambda^d iG_{0K}(\Lambda,t,t) = \frac{\mathrm{d}\Lambda}{\Lambda}\frac{N+2}{12N}a_d\frac{\Lambda^d}{\omega_\Lambda}\left[K_+ + K_-\cos(2\omega_\Lambda t)\right]; \tag{4.190}$$

$$\begin{aligned} I_2 &= \frac{N+8}{6N}\int_0^t \mathrm{d}t'\int_{>}\frac{\mathrm{d}^d k}{(2\pi)^d}\, iG_{0K}(k,t,t')G_{0R}(k,t-t') \\ &\simeq \frac{N+8}{6N}a_d\frac{\mathrm{d}\Lambda}{\Lambda}\Lambda^d\int_0^t \mathrm{d}t'\, iG_{0K}(\Lambda,t,t')G_{0R}(\Lambda,t-t') \\ &= -\frac{N+8}{24N}a_d\frac{\mathrm{d}\Lambda}{\Lambda}\frac{\Lambda^d}{\omega_\Lambda^3}\left\{K_-2\omega_\Lambda\, t\,\sin(2\omega_\Lambda t) + (K_+ - K_-)[1-\cos(2\omega_\Lambda t)]\right\}, \end{aligned} \tag{4.191}$$

where $\int_> \equiv \int_{\Lambda-\mathrm{d}\Lambda\le|\mathbf{k}|\le\Lambda}$ and $K_\pm$ are given in Eq. (4.82) and their argument is calculated for $k=\Lambda$. Finally, the generated dissipative vertices $\propto|\boldsymbol{\phi}_c|^2|\boldsymbol{\phi}_q|^2$ and $\propto(\boldsymbol{\phi}_c\cdot\boldsymbol{\phi}_q)^2$ due to the interaction vertices $\propto u_c^2$ and $\propto u_c u_q$ can be calculated analogously. For the latter we find,

$$\begin{aligned} \delta S^{(2)}_{\mathrm{diss}}\Big|_{u_c u_q} = &-i\left(\frac{2}{4!N}\right)^2\sum_{jklm=1}^{N} u_c u_q\times\int_{1,2}\left[2\phi^<_{qj}(1)\phi^>_{cj}(1)\phi^>_{cl}(1)\phi^<_{cl}(1)+\phi^<_{qj}(1)\phi^<_{cj}(1)\phi^{>2}_{cl}(1)\right] \\ &\times\left[2\phi^>_{qk}(2)\phi^<_{ck}(2)\phi^>_{qm}(2)\phi^<_{qm}(2)+\phi^<_{qk}(2)\phi^<_{ck}(2)\phi^{>2}_{qm}(2)\right], \end{aligned} \tag{4.192}$$

where, for convenience, we reinstated the explicit indication of the fast and the slow components of the involved fields, with the understanding that one has eventually to integrate out the fast components, as discussed in Sec. 4.4. The previous equation is a sum of four terms, where, for instance, the first one is:

$$4\left(\frac{2}{4!N}\right)^2 u_c u_q\int_{1,2} G^2_{0R}(1,2)\Big\{\left[\boldsymbol{\phi}^<_c(2)\cdot\boldsymbol{\phi}^<_q(2)\right]^2+\left[\boldsymbol{\phi}^<_c(2)\right]^2\left[\boldsymbol{\phi}^<_q(2)\right]^2\Big\}. \tag{4.193}$$

All the remaining terms can be analogously evaluated. Summing all terms, including the $u_c u_q$ and u_c^2 vertices, one obtains

$$\delta S^{(2)}_{\mathrm{diss}} = -i\frac{2u_c}{144N^2}\int_{1,2}\left[u_q G^2_{0R}(1,2)+u_c G^2_{0K}(1,2)\right]\Big\{(N+6)\left(\boldsymbol{\phi}^<_c(1)\cdot\boldsymbol{\phi}^<_q(1)\right)^2+2\left|\boldsymbol{\phi}^<_c(1)\right|^2\left|\boldsymbol{\phi}^<_q(1)\right|^2\Big\}. \tag{4.194}$$

Performing the integrations, one obtains,

$$\delta S^{(2)}_{\mathrm{diss}} = -iu_c\frac{\mathrm{d}\Lambda}{\Lambda}\frac{a_d}{144N^2}\frac{\Lambda^d}{\omega_\Lambda^2}\left[u_q - u_c\left(K_+^2+K_-^2\right)\right]\int_1 t_1\Big\{(N+6)\left[\boldsymbol{\phi}^<_c(1)\cdot\boldsymbol{\phi}^<_q(1)\right]^2+2\left[\boldsymbol{\phi}^<_c(1)\right]^2\left[\boldsymbol{\phi}^<_q(1)\right]^2\Big\} \tag{4.195}$$

where we neglected the oscillating terms coming from the integration of $G_{R,K}$ in time. The coefficients $K_\pm$ are given in Eq. (4.82) and their argument is calculated for $k=\Lambda$.

4.G Four-point function at one-loop

In this Appendix we calculate explicitly the one-loop contribution to the four-point function introduced in Sec. 4.5. As anticipated in the main text, among the many terms generated by the repeated use of the Wick's theorem, we need to consider only those which renormalize the vertex. In particular, several terms which arise in the perturbative expansion actually renormalize the Green's functions rather then the interaction vertex. Those we are interested in can be written as

$$\begin{aligned} I_2 &= -\frac{1}{2}\left(\frac{2u_c}{4!N}\right)^2 \int_{1',2'} \langle \phi_{cj}(1)\phi_{ql}(2)\phi_{qm}(3)\phi_{qn}(4)[\boldsymbol{\phi}_q(1')\cdot\boldsymbol{\phi}_c(1')]\boldsymbol{\phi}_c^2(1')[\boldsymbol{\phi}_q(2')\cdot\boldsymbol{\phi}_c(2')\boldsymbol{\phi}_c^2(2')\rangle_0 \\ &= \frac{2u_c^2}{4!N}\frac{N+8}{6}\int_{1',2'} \left[\langle \phi_{cj}(1)\phi_{ql}(2)\phi_{qm}(3)\phi_{qn}(4)[\boldsymbol{\phi}_c(1')\cdot\boldsymbol{\phi}_q(1')]\boldsymbol{\phi}_c^2(2')\rangle_0 \, G_{0K}(1',2')G_{0R}(1',2')\right], \end{aligned} \tag{4.196}$$

where $\langle ...\rangle_0$ denotes the average over the Gaussian part of the action (4.8), while in the last equality we relabelled the integration variables. In order to select only the local contribution to the vertex, we expand the fields contracted with the external legs around the point indicated as α (first term) and we retain only the zeroth order term (cf. Eq. (4.187)). Accordingly, we have

$$\begin{aligned} I_2 &= \frac{2u_c^2}{4!N}\frac{N+8}{6}\int_{1'}\langle \phi_{cj}(1)\phi_{ql}(2)\phi_{qm}(3)\phi_{qn}(4)(\boldsymbol{\phi}_q\cdot\boldsymbol{\phi}_c)\boldsymbol{\phi}_c^2\rangle_0 \int_{2'} G_{0K}(1',2')G_{0R}(1',2') \\ &= \frac{N+8}{36N}F_{jlmn}\, u_c^2 \int_{1'} G_{0R}(1,1')G_{0R}(1',2)G_{0R}(1',3)G_{0R}(1',4)\int_{2'} G_{0K}(1',2')G_{0R}(1',2') \\ &\equiv \frac{-iu_c}{6N}F_{jlmn}\int_{1'} G_{0R}(1,1')G_{0R}(1',2)G_{0R}(1',3)G_{0R}(1',4)J \end{aligned} \tag{4.197}$$

where F_{jlmn} is defined below Eq. (4.101), while the last integral J can be easily calculated:

$$\begin{aligned} J &= \frac{N+8}{6N}u_c\int_{\mathbf{x}}\int_0^t \mathrm{d}t'\, iG_{0K}\left(\mathbf{x},t,t'\right)G_{0R}(\mathbf{x},t-t') \\ &= \frac{N+8}{6N}u_c\int_{\mathbf{q}}\int_0^t \mathrm{d}t'\, iG_{0K}\left(q,t,t'\right)G_{0R}(q,t-t')\,\mathrm{e}^{-2q/\Lambda} \\ &= -\frac{N+8}{48N}u_c\Omega_{0q}a_4\left\{-\frac{(\Lambda t)^2}{1+(\Lambda t)^2}+\ln\left[1+(\Lambda t)^2\right]\right\}, \end{aligned} \tag{4.198}$$

where $\mathrm{e}^{-2q/\Lambda}$ implements the UV regularization of the integral over momenta k, and in the last equality we set $d=4$. Finally, taking the limit $\Lambda t \gg 1$, we find the logarithmic dependence on Λ

$$J = -\frac{N+8}{24N}a_4 u_c\Omega_{0q}\ln(\Lambda t), \tag{4.199}$$

reported in Eq. (4.104).

Chapter 5

Aging through FRG

Abstract

We present a method to calculate short-time non-equilibrium universal exponents within the functional renormalization-group (FRG) scheme. As an example, we consider the classical critical dynamics of the relaxional model A after a quench of the temperature and calculate the initial-slip exponent θ which characterizes the non-equilibrium universal short-time behaviour of both the order parameter and correlation functions. The value of θ is found to be consistent with the result of a perturbative dimensional expansion and of Monte Carlo simulations in spatial dimensionality $d = 3$.

5.1 Critical quench of model A

The so-called model A [121, 232] captures the universal aspects of relaxional dynamics of a system belonging to the Ising universality class and coupled to a thermal bath. This model prescribes an effective dynamics for the coarse-grained order parameter (i.e., the local magnetization), described by the classical field $\varphi \equiv \varphi(\mathbf{r}, t)$ and evolving according to the Langevin equation

$$\dot{\varphi} = -\Omega \frac{\delta \mathcal{H}}{\delta \varphi} + \zeta, \tag{5.1}$$

where Ω is the diffusion coefficient, ζ is a zero-mean Markovian and Gaussian noise with correlation $\langle \zeta(\mathbf{r}, t)\zeta(\mathbf{r}', t')\rangle = 2\Omega\, T \delta^{(d)}(\mathbf{r} - \mathbf{r}')\delta(t - t')$, describing the thermal fluctuations induced by the bath at temperature T (measured in units of Boltzmann constant); $\mathcal{H}$ is given by

$$\mathcal{H} = \int_{\mathbf{r}} \left[\frac{1}{2}(\nabla\varphi)^2 + \frac{r}{2}\varphi^2 + \frac{g}{4!}\varphi^4 \right], \tag{5.2}$$

where $\int_{\mathbf{r}} \equiv \int \mathrm{d}^d r$ with d the spatial dimensionality, r parametrizes the distance from the critical point and $g \geq 0$ controls the strength of the interaction. The parameter r depends on T and it takes a critical value r_c at the critical temperature $T = T_c$.

We assume that the system is prepared at $t = t_0$ in the high-temperature phase $T \to +\infty$ with an external magnetic field h_0, i.e., that the initial condition $\varphi(\mathbf{r}, t = t_0) = \varphi_0(\mathbf{r})$ is a random field with probability distribution $P_0[\varphi_0]$ given by

$$P_0[\varphi_0] \propto \exp\left[-\int_{\mathbf{r}} \frac{\tau_0}{2}(\varphi_0 - h_0)^2\right]. \tag{5.3}$$

Equation (5.3) implies that the initial field φ_0, with average $\langle\varphi(\mathbf{r})\rangle = h_0(\mathbf{r})$, is characterized by short-range correlations

$$\langle[\varphi_0(\mathbf{r}) - h_0(\mathbf{r})]\left[\varphi_0(\mathbf{r}') - h_0(\mathbf{r}')\right]\rangle = \tau_0^{-1}\delta^{(d)}(\mathbf{r} - \mathbf{r}'). \tag{5.4}$$

We recall that the correlation function G_C is defined as [121]

$$G_C(\mathbf{r}, t, t') = \langle\varphi(\mathbf{r}, t)\varphi(\mathbf{0}, t')\rangle, \tag{5.5}$$

where $\langle\dots\rangle$ denotes the average over the dynamics generated by Eq. (5.1), which includes averaging over both the initial condition φ_0 and the realizations of the noise ζ. The response function G_R is defined as the linear response to an external field $h(\mathbf{r}, t)$, which couples linearly to φ and which modifies the Hamiltonian $\mathcal{H}$ in Eq. (5.2) as $\mathcal{H}_h = \mathcal{H} - \int_{\mathbf{r}} h\varphi$; specifically, we have

$$G_R(\mathbf{r}, t, t') \equiv \left.\frac{\delta\langle\varphi(\mathbf{r}, t)\rangle_h}{\delta h(\mathbf{0}, t')}\right|_{h=0}, \tag{5.6}$$

where $\langle\dots\rangle_h$ denotes the average over the dynamics generated by Eq. (5.1) with the Hamiltonian $\mathcal{H}_h$. Note that in Eqs. (5.5) and (5.6) we made use of the spatial translational invariance of the dynamical equation (5.1), as G_C and G_R only depend on the distance between the two spatial points involved in these equations. Accordingly, one can take the Fourier transform with respect to $\mathbf{r}$ and express more conveniently $G_{C,R}$ in momentum space.

We assume that the temperature T of the bath takes the critical value T_c, so that the system will eventually relax to a critical equilibrium state. As a consequence of being at criticality, this relaxation dynamics exhibits self-similar properties, signalled by the emergence of a scaling behaviour referred to as aging: for example, correlation and response functions in momentum space read [117, 119, 233], after a quench occurring at $t = t_0$,

$$G_R(q, t, t') \simeq q^{-2+\eta+z}\left(\frac{t}{t'}\right)^{\theta} \mathcal{G}_R(q^z t), \tag{5.7a}$$

$$G_C(q, t, t') \simeq q^{-2+\eta}\left(\frac{t}{t'}\right)^{\theta-1} \mathcal{G}_C(q^z t), \tag{5.7b}$$

with η the anomalous dimension [178, 195], z the dynamical critical exponent [121, 177], and $\mathcal{G}_{R,C}(x)$ scaling functions. The scaling forms (5.7) are valid for $h_0 = 0$, $t' \ll t$ and $t' \to t_m$, where t_m is a microscopic time which depends on the specific details of the underlying microscopic model. The dynamics at times shorter than t_m has a non-universal character and it depends on the material properties of the system. The scaling forms (5.7) are characterized by the so-called initial-slip exponent

θ, which is generically independent of the static critical exponents η, ν [178,195] and of the dynamical critical exponent z characterizing the equilibrium dynamics of model A. The physical origin of θ can be eventually traced back to the (transient) violation of detailed balance due to the breaking of the time-translational invariance induced by the quench [117].

In the presence of a non-vanishing initial homogeneous external field h_0, the evolution of the magnetization $M(t) \equiv \langle \varphi(\mathbf{r}, t) \rangle$ displays an interesting non-equilibrium evolution. In fact, for $t \gg t_m$, it follows the scaling form [117]

$$M(t) = M_0 \, t^{\theta'} \mathcal{F}\left(M_0 \, t^{\theta' + \beta/(\nu z)} \right), \tag{5.8}$$

where $\theta' = \theta + (2 - z - \eta)/z$, β is the equilibrium critical exponent of the magnetization [178, 195], $M_0 \equiv h_0$ is the initial value of the magnetization and $\mathcal{F}(x)$ is a function with the following asymptotic properties:

$$\mathcal{F}(x) \approx \begin{cases} x^{-1} & \text{for} \quad x \to \infty, \\ 1 & \text{for} \quad x \to 0. \end{cases} \tag{5.9}$$

Accordingly, $M(t)$ exhibits the non-monotonic behavior depicted in Fig. 5.1: for times $t \lesssim t_{M_0} \propto M_0^{1/[\theta' + \beta/(\nu z)]}$ it grows as an algebraic function with the non-equilibrium exponent θ', while for $t \gtrsim t_{M_0}$ it relaxes towards its equilibrium value $M_{\rm eq} = 0$, with an algebraic decay controlled by a combination of universal equilibrium (static and dynamic) critical exponents.

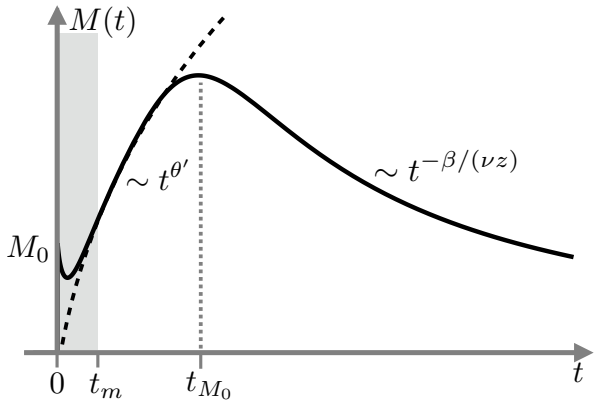

Figure 5.1: Sketch of the time evolution of the magnetization $M(t)$ after a quench at $t = t_0$ from a disordered initial state with a small value M_0 of the magnetization to the critical temperature. The grey area indicates the time interval up to t_m within which the dynamics does not display universal features.

5.1.1 Gaussian approximation

In the absence of interaction ($g = 0$), Eq. (5.1) is linear and therefore it is possible to calculate exactly the correlation and response functions. By solving Eq. (5.1) with $g = 0$ and $h_0 = 0$, based on the

definitions (5.5) and (5.6), one finds after a Fourier transform in space with momentum q

$$G_{0R}(q,t,t') = \vartheta(t-t')\mathrm{e}^{-\Omega\omega_q(t-t')}, \tag{5.10}$$

$$G_{0C}(q,t,t') = \frac{T}{\omega_q}\Big[\mathrm{e}^{-\Omega\omega_q|t-t'|} + \left(\frac{\omega_q}{T\tau_0} - 1\right)\mathrm{e}^{-\Omega\omega_q(t+t'-2t_0)}\Big], \tag{5.11}$$

where $\omega_q = q^2 + r$ is the dispersion relation, $\vartheta(t)$ is the Heaviside step function and t_0 is the time at which the quench occurs. The subscript 0 in $G_{0C,0R}$ indicates that these expressions refer to the Gaussian approximation. Notice that, while G_{0R} is a time-translational invariant function, as it depends only on the difference of times $t - t'$, G_{0C} breaks time-translational invariance. However, by taking the initial time $t_0 \to -\infty$ and as long as $\omega_q \neq 0$, G_{0C} recovers its equilibrium time-translational invariant form [121]: this is, in fact, a consequence of the relaxional nature of model A, which erases at long times the information about the initial state. In the presence of a non-vanishing initial homogeneous external field h_0, it is also possible to calculate exactly the evolution of the magnetization $M(t)$, i.e.,

$$M(t) = M_0\mathrm{e}^{-\Omega r(t-t_0)}, \tag{5.12}$$

which vanishes exponentially fast in time for $r > 0$, while it keeps its initial value $M_0 = h_0$ for $r = 0$.

Within this Gaussian approximation, the dynamics (5.1) becomes critical for $r = 0$: in this case, by comparing Eqs. (5.10), (5.11) and (5.12) with Eqs. (5.7a), (5.7b) and Eq. (5.8), one finds $\theta = 0$, i.e., the initial-slip exponent vanishes.

As a result of a finite interaction strength $g \neq 0$, the Gaussian value of the initial-slip exponent acquires sizeable corrections [117, 119]. In Sec. 5.2 we introduce a functional renormalization group formalism, which we employ in Sec. 5.3 and 5.4 in order to calculate these corrections to θ.

5.2 Functional renormalization group for a quench

In general, breaking translational invariance in space and/or time prevents the use of ordinary computational strategies of FRG [234], primarily based on writing the corresponding flow equations in Fourier space, where they acquire a particularly simple form. In this Section, we show how, in spite of this difficulty, the case of broken time-translational invariance can be successfully studied.

5.2.1 Response functional and FRG equation

The Langevin formulation of model A in Eq. (5.1) can be converted into a functional form by using the response functional [118, 121, 235–239]. The corresponding action is given by

$$S[\varphi,\widetilde{\varphi}] = S_0[\varphi_0,\widetilde{\varphi}_0] + \int_{\mathbf{r}}\int_{t_0}^{+\infty}\mathrm{d}t\,\widetilde{\varphi}\left(\dot{\varphi} + \Omega\frac{\delta\mathcal{H}}{\delta\varphi} - \Omega T\widetilde{\varphi}\right), \tag{5.13}$$

where $\widetilde{\varphi} = \widetilde{\varphi}(\mathbf{r},t)$ is the so-called response field, while $\widetilde{\varphi}_0 = \widetilde{\varphi}(\mathbf{r},t=t_0)$. The action $S_0[\varphi_0,\widetilde{\varphi}_0]$ contains information about the initial state and can be derived by including the initial probability distribution (5.3) into the functional description [117–119]. We postpone the discussion on its precise form to Sec. 5.2.2. The quench occurs at time t_0: if one is only interested in the stationary properties

of model A, the limit $t_0 \to -\infty$ can be taken, thus recovering a full time-translational invariant behaviour, as discussed in Sec. 5.3.3.

In order to implement FRG [234, 240], it is necessary to supplement the action $S[\varphi, \widetilde{\varphi}]$ with a cutoff function $R_k(q)$, and to trade $S[\varphi, \widetilde{\varphi}]$ for the effective action $\Gamma[\phi, \widetilde{\phi}]$, obtained from the Legendre transform of the generating function associated with S (see App. 5.A, in particular Eq. (5.57)). $R_k(q)$ introduces an effective "mass" parametrized by the momentum scale k, and it provides an infrared cutoff for momenta $q \lesssim k$, with $R_k(q) \simeq k^2$ for $q \to 0$. As a result, this cutoff function regularizes the infrared divergences of RG loop corrections at criticality [234,240,241]. The effective action Γ_k can be thus interpreted as an action which interpolates between the microscopic one $S[\varphi, \widetilde{\varphi}]$ for $k \to \Lambda$, where Λ is the ultraviolet cutoff of the model, and the long-distance effective action for $k \to 0$, since the cutoff function R_k, as a function of k, is characterized by the following limiting behaviours [234, 240, 241]:

$$R_k(q) \simeq \begin{cases} \Lambda^2 & \text{for} \quad k \to \Lambda, \\ 0 & \text{for} \quad k \to 0. \end{cases} \tag{5.14}$$

The dependence on k of the effective action Γ_k, which can be regarded as an action which has been coarse-grained on a volume k^{-d}, is then determined by the following equation [234, 242],

$$\frac{\mathrm{d}\Gamma}{\mathrm{d}k} = \frac{1}{2} \int_x \mathrm{tr} \left[\vartheta(t - t_0) G(x, x) \frac{\mathrm{d}R}{\mathrm{d}k} \sigma \right], \tag{5.15}$$

where, in order to simplify the notation, we no longer indicate explicitly the dependence on k of Γ and R, while we defined $x \equiv (\mathbf{r}, t)$, $\int_x \equiv \int \mathrm{d}^d r \int_{-\infty}^{+\infty} \mathrm{d}t$, and $\sigma = \left(\begin{smallmatrix} 0 & 1 \\ 1 & 0 \end{smallmatrix}\right)$. The matrix $G(x, x')$ is defined as

$$G(x, x') = \left(\Gamma^{(2)} + R\,\sigma \right)^{-1} (x, x'), \tag{5.16}$$

where the inverse of the matrix on the r.h.s. is taken with respect to spatial and temporal variables, as well as to the internal matrix structure. The kernel $\Gamma^{(2)}(x, x')$ is the second variation of the effective action Γ with respect to the fields, i.e.,

$$\Gamma^{(2)}(x, x') = \begin{pmatrix} \dfrac{\delta^2 \Gamma}{\delta\phi(x)\delta\phi(x')} & \dfrac{\delta^2 \Gamma}{\delta\widetilde{\phi}(x)\delta\phi(x')} \\ \dfrac{\delta^2 \Gamma}{\delta\phi(x)\delta\widetilde{\phi}(x')} & \dfrac{\delta^2 \Gamma}{\delta\widetilde{\phi}(x)\delta\widetilde{\phi}(x')} \end{pmatrix}. \tag{5.17}$$

While Eq. (5.15) is exact, it is generically not possible to solve it. Accordingly, one resorts to approximation schemes which render Eq. (5.15) amenable to analytic and numerical calculations. A first step in this direction is to provide an ansatz for the form of the effective action Γ which, once inserted into Eq. (5.15), results in a set of coupled non-linear differential equations for the couplings which parametrize it. In fact, any coupling $g_{n,l} \phi^n \widetilde{\phi}^l / (n!\, l!)$ (with n and l positive integers) appearing in Γ corresponds to a term of its vertex expansion [243–245], as

$$g_{n,l} = \left. \frac{\delta^{l+n} \Gamma}{\delta\phi^n \delta\widetilde{\phi}^l} \right|_{\substack{\widetilde{\phi}=0 \\ \phi=\phi_m}}, \tag{5.18}$$

where the derivatives of Γ are evaluated at some homogeneous field configurations $\widetilde{\phi} = 0$ and $\phi = \phi_m$. The field ϕ_m, referred to as background field, is typically chosen as the minimum of the effective action.

We consider the following ansatz for model A:

$$\Gamma[\phi, \widetilde{\phi}] = \Gamma_0[\phi_0, \widetilde{\phi}_0] + \int_x \vartheta(t - t_0)\widetilde{\phi}\left(Z\dot{\phi} + K\nabla^2\phi + \frac{\partial \mathcal{U}}{\partial \phi} - D\widetilde{\phi}\right). \tag{5.19}$$

The boundary action $\Gamma_0[\phi_0, \widetilde{\phi}_0]$ accounts for the initial conditions and its form will be discussed in detail in Sec. 5.2.2. For the time being, we just assume that it is a quadratic function of the fields. Note that the effective action (5.19) can generally describe a quench because of the presence of the Heaviside step function. The field-independent factors Z, K and D account for possible renormalizations of the derivatives and of the Markovian noise, while the generic potential $\mathcal{U}(\phi)$ is a $\mathbb{Z}_2$-symmetric local polynomial of the order parameter ϕ. For constructing the FRG equations, we consider the following cutoff function

$$R(q) = K(k^2 - q^2)\vartheta(k^2 - q^2), \tag{5.20}$$

which has the advantage of minimizing spurious effects introduced by the specific truncation ansatz of the effective action [241].

The kernel $\Gamma^{(2)} + R\sigma$ appearing in Eq. (5.16) — which is obtained by deriving Eq. (5.19) — can be conveniently re-expressed by separating the field-independent part G_0^{-1} (which receives contributions from the quadratic part of Γ and from σR) from the field-dependent part V, i.e.,

$$\Gamma^{(2)}(x, x') + R(x, x')\sigma = G_0^{-1}(x, x') - V(x, x'), \tag{5.21}$$

such that (see Eq. (5.16))

$$G^{-1}(x, x') = G_0^{-1}(x, x') - V(x, x'). \tag{5.22}$$

Note that, since we assumed $\Gamma_0[\phi_0, \widetilde{\phi}_0]$ to be quadratic, its presence is completely encoded in the function G_0^{-1}. For the ansatz (5.19), the field-dependent part V reads:

$$V(x, x') = V(x)\,\delta(x - x'), \tag{5.23}$$

where the delta function $\delta(x - x') \equiv \delta(t - t')\delta^{(d)}(\mathbf{r} - \mathbf{r}')$ appears as a consequence of the locality in space and time of the potential $\mathcal{U}$, and where the function $V(x)$ is defined as

$$V(x) = -\vartheta(t - t_0)\begin{pmatrix} \widetilde{\phi}(x)\dfrac{\partial^3 \mathcal{U}}{\partial \phi^3}(x) & \dfrac{\partial^2 \mathcal{U}}{\partial \phi^2}(x) \\ \dfrac{\partial^2 \mathcal{U}}{\partial \phi^2}(x) & 0 \end{pmatrix}. \tag{5.24}$$

The function ϑ in this expression of $V(x)$ appears as a consequence of the one in Eq. (5.19): as it will become clear below, the presence of ϑ allows one to encompass both the case of the quench and of a stationary state in the calculation of G (see Sec. 5.3.3).

Finally, in order to derive the RG equations for the couplings appearing in the effective action (5.19), one has to take the derivative with respect to k on both sides of Eq. (5.18) and, using Eq. (5.15), one finds

$$\frac{\mathrm{d}g_{n,l}}{\mathrm{d}k} = \frac{\delta^{l+n}}{\delta\phi^n \delta\widetilde{\phi}^l} \frac{1}{2} \int_x \mathrm{tr}\left[\vartheta(t-t_0) G(x,x) \frac{\mathrm{d}R}{\mathrm{d}k}\sigma\right]\Big|_{\substack{\widetilde{\phi}=0 \\ \phi=\phi_m}} + \frac{\delta^{l+n+1}\Gamma}{\delta\phi^{n+1}\delta\widetilde{\phi}^l}\Big|_{\substack{\widetilde{\phi}=0 \\ \phi=\phi_m}} \frac{\mathrm{d}\phi_m}{\mathrm{d}k}, \tag{5.25}$$

from which one can evaluate the flow equation for the couplings $g_{n,m}$, once the derivative of ϕ_m is calculated, where ϕ_m corresponds to the minimum of the potential $\mathcal{U}$.

5.2.2 Quench functional renormalization group

In order to study the critical properties of the quench described in Sec. 5.1, we consider the effective action (5.19), in which one has still to specify the form of the boundary action Γ_0. The Gaussian probability distribution of the initial condition (5.3) can be effectively encoded by taking

$$\Gamma_0 = \int_{\mathbf{r}} \left(-\frac{Z_0^2}{2\tau_0}\widetilde{\phi}_0^2 + Z_0 \widetilde{\phi}_0 \phi_0 + Z_0 h_0 \widetilde{\phi}_0 \right). \tag{5.26}$$

This form is uniquely fixed by requiring that it does not result in a violation of causality in the response functional [1] and that it reproduces the Gaussian Green's functions (5.10) and (5.11), see App. 5.B. The factor Z_0 accounts for a possible renormalization of the initial response field $\widetilde{\phi}_0$: the way in which corrections to Z_0 are generated is discussed further below in this section. Note also that the term $\widetilde{\phi}_0^2$ can be regarded as a Gaussian noise located at the initial time t_0. The boundary action Γ_0 may in principle contain higher powers of ϕ_0 and $\widetilde{\phi}_0$, and spatial and temporal derivatives of these fields: however, based on their engineering dimension one can argue [117] that they are irrelevant in the renormalization-group sense, and therefore they have not been included. The presence of a non-vanishing initial field h_0 induces a non-trivial evolution of the magnetization $M(t)$, but it does not generate new additional critical exponents (see Sec. 5.1 and Ref. [117]), and therefore in the rest of this Chapter we will assume $h_0 = 0$ without loss of generality.

In order to study the flow of the couplings of the effective action Γ in Eq. (5.19) from the FRG equation (5.15) it is necessary to evaluate the matrix G defined in Eq. (5.16). However, the presence of the boundary action given in Eq. (5.26) as well as the breaking of time-translational invariance in Eq. (5.19) makes the calculation of $G(x,x')$ non-trivial, since now G depends separately on the two times t and t'. In order to overcome this difficulty, we notice that G satisfies the following integral equation (see App. 5.C):

$$G(x,x') = G_0(x,x') + \int_y G_0(x,y)\, V(y) G(y,x'), \tag{5.27}$$

[1] In fact, one may be tempted to include in Γ_0 the term $\propto \phi_0^2$ appearing into the initial probability (5.3): however, this would cause a violation of causality in the response functional, since each term in the action Γ in Eq. (5.19) must contain at least one response field $\widetilde{\phi}$ (see ,for instance, Ref. [121]). Instead, the term $\propto \widetilde{\phi}_0^2$ in Eq. (5.26) is allowed in this respect.

with G_0 and V defined in Eq. (5.21). The explicit form of G_0 can be evaluated by using the boundary action Γ_0 in Eq. (5.26) and it reads (see App. 5.B):

$$G_0(t,t') = \begin{pmatrix} G_{0C}(t,t') & G_{0R}(t,t') \\ G_{0R}(t',t) & 0 \end{pmatrix}, \tag{5.28}$$

where G_{0R} and G_{0C} are given by Eqs. (5.10) and Eqs. (5.11) (with $\Omega = 1$ and T replaced by D), respectively, with the dispersion relation ω_q replaced by the regularized one $\omega_{k,q}$, defined as:

$$\omega_{k,q} \equiv Kq^2 + r + K(k^2 - q^2)\vartheta(k^2 - q^2). \tag{5.29}$$

Equation (5.27) can then be solved iteratively and, once this formal solution has been replaced into the FRG equation (5.15), the latter can be cast in the form (see Eqs. (5.72) and (5.74)):

$$\frac{\mathrm{d}\Gamma}{\mathrm{d}k} = \sum_{n=1}^{+\infty} \Delta\Gamma_n, \tag{5.30}$$

where the functions $\Delta\Gamma_n$ are defined as (see App. 5.C for details)

$$\Delta\Gamma_n = \frac{1}{2}\int_{x,y_1\ldots y_n} \mathrm{tr}\left[G_0(x,y_1)V(y_1)G_0(y_1,y_2)\ldots V(y_n)G_0(y_n,x)\frac{\mathrm{d}R}{\mathrm{d}k}\sigma\right]. \tag{5.31}$$

As discussed in App. 5.C, the FRG equation in the form of Eq. (5.30) is more convenient for calculations when, as in the present case, time-translational invariance is broken and it is therefore not possible to simplify this equation by expressing it in the Fourier frequency space.

For simplicity, let us assume that the potential $\mathcal{U}$ which appears in Eq. (5.19) is quartic in the field ϕ, i.e.,

$$\mathcal{U}(\phi) = \frac{r}{2}\phi^2 + \frac{g}{4!}\phi^4, \tag{5.32}$$

such that, from Eq. (5.24), the field-dependent function $V(x)$ reads

$$V(x) = -\vartheta(t - t_0)\, g \begin{pmatrix} \widetilde{\phi}\phi & \phi^2/2 \\ \phi^2/2 & 0 \end{pmatrix}. \tag{5.33}$$

Accordingly, since this V appears n times in the convolution (5.31) which defines $\Delta\Gamma_n$ on the r.h.s. of Eq. (5.30), it follows that $\Delta\Gamma_n$ contains products of $2n$ possibly different fields. Since also the l.h.s. of Eq. (5.30) is a polynomial of the fields because of the ansatz (5.19), each term on the l.h.s. is thus uniquely matched by a term of the expansion on the r.h.s. Accordingly, in order to derive the RG equation for the coupling of a term involving a product of $2n$ fields, it is sufficient to evaluate the corresponding $\Delta\Gamma_n$. Note that this line of argument applies also to the time-translational invariant case, and, moreover, it can be easily generalized to the case in which the potential contains powers of ϕ of higher orders than it does in Eq. (5.32).

5.3 Truncation for $\phi_m = 0$

In this section we discuss the derivation of the RG equations from the ansatz (5.19) with the quartic potential $\mathcal{U}$ introduced in Eq. (5.32). Considering this simple case allows us to detail how the boundary action (5.26) is renormalized by the post-quench interaction. Since this ansatz corresponds to a local potential approximation [234, 240, 246], the anomalous dimensions of the derivative terms and of the Markovian noise strength D vanish, and therefore in the following we set, for simplicity, $K = Z = 1$. The only non-irrelevant terms which are renormalized within this scheme are those proportional to quadratic and quartic powers of the fields ϕ and $\widetilde{\phi}$, i.e., those associated with post-quench parameter r, the anomalous dimension Z_0 and the coupling g. As discussed in Sec. 5.2.2, the renormalization of the quadratic terms is determined by the contribution $\Delta\Gamma_1$ appearing on the r.h.s. of Eq. (5.30), while the renormalization of the quartic one by the contribution $\Delta\Gamma_2$.

5.3.1 Derivation of the RG equations

Let us now consider Eq. (5.30) and focus on the term $\Delta\Gamma_1$, as defined in Eq. (5.31). A simple calculation renders (see App. 5.D for details)

$$\Delta\Gamma_1 = -k^{d+1}\frac{a_d}{d}\frac{gD}{\omega_k^2}\int_{\mathbf{r}}\int_{t_0}^{+\infty} \mathrm{d}t\, \widetilde{\phi}(t,\mathbf{r})\phi(t,\mathbf{r})\left[1 - f_r(t-t_0)\right], \tag{5.34}$$

where $a_d = 2/[\Gamma(d/2)(4\pi)^{d/2}]$, with d the spatial dimensionality of the system and $\Gamma(x)$ the gamma function. The integration over the intermediate time variable in Eq. (5.31) for $n = 1$ generates, within the square brackets in the integrand of Eq. (5.34), a term which is independent of time and one which depends on it via the function $f_r(t - t_0)$, defined as

$$f_r(t) = \mathrm{e}^{-2\omega_k t}\left[1 + 2\omega_k t\left(1 - \frac{\omega_k}{D\tau_0}\right)\right], \tag{5.35}$$

where $\omega_k \equiv \omega_{q=k}$ or, equivalently, $\omega_k \equiv \omega_{k,q=k}$ (see Eq. (5.29)). Since $f_r(t)$ vanishes exponentially fast upon increasing time, its contribution to the renormalization of the time-independent parameter r can be neglected [2]. Accordingly, the flow equation for r can be simply obtained by comparing the l.h.s. of Eq. (5.30) with Eq. (5.34), where we introduced the potential (5.32) in the truncated action (5.19), finding

$$\frac{\mathrm{d}r}{\mathrm{d}k} = -k^{d+1}\frac{a_d}{d}\frac{gD}{(k^2+r)^2}. \tag{5.36}$$

On the other hand, at short times, the function $f_r(t)$ singles out contributions containing fields which live on the temporal boundary, thus renormalizing the boundary action Γ_0 introduced in Eq. (5.26). In fact, the formal identity

$$\int_{t_0}^{+\infty} \mathrm{d}t\, g(t)\mathrm{e}^{-c(t-t_0)} = \sum_{n=0}^{+\infty}\frac{1}{c^{n+1}}\frac{\mathrm{d}^n g}{\mathrm{d}t^n}\bigg|_{t=t_0}, \tag{5.37}$$

[2] In this calculation and in those which follow, we always take first the limit $t \to \infty$, and then the limit $k \to 0$.

with $c > 0$ and $g(t)$ an arbitrary smooth function, can be used in order to express formally the part of the integral involving $f_r(t)$ on the r.h.s. of Eq. (5.34) as

$$\int_{t_0}^{+\infty} \mathrm{d}t\, \widetilde{\phi}(t)\phi(t) f_r(t-t_0) = \sum_{n=0}^{+\infty} \frac{c_{n,k}(\tau_0)}{(2\omega_k)^{n+1}}\, Z_{0,n} \frac{\mathrm{d}^n}{\mathrm{d}t^n} \left[\widetilde{\phi}(t)\phi(t)\right]\Big|_{t=t_0}, \tag{5.38}$$

with

$$c_{n,k}(\tau_0) \equiv (n+2) - \frac{(n+1)\omega_k}{D\tau_0}. \tag{5.39}$$

Accordingly, the time-dependent part in the integrand of Eq. (5.34) generates an infinite series of operators contributing to the boundary action Γ_0. For future convenience, we introduced in Eq. (5.38) additional numerical factors $Z_{0,n}$, which account for for possible renormalization of the boundary operators and which equal one in the non-renormalized theory. Most of the operators in the sum (5.38) renormalize irrelevant operators which were not included into the initial ansatz for the boundary action (5.26), and therefore one can neglect them. The only non-irrelevant term corresponds to $n = 0$ in Eq. (5.38): by inserting the boundary action Γ_0 (see Eq. (5.26)) into the l.h.s. of Eq. (5.30), and by combining it with Eqs. (5.34) and (5.38), one finds the flow equation for $Z_0 \equiv Z_{0,0}$, i.e.,

$$\frac{\mathrm{d}Z_0}{\mathrm{d}k} = k^{d+1} \frac{a_d}{d} \frac{gD}{(k^2+r)^3} \left[1 - \frac{k^2+r}{2D\tau_0}\right] Z_0. \tag{5.40}$$

We consider now the renormalization of the quartic term, which can be read off from $\Delta\Gamma_2$. A simple calculation renders (see App. 5.D for details)

$$\begin{aligned}\Delta\Gamma_2 = {} & \frac{3}{2} k^{d+1} \frac{a_d}{d} \frac{g^2 D^2}{\omega_k^4} \int_{\mathbf{r}} \int_{t_0}^{+\infty} \mathrm{d}t\, \widetilde{\phi}^2(t)\phi^2(t) \left[1 - f_D(t-t_0)\right] \\ & + k^{d+1} \frac{a_d}{d} \frac{g^2 D}{\omega_k^3} \int_{\mathbf{r}} \int_{t_0}^{+\infty} \mathrm{d}t\, \widetilde{\phi}(t')\phi^3(t) \left[1 - f_g(t-t_0)\right], \end{aligned} \tag{5.41}$$

where f_D and f_g, given in Eqs. (5.85) and (5.86), respectively, decay exponentially upon increasing time, and therefore they do not contribute to the renormalization of the couplings at long times. Note that the integration produces a term proportional to $\widetilde{\phi}^2\phi^2$ in Eq. (5.41): however, this operator is irrelevant for $d > 2$ and it can be neglected, since our truncation includes only relevant couplings. On the other hand, the term proportional to $\widetilde{\phi}\phi^3$ in Eq. (5.41) renormalizes the relevant coupling g and, comparing Eq. (5.41) with the l.h.s. of Eq. (5.30) after using the ansatz (5.19) for Γ with the potential (5.32), one finds the flow equation

$$\frac{\mathrm{d}g}{\mathrm{d}k} = 6k^{d+1} \frac{a_d}{d} \frac{g^2 D}{(k^2+r)^3}. \tag{5.42}$$

5.3.2 Flow equations

In order to study the flow of r and g prescribed by Eqs. (5.36) and (5.42), it is convenient to introduce the dimensionless quantities $\widetilde{r} = r/k^2$, and $\widetilde{g} = gDk^{d-4}a_d/d$. The corresponding flow follow from

Eqs. (5.36) and (5.42):

$$k\frac{\mathrm{d}\widetilde{r}}{\mathrm{d}k} = -2\widetilde{r} - \frac{\widetilde{g}}{(1+\widetilde{r})^2}, \tag{5.43}$$

$$k\frac{\mathrm{d}\widetilde{g}}{\mathrm{d}k} = \widetilde{g}\left[-\epsilon + 6\frac{\widetilde{g}}{(1+\widetilde{r})^3}\right], \tag{5.44}$$

where $\epsilon = 4-d$. These equations describe the RG flow of the couplings in the equilibrium state which is asymptotically reached by the system at long times. Accordingly, they are independent of both Z_0 and τ_0: the relaxional nature of model A erases the information about the initial state in the long time. Since the final state corresponds to an equilibrated system, the equations for $\widetilde{r}$ and $\widetilde{g}$ must provide the same critical exponents as in the equilibrium Ising universality class [121, 177, 178]. This can be seen, for instance, by comparing Eqs. (5.43) and (5.44) (at leading order in ϵ) with the results obtained within the perturbative RG at one loop in the equilibrium theory [121]. Note that Eqs. (5.43) and (5.44) do not have the same form as the corresponding equations derived within perturbative RG, as they are obtained within a different renormalization scheme; nevertheless, they provide the same critical exponents, as discussed further below.

Equations (5.43) and (5.44) admit two fixed points: the Gaussian one $(\widetilde{r}^*_{\mathrm{G}}, \widetilde{g}^*_{\mathrm{G}}) = (0,0)$ and the Wilson-Fisher one, which at leading order in ϵ, reads $(\widetilde{r}^*_{\mathrm{WF}}, \widetilde{g}^*_{\mathrm{WF}}) = (-\epsilon/12, \epsilon/6) + O(\epsilon^2)$ (in general we will denote by the superscript * any quantity which is evaluated at a fixed point). By linearizing Eqs. (5.43) and (5.44) around these fixed points, one finds that the Gaussian one is stable only for $\epsilon < 0$, while the Wilson-Fisher fixed point is stable only for $\epsilon > 0$. The latter has an unstable direction, and from the inverse of the negative eigenvalue of the associated stability matrix, one derives the critical exponent ν, which reads $\nu = 1/2 + \epsilon/12 + O(\epsilon^2)$, the same as in equilibrium [121, 177, 178]. As mentioned at the beginning of this section, the ansatz (5.32) for the potential does not allow for a renormalization of the time and spatial derivatives in the effective action (5.19). Accordingly, the anomalous dimension η and the dynamical critical exponent z are equal to their Gaussian values $\eta = 0$ and $z = 2$.

Let us now focus on the renormalization of the terms in the boundary action Γ_0 in Eq. (5.26). From Eq. (5.40), we define the anomalous dimension η_0 of the response field $\widetilde{\phi}_0$ at initial time as

$$\eta_0 \equiv -\frac{k}{Z_0}\frac{\mathrm{d}Z_0}{\mathrm{d}k} = -\frac{\widetilde{g}}{(1+\widetilde{r})^3}\left(1 - \frac{1+\widetilde{r}}{2\widetilde{\tau}_0}\right), \tag{5.45}$$

where we introduced the rescaled pre-quench parameter $\widetilde{\tau}_0 = \tau_0/k^2$ and we used Eq. (5.40). Since τ_0 does not receive any correction from the renormalization, its flow equation is simply determined by its canonical dimension and thus

$$k\frac{\mathrm{d}\widetilde{\tau}_0}{\mathrm{d}k} = -2\widetilde{\tau}_0. \tag{5.46}$$

Accordingly, $\widetilde{\tau}_0$ has only one stable fixed point in the infrared regime (i.e., for $k \to 0$), that is $\widetilde{\tau}^*_0 = +\infty$. Close to this fixed point, any possible term in the boundary action Γ_0 (except for $\widetilde{\phi}_0\phi_0$) is irrelevant for $d > 2$, and therefore the ansatz (5.26) is consistent. Note that the r.h.s. of Eq. (5.45) diverges at the unstable fixed point $\widetilde{\tau}^*_0 = 0$: this is expected since $\tau_0 = 0$ is unphysical [117] for the initial probability in Eq. (5.3) and hence for the ansatz in Eq. (5.26), as it would correspond to a non-normalizable probability.

The value η_0^* of the anomalous dimension η_0 of the initial response field at the Wilson-Fisher fixed point can be straightforwardly derived by substituting in Eq. (5.45) the fixed-point values $\widetilde{r}^*_{\rm WF}$ and $\widetilde{g}^*_{\rm WF}$ of the couplings, obtaining $\eta_0^* = -\epsilon/6$. The initial-slip exponent θ is then defined as [117, 119]:

$$\theta = -\frac{\eta_0^*}{z}, \tag{5.47}$$

and therefore, in the present case, it takes the value

$$\theta = -\frac{\eta_0^*}{2} = \frac{\epsilon}{12}, \tag{5.48}$$

which is in agreement, up to first order in ϵ, with the expression

$$\theta = \frac{\epsilon}{12}\left[1 + \epsilon\left(\frac{8}{27} + \frac{2\log 2}{3}\right)\right] + O(\epsilon^3), \tag{5.49}$$

obtained in Ref. [117].

5.3.3 Comparison with equilibrium dynamics

In this section, we show how one can recover the flow equations for the equilibrium case in the limit $t_0 \to -\infty$. First of all, we note that, in the expressions for $\Delta\Gamma_1$ and $\Delta\Gamma_2$ given in Eqs. (5.34) and (5.41), respectively, the only dependence on t_0 occurs in the lower limit of the integration domain of the integrals on t and in the functions $f_r(t-t_0)$, $f_g(t-t_0)$, and $f_D(t-t_0)$. For $t_0 \to -\infty$ these functions vanish exponentially fast (see Eqs. (5.35), (5.86) and (5.85)) and Eqs. (5.34) and (5.41) read

$$\Delta\Gamma_1^{\rm eq} = -k^{d+1}\frac{a_d}{d}\frac{gD}{\omega_k^2}\int_x \widetilde{\phi}(x)\phi(x), \tag{5.50a}$$

$$\Delta\Gamma_2^{\rm eq} = k^{d+1}\frac{a_d}{d}\frac{g^2D}{\omega_k^3}\int_x \left[\frac{3D}{2\omega_k}\widetilde{\phi}^2(x)\phi^2(x) + \widetilde{\phi}(x)\phi^3(x)\right], \tag{5.50b}$$

with $x \equiv (\mathbf{r}, t)$ and $\int_x \equiv \int \mathrm{d}^d r \int_{-\infty}^{+\infty} \mathrm{d}t$.

Alternatively, one could have taken the limit $t_0 \to -\infty$ from the outset, i.e., before evaluating $\Delta\Gamma_1$ and $\Delta\Gamma_2$: in this case one simply needs to replace $\vartheta(t-t_0)$ with its limiting value 1 in Eqs. (5.15) and (5.24), while G_{0R} is modified inasmuch G_{0C} becomes time-translational invariant as $t_0 \to -\infty$ (see Eqs. (5.11) and (5.28)). This gives rise again to Eqs. (5.50), since the operations of taking the limit $t_0 \to -\infty$ and of calculating the integrals over time (and momenta) on the r.h.s. of Eq. (5.30) do commute (because all the integrals in time are convergent due to the decreasing exponentials in G_{0R} and G_{0C}).

Taking the limit $t_0 \to -\infty$ in the action (5.19) just corresponds to consider the equilibrium, time-translational invariant theory [121], and therefore one concludes that Eqs. (5.50) give rise to the equilibrium flow equations. Since the flow equations (5.43) and (5.44) can also be derived from Eqs. (5.50), they thus represent the equilibrium ones: this is an expected result, since the relaxional nature of model A leads the system to its equilibrium state (yet for asymptotically long times at the critical point), regardless of the quench protocol [117].

5.4 Truncation for $\phi_m \neq 0$

In this section, we discuss the results of a different, improved ansatz for the potential $\mathcal{U}$ in the effective action (5.19), namely

$$\mathcal{U} = \frac{g}{4!}(\phi^2 - \phi_m^2)^2 + \frac{\lambda}{6!}(\phi^2 - \phi_m^2)^3, \tag{5.51}$$

the flow of which is derived in App. 5.E. This potential differs from the one considered in Eq. (5.32) in two respects. First, it corresponds to an expansion around a finite homogeneous value ϕ_m: this choice has the leverage to capture the leading divergences of two-loops corrections in a calculation which is technically carried at one-loop, in the same logic as the background field methods (see, e.g., Refs. [234, 240, 244, 245]), and thus it allows us to calculate, for instance, the renormalization of the factors Z, K and D. Second, we added a sextic interaction, which is marginal for $d = 3$ and therefore it is expected to contribute with sizeable corrections to the value of the critical exponents for spatial dimensionalities close to $d = 3$. In fact, the effective action (5.19) with the potential (5.51) contains all the non-irrelevant operators in $d = 3$. As anticipated, this ansatz allows the renormalization of the time and spatial derivatives terms and of the Markovian noise, i.e., of the coefficients K, Z and D in Eq. (5.19), which therefore will be reinstated in the following analysis. The flow equations for these coefficients can be conveniently expressed in terms of the corresponding anomalous dimensions η_D, η_Z and η_K, defined as:

$$\eta_D \equiv -\frac{k}{D}\frac{\mathrm{d}D}{\mathrm{d}k}, \quad \eta_Z \equiv -\frac{k}{Z}\frac{\mathrm{d}Z}{\mathrm{d}k}, \quad \eta_K \equiv -\frac{k}{K}\frac{\mathrm{d}K}{\mathrm{d}k}. \tag{5.52}$$

The calculation of η_D, η_Z and η_K is detailed, respectively, in Apps. 5.F.1, 5.F.2 and 5.F.3.

The somewhat lengthy flow equations for the corresponding dimensionless couplings

$$\widetilde{m} = \frac{1}{3}\frac{\phi_m^2 g}{K k^2}, \quad \widetilde{g} = \frac{a_d}{d}\frac{D}{ZK^2}\frac{g}{k^{4-d}}, \quad \widetilde{\lambda} = \frac{a_d}{d}\frac{D^2}{Z^2K^3}\frac{\lambda}{k^{6-2d}} \tag{5.53}$$

and for the anomalous dimensions $\eta_{D,Z,K}$ is reported in Eqs. (5.131)-(5.136) of App. 5.G. First of all, we note that $\eta_D = \eta_Z$: this a consequence of detailed balance [121, 244, 245], which characterizes the equilibrium dynamics of model A. In fact, while the short-time dynamics after the quench violates detailed balance inasmuch time-translational invariance is broken, in the long-time limit (in which the flow equations are valid) detailed balance is restored.

The fixed points $(\widetilde{m}^*, \widetilde{g}^*, \widetilde{\lambda}^*)$ of Eqs. (5.131)-(5.134) can be determined numerically and they can be used in order to calculate the anomalous dimension η and the dynamical critical exponent z as

$$\eta = \eta_K^*, \qquad z = 2 - \eta_K^* + \eta_Z^*. \tag{5.54}$$

The critical exponent ν can be determined after linearizing the flow equations around the fixed point, as the inverse of the negative eigenvalue of the stability matrix.

As a consistency check, we compare our values $\nu = 0.64$, $\eta = 0.11$ and $z = 2.05$ in $d = 3$ with the ones determined in Ref. [244] for the equilibrium dynamics of model A within the same truncation ansatz for the effective action Γ as the one employed here, i.e., $\nu = 0.65$, $\eta = 0.11$ and $z = 2.05$, finding very good agreement. For completeness, we also report the Monte Carlo values (see Ref. [244] for a summary), given by $\nu_{\mathrm{MC}} = 0.6297(5)$, $\eta_{\mathrm{MC}} = 0.0362(8)$, and $z_{\mathrm{MC}} = 2.055(10)$.

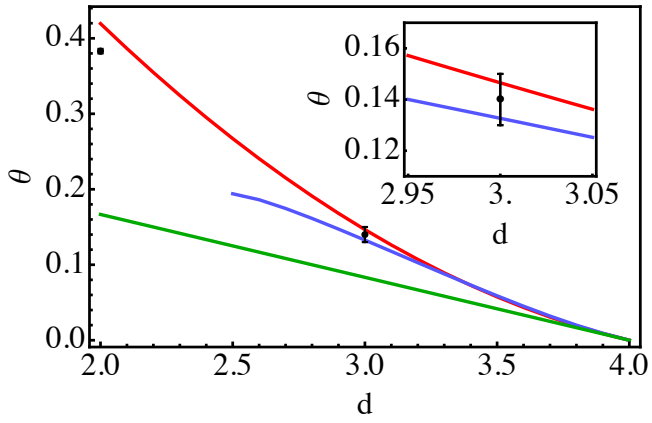

Figure 5.1: Main plot: initial-slip exponent θ as a function of the spatial dimensionality d, evaluated from the FRG discussed here (blue, central line) and from the ϵ-expansion to first (green, lower line) and second (red,upper line) order in $\epsilon = 4 - d$ provided in Eq. (5.49). The value of θ obtained from numerical simulations are indicated for $d = 2$ and 3 (symbols with error bars). For $d = 2$, the error bars are within the symbol size. Inset: magnification of the main plot for $d \simeq 3$.

In Fig. 5.1, we compare the values of $\theta = -\eta_0^*/z$ obtained from Eq. (5.47) on the basis of the present analysis (blue line), and of the first- (green line) and second-order (red line) ϵ-expansion of Ref. [117] reported in Eq. (5.49), as a function of the spatial dimensionality d. The first-order term in the ϵ-expansion is accurate only for dimensions close to $d = 4$, while the second-order contribution provides a sizeable correction and it gives remarkably good results also at smaller dimensionalities. Our results are in remarkable agreement with the latter expansion for $d \gtrsim 3.2$, while increasing discrepancies emerge at smaller values of the spatial dimensionality. In particular, for $d \leq 3$ additional stable fixed points appears in the solution of Eqs. (5.131)-(5.134) in addition to the Wilson-Fisher one, while for $d \leq 2.5$ the latter disappears. This is not surprising, since for $d \leq 3$ new non-irrelevant terms are allowed, and therefore the potential in Eq. (5.51) is no longer an appropriate ansatz and additional terms have to be introduced [240, 244].

For comparison, we report in Fig. 5.1 also the two values of θ obtained from numerical simulations (see, e.g., the summary in Ref. [119]) in $d = 2$ and $d = 3$ (symbols). Remarkably, the predictions of both FRG and ϵ-expansion are compatible (within error bars) with the numerical value in $d = 3$, where the ansatz for the potential (5.51) is reliable, while the FRG predicts a smaller value compared to the one predicted by the ϵ-expansion. For $d = 2$, instead, our ansatz (5.51) is unable to provide reliable results for the reasons reported above, while the ϵ-expansion still provides an unexpectedly accurate prediction, yet outside the error bars of the best available numerical estimate $\theta = 0.383(3)$.

5.5 Concluding remarks

In this Chapter we generalized the functional renormalization group scheme in order to describe the universal dynamical behaviour emerging at short times in a classical statistical system after a temperature quench to its critical point. Specifically, we focused on the relaxional dynamics described by

the model A [121] for a scalar order parameter and a Landau-Ginzburg effective Hamiltonian, and we evaluated the initial-slip exponent θ, which controls the universal scaling of correlation functions and magnetization after the quench within the Ising universality class with spin-flip (Glauber) dynamics. The value of θ is found to be in good agreement with the one obtained via an ϵ-expansion and numerical simulations in $d = 3$. Our prediction for θ can be systematically improved by using a more refined ansatz for the effective action, taking advantage of the existing FRG schemes for equilibrium systems [234, 240].

The approach developed in this Chapter can be extended to different static universality classes, such as $O(N)$ and Potts models, or to different dynamics, e.g., with conserved quantities [247, 248]. In addition, it can also be used in order to study equilibrium phase transitions in systems with a spatial boundary, whose description is formally similar to the case of a quench [229], and possibly also their non-equilibrium dynamics [249, 250]. Moreover, this FRG approach can provide quantitative predictions for additional relevant non-equilibrium universal quantities such as the fluctuation-dissipation ratio and the effective temperatures in the aging regime [119, 182, 251–253].

Finally, this approach constitutes a first step towards the exploration of universality in the dynamics of isolated quantum many-body systems after a parameter quench. It is being currently used to address the dynamical phase transition studied in Chapters 2, 3 and 4.

Appendix

5.A Derivation of the FRG equation

In this Appendix we briefly review the derivation of Eq. (5.15) for the response functional [234]. Let us consider the action $S[\Psi]$, where $\Psi^{\mathrm{t}} = (\varphi, \widetilde{\varphi})$, with φ the order parameter and $\widetilde{\varphi}$ the response field. We define a modified action $S_k[\Psi] = S[\Psi] + \Delta S_k[\Psi]$ where $\Delta S_k[\Psi] = \frac{1}{2}\int_{t,\mathbf{r}} \Psi^{\mathrm{t}} \sigma \Psi R_k$, where $\sigma = \left(\begin{smallmatrix} 0 & 1 \\ 1 & 0 \end{smallmatrix}\right)$ and R_k is a function which implements the infrared cutoff. Then we define the generating function $W_k[J]$ as

$$W_k[J] = \log\left[\int \mathrm{D}\Psi\, \mathrm{e}^{-S_k[\Psi] + \int_{t,\mathbf{r}} \Psi^{\mathrm{t}} J}\right], \tag{5.55}$$

where $\mathrm{D}\Psi$ denotes functional integration over both the fields φ and $\widetilde{\varphi}$, while $J^{\mathrm{t}} = (j, \widetilde{j})$ is an external field. Defining the expectation value $\langle\Psi\rangle$, where the average is taken with respect to the action $-S_k[\Psi] + \int_{t,\mathbf{r}} \Psi^{\mathrm{t}} J$, it is straightforward to check that the following properties follows from Eq. (5.55) [234]:

$$\langle\Psi\rangle = \frac{\delta W_k}{\delta J^{\mathrm{t}}}, \qquad \langle\Psi\Psi^{\mathrm{t}}\rangle - \langle\Psi\rangle\langle\Psi^{\mathrm{t}}\rangle = \frac{\delta^2 W_k}{\delta J^{\mathrm{t}} \delta J} = \frac{\delta\langle\Psi^{\mathrm{t}}\rangle}{\delta J^{\mathrm{t}}}. \tag{5.56}$$

The effective action $\Gamma_k[\Phi]$ is defined as

$$\Gamma_k[\Phi] = -W_k[J] + \int_{t,\mathbf{r}} J^{\mathrm{t}}\Phi - \Delta S_k[\Phi], \tag{5.57}$$

where J is fixed by the condition

$$\Phi = \frac{\delta W_k}{\delta J^{\mathrm{t}}}. \tag{5.58}$$

By comparing the previous equation with the first one in Eq. (5.56), it follows that $\Phi = \langle\Psi\rangle$: accordingly, by using Eq. (5.56), the following relationships can be derived [234]:

$$\frac{\delta\Gamma_k}{\delta\Phi^{\mathrm{t}}} = J - \sigma R_k \Phi, \qquad \frac{\delta^2\Gamma_k}{\delta\Phi^{\mathrm{t}}\delta\Phi} + \sigma R_k = \frac{\delta J^{\mathrm{t}}}{\delta\Phi^{\mathrm{t}}} = \left[\frac{\delta^2 W_k}{\delta J^{\mathrm{t}}\delta J}\right]^{-1}. \tag{5.59}$$

The definition of $\Gamma_k[\Phi]$ in Eq. (5.57) is such that [234] $\Gamma_{k=\Lambda}[\Phi] \approx S[\Phi]$, i.e., when k is equal to the ultraviolet cutoff Λ of the theory, the effective action Γ_k reduces to the "microscopic" action $S[\Phi]$ evaluated on the expectation value Φ. This can also be easily seen by taking a Gaussian microscopic

action $S[\Psi]$: in this case a simple calculation shows that $\Gamma_k[\Phi] = S[\Phi]$. We can now derive the FRG equation by taking the total derivative of the effective action with respect to k:

$$\begin{aligned}\frac{\mathrm{d}\Gamma_k}{\mathrm{d}k} &= -\frac{\partial W_k}{\partial k} - \int_{t,\mathbf{r}} \left(\frac{\delta W}{\delta J} - \Phi^{\mathrm{t}}\right) \frac{\mathrm{d}J}{\mathrm{d}k} - \frac{1}{2}\int_{t,\mathbf{r}} \Phi^{\mathrm{t}}\sigma\frac{\mathrm{d}R_k}{\mathrm{d}k}\Phi \\ &= \frac{1}{2}\int_{t,\mathbf{r}} \langle \Psi^{\mathrm{t}}\sigma\frac{\mathrm{d}R_k}{\mathrm{d}k}\Psi\rangle - \frac{1}{2}\int_{t,\mathbf{r}} \Phi^{\mathrm{t}}\sigma\frac{\mathrm{d}R_k}{\mathrm{d}k}\Phi \\ &= \frac{1}{2}\int_{t,\mathbf{r}} \mathrm{tr}\left[\langle \Psi\Psi^{\mathrm{t}}\rangle\sigma\frac{\mathrm{d}R_k}{\mathrm{d}k}\right] - \frac{1}{2}\int_{t,\mathbf{r}} \mathrm{tr}\left[\Phi\Phi^{\mathrm{t}}\sigma\frac{\mathrm{d}R_k}{\mathrm{d}k}\right] \\ &= \frac{1}{2}\int_{t,\mathbf{r}} \mathrm{tr}\left[\left(\frac{\delta^2\Gamma_k}{\delta\Phi^{\mathrm{t}}\delta\Phi} + \sigma R_k\right)^{-1}\sigma\frac{\mathrm{d}R_k}{\mathrm{d}k}\right], \end{aligned} \tag{5.60}$$

where we repeatedly used Eqs. (5.56) and (5.59) and we expressed the scalar products $\Psi^{\mathrm{t}}\sigma\Psi$ and $\Phi^{\mathrm{t}}\sigma\Phi$ as traces over the internal degrees of freedom. Equation (5.60) is the FRG equation which describes the flow of the effective action Γ_k upon varying the infrared cutoff k.

5.B Derivation of Gaussian Green's functions from Γ_0

In this Appendix we show how the boundary action Γ_0 in Eq. (5.26) contributes to the matrix G_0 defined in Eq. (5.28). Let us consider the quadratic part of the effective action (we consider $Z_0 = 1$ and $h_0 = 0$ for the sake of simplicity) expressed in momentum space:

$$\Gamma = \int_{\mathbf{q}} \left(-\frac{1}{2\tau_0}\widetilde{\phi}_0^2 + \widetilde{\phi}_0\phi_0\right) + \int_{t,\mathbf{q}} \vartheta(t-t_0)\,\widetilde{\phi}\left(\dot{\phi} + \omega_q\phi - D\widetilde{\phi}\right), \tag{5.61}$$

where $\omega_q = q^2 + r$ is the dispersion law, $\int_{\mathbf{q}} \equiv \int \mathrm{d}^d q/(2\pi)^d$ and $\phi \equiv \phi(t,\mathbf{q}), \widetilde{\phi} \equiv \widetilde{\phi}(t,\mathbf{q})$. By taking its second variation $\Gamma^{(2)}(q,t,t')$ as defined in Eq. (5.17), one finds

$$\Gamma^{(2)}(q,t,t') = \left[-V_0\,\delta(t-t_0) + \hat{B}_q(t)\right]\delta(t-t'), \tag{5.62}$$

where the matrices V_0 and $\hat{B}_q(t)$ are defined as

$$V_0 = \begin{pmatrix} 0 & -1 \\ -1 & \tau_0^{-1}\end{pmatrix}, \qquad \hat{B}_q(t) = \begin{pmatrix} 0 & -\partial_t + \omega_q \\ \partial_t + \omega_q & -2D\end{pmatrix}. \tag{5.63}$$

The matrix V_0 is obtained from the boundary action, and consequently it appears in Eq. (5.62) multiplied by a delta function localized at $t = t_0$, while the term proportional to $\hat{B}_q(t)$ is, instead, related to the bulk action. The matrix $G_0(t,t')$ of the correlation functions, defined in Eq. (5.28), is given by $G_0(q,t,t') = [\Gamma^{(2)}]^{-1}(q,t,t')$, where the inverse is taken with respect to the internal matrix structure, the times t, t', and the momentum q. However, since the matrix is diagonal in q, the inversion with respect to the dependence on momenta is trivial. Making use of the definition of $G(q,t,t')$ in Eq. (5.16), multiplying both sides by $G_{\mathrm{eq}}(q,t,t') \equiv [\hat{B}_q(t,t')]^{-1}$ and integrating over the intermediate times, one finds

$$G_0(t,t') = G_{\mathrm{eq}}(t,t') + G_{\mathrm{eq}}(t,t_0)V_0G_0(t_0,t'). \tag{5.64}$$

The explicit form of $G_{\rm eq}(q,t,t')$ can be calculated by inverting the Fourier transform of $\hat{B}_q(t,t')$ and anti-transforming in real time:

$$G_{\rm eq}(q,t,t') = \int \frac{{\rm d}\omega}{2\pi}\, {\rm e}^{-i\omega(t-t')}[B_q(\omega)]^{-1} = \begin{pmatrix} D\omega_q^{-1}{\rm e}^{-\omega_q|t-t'|} & \vartheta(t-t'){\rm e}^{-\omega_q(t-t')} \\ \vartheta(t'-t){\rm e}^{-\omega_q(t'-t)} & 0 \end{pmatrix}. \tag{5.65}$$

Notice that $B_q(\omega)$ is diagonal in the frequency ω, since $\hat{B}_q(t,t')$ depends only on the difference of times $t-t'$. In fact, $G_{\rm eq}(t,t')$ is a time-translational invariant function which corresponds to the correlation matrix of the model at thermal equilibrium. Equation (5.64) can be solved by iteration, and it yields the formal solution:

$$G_0(q,t,t') = G_{\rm eq}(q,t,t') + G_{\rm eq}(q,t,t_0)V_0 \sum_{n=0}^{+\infty} [G_{\rm eq}(q,t_0,t_0)V_0]^n\, G_{\rm eq}(q,t_0,t'). \tag{5.66}$$

Recalling that within the response functional formalism adopted here we set $\vartheta(0) = 0$ in order to ensure causality [121], we get

$$V_0 \sum_{n=0}^{+\infty} [G_{\rm eq}(q,t_0,t_0)V_0]^n = V_0[1 - G_{\rm eq}(q,t_0,t_0)V_0]^{-1} = \begin{pmatrix} 0 & -1 \\ -1 & D\omega_q^{-1} + \tau_0^{-1} \end{pmatrix}. \tag{5.67}$$

Combining Eqs. (5.66), (5.65) and (5.67), one finds the same Gaussian Green's functions as those in Eqs. (5.11) and (5.10), with $\Omega = 1$ and T replaced by D.

5.C Integral equation for G

In this Appendix we derive and discuss Eq. (5.27) for the matrix G defined in Eq. (5.16). The former can be obtained by multiplying both sides of the latter by $G_0^{-1} - V$ defined in Eq. (5.21) and by integrating over intermediate coordinates, which yields

$$\int_y \left[G_0^{-1}(x,y) - V(x,y)\right] G(y,x') = \delta(x-x'), \tag{5.68}$$

where the delta function on the r.h.s. of Eq. (5.68) appears as a consequence of Eq. (5.22). Accordingly, by multiplying both sides of Eq. (5.68) by G_0 and integrating over the intermediate coordinates, and by using Eq. (5.23), one finds the integral equation for G

$$G(x,x') = G_0(x,x') + \int_y G_0(x,y)\, V(y) G(y,x'). \tag{5.69}$$

This equation can be formally solved by iteration, and the solution can be expressed as the infinite series

$$G(x,x') = G_0(x,x') + \sum_{n=1}^{+\infty} G_n(x,x'), \tag{5.70}$$

where G_n are convolutions given by

$$G_n(x,x') \equiv \int_{y_1 \ldots y_n} G_0(x,y_1) V(y_1) G_0(y_1,y_2) \ldots V(y_n) G_0(y_n,x'). \tag{5.71}$$

The formal solution Eq. (5.70) can be inserted into Eq. (5.15), providing a convenient expression for the FRG equation, which now reads (as in the main text, the dependence of Γ and R on k is understood):

$$\frac{\mathrm{d}\Gamma}{\mathrm{d}k} = \sum_{n=0}^{+\infty} \Delta\Gamma_n, \tag{5.72}$$

where

$$\Delta\Gamma_0 \equiv \frac{1}{2} \int_x \mathrm{tr} \left[G_0(x,x) \frac{\mathrm{d}R}{\mathrm{d}k} \sigma \right], \tag{5.73}$$

and

$$\Delta\Gamma_n = \frac{1}{2} \int_x \mathrm{tr} \left[G_n(x,x) \frac{\mathrm{d}R}{\mathrm{d}k} \sigma \right] \quad \text{for} \quad n \geq 1. \tag{5.74}$$

A straightforward calculation shows that $\Delta\Gamma_0 \propto \vartheta(0)$ and therefore this term vanishes, since we assumed from the outset $\vartheta(0) = 0$ in order to ensure causality [121]. As a result, the sum over n in Eq. (5.72) actually starts from $n = 1$, as in Eq. (5.30).

The FRG equation in the form of Eq. (5.72) can be used to study the case of systems with broken time-translational symmetry, since each $\Delta\Gamma_n$ can now be calculated independently of the presence of such a symmetry. However, we emphasize that in general it is not possible to sum the series on the r.h.s. of Eq. (5.72) in a closed form, because the convolutions in $\Delta\Gamma_n$ are generically rather complicated non-local functions of the fields ϕ and $\widetilde{\phi}$.

If, instead, time-translational invariance is not broken, e.g., when one takes the limit $t_0 \to -\infty$ in the action (5.19), the matrix G determined from Eq. (5.70) is identical to the one obtained by the direct inversion of Eq. (5.16). In order to show this, let us assume that one is interested only in the renormalization of the potential $\mathcal{U}$, disregarding those of K, D and Z. Then one makes use of the so-called local-potential approximation [234, 240, 246], in which the field-dependent function $V(\mathbf{r},t)$ introduced in Eq. (5.24) is evaluated on configurations of the fields ϕ and $\widetilde{\phi}$ which are constant in space and time, such that $V(\mathbf{r},t)$ is actually independent of $\mathbf{r}$ and t. As a consequence of time-translational invariance, G depends only on the difference of its arguments, i.e., $G_0(x,x') = G_0(x-x')$ and $G(x,x') = G(x-x')$. Then, after taking the Fourier transform with respect to the relative coordinates $\mathbf{r} - \mathbf{r}'$ and $t - t'$, the convolutions in Eq. (5.70) become products of the $G_0(\mathbf{k},\omega)$, which are functions of the momentum $\mathbf{k}$ and of the frequency ω. Accordingly, this equation becomes

$$\begin{aligned} G(\mathbf{k},\omega) &= \sum_{n=0}^{+\infty} G_0(\mathbf{k},\omega) \left[V G_0(\mathbf{k},\omega) \right]^n \\ &= \left[G_0^{-1}(\mathbf{k},\omega) - V \right]^{-1}. \end{aligned} \tag{5.75}$$

This expression can thus be used in Eq. (5.15), which then acquires a closed form. Notice that Eq. (5.75) could have been obtained directly by simply taking the Fourier transform of Eq. (5.16) with the definition (5.21).

5.D Calculation of $\Delta\Gamma_1$ and $\Delta\Gamma_2$

In this Appendix, we detail the calculations which lead to Eqs. (5.34) and (5.41). Starting from Eq. (5.74), we find:

$$\begin{aligned}\Delta\Gamma_1 &= \frac{1}{2}\int_{t,t',\mathbf{r},\mathbf{r}'} \mathrm{tr}\left[G_0(\mathbf{r}-\mathbf{r}',t,t')\,V(t',\mathbf{r}')G_0(\mathbf{r}'-\mathbf{r},t',t)\sigma\frac{\mathrm{d}R}{\mathrm{d}k}\right] \\ &= \frac{1}{2}\int_{t,t',\mathbf{q},\mathbf{r}'} \mathrm{tr}\left[G_0(q,t,t')\,V(t',\mathbf{r}')G_0(q,t',t)\sigma\frac{\mathrm{d}R}{\mathrm{d}k}(q)\right] \\ &= k^{d+1}\frac{a_d}{d}\int_{t,t',\mathbf{r}'} \mathrm{tr}\left[G_0(k,t,t')\,V(t',\mathbf{r}')G_0(k,t',t)\sigma\right], \end{aligned} \tag{5.76}$$

where $a_d = 2/[\Gamma(d/2)(4\pi)^{d/2}]$, with d the spatial dimensionality and $\Gamma(x)$ the gamma function. In the second equality of Eq. (5.76) one expresses $G_0(\mathbf{r},t,t')$ in terms of its Fourier transforms $G_0(q,t,t')$ and then calculates the integral over the spatial coordinates $\mathbf{r}$. In the third equality, instead, after performing the integration over angular variables (which generates the factor a_d), the integral over momenta q becomes trivial since the function (see Eq. (5.20))

$$\frac{\mathrm{d}R(q)}{\mathrm{d}k} = 2k\,\vartheta(k^2-q^2) \tag{5.77}$$

restricts the integration domain to $0 \le q \le k$, within which $G_0(q,t,t')$ is constant and equal to $G_0(k,t,t')$ as a consequence of the modified dispersion relation in Eq. (5.29). Similarly, $\omega_{k,q}$ is replaced by $\omega_{k,q\le k} = \omega_{k,k} = \omega_{q=k}$ (see Eq. (5.29) and after Eq. (5.11)). Note that, since K is not renormalized within this approximation, it does not contribute to Eq. (5.77) and, for simplicity, we set $K = 1$. Finally, by using the definitions (5.28) and (5.33), one evaluates the trace in Eq. (5.76), finding

$$\begin{aligned}\Delta\Gamma_1 &= -2k^{d+1}\frac{a_d}{d}g\int_{\mathbf{r}'}\int_{t_0}^{+\infty}\mathrm{d}t'\,\widetilde{\phi}(\mathbf{r}',t')\phi(\mathbf{r}',t')\int_{t_0}^{+\infty}\mathrm{d}t\,G_R(k,t',t)G_C(k,t',t) \\ &= -k^{d+1}\frac{a_d}{d}\frac{gD}{\omega_k^2}\int_{\mathbf{r}}\int_{t_0}^{+\infty}\mathrm{d}t'\,\widetilde{\phi}(t',\mathbf{r})\phi(t',\mathbf{r})\left[1-f_r(t'-t_0)\right], \end{aligned} \tag{5.78}$$

where in the last equality the integral over time t was calculated. The function $f_r(t)$ is defined in Eq. (5.35) and corresponds to the time-dependent part of the result of the integration over t. Note that the terms proportional to ϕ^2 contained in V, do not appear in the final result (as required by causality [121,215]) since they would be multiplied by a factor $\vartheta(t-t')\vartheta(t'-t) = 0$. The last equality of Eq. (5.78) is nothing but Eq. (5.34) of the main text.

The calculation of $\Delta\Gamma_2$ is lengthier, but it proceeds as discussed above for $\Delta\Gamma_1$. From the definition

in Eq. (5.74) one has

$$\begin{aligned}\Delta\Gamma_2 &= \frac{1}{2}\int_{t,t',t'',\mathbf{r},\mathbf{r}',\mathbf{r}''} \mathrm{tr}\left[G_0(\mathbf{r}-\mathbf{r}',t,t')V(t',\mathbf{r}')G_0(\mathbf{r}'-\mathbf{r}'',t',t'')V(t'',\mathbf{r}'')G_0(\mathbf{r}''-\mathbf{r},t'',t)\frac{\mathrm{d}R}{\mathrm{d}k}\right] \\ &= \frac{1}{2}\int_{t,t',t'',\mathbf{r}',\mathbf{r}'',\mathbf{q},\mathbf{q}'} \mathrm{e}^{i\mathbf{r}'\cdot(\mathbf{q}'-\mathbf{q})}\,\mathrm{tr}\left[G_0(q,t,t')V(t',\mathbf{r}'+\mathbf{r}'')G_0(q',t',t'')V(t'',\mathbf{r}'')G_0(q,t'',t)\frac{\mathrm{d}R(q)}{\mathrm{d}k}\right] \\ &\approx \frac{1}{2}\int_{t,t',t'',\mathbf{r}',\mathbf{r}'',\mathbf{q},\mathbf{q}'} \mathrm{e}^{i\mathbf{r}'\cdot(\mathbf{q}'-\mathbf{q})}\mathrm{tr}\left[G_0(q,t,t')V(t',\mathbf{r}'')G_0(q',t',t'')V(t'',\mathbf{r}'')G_0(q,t'',t)\frac{\mathrm{d}R(q)}{\mathrm{d}k}\right] \\ &= k^{d+1}\frac{a_d}{d}\int_{t,t',t'',\mathbf{r}''} \mathrm{tr}\left[G_0(k,t,t')V(t',\mathbf{r}'')G_0(k,t',t'')V(t'',\mathbf{r}'')G_0(k,t'',t)\sigma\right], \end{aligned} \tag{5.79}$$

where in the second equality we expressed the various $G_0(\mathbf{r},t,t')$ (see Eq. (5.28)) in terms of their Fourier transforms, we made the change of variables $\mathbf{r}' \to \mathbf{r}'+\mathbf{r}''$ and integrated over the spatial coordinate $\mathbf{r}$. In the third step we expanded $V(t',\mathbf{r}'+\mathbf{r}'') \approx V(t',\mathbf{r}'')$ in order to retain only local combinations of fields, while in the last step we integrated over $\mathbf{r}'$ and calculated the trivial integrals over $\mathbf{q}$ and $\mathbf{q}'$. After determining the trace on the basis of the definitions (5.28) and (5.33), and by noticing that the prefactor of the term $\propto \phi^4$ vanishes (as required by causality [121,215]) as it contains the factor $\vartheta(t-t')\vartheta(t'-t'')\vartheta(t''-t)=0$, Eq. (5.79) becomes

$$\begin{aligned}\Delta\Gamma_2 &= k^{d+1}\frac{a_d}{d}g^2\int_{\mathbf{r}''}\int_{t_0}^{+\infty}\mathrm{d}t\,\mathrm{d}t'\mathrm{d}t''\left\{2\,\widetilde{\phi}(t')\phi(t')\widetilde{\phi}(t'')\phi(t'')\,G_{0C}(k,t',t'')G_{0C}(k,t'',t)G_{0R}(k,t',t)\right. \\ &\quad + \widetilde{\phi}(t')\phi(t')\phi^2(t'')\Big[G_{0C}(k,t',t'')G_{0R}(k,t,t'')G_{0R}(k,t',t) \\ &\quad \left. + G_{0C}(k,t',t'')G_{0R}(k,t,t'')G_{0R}(k,t',t) + G_{0C}(k,t,'t)G_{0R}(k,t',t'')G_{0R}(k,t'',t)\Big]\right\} \\ &\simeq k^{d+1}\frac{a_d}{d}g^2\int_{\mathbf{r}''}\int_{t_0}^{+\infty}\mathrm{d}t'\,\left[2\widetilde{\phi}^2(t')\phi^2(t')F_D(t') + \widetilde{\phi}(t')\phi^3(t')F_g(t')\right], \end{aligned} \tag{5.80}$$

where we omitted the dependence on $\mathbf{r}''$ of the fields for the sake of clarity. In the last step of Eq. (5.80), we expanded the fields for $t' \simeq t''$ as $\phi(t'') \simeq \phi(t')$ and $\widetilde{\phi}(t'') \simeq \widetilde{\phi}(t')$ in order to retain only combinations of the fields local in time, and we introduced the functions

$$F_D(t') = \int_{t_0}^{+\infty}\mathrm{d}t\,\mathrm{d}t''G_{0C}(k,t,t')G_{0C}(k,t',t'')G_{0R}(k,t'',t), \tag{5.81}$$

and

$$\begin{aligned}F_g(t') = \int_{t_0}^{+\infty}\mathrm{d}t\,\mathrm{d}t''\Big[&G_{0C}(k,t',t'')G_{0R}(k,t,t'')G_{0R}(k,t',t) + G_{0C}(k,t,t'')G_{0R}(k,t',t'')G_{0R}(k,t',t) \\ &+ G_{0C}(k,t,t')G_{0R}(k,t',t'')G_{0R}(k,t'',t)\Big]. \end{aligned} \tag{5.82}$$

The functions F_D and F_g can be easily evaluated using Eqs. (5.11) and (5.10), and they render

$$F_D(t) = \frac{1}{4}\frac{D^2}{\omega_k^4}\left[3 - f_D(t-t_0)\right], \tag{5.83}$$

$$F_g(t) = \frac{D}{\omega_k^3}\left[1 - f_g(t-t_0)\right], \tag{5.84}$$

with

$$f_D(t) = \left\{2 + 2\omega_k t - 2(1+\omega_k t)^2\left(\frac{\omega_k}{D\tau_0} - 1\right) - \left(\frac{\omega_k}{D\tau_0} - 1\right)^2\right\}\mathrm{e}^{-2\omega_k t}, \tag{5.85}$$

$$f_g(t) = \left[1 + 2\omega_k t - 2(\omega_k t)^2\left(\frac{\omega_k}{D\tau_0} - 1\right)\right]\mathrm{e}^{-2\omega_k t}. \tag{5.86}$$

Finally, substituting Eqs. (5.83) and (5.84) into Eq. (5.80), we find Eq. (5.41) of the main text.

5.E Flow equations in the ordered phase

In this Appendix, we will detail the derivation of the flow equations for the potential expanded around a finite homogeneous value $\phi = \phi_m$ and $\widetilde{\phi} = 0$. For the sake of clarity, we consider the potential $\mathcal{U}$ in Eq. (5.51) with $\lambda = 0$. The generalization to the case $\lambda \neq 0$ is straightforward and proceeds as in the equilibrium case (see, for instance, Refs. [234] and [245]).

First of all, since the factor K is renormalized within the ansatz discussed here, the derivative with respect to k of the regulator $R(q)$ defined in Eq. (5.20), has also to account for the renormalization factor K on k, as

$$\frac{\mathrm{d}R(q)}{\mathrm{d}k} = \frac{K}{k}\vartheta(k^2 - q^2)\left[2k^2 - \eta_K\left(k^2 - q^2\right)\right], \tag{5.87}$$

where we made use of the definition of η_K in Eq. (5.52), see also Ref. [245]. In fact, since the factor K depends on k within this approximation, the derivative with respect to k of Eq. (5.20) produces a contribution proportional to η_K.

Then, by taking the second variation of the effective action Γ in Eq. (5.19) (see Eq. (5.17)), we cast the equation for the function G defined in Eq. (5.16) into the same form as Eq. (5.69), with the field-dependent function V defined as (we assume $t_0 = 0$ for simplicity):

$$V(x) = -g\,\vartheta(t)\begin{pmatrix}\widetilde{\rho}(x) & \rho(x) - \rho_m \\ \rho(x) - \rho_m & 0\end{pmatrix}, \tag{5.88}$$

where we define

$$\rho \equiv \frac{\phi^2}{2}, \qquad \widetilde{\rho} = \widetilde{\phi}\phi, \qquad \rho_m \equiv \frac{\phi_m^2}{2}, \tag{5.89}$$

while G_0 is defined according to Eq. (5.28), but with the post-quench parameter r replaced by

$$m = \frac{2}{3}\rho_m g. \tag{5.90}$$

The use of the $\mathbb{Z}_2$ invariants ρ and $\widetilde{\rho}$ is customary in the context of FRG [245] and it helps in simplifying the notation in what follows. The form of $V(x)$ in Eq. (5.88) allows us to express the r.h.s. of the FRG equation (5.30) as a power series of $\rho - \rho_m$, in the spirit of Eq. (5.72): this provides, together with the vertex expansion (5.18), a way to unambiguously identify the renormalization of the terms appearing in the potential $\mathcal{U}$ in Eq. (5.51). In fact, ρ_m and the couplings g and λ are identified as [240]:

$$\left.\frac{\mathrm{d}\mathcal{U}}{\mathrm{d}\rho}\right|_{\rho=\rho_m} = 0, \quad \frac{g}{3} = \left.\frac{\mathrm{d}^2\mathcal{U}}{\mathrm{d}\rho^2}\right|_{\rho=\rho_m}, \quad \frac{\lambda}{15} = \left.\frac{\mathrm{d}^3\mathcal{U}}{\mathrm{d}\rho^3}\right|_{\rho=\rho_m}, \tag{5.91}$$

where the first condition actually defines ρ_m as the minimum of the potential. In terms of the effective action Γ, Eqs. (5.91) become [244, 245]

$$\left.\frac{\delta\Gamma}{\delta\widetilde{\rho}}\right|_{\substack{\widetilde{\rho}=0\\ \rho=\rho_m}} = 0, \quad \frac{g}{3} = \left.\frac{\delta^2\Gamma}{\delta\widetilde{\rho}\,\delta\rho}\right|_{\substack{\widetilde{\rho}=0\\ \rho=\rho_m}}, \quad \frac{\lambda}{15} = \left.\frac{\delta^3\Gamma}{\delta\widetilde{\rho}\,\delta\rho^2}\right|_{\substack{\widetilde{\rho}=0\\ \rho=\rho_m}}. \tag{5.92}$$

By taking a total derivative with respect to k of each equality in Eqs. (5.92), one finds

$$\left.\frac{\delta}{\delta\widetilde{\rho}}\frac{\partial\Gamma}{\partial k}\right|_{\substack{\widetilde{\rho}=0\\ \rho=\rho_m}} + \left.\frac{\delta^2\Gamma}{\delta\widetilde{\rho}\,\delta\rho}\right|_{\substack{\widetilde{\rho}=0\\ \rho=\rho_m}} \frac{\mathrm{d}\rho_m}{\mathrm{d}k} = 0, \tag{5.93}$$

$$\frac{1}{3}\frac{\mathrm{d}g}{\mathrm{d}k} = \left.\frac{\delta^2}{\delta\widetilde{\rho}\,\delta\rho}\frac{\partial\Gamma}{\partial k}\right|_{\substack{\widetilde{\rho}=0\\ \rho=\rho_m}} + \left.\frac{\delta^3\Gamma}{\delta\widetilde{\rho}\,\delta^2\rho}\right|_{\substack{\widetilde{\rho}=0\\ \rho=\rho_m}} \frac{\mathrm{d}\rho_m}{\mathrm{d}k}, \tag{5.94}$$

$$\frac{1}{15}\frac{\mathrm{d}\lambda}{\mathrm{d}k} = \left.\frac{\delta^3}{\delta\widetilde{\rho}\,\delta\rho^2}\frac{\partial\Gamma}{\partial k}\right|_{\substack{\widetilde{\rho}=0\\ \rho=\rho_m}} + \left.\frac{\delta^4\Gamma}{\delta\widetilde{\rho}\,\delta^3\rho}\right|_{\substack{\widetilde{\rho}=0\\ \rho=\rho_m}} \frac{\mathrm{d}\rho_m}{\mathrm{d}k}, \tag{5.95}$$

which, after replacing $\partial\Gamma/\partial k$ with the FRG equation (5.15), render the flow equations for ρ_m, g, and λ. For the case of the potential $\mathcal{U}$ in Eq. (5.51) with $\lambda = 0$, by using Eq. (5.92), the set of flow equations (5.93) and (5.94) simplifies as

$$\frac{\mathrm{d}\rho_m}{\mathrm{d}k} = -\frac{3}{g}\left.\frac{\delta}{\delta\widetilde{\rho}}\frac{\partial\Gamma}{\partial k}\right|_{\substack{\widetilde{\rho}=0\\ \rho=\rho_m}} = -\frac{3}{g}\left.\frac{\delta\Delta\Gamma_1}{\delta\widetilde{\rho}}\right|_{\substack{\widetilde{\rho}=0\\ \rho=\rho_m}}, \tag{5.96}$$

$$\frac{1}{3}\frac{\mathrm{d}g}{\mathrm{d}k} = \left.\frac{\delta^2}{\delta\widetilde{\rho}\,\delta\rho}\frac{\partial\Gamma}{\partial k}\right|_{\substack{\widetilde{\rho}=0\\ \rho=\rho_m}} = \left.\frac{\delta^2\Delta\Gamma_2}{\delta\widetilde{\rho}\,\delta\rho}\right|_{\substack{\widetilde{\rho}=0\\ \rho=\rho_m}}, \tag{5.97}$$

where we used Eq. (5.72) with $\Delta\Gamma_1$ and $\Delta\Gamma_2$ defined as in Eqs. (5.74) and (5.71) in terms of the $V(x)$ in Eq. (5.88). The explicit form of the flow equations comes from a calculation analogous to the one discussed in Sec. 5.3 and in App. 5.D (see Eqs. (5.34) and (5.41)). In particular, the flow of m, defined in Eq. (5.90), takes contributions from both the flow equations for ρ_m and g. Similarly, the renormalization of Z_0 is determined by the contribution localized at $t = 0$ of the coefficient of the quadratic term $\widetilde{\phi}\phi$ in the effective action (5.19) equipped with the potential (5.51).

5.F Anomalous dimensions

In this Appendix we discuss the derivation of the renormalization of K, Z, and D resulting from the potential $\mathcal{U}$ in Eq. (5.51) and from the effective action Γ in Eq. (5.19).

5.F.1 Renormalization of D

The strength D of the Markovian noise can be unambiguously defined from the effective action Γ in Eq. (5.19) as [245]

$$D = -\rho_m \left. \frac{\delta^2 \Gamma}{\delta^2 \widetilde{\rho}} \right|_{\substack{\widetilde{\rho}=0 \\ \rho=\rho_m}}, \tag{5.98}$$

where ρ and $\widetilde{\rho}$ are defined in Eq. (5.89). By differentiating the previous equation with respect to k, we find

$$\frac{\mathrm{d}D}{\mathrm{d}k} = -\left(\frac{\delta^2 \Gamma}{\delta^2 \widetilde{\rho}} + \frac{\delta^3 \Gamma}{\delta^2 \widetilde{\rho} \delta \rho} \right) \Bigg|_{\substack{\widetilde{\rho}=0 \\ \rho=\rho_m}} \frac{\mathrm{d}\rho_m}{\mathrm{d}k} - \rho_m \frac{\delta^2}{\delta^2 \widetilde{\rho}} \frac{\partial \Gamma}{\partial k} \Bigg|_{\substack{\widetilde{\rho}=0 \\ \rho=\rho_m}}. \tag{5.99}$$

For the effective action Γ in Eq. (5.19) with the potential $\mathcal{U}$ in Eq. (5.51), the terms in brackets in Eq. (5.99) vanish and the flow equation for D simplifies as

$$\frac{\mathrm{d}D}{\mathrm{d}k} = -\rho_m \frac{\delta^2}{\delta^2 \widetilde{\rho}} \frac{\partial \Gamma}{\partial k} \Bigg|_{\substack{\widetilde{\rho}=0 \\ \rho=\rho_m}} = -\rho_m \frac{\delta^2 \Delta\Gamma_2}{\delta^2 \widetilde{\rho}} \Bigg|_{\substack{\widetilde{\rho}=0 \\ \rho=\rho_m}}, \tag{5.100}$$

where we used Eqs. (5.72) and (5.74) with $V(x)$ as in Eq. (5.88). In fact, a direct inspection of Eq. (5.41) shows that $\Delta\Gamma_2$ contains a term proportional to $\widetilde{\rho}^2$, while any other term $\Delta\Gamma_n$ with $n > 2$ generated by the field-dependent function (5.88) vanishes when evaluated for $\rho = \rho_m$. Accordingly, by calculating $\Delta\Gamma_2$ as in Eq. (5.41) (see also App. 5.D), in the long-time limit within which the function $f_D(t)$ (see Eqs. (5.41) and (5.85)) vanishes, and by applying Eq. (5.100), we find the equation

$$\frac{\mathrm{d}D}{\mathrm{d}k} = -3k^{d+1} \frac{a_d}{d} \frac{KD^2}{Z} \left(1 - \frac{\eta_K}{d+2} \right) \frac{\rho_m g^2}{(Kk^2 + m)^4}, \tag{5.101}$$

with m given in Eq. (5.90). Note that the factor $1 - \eta_K/(d+2)$ comes from the integration over momenta with $\mathrm{d}R/\mathrm{d}k$ given by Eq. (5.87). According to definition (5.52), η_D is eventually given by:

$$\eta_D = 3k^{d+2} \frac{a_d}{d} \frac{KD}{Z} \left(1 - \frac{\eta_K}{d+2} \right) \frac{\rho_m g^2}{(Kk^2 + m)^4}. \tag{5.102}$$

5.F.2 Renormalization of Z

Following the general procedure described, e.g., in Refs. [244, 245], in order to evaluate the correction to the coefficient Z, we express the fields ϕ and $\widetilde{\phi}$ as fluctuations around the homogeneous field ϕ_m:

$$\phi(\mathbf{r}, t) = \phi_m + \delta\phi(\mathbf{r}, t), \quad \widetilde{\phi}(\mathbf{r}, t) = \delta\widetilde{\phi}(\mathbf{r}, t). \tag{5.103}$$

By replacing Eq. (5.103) into the field-dependent function $V(x)$ defined in Eq. (5.88), we find

$$V(x) = V_1(x) + V_2(x), \tag{5.104}$$

with V_1 being linear in the fluctuations $\delta\phi$ and $\delta\widetilde{\phi}$, i.e.,

$$V_1(x) = -g\phi_m \vartheta(t) \begin{pmatrix} \delta\widetilde{\phi}(x) & \delta\phi(x) \\ \delta\phi(x) & 0 \end{pmatrix}, \tag{5.105}$$

while V_2 contains only terms quadratic in the fluctuations, i.e.,

$$V_2(x) = -g\vartheta(t) \begin{pmatrix} \delta\phi(x)\delta\widetilde{\phi}(x) & [\delta\phi(x)]^2/2 \\ [\delta\phi(x)]^2/2 & 0 \end{pmatrix}. \tag{5.106}$$

When V in Eq. (5.104) is substituted in the expression of $\Delta\Gamma_2$ in Eq. (5.79), it produces a term which contains a product of two V_1 calculated at different spatial and temporal coordinates, generating a quadratic term $\propto \delta\phi\delta\widetilde{\phi}$, non-local in both spatial and temporal coordinates. Since we are interested in the renormalization of Z, we can restrict to terms which are local in space and therefore we can use Eq. (5.79) and replace V by V_1 in it: this gives (cf. Eq. (5.80))

$$\begin{aligned}\Delta\Gamma_2\big|_{V\to V_1} = 4k^{d+1}\frac{a_d}{d}K\left(1-\frac{\eta_K}{d+2}\right)g^2\rho_m\int_{\mathbf{r}}\int_{t_0}^{+\infty}\mathrm{d}t\,\mathrm{d}t'\mathrm{d}t''\Big\{2\,\delta\widetilde{\phi}(t')\delta\widetilde{\phi}(t'')\,G_{0C}(k,t',t'')G_{0C}(k,t'',t)G_{0R}(k,t',t)\\ + \delta\widetilde{\phi}(t')\delta\phi(t'')\Big[G_{0C}(k,t',t'')G_{0R}(k,t,t'')G_{0R}(k,t',t)\\ + G_{0C}(k,t',t'')G_{0R}(k,t,t'')G_{0R}(k,t',t) + G_{0C}(k,t,'t)G_{0R}(k,t',t'')G_{0R}(k,t'',t)\Big]\Big\},\end{aligned} \tag{5.107}$$

where the dependence of the fluctuations on the spatial coordinates $\mathbf{r}$ has been omitted for simplicity. Then, by neglecting the term $\propto \delta\widetilde{\phi}^2$, which generates only additional irrelevant terms, and by expanding $\delta\phi(t'')$ for $t''\simeq t'$ as $\delta\phi(t'')\simeq\delta\phi(t')+(t''-t')\delta\dot{\phi}(t')$, keeping only the derivative, from Eq. (5.107) we find

$$\Delta\Gamma_2\big|_{V\to V_1} \simeq 4k^{d+1}\frac{a_d}{d}K\left(1-\frac{\eta_K}{d+2}\right)g^2\rho_m\int_{\mathbf{r}}\int_{t_0}^{+\infty}\mathrm{d}t'\delta\widetilde{\phi}(t')\delta\dot{\phi}(t')F_Z(t'), \tag{5.108}$$

where

$$\begin{aligned}F_Z(t') = \int_{t_0}^{+\infty}\mathrm{d}t\,\mathrm{d}t''(t''-t')\Big[G_{0C}(k,t',t'')G_{0R}(k,t,t'')G_{0R}(k,t',t)+G_{0C}(k,t,t'')G_{0R}(k,t',t'')G_{0R}(k,t',t)\\ + G_{0C}(k,t,t')G_{0R}(k,t',t'')G_{0R}(k,t'',t)\Big].\end{aligned} \tag{5.109}$$

The function $F_Z(t)$ can be easily evaluated using Eqs. (5.11) and (5.10), and reads

$$F_Z(t) = \frac{D}{4\omega_k^4}\left[3 - f_Z(t-t_0)\right], \tag{5.110}$$

where $f_Z(t)$ is a function which vanishes exponentially fast upon increasing t and therefore does not contribute to the renormalization of Z at long times. Finally, by replacing Eq. (5.110) into Eq. (5.108), and by comparing the r.h.s. of Eq. (5.72) with its l.h.s. in which the effective action (5.19) has been inserted, one finds the flow equation for Z:

$$\frac{\mathrm{d}Z}{\mathrm{d}k} = -3k^{d+1}\frac{a_d}{d}\frac{KD}{Z}\left(1-\frac{\eta_K}{d+2}\right)\frac{g^2\rho_m}{(Kk^2+m)^4}Z, \tag{5.111}$$

where m is given in Eq. (5.90). By using the definitions in Eq. (5.52), one thus finds the expression of the anomalous dimension η_Z:

$$\eta_Z = 3k^{d+2}\frac{a_d}{d}\frac{KD}{Z}\left(1-\frac{\eta_K}{d+2}\right)\frac{g^2\rho_m}{(Kk^2+m)^4}. \tag{5.112}$$

5.F.3 Renormalization of K

The calculation of the flow equation for K proceeds as in the case of Z discussed in the previous section, i.e., we expand the field ϕ around the homogeneous configuration as in Eq. (5.103). This renders the same field-dependent function $V(x)$ as in Eq. (5.104), containing a term V_1 linear in the fluctuations which — when inserted in the expression (5.79) for $\Delta\Gamma_2$ — generates quadratic terms which are non-local in spatial and temporal coordinates. It is convenient to define K as follows [244]:

$$K = \mathcal{N}\frac{\partial}{\partial p^2}\frac{\delta^2\Gamma}{\delta\widetilde{\phi}(t,-\mathbf{p})\delta\phi(t,\mathbf{p})}\bigg|_{\substack{\mathbf{p}=0\\ \delta\widetilde{\phi}=\delta\phi=0}}, \tag{5.113}$$

where $\mathcal{N}$ is a normalization factor formally given by $\mathcal{N} = (2\pi)^d/[\delta^{(d)}(q=0)\delta(t=0)]$, and $\mathbf{p}$ is a given momentum, eventually vanishing. By taking the total derivative with respect to k of the previous expressions, we find

$$\frac{\mathrm{d}K}{\mathrm{d}k} = \mathcal{N}\frac{\partial}{\partial p^2}\frac{\delta^2}{\delta\widetilde{\phi}(t,-\mathbf{p})\delta\phi(t,\mathbf{p})}\frac{\partial\Gamma}{\partial k}\bigg|_{\substack{\mathbf{p}=0\\ \delta\widetilde{\phi}=\delta\phi=0}} = \mathcal{N}\frac{\partial}{\partial p^2}\frac{\delta^2\Delta\Gamma_2\big|_{V\to V_1}}{\delta\widetilde{\phi}(t,-\mathbf{p})\delta\phi(t,\mathbf{p})}\bigg|_{\substack{\mathbf{p}=0\\ \delta\widetilde{\phi}=\delta\phi=0}},$$

where in the last equality we used Eq. (5.72) and the fact that the sole non-trivial contribution comes from the part of $\Delta\Gamma_2$ (indicated as $\Delta\Gamma_2\big|_{V\to V_1}$ in the previous equation) involving the product of two V_1 (see App. 5.F.2). From Eq. (5.79), we find with some simple calculations:

$$\Delta\Gamma_2\big|_{V\to V_1} = \frac{1}{2}\int_{t,t',t'',\mathbf{q},\mathbf{q}'}\mathrm{tr}\bigg[G_0(q,t,t')V(t',\mathbf{q}-\mathbf{q}')G_0(q',t',t'')V(t'',\mathbf{q}'-\mathbf{q})G_0(q,t'',t)\frac{\mathrm{d}R}{\mathrm{d}k}(q)\bigg] \tag{5.114}$$

$$\simeq 2g^2\rho_m\int_{t',\mathbf{q},\mathbf{q}'}\delta\widetilde{\phi}(\mathbf{q}-\mathbf{q}',t')\delta\phi(\mathbf{q}'-\mathbf{q},t')F_K(q,q',t')\frac{\mathrm{d}R(q)}{\mathrm{d}k}, \tag{5.115}$$

where $V(t,\mathbf{q}) = \int_{\mathbf{r}}\mathrm{e}^{-i\mathbf{q}\cdot\mathbf{r}}V(t,\mathbf{r})$ and in the last step we retained only the part of the fields which is local in time by expanding them as $\delta\phi(t'') \simeq \delta\phi(t')$ for $t'' \simeq t'$. In the last equality of Eq. (5.114), we also discarded the term proportional to $\delta\widetilde{\phi}^2$, which does not contribute to the renormalization of K. The function $F_K(q,q',t')$ in Eq. (5.114) is defined as

$$F_K(q,q',t') = \int_{t_0}^{+\infty}\mathrm{d}t\,\mathrm{d}t''\bigg[G_{0C}(q',t',t'')G_{0R}(q,t,t'')G_{0R}(q,t',t)+G_{0C}(q,t,t'')G_{0R}(q',t',t'')G_{0R}(q,t',t)$$
$$+\,G_{0C}(q,t,t')G_{0R}(q',t',t'')G_{0R}(q,t'',t)\bigg]. \tag{5.116}$$

Then, combining Eqs. (5.114) and (5.114), one finds

$$\frac{\delta^2\Delta\Gamma_2\big|_{V\to V_1}}{\delta\widetilde{\phi}(t,-\mathbf{p})\delta\phi(t,\mathbf{p})} = \frac{2g^2\rho_m}{\mathcal{N}}\int_{\mathbf{q}}F_K(q,|\mathbf{q}-\mathbf{p}|,t)\frac{\mathrm{d}R(q)}{\mathrm{d}k}. \tag{5.117}$$

In order to evaluate Eq. (5.114), we need to retain the contribution proportional to p^2 from $F_K(q,|\mathbf{q}-\mathbf{p}|,t)$ defined in Eq. (5.116). To this end, we define the function $P(q) \equiv K[q^2 + (k^2-q^2)\vartheta(k^2-q^2))]$

and note that $G_{0R,0C}(q,t,t')$ depend on q via $P(q)$, as their explicit expression is given by Eqs. (5.5) and (5.6) with ω_q replaced by $\omega_{k,q} = P(q) + r$ given in Eq. (5.29). For a generic function of $P(q)$ one can write

$$\frac{\partial^2}{\partial q_i \partial q_j} = \frac{\partial P(q)}{\partial q_i}\frac{\partial P(q)}{\partial q_j}\frac{\partial^2}{\partial P^2} + \frac{\partial^2 P}{\partial q_i \partial q_j}\frac{\partial}{\partial P}, \tag{5.118}$$

where $i, j = 1, \ldots, d$ label the components of the momenta q_i. A simple calculation shows that

$$\begin{aligned}
\frac{\partial P(q)}{\partial q_i} &= 2Kq_i\left[1 - \vartheta(k^2 - q^2)\right], \\
\frac{\partial^2 P(q)}{\partial q_i \partial q_j} &= 2K\delta_{ij}\left[1 - \vartheta(k^2 - q^2)\right] + 4Kq_iq_j\delta(k^2 - q^2),
\end{aligned} \tag{5.119}$$

and therefore, all contributions proportional to $1 - \vartheta(k^2 - q^2)$ vanish when inserted into the integral in the r.h.s. of Eq. (5.117), because they multiply the term $\propto \vartheta(k^2 - q^2)$ contained in $\mathrm{d}R/\mathrm{d}k$ (see Eq. (5.87)). Accordingly, by discarding these contributions, the derivatives $\partial^2 G_{0R,0C}(q,t,t')/\partial q_i \partial q_j$ which are involved in the expansion of the function F_K in the integrand of Eq. (5.117) can be effectively replaced by

$$\frac{\partial^2 G_{0R/0K}(q,t,t')}{\partial q_i \partial q_j} \mapsto \frac{\partial G_{0R/0K}(q,t,t')}{\partial P(q)} 4Kq_iq_j\delta(k^2 - q^2), \tag{5.120}$$

where, from Eqs. (5.10) and (5.11) with $\omega_q \to \omega_{k,q}$ given in Eq. (5.29), we have

$$\frac{\partial G_{0R}(q,t,t')}{\partial P(q)} = -(t - t')G_{0R}(q,t,t'), \tag{5.121}$$

$$\frac{\partial G_{0C}(q,t,t')}{\partial P(q)} = -\frac{D}{\omega_{k,q}}\left[\left(\frac{1}{\omega_{k,q}} + |t - t'|\right)\mathrm{e}^{-\omega_{k,q}|t-t'|} + \left(\frac{1}{\omega_{k,q}} + t + t'\right)\left(\frac{\omega_{k,q}}{D\tau_0} - 1\right)\mathrm{e}^{-\omega_{k,q}(t+t')}\right]. \tag{5.122}$$

Accordingly, terms proportional to p^2 in the Taylor expansion of $F_K(q, |\mathbf{q} - \mathbf{p}|, t)$ can be obtained by using Eqs. (5.116), (5.120), (5.121) and (5.122), and they eventually read

$$\frac{1}{2}\sum_{i,j=1}^{d} p_i p_j \frac{\partial^2 F_K(q,q,t)}{\partial q_i \partial q_j} = 2K(\mathbf{q}\cdot\mathbf{p})^2\delta(k^2 - q^2)\widetilde{F}_K(q,t), \tag{5.123}$$

with

$$\begin{aligned}
\widetilde{F}_K(q,t') = \int_{t_0}^{+\infty} \mathrm{d}t\,\mathrm{d}t''\Bigg[&\frac{\partial G_{0C}(q,t',t'')}{\partial P(q)} G_{0R}(q,t,t'')G_{0R}(q,t',t) \\
&+ G_{0C}(q,t,t'')\frac{G_{0R}(q,t',t'')}{\partial P(q)}G_{0R}(q,t',t) + G_{0C}(q,t,t')\frac{\partial G_{0R}(q,t',t'')}{\partial P(q)}G_{0R}(q,t'',t)\Bigg].
\end{aligned} \tag{5.124}$$

Then, by inserting Eq. (5.123) into Eq. (5.117), and by using the fact that, from Eq. (5.87)

$$\frac{\mathrm{d}R_k}{\mathrm{d}k}\delta(k^2 - q^2) = \frac{1}{2}K\delta(k - q), \tag{5.125}$$

as well as the identity for the d-dimensional integral of a rotational-invariant function $f(q)$

$$\int \mathrm{d}^d q\, (\mathbf{q}\cdot\mathbf{p})^2 f(q) = \frac{p^2}{d}\int \mathrm{d}^d q\, q^2\, f(q), \tag{5.126}$$

we find

$$\frac{\partial^2}{\partial p^2}\frac{\delta^2\Delta\Gamma_2\big|_{V_1^2}}{\delta\widetilde{\phi}(t,-\mathbf{p})\delta\phi(t,\mathbf{p})}\bigg|_{\mathbf{p}=0} = 2\frac{a_d}{d}k^{d+1}\frac{g^2\rho_m}{\mathcal{N}}K^2\widetilde{F}_K(k,t). \tag{5.127}$$

Finally, a lengthy but straightforward evaluation of $\widetilde{F}_K(k,t)$, using Eqs. (5.116), (5.10) and (5.11) with $\omega_q \to \omega_{k,q}$ (see Eq. (5.29)), yields

$$\widetilde{F}_K(k,t) = -\frac{D}{Z\omega_k^4}\left[1 - f_K(t)\right], \tag{5.128}$$

where $\omega_k = \omega_{q=k}$ and $f_K(t)$ is a function which vanishes exponentially fast upon increasing t and therefore does not contribute to the renormalization of K at long times. By inserting Eqs. (5.128) and (5.127) into Eq. (5.114), we finally find the flow equation for K, which reads

$$\frac{\mathrm{d}K}{\mathrm{d}k} = -2k^{d+1}\frac{a_d}{d}\frac{DK^2}{Z}\frac{g^2\rho_m}{(Kk^2+m)^4}, \tag{5.129}$$

and, according to Eq. (5.52), the anomalous dimension η_K reads

$$\eta_K = 2k^{d+2}\frac{a_d}{d}\frac{DK}{Z}\frac{g^2\rho_m}{(Kk^2+m)^4}. \tag{5.130}$$

5.G Flow equations

In this Appendix we report the explicit form of the flow equations derived from the effective action Γ in Eq. (5.19) with the potential $\mathcal{U}$ in Eq. (5.51) and $\lambda \neq 0$. These equations can be derived by repeating the calculations presented in Apps. 5.E and 5.F but by keeping λ finite; here we report only the final result of this somewhat lengthy calculation. The flow equations for the couplings $\widetilde{m}$, $\widetilde{g}$ and $\widetilde{\lambda}$, defined in Eq. (5.53), turn out to be

$$k\frac{\mathrm{d}\widetilde{m}}{\mathrm{d}k} = (-2+\eta_K)\widetilde{m} + \left(1-\frac{\eta_K}{d+2}\right)\frac{2\widetilde{g}}{(1+\widetilde{m})^2}\left[1+\frac{3}{2}\left(\frac{\widetilde{m}\widetilde{\lambda}}{\widetilde{g}^2}\right)^2 + \frac{3\widetilde{m}}{1+\widetilde{m}}\left(1+\frac{\widetilde{m}\widetilde{\lambda}}{\widetilde{g}^2}\right)^2\right], \tag{5.131}$$

$$k\frac{\mathrm{d}\widetilde{g}}{\mathrm{d}k} = g\left[d-4+2\eta_K + \left(1-\frac{\eta_K}{d+2}\right)\frac{6g}{(1+\widetilde{m})^3}\left(1+\frac{\widetilde{m}\widetilde{\lambda}}{\widetilde{g}^2}\right)^2\right] + \left(1-\frac{\eta_K}{d+2}\right)\frac{\widetilde{\lambda}}{(1+\widetilde{m})^2}\left(-2+3\frac{\widetilde{m}\widetilde{\lambda}}{\widetilde{g}^2}\right), \tag{5.132}$$

$$k\frac{\mathrm{d}\widetilde{\lambda}}{\mathrm{d}k} = \widetilde{\lambda}\left[2d-6+3\eta_K+30\left(1-\frac{\eta_K}{d+2}\right)\frac{\widetilde{g}}{(1+\widetilde{m})^3}\left(1+\frac{\widetilde{m}\widetilde{\lambda}}{\widetilde{g}^2}\right)\right] - 18\left(1-\frac{\eta_K}{d+2}\right)\frac{\widetilde{g}^2}{(1+\widetilde{m})^4}\left(1+\frac{\widetilde{m}\widetilde{\lambda}}{\widetilde{g}^2}\right), \tag{5.133}$$

while the anomalous dimensions η_K, η_D, η_Z and η_0, defined, respectively, in Eqs. (5.52) and (5.45), read

$$\eta_K = \frac{3\widetilde{m}\widetilde{g}}{(1+\widetilde{m})^4}\left(1+\frac{\widetilde{m}\widetilde{\lambda}}{\widetilde{g}^2}\right)^2, \tag{5.134}$$

$$\eta_Z = \eta_D = \left(1-\frac{\eta_K}{d+2}\right)\frac{9\widetilde{m}\widetilde{g}}{2(1+\widetilde{m})^4}\left(1+\frac{\widetilde{m}\widetilde{\lambda}}{\widetilde{g}^2}\right)^2, \tag{5.135}$$

$$\eta_0 = -\left(1-\frac{\eta_K}{d+2}\right)\frac{\widetilde{g}}{(1+\widetilde{m})^3}\left[1+\frac{3}{2}\left(\frac{\widetilde{m}\widetilde{\lambda}}{\widetilde{g}^2}\right)^2+\frac{9\widetilde{m}}{2(1+\widetilde{m})}\left(1+\frac{\widetilde{m}\widetilde{\lambda}}{\widetilde{g}^2}\right)^2\right]. \tag{5.136}$$

Part II

Open quantum systems

Chapter 6

Introduction

6.1 Motivation

As discussed in the first part of this Thesis, non-equilibrium features in isolated quantum many-body systems may appear in both the transient dynamics and in the non-thermal stationary states of integrable systems. However, these steady states are fragile against the presence of non-integrable perturbations (with the remarkable exception of many-body localized systems, possibly). By contrast, robust non-equilibrium steady states may be created by coupling a system to an environment, theoretically modelled with *reservoirs*, i.e., collections of particles (or other degrees of freedom) much larger than the system, which are therefore able to impose an *irreversible* dynamics on the systems variables. Reservoirs are, in fact, typically used to model dissipative processes, or to model the incoherent injection of particles or energy into the system [254–256].

The physics of open systems has been widely studied in the context of classical systems, for which the concepts of emerging collective phenomena and universality, initially developed in equilibrium systems, also apply [120,121,128–130,232,257]. For open quantum systems, instead, this understanding is much less developed, but it has gained increasing attention in last years, as a consequence of a surge of experiments in cold atomic gases [258–260], trapped ions [261,262] and quantum optical platforms [263–268]. The steady-state of these systems is not determined by some equilibrium distribution, but rather by a dynamical balance of pumping and losses: they are thus not guaranteed to thermalize, as detailed balance is typically broken by the presence of the driving. These non-equilibrium steady states thus realize scenarios without counterpart in condensed, equilibrium matter: this rules out the usual theoretical equilibrium concepts and techniques, and calls for the development of new theoretical tools [269]. This posed theoretical questions on the existence of novel phases of matter [270–274] and the nature of phase transitions in these driven systems [264, 275–279].

In the following, we will discuss more in detail the specific case of non-equilibrium Bose-Einstein condensation, which represents a paradigm of this quest for non-equilibrium phenomena in open quantum systems.

6.2 Equilibrium Bose-Einstein condensation

Before addressing the case of nonequilibrium Bose-Einstein condensation (BEC), we briefly review its basic features in the equilibrium case. The simplest approach to the equilibrium BEC in statistical physics [280, 281] is based on a grand-canonical description of an ideal three-dimensional Bose gas in thermal equilibrium with inverse temperature $\beta = 1/k_B T$ and chemical potential $\mu \leq 0$ in terms of the Bose distribution, $n_{\mathbf{k}} = [e^{\beta(\epsilon_{\mathbf{k}}-\mu)} - 1]^{-1}$, where $\epsilon_{\mathbf{k}} = \hbar^2 k^2/2m$ is the energy of the state of momentum $\hbar\mathbf{k}$ and m the mass of the particles. For any given temperature T, the maximum density of particles that can be accommodated in the excited states at $\mathbf{k} \neq 0$ grows upon increasing μ and then saturates at $n_{\max}(T)$ for $\mu = 0$. If the actual density of particles n exceeds this threshold, the extra particles must accumulate into the lowest state at $\mathbf{k} = 0$, forming the so-called condensate. This happens for spatial dimensions $d \geq 3$, and therefore BEC cannot occurs for dimensions lower than $d = 3$. In fact, in spatial dimension $d < 3$, the long-range order of the condensate is not stable against thermal fluctuations and is replaced by a so-called quasi-condensate, in agreement with the Hohenberg-Mermin-Wagner theorem of statistical physics [280]: while order is present up to intermediate length scales, upon increasing the distance, it decays (at finite T) with an exponential (in $d = 1$) or algebraic (in $d = 2$) law.

An alternative, mathematically equivalent condition — the so-called Penrose-Onsager criterion [282] — involves the long-distance limit of the coherence function of the matter field $\hat{\Psi}(\mathbf{r})$ describing the Bose particles undergoing condensation, i.e.,

$$\lim_{|\mathbf{r}-\mathbf{r}'|\to\infty} \left\langle \hat{\Psi}^\dagger(\mathbf{r})\, \hat{\Psi}(\mathbf{r}') \right\rangle = n_{BEC} > 0; \tag{6.1}$$

as the coherence in Eq. (6.1) is the Fourier transform of the momentum distribution $n_{\mathbf{k}}$, it is immediate to see that the two different definitions of condensate fraction n_{BEC} in terms of a macroscopic occupation $n_{\mathbf{k}=0}$ of the lowest mode and of the long-distance behavior of the coherence actually coincide.

Moreover, a further equivalent description of the condensation was presented in Ref. [283]: in order to highlight the mechanism of spontaneous symmetry breaking it is convenient to introduce a fictitious external field η coupling to the quantum matter field via the Hamiltonian

$$H_{\text{ext}} = -\int d^3\mathbf{r} \left[\eta \hat{\Psi}^\dagger(\mathbf{r}) + \eta^* \hat{\Psi}(\mathbf{r})\right], \tag{6.2}$$

which explicitly breaks the $U(1)$ symmetry. As in a ferromagnet the direction of the magnetization is selected by an external magnetic field B, in the presence of an η field the quantum matter field $\hat{\Psi}(\mathbf{r})$ acquires a finite expectation value. For $T < T_{BEC}$, this expectation value

$$\Psi_0 = \lim_{\eta\to 0} \lim_{V\to\infty} \left\langle \hat{\Psi}(\mathbf{r}) \right\rangle \tag{6.3}$$

remains finite even for vanishing η in the thermodynamic limit $V \to \infty$, and is related to the condensate density by $n_{BEC} = |\Psi_0|^2$. As usual for phase transitions, the order in which the zero-field and the infinite-volume limits are taken in Eq. (6.3) is crucial [280].

In the presence of inter-particle pair interactions, all condensation criteria based on the lowest mode occupation, on the long-distance coherence and on the spontaneous coherent matter field remain

valid. However, the underlying physics is much more complex and we refer the reader to the specialized literature on the subject, e.g. Ref. [281]. For our purposes, we only need to mention that at equilibrium at $T = 0$ the condensate order parameter $\Psi_0(\mathbf{r})$ in the presence of an external potential $V(\mathbf{r})$ can be obtained in the dilute-gas regime by minimizing the so-called Gross-Pitaevskii (GP) energy functional,

$$E[\Psi_0] = \int d^3\mathbf{r} \left\{ \frac{\hbar^2 |\nabla \Psi_0(\mathbf{r})|^2}{2m} + V(\mathbf{r}) |\Psi_0(\mathbf{r})|^2 + \frac{g}{2} |\Psi_0(\mathbf{r})|^4 \right\}, \tag{6.4}$$

where the normalization of Ψ_0 is set by the total number N of particles in the system, i.e., $N = \int d^3\mathbf{r} |\Psi_0(\mathbf{r})|^2$, and $g = 4\pi\hbar^2 a_0/m$ quantifies the strength of the (local) interactions, proportional to the s-wave inter-particle scattering length a_0. In terms of a_0, the dilute-gas regime corresponds to $n a_0^3 \ll 1$. The mathematical form of the GP energy functional (6.4) guarantees that the condensate wavefunction $\Psi_0(\mathbf{r})$ keeps a constant phase throughout the whole system even in the presence of the external potential $V(\mathbf{r})$, while the density profile $|\Psi_0(\mathbf{r})|^2$ develops large variations in space.

Finally, at this same level of approximation, the condensate dynamics is ruled by the time-dependent Gross-Pitaevskii equation,

$$i\hbar \frac{\partial \Psi_0(\mathbf{r},t)}{\partial t} = -\frac{\hbar^2 \nabla^2 \Psi_0(\mathbf{r},t)}{2m} + V(\mathbf{r}) \Psi_0(\mathbf{r},t) + g |\Psi_0(\mathbf{r},t)|^2 \Psi_0(\mathbf{r},t), \tag{6.5}$$

which has the mathematical form of a nonlinear Schrödinger equation.

6.3 Bose-Einstein condensation in driven-dissipative systems

In the early 1970's, the pioneering studies in Refs. [284, 285] proposed a very insightful interpretation of the laser threshold in terms of a spontaneous breaking of the $U(1)$ symmetry associated with the phase of the emitted light. Similarly to what happens to the order parameter at a second-order phase transition, such an optical phase is randomly chosen every time the device is switched on and it remains constant for macroscopically long times. Moreover, a long-range spatial order is established, as light emitted by a laser device above threshold is phase-coherent on macroscopically large distances. While textbooks typically discuss this interpretation of laser operation in terms of a phase transition for the simplest case of a single-mode laser cavity, rigorously speaking it is valid only in spatially infinite systems. In fact, only in this case one can observe non-analytic behaviors of the physical quantities at the transition point. In particular, the onset of long-range order is typically assessed by looking at the long-distance behavior of the correlation function of the order parameter, which, for a laser, corresponds to the first-order spatial coherence of the emitted electric field $\hat{E}(\mathbf{r})$,

$$\lim_{|\mathbf{r}-\mathbf{r}'|\to\infty} \left\langle \hat{E}^\dagger(\mathbf{r})\, \hat{E}(\mathbf{r}') \right\rangle : \tag{6.6}$$

the spontaneous symmetry breaking is signalled by this quantity becoming non-zero. The average $\langle \dots \rangle$ is taken on the stationary density matrix of the system. In order to be able to probe the long-distance behavior, experimental studies need devices with a spatially extended active region. The so-called VCSELs (vertical cavity surface emitting lasers) (see Fig. 6.1, left panel for a schematic structure of a VCSEL) are perhaps the most studied examples in this class [286, 287]: by using an

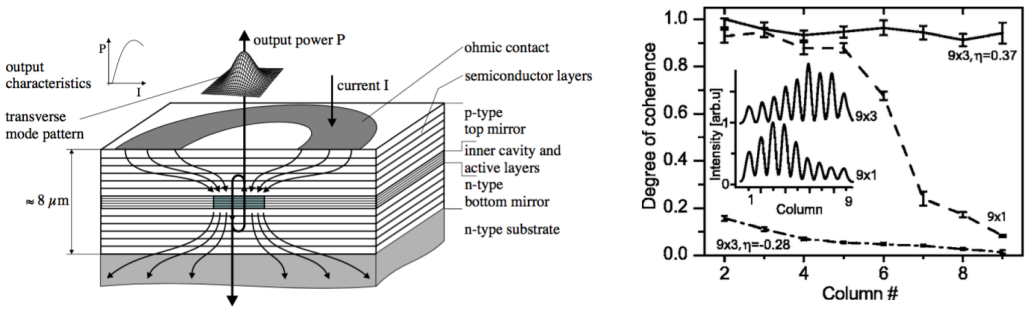

Figure 6.1: Left panel: schematic structure of a VCSEL (from Ref. [286]). Right panel: coherence of an array of VCSELs, measured for different values of the pump rate (from Ref. [287]).

active medium sandwiched between a pair of plane-parallel semiconductor mirrors, one can realize devices of arbitrarily large size, the only limitation coming from extrinsic effects such as the difficulty of having a spatially homogeneous pumping of the active material and of avoiding disorder of the semiconductor microstructure.

There is an important difference between the equilibrium BEC discussed in the previous Section and laser operation: in the former, the system is assumed to be in thermal equilibrium at temperature T, so the density matrix $\rho_{\rm eq}$ of the system is given by the Boltzmann factor of equilibrium statistical mechanics $\rho_{\rm eq} \propto \exp(-H/k_B T)$. A laser is, instead, an intrinsically non-equilibrium device, whose steady state is determined by a dynamical balance of pumping and losses, the latter being essential in order to generate the output laser beam used in any application. As a result, one can think of laser operation in spatially extended devices as an example of *non-equilibrium BEC*.

In between the two extreme cases of equilibrium BEC and laser operation, experiments with gases of exciton-polaritons in microcavities [266], of magnons [288] and of photons [289] have explored the full range of partially thermalized regimes depending on the ratio between the loss and the thermalization rates, the latter being typically due to interparticle collisions within the gas and/or to interactions with the host material. In particular, exciton-polaritons have proved to be a versatile experimental platform for studying condensation [267,290,291]. Exciton-polaritons are quasi-particles which emerge in planar semiconductor microcavities embedding a quantum well (see Fig. 6.2 for a schematic description). In a microcavity, photons are confined inside metallic and/or dielectric planar mirrors: as a consequence of confinement along one (or more) directions, their motion along the remaining extended directions is characterized by an effective mass. The high reflectivity of the mirrors allow the photons to strongly interact with the excitonic modes in the quantum well, thus originating polaritonic quasiparticles. These new quasiparticles are characterized by a two-fold dispersion law (lower and upper polaritons), which derives from the hybridization of the photonic and excitonic bands (see Fig. 6.2, right panel). Moreover, polaritons have a finite lifetime, and they need to be continuously replenished in order to maintain their population constant. Most importantly, they are interacting particles, as they inherit the screened Coulomb interaction from their excitonic component.

While the shape of an equilibrium condensate is obtained by minimizing the Gross-Piteavskii energy functional, non-equilibrium BECs appear to be significantly less universal as their theoretical description typically requires some microscopic modelling of the specific dissipation and pumping

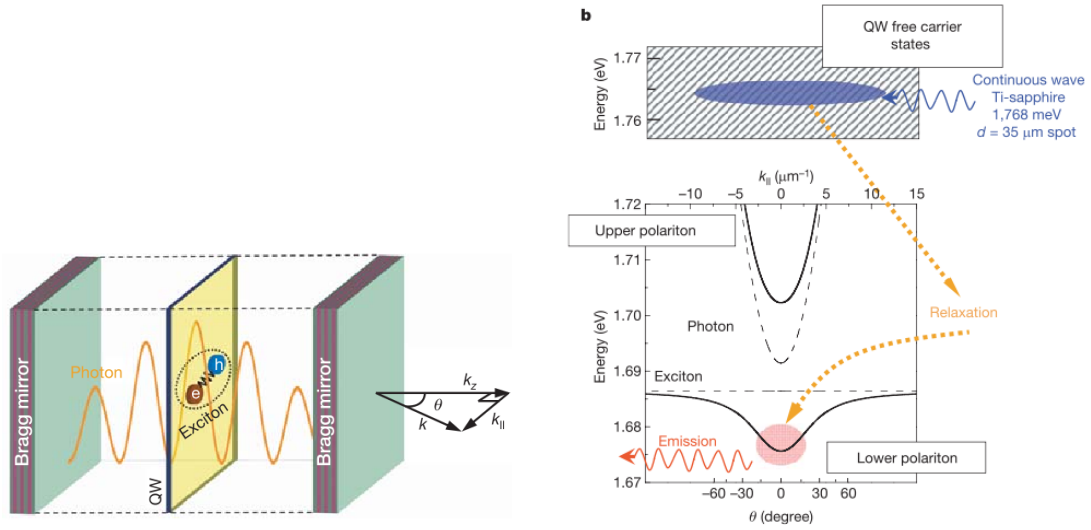

Figure 6.2: Left panel: Sketch of a planar semiconductor microcavity delimited by two Bragg mirrors and embedding a quantum well (from Ref. [266]). Right panel: dispersion of the polariton modes versus in-plane wave vector. The exciton dispersion is almost flat due to the heavy mass of the exciton compared to that of the cavity photon. In the polariton condensation experiments under incoherent pumping reported in this figure, the system is incoherently excited by a laser beam tuned at a very high energy. Relaxation of the excess energy (via phonon emission, exciton-exciton scattering, etc.) leads to a population of the lowest-energy modes of the polaritonic band (from Ref. [266]).

mechanisms present in a given experimental set-up. For a comprehensive discussion of the main configurations, we refer the interested reader to the recent review article [267]. Here we summarize the simplest and most transparent of such descriptions, which is based on the following complex Ginzburg-Landau evolution equation for the order parameter,

$$i\hbar\frac{\partial\Psi_0}{\partial t} = -\frac{\hbar^2}{2m}\nabla^2\Psi_0 + V(\mathbf{r})\Psi_0 + g|\Psi_0|^2\Psi_0 - \frac{i\hbar}{2}\left[\gamma - \frac{P}{1+\frac{|\Psi_0|^2}{n_{\rm sat}}}\right]\Psi_0, \tag{6.7}$$

inspired by the so-called semiclassical theory of the laser. In addition to coherent terms present in the equilibrium description (6.5), Eq. (6.7) accounts for the losses occurring with rate γ and for the stimulated pumping of new particles into the condensate at a bare rate P, which then saturates once the condensate density exceeds the saturation density $n_{\rm sat}$. Given the driven-dissipative nature of this evolution equation, the steady state has to be determined as the long-time limit of the dynamical evolution. This apparently minor difference has profound implications, as the breaking of time-reversal symmetry by the pumping and loss terms in (6.7) allows for steady-state configurations with a spatially varying phase of the order parameter, which physically corresponds to finite particle currents through the condensate. This feature was first observed in Ref. [292] as a ring-shaped condensate emission in the wavevector $\mathbf{k}$-space and, in the presence of disorder, as an asymmetry of the emission pattern under reflections, $n(\mathbf{k}) \neq n(-\mathbf{k})$ [293]. The theoretical interpretation proposed in Ref. [294] was soon confirmed by the more detailed experiments in Ref. [295]. Another feature of Eq. (6.7) which

clearly distinguishes non-equilibrium systems from their equilibrium counterparts is the dispersion of the collective excitations on top of a condensate. As first predicted in Refs. [296–298], the usual Bogoliubov dispersion $\hbar\omega_{\mathrm{eq},\mathbf{k}} = [\epsilon_{\mathbf{k}}(\epsilon_{\mathbf{k}} + 2g|\Psi_0|^2)]^{1/2}$ of spatially homogeneous condensates is modified by pumping and dissipation to $\omega_{\mathrm{neq},\mathbf{k}} = -i\Gamma/2 + [\omega^2_{\mathrm{eq},\mathbf{k}} - \Gamma^2/4]^{1/2}$, where the dissipation parameter $\Gamma = \gamma(1 - P_c/P)$ depends on the pumping power P in units of its threshold value P_c. In particular, the usual sonic (linear) dispersion of low-wavevector excitations in equilibrium condensates is strongly modified into a flat, diffusive region [299].

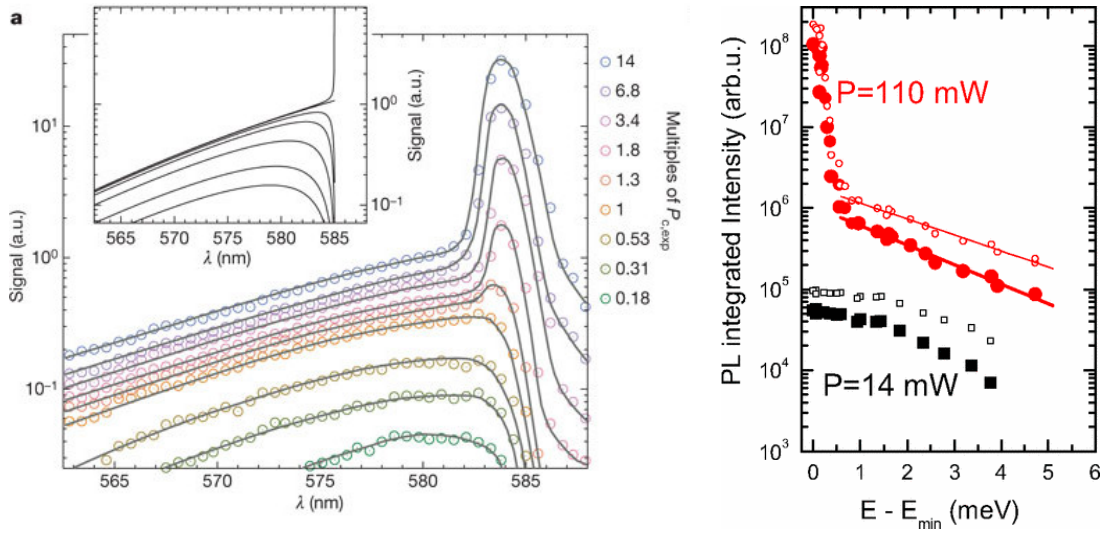

Figure 6.3: Left panel: Intensity of the emitted light as a function of the wavelength for a photon condensate above the condensation threshold (from Ref. [289]). Right panel: Integrated photoluminescence of as a function of the emission energy for a lasing microcavity. The red (black) curve corresponds to measurements above (below) the condensation threshold (from Ref. [300]).

A remarkable question is how the spatial dimensionality affects the nature of such transition. As anticipated in the previous Section, below $d < 3$, the long-range order of the condensate is not stable against thermal fluctuations in agreement with the Hohenberg-Mermin-Wagner theorem. In $d = 2$, the systems undergoes a continuous Berezinskii-Kosterlitz-Thouless (BKT) transition [301, 302], where a vortex binding-unbinding mechanism mediates between two phases characterized by exponentially decaying and algebraic correlations. In $d = 1$ the system only display exponentially decaying correlations.

While this result was first discussed in the late 60's for equilibrium systems [303,304], a first mention in the non-equilibrium context was already present in the above-cited seminal work by Graham and Haken [284]: in this latter case, however, fluctuations did not have a thermal origin, but were an unavoidable consequence of the quantum nature of the field undergoing condensation. Independently of this pioneering work, this result was rediscovered later on in Refs. [296, 298] and then extended to the critical region using renormalization-group techniques. Within this approach, several new features emerged: in $d = 3$ novel critical exponents appear [278] while the $d = 2$ algebraic long-range decay of correlations is destroyed and replaced by a stretched exponential [271].

6.4 Thermalization in photonic and polaritonic gases

In most of the experiments on BEC in polariton and photon gases conducted so far, a special effort was made in order to understand whether the system was thermalized or not. One can in fact expect that some effective thermalization might occur even in non-equilibrium regimes as soon as the thermalization time is shorter than the lifetime of the particles. In order to experimentally assess this *quasi-equilibrium* condition, the measured momentum and/or energy distribution of the non-condensed particle was typically compared with a Bose distribution. The observation of this thermal distribution is to be expected in polariton and photon gases showing frequent collisions [266, 289] as illustrated in the left panel of Fig. 6.3. The mechanism leading to this thermal distribution for photon gases in dye-filled microcavities is quite distinct from that in polaritons, where it is mediated by inter-particle collisions. In the photon gas [289, 305], the dye acts as a reservoir which, via repeated absorption and reemission of photons, can establish a thermal distribution, provided that the Kennard-Stepanov relation between absorption and emission is satisfied. On the other hand, it was quite a surprise when the experiment in Ref. [300] reported a momentum distribution with a thermal-like tail even in a lasing regime where the photons should not be thermalized — see the right panel of Fig. 6.3. This observation cast some doubts on the interpretation of similar available experimental results; in particular, several authors have tried to develop alternative models to justify the observed thermal tail in terms of generalized, strongly non-equilibrium laser theories [5, 306].

In general it is unclear, *a priori*, by which physical mechanism an effective temperature is possibly established in these systems and, in case, what determines its value. Recent work, however, suggests possible mechanisms where an effective temperature can occur as a consequence of the competition between driven-dissipative and coherent dynamics [277,278,307–313]. Irrespective of its cause, effective thermalization often affects only the low-energy degrees of freedom [184, 219, 277, 278, 296, 307–314].

All these examples show clearly that the presence of effective thermodynamic equilibrium (which might be established only in a subsystem or within a specific range of frequencies) in the steady state of a system is often by no means obvious. Hence, before addressing the question of whether the time evolution of a certain system leads to thermalization or not, it is imperative to identify criteria which allow a clear-cut detection of thermodynamic equilibrium conditions in the stationary state. In this regard, it is important to consider not only the *static* properties of the density matrix of the system, which describes its stationary state, but also the *dynamics* of fluctuations: being encoded, e.g., in two-time correlation and response functions (through the so-called fluctuation-dissipation theorem), it might or might not be compatible with equilibrium.

6.5 Paraxial quantum optics

As discussed in Sec. 6.1, in the last few years many-body physics has embraced a novel class of systems, the so-called quantum fluids of light [267]. In these optical systems, light and matter combine to generate new photonlike particles that, differently from vacuum photons, are characterized by sizeable effective masses and mutual interactions and, therefore, may give rise to novel states of matter. One of the most used platforms to study the physics of quantum fluids of light is the semiconductor planar microcavity, in which the cavity photons and the quantum-well excitons strongly couple to form mixed light-matter interacting bosonic quasiparticles called exciton polaritons [290]. Numerous

quantum-hydrodynamics collective phenomena have been investigated theoretically and successfully observed experimentally in such exciton-polariton fluids [267]. Nevertheless, fluids of light in cavity-based systems are inevitably subject to losses, which is typically detrimental for the experimental observation of coherent quantum dynamical features, as the ones described in the first part of this Thesis.

An alternative platform for studying many-body physics in photon fluids is based on light propagating in a bulk nonlinear (of Kerr type) optical medium. In classical optics, in fact, the paraxial propagation of a beam of light can be described by a nonlinear equation formally identical to the Gross-Pitaevskii equation for a dilute Bose-Einstein condensate [281], if the so-called paraxial and slowly-varying-envelope approximations are satisfied [315–318]. This similarity has been used in a number of theoretical and experimental works where the physics of lasing non-linear systems has been reformulated in the hydrodynamics language [319–325].

The question if this framework could be extended to quantum optics has been recently addressed in a series of works [208, 326], in which it was shown that the paraxial propagation of quantum light can be mapped to a many-body quantum nonlinear Schrödinger formalism with the roles of the propagation coordinate and time exchanged. These investigations exemplified the potential of nonlinear paraxial optics as a novel platform for experimental studies of non-equilibrium dynamical problems in many-body quantum physics.

Chapter 7

A quantum Langevin model for non-equilibrium condensation

Abstract

We develop a quantum model for non-equilibrium Bose-Einstein condensation of photons and polaritons in planar microcavity devices. The model builds upon laser theory and includes the spatial dynamics of the cavity field, a saturation mechanism and some frequency-dependence of the gain: quantum Langevin equations are written for a cavity field coupled to a continuous distribution of externally pumped two-level emitters with a well-defined frequency. As a an example of application, the method is used to study the linearised quantum fluctuations around a steady-state condensed state. In the good-cavity regime, an effective equation for the cavity field only is proposed in terms of a stochastic Gross-Pitaevskii equation. Perspectives in view of a full quantum simulation of the non-equilibrium condensation process are finally sketched.

As anticipated in Chapter 6.3, the common starting point of the descriptions of BEC in driven-dissipative systems relies on the phenomenological stochastic Gross-Pitaevskii equations (SGPE) reported in Eq. (6.7). The only exception is the numerical simulation reported in [327] where the BEC phase transition was studied in the so-called Optical Parametric Oscillator (OPO) configuration which is amenable to an almost *ab initio* truncated-Wigner description of the field dynamics. In all other cases, the strength and the functional form of the noise terms had to be introduced in a phenomenological way [312,328]. The purpose of this Chapter is to develop a fully quantum model of the system from which one can derive a SGPE under controlled approximations. In contrast to previous derivations of the SGPE based, e.g., on Keldysh formalism [329] or on the truncated-Wigner representations of the field [327,328], our derivation is performed through the quantum Langevin approach [256]: on one hand, this approach offers a physically transparent description of the baths and, in particular, of the incoherent pumping mechanism. On the other hand, it allows to capture within a simple Markovian theory the frequency-dependence of the pumping and dissipation baths. In the good cavity limit, we can then adiabatically eliminate the matter degrees of freedom, which results in an effective dynamics for the cavity photon field only: in particular, explicit expressions for the Langevin terms are pro-

vided, which can eventually be used as a starting point for more sophisticated statistical mechanics calculations.

This Chapter is organised as follows. In Sec. 7.1 we present the model and we derive the quantum Langevin equations. In Sec. 7.2, we present the mean-field theory of the condensation process and we illustrate the $U(1)$ spontaneous symmetry breaking phenomenon. In the following Sec. 7.3 we study the excitation modes of the system and the effect of fluctuations around the condensate: in particular, predictions for the momentum distribution of the thermal component and for the luminescence spectrum are given. In Sec. 7.4 we discuss the good cavity limit where our equations can be reduced to a stochastic Gross-Pitaevskii equation. Conclusions are finally drawn in Sec. 7.5.

7.1 The model

Our microscopic theory extends early models on laser operation [330–333] to the spatially extended case of planar cavities with a parabolic dispersion of the cavity photon as a function of the in-plane wavevector $\mathbf{k}$,

$$\omega_{\mathbf{k}} = \omega_0 + \frac{k^2}{2m}. \tag{7.1}$$

with a cut-off frequency ω_0 and an effective mass m [267]. This simple description of cavity modes well captures the physics of planar DBR semiconductor microcavities in both the weak and the strong light-matter coupling regimes: in particular, low-momentum polaritons used in the condensation experiment [266] are straightforwardly included as dressed photon modes with suitably renormalised ω_0 and m parameters. When supplemented with an harmonic potential term accounting for the mirror curvature, this same formalism also describes the mesoscopic cavity of [289].

As it is sketched in Fig.7.1, the cavity field is then coupled to a set of two-level emitters. Both the emitters and the cavity are subject to losses of different natures, while energy is continuously injected into the system by pumping the emitters to their excited state. The steady-state of the system is therefore determined by a dynamical balance of pumping and losses. In this description, both Bose-Einstein condensation and lasing consist in the appearance of a macroscopic coherent field in a single mode of the cavity (typically the $\mathbf{k} = 0$ one), monochromatically oscillating at a given frequency ω and with a long-distance coherence extending in the whole system. Part of the in-cavity light eventually leaves the cavity via the non-perfectly reflecting mirror and end up forming a coherent output beam of light.

While this theory directly builds on standard laser theory, it is generic enough to capture the main specificities of exciton-polariton condensation under an incoherent pumping scheme which was experimentally demonstrated in [266]. In this case, the dispersion is the polariton one and the two-level emitters provide a model description of the complex irreversible polariton scattering processes replenishing the condensate [290, 329]. The main gain process consists of binary polariton scattering where two polaritons located around the inflection point of their dispersion are scattered into one condensate polariton and one exciton (which is then quickly lost). In our model, the excited state of the emitters correspond to pairs of polaritons located around the inflection point of their dispersion, while the ground state of the emitter corresponds to having one exciton resulting from the collision. At simplest order, the emitter energy ν is then approximately equal to the difference of the energy of the pair around the inflection point and of the exciton, $\hbar\nu \approx 2E_{\rm infl} - E_{\rm exc}$, that is the energy where

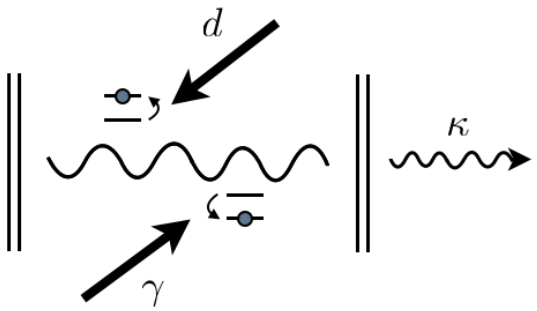

Figure 7.1: A pictorial representation of the model. Emitters lose energy at a rate γ while energy is pumped in at a rate d. Photons can leave the cavity after a time κ^{-1}.

the collisional gain is expected to be maximum. Extensions of this theory including more complicate emitters can be used to describe the dye molecules involved in the photon condensation experiments of [289]. Several possibilities in this direction are explored in [334, 335].

7.1.1 The field and emitter Hamiltonians and the radiation-emitter coupling

Given the translational symmetry of the system along the cavity plane, the in-plane momentum $\mathbf{k}$ of the photon is a good quantum number and the (bare) photon dispersion of a given longitudinal mode is well described by the parabolic dispersion (7.1). The emitters are fixed in space according to a regular square lattice and do not have any direct interaction.

Taking for notational simplicity $\hbar = 1$, the free Hamiltonian of the field and of the emitters has the usual form

$$H_{\text{free}} = \sum_{\mathbf{k}} \omega_{\mathbf{k}} \hat{b}^\dagger_{\mathbf{k}} \hat{b}_{\mathbf{k}} + \sum_i \nu S^z_i \tag{7.2}$$

where $\omega_{\mathbf{k}}$ is the cavity dispersion defined in (7.1) and ν is the emitter frequency. The $\hat{b}_{\mathbf{k}}, \hat{b}^\dagger_{\mathbf{k}}$ operators satisfy bosonic commutation rules $[\hat{b}_{\mathbf{k}}, \hat{b}^\dagger_{\mathbf{k}'}] = \delta_{\mathbf{k},\mathbf{k}'}$, while the emitter operators $S^{\pm,z}$ satisfy the usual algebra of spin-1/2 operators.

Within the usual rotating-wave approximation, the radiation-matter coupling is then:

$$H_{\text{int}} = \frac{ig}{\sqrt{V}} \sum_i \sum_{\mathbf{k}} \left(\mathrm{e}^{i\mathbf{k}\cdot\mathbf{x}_i} \, \hat{b}_{\mathbf{k}} \, S^+_i - \mathrm{e}^{-i\mathbf{k}\cdot\mathbf{x}_i} \, \hat{b}^\dagger_{\mathbf{k}} \, S^-_i \right), \tag{7.3}$$

where $\mathbf{x}_i$ is the position of the i-th emitter and V is the total volume of the system.

Assuming periodic boundary conditions, we can introduce the D-dimensional real-space cavity field

$$\phi(\mathbf{x}) = \frac{1}{\sqrt{V}} \sum_{\mathbf{k}} e^{i\mathbf{k}\cdot\mathbf{x}} \, \hat{b}_{\mathbf{k}}. \tag{7.4}$$

In terms of the field $\phi(\mathbf{x})$, local binary interactions between the cavity photons can be added to the

model via a two-body interaction term of the form

$$H^{(4)} = \frac{\lambda}{2}\int_V \mathrm{d}^D x\, \phi^\dagger(\mathbf{x})\phi^\dagger(\mathbf{x})\phi(\mathbf{x})\phi(\mathbf{x}), \tag{7.5}$$

which in momentum space reads:

$$H^{(4)} = \frac{\lambda}{2V}\sum_{\mathbf{kk'q}} \hat{b}^\dagger_{\mathbf{k+q}}\hat{b}^\dagger_{\mathbf{k'-q}}\hat{b}_{\mathbf{k'}}b_{\mathbf{k}}. \tag{7.6}$$

Physically, such a term can describe a Kerr $\chi^{(3)}$ optical non-linearity of the cavity material or, equivalently, polariton-polariton interactions [267].

7.1.2 Dissipative field dynamics: radiative losses

The cavity field is coupled to an external bath of radiative modes via the non-perfectly reflecting cavity mirrors. As usual, this can be modelled by coupling each $\mathbf{k}$ mode of the field with a bath of harmonic oscillators [336]. The resulting quantum Langevin equations [256] then have the form

$$\frac{d\hat{b}^\dagger_{\mathbf{k}}}{dt} = \left(i\omega_{\mathbf{k}} - \frac{\kappa}{2}\right)\hat{b}^\dagger_{\mathbf{k}} + F^\dagger_{\mathbf{k}}. \tag{7.7}$$

Here, κ is the decay rate of the field and the zero-mean quantum noises $F^\dagger_{\mathbf{k}}$ are uncorrelated and have a delta-like correlation in time

$$\langle F^\dagger_{\mathbf{k}}(t)F_{\mathbf{k'}}(t')\rangle = 0 \tag{7.8}$$

$$\langle F_{\mathbf{k}}(t)F^\dagger_{\mathbf{k'}}(t')\rangle = \kappa\,\delta(t-t')\,\delta_{\mathbf{k},\mathbf{k'}}. \tag{7.9}$$

This form of the quantum Langevin equation requires that the initial total density matrix factorizes in the cavity and bath parts and that the bath density matrix corresponds to an equilibrium state at very low temperature. Both approximations are well satisfied by realistic systems, since the frequencies involved in optical experiments are very high as compared to the device temperature, typically at or below room temperature. As a result, cavity photons can only spontaneously quit the cavity after a lifetime κ^{-1}, while no radiation can enter the cavity from outside.

7.1.3 Dissipative emitter dynamics: losses and pumping

The dissipative dynamics of the emitter requires a bit more care because of the intrinsic nonlinearity of a two-level system.

We take each emitter to be independently coupled to its own loss bath with a Hamiltonian of the form

$$H_\gamma = \sum_q \left(\gamma^*_q S^+ A_q + \gamma_q A^\dagger_q S^-\right). \tag{7.10}$$

Here, q indicates the modes of the bath, γ_q are the coupling constants, and A_q are the bath operators, assumed to have bosonic nature and an initially very low temperature. Performing a Markov approximation, the quantum Langevin equations for the spin-like operators of the emitter read

$$\begin{cases} \frac{dS^z}{dt}\big|_\gamma = -\gamma\left(\frac{1}{2}+S^z\right)+G^z_\gamma \\ \frac{dS^+}{dt}\Big|_\gamma = \left(i\nu-\frac{\gamma}{2}\right)S^+ + G^+_\gamma. \end{cases} \tag{7.11}$$

The deterministic part of these equations shows that each emitter tends to decay towards its lower state independently of its neighbors. Differently from what happened to the cavity mode in (7.8) and (7.9), the noise operators G^+_γ and G^z_γ now depend on the initial state of the bath $A_q(t_0)$ as well as on the instantaneous spin operators:

$$G^z_\gamma(t) = -i\sum_q \left[\gamma_q^* \mathrm{e}^{-i\omega_q(t-t_0)} S^+(t) A_q(t_0) \gamma_q \mathrm{e}^{i\omega_q(t-t_0)} A_k^\dagger(t_0) S^-(t)\right], \tag{7.12}$$

$$G^+_\gamma(t) = -2i\sum_k \gamma_k \mathrm{e}^{i\omega_k(t-t_0)} A_k^\dagger(t_0) S^z(t). \tag{7.13}$$

Under the same conditions assumed for the cavity operators, the quantum noises on the different emitters are uncorrelated and have a delta-like temporal correlation,

$$\langle G^\alpha_{\gamma,i}(t) G^{\alpha'}_{\gamma,j}(t')\rangle = 2D^{\alpha\alpha'}_\gamma(t)\delta(t-t')\,\delta_{ij}. \tag{7.14}$$

Among the many $\alpha,\alpha' = +,-,z$ terms, the only non-zero diffusion coefficients are:

$$D^{-+}_\gamma = \frac{\gamma}{2}, \qquad D^{-z}_\gamma = \frac{\gamma}{2}\langle S^-\rangle, \qquad D^{z+}_\gamma = \frac{\gamma}{2}\langle S^+\rangle, \qquad D^{zz}_\gamma = \frac{\gamma}{2}\left(\frac{1}{2}+\langle S^z\rangle\right). \tag{7.15}$$

The dependence of the diffusion coefficients on the spin operator averages stems from the intrinsic optical nonlinearity of two-level emitter and makes calculations much harder.

The incoherent external pumping of the system is modelled by coupling each emitter with a bath of inverted oscillators as typically done in laser theory [256]. This leads to quantum Langevin equations of the form

$$\begin{cases} \frac{dS^z}{dt}\big|_d = d\left(\frac{1}{2}-S^z\right)+G^z_d, \\ \frac{dS^+}{dt}\Big|_d = \left(i\nu-\frac{d}{2}\right)S^+ + G^+_d \end{cases} \tag{7.16}$$

Again, the noise operators G^α_d depend on the spin operators and satisfy delta-like correlation functions in time. The only non-zero diffusion coefficients are now:

$$D^{+-}_d = \frac{d}{2}, \qquad D^{+z}_d = -\frac{d}{2}\langle S^+\rangle, \tag{7.17}$$

$$D^{z-}_d = -\frac{d}{2}\langle S^-\rangle, \qquad D^{zz}_d = \frac{d}{2}\left(\frac{1}{2}-\langle S^z\rangle\right). \tag{7.18}$$

Combining the two loss and pumping contributions to the emitter dissipative dynamics, one finally obtains

$$\begin{cases} \frac{dS^z}{dt}\big|_{\gamma+d} &= \Gamma\left(\frac{\mathcal{D}}{2}-S^z\right)+G^z, \\ \frac{dS^+}{dt}\Big|_{\gamma+d} &= \left(i\nu-\frac{\Gamma}{2}\right)S^+ + G^+, \end{cases} \tag{7.19}$$

where $\Gamma = d + \gamma$ and $G^\alpha(t) = G^\alpha_\gamma(t) + G^\alpha_d(t)$. The stationary value of the average inversion operator S^z in the absence of any cavity field can be called *unsaturated population inversion* and depends only on the ratio between damping rates $x = d/\gamma$,

$$\mathcal{D} = \frac{d-\gamma}{d+\gamma}. \tag{7.20}$$

In the $\alpha, \alpha' = +, -, z$ basis, the diffusion matrix $D^{\alpha\alpha'}$ of the total external noise operators G^α is given by:

$$D^{\alpha\alpha'} = \begin{pmatrix} 0 & \frac{\gamma}{2} & \frac{\gamma}{2}\langle S^+\rangle \\ \frac{d}{2} & 0 & -\frac{d}{2}\langle S^-\rangle \\ -\frac{d}{2}\langle S^+\rangle & \frac{\gamma}{2}\langle S^-\rangle & \frac{\Gamma}{2}\left(\frac{1}{2} - \mathcal{D}\langle S^z\rangle\right) \end{pmatrix}. \tag{7.21}$$

7.1.4 The quantum Langevin equations

Putting all terms together, we obtain the final quantum Langevin equations for the i-th emitter and the $\mathbf{k}$ cavity mode operators,

$$\frac{dS^z_i}{dt} = \Gamma\left(\frac{\mathcal{D}}{2} - S^z_i\right) + \frac{g}{\sqrt{V}}\sum_{\mathbf{k}}\left(\mathrm{e}^{i\mathbf{k}\cdot\mathbf{x}_i}\, S^+_i\, \hat{b}_{\mathbf{k}} + \mathrm{e}^{-i\mathbf{k}\cdot\mathbf{x}_i}\, \hat{b}^\dagger_{\mathbf{k}}\, S^-_i\right) + G^z_i, \tag{7.22}$$

$$\frac{dS^+_i}{dt} = \left(i\nu - \frac{\Gamma}{2}\right) S^+_i - \frac{2g}{\sqrt{V}}\sum_{\mathbf{k}} \mathrm{e}^{-i\mathbf{k}\cdot\mathbf{x}_i}\, \hat{b}^\dagger_{\mathbf{k}}\, S^z_i + G^+_i, \tag{7.23}$$

$$\frac{d\hat{b}^\dagger_{\mathbf{k}}}{dt} = \left(i\omega_{\mathbf{k}} - \frac{\kappa}{2}\right)\hat{b}^\dagger_{\mathbf{k}} - \frac{g}{\sqrt{V}}\sum_i \mathrm{e}^{i\mathbf{k}\cdot\mathbf{x}_i}\, S^+_i + F^\dagger_{\mathbf{k}}. \tag{7.24}$$

These equations can be rewritten in *real space* in terms of field and spin-density operators. Assuming the emitters to be arranged on a regular square lattice with density n_A and to have a fictitious size equal to the lattice cell volume $a = n_A^{-1}$, these latter can be defined as

$$S^\alpha(\mathbf{x}) = \sum_i \delta^{(D)}_a(\mathbf{x} - \mathbf{x}_i)\, S^\alpha_i \tag{7.25}$$

in terms of delta distributions broadened over a spatial area a. Assuming that the bosonic field $\phi(\mathbf{x})$ is almost constant over a length $\sim a$ allows us to approximate $\delta^{(D)}_a(\mathbf{x})$ as a delta function, simplifying the algebra of the spin densities and the form of the quantum Langevin equations. In this representation, the spin algebra in the cartesian $\alpha_i = x, y, z$ basis has the form

$$[S^{\alpha_1}(\mathbf{x}), S^{\alpha_2}(\mathbf{x}')] = i\varepsilon_{\alpha_1\alpha_2\alpha_3} S^{\alpha_3}(\mathbf{x})\delta^{(D)}_a(\mathbf{x} - \mathbf{x}'). \tag{7.26}$$

Summing up, the real space quantum Langevin equations can be written as

$$\frac{\partial S^z(\mathbf{x})}{\partial t} = \Gamma\left[n_A\frac{\mathcal{D}}{2} - S^z(\mathbf{x})\right] + g\left[S^+(\mathbf{x})\phi(\mathbf{x}) + \phi^\dagger(\mathbf{x})S^-(\mathbf{x})\right] + G^z(\mathbf{x}), \tag{7.27}$$

$$\frac{\partial S^+(\mathbf{x})}{\partial t} = \left[i\nu - \frac{\Gamma}{2}\right] S^+(\mathbf{x}) - 2g\phi^\dagger(\mathbf{x})S^z(\mathbf{x}) + G^+(\mathbf{x}), \tag{7.28}$$

$$\frac{\partial \phi^\dagger(\mathbf{x})}{\partial t} = \left[i\omega(i\nabla_{\mathbf{x}}) - \frac{\kappa}{2}\right]\phi^\dagger(\mathbf{x}) - gS^+(\mathbf{x}) + F^\dagger(\mathbf{x}). \tag{7.29}$$

with a spatially local noise correlation

$$\langle G^{\alpha}(t,\mathbf{x})G^{\alpha'}(t',\mathbf{x}')\rangle = D^{\alpha\alpha'}(\mathbf{x})\delta_a^{(D)}(\mathbf{x}-\mathbf{x}')\delta(t-t'), \tag{7.30}$$

with

$$D^{\alpha\alpha'}(\mathbf{x}) = \begin{pmatrix} 0 & \frac{\gamma}{2}\,n_A & \frac{\gamma}{2}\langle S^{+}(\mathbf{x})\rangle \\ \frac{d}{2}\,n_A & 0 & -\frac{d}{2}\langle S^{-}(\mathbf{x})\rangle \\ -\frac{d}{2}\langle S^{+}(\mathbf{x})\rangle & \frac{\gamma}{2}\langle S^{-}(\mathbf{x})\rangle & \frac{\Gamma}{2}\left(\frac{n_A}{2}-\mathcal{D}\langle S^{z}(\mathbf{x})\rangle\right) \end{pmatrix}. \tag{7.31}$$

Another useful representation of the previous equations is in *momentum space*: defining the Fourier transform of the spin-density as

$$S^{\alpha}_{\mathbf{k}} = \int \mathrm{d}^d x\, S^{\alpha}(\mathbf{x})\mathrm{e}^{-i\mathbf{k}\cdot\mathbf{x}}, \qquad S^{\alpha}(\mathbf{x}) = \frac{1}{V}\sum_{\mathbf{k}} S^{\alpha}_{\mathbf{k}}\mathrm{e}^{i\mathbf{k}\cdot\mathbf{x}}, \tag{7.32}$$

we have the spin commutation relations

$$[S^{\alpha_1}_{\mathbf{k}}, S^{\alpha_2}_{\mathbf{k}'}] = i\varepsilon_{\alpha_1\alpha_2\alpha_3}S^{\alpha_3}_{\mathbf{k}+\mathbf{k}'}, \tag{7.33}$$

and the quantum Langevin equations

$$\frac{dS^{z}_{\mathbf{k}}}{dt} = \Gamma\left(\delta_{\mathbf{k},0}N_A\frac{\mathcal{D}}{2} - S^{z}_{\mathbf{k}}\right) + \frac{g}{\sqrt{V}}\sum_{\mathbf{q}}\left(S^{+}_{\mathbf{k}-\mathbf{q}}\hat{b}_{\mathbf{q}} + \hat{b}^{\dagger}_{\mathbf{q}}S^{-}_{\mathbf{k}+\mathbf{q}}\right) + G^{z}_{\mathbf{k}} \tag{7.34}$$

$$\frac{dS^{+}_{\mathbf{k}}}{dt} = \left(i\nu - \frac{\Gamma}{2}\right)S^{+}_{\mathbf{k}} - 2\frac{g}{\sqrt{V}}\sum_{\mathbf{q}}\hat{b}^{\dagger}_{\mathbf{q}}S^{z}_{\mathbf{k}+\mathbf{q}} + G^{+}_{\mathbf{k}}, \tag{7.35}$$

$$\frac{d\hat{b}^{\dagger}_{\mathbf{k}}}{dt} = \left(i\omega_{\mathbf{k}} - \frac{\kappa}{2}\right)\hat{b}^{\dagger}_{\mathbf{k}} - \frac{g}{\sqrt{V}}S^{+}_{-\mathbf{k}} + F^{\dagger}_{\mathbf{k}}. \tag{7.36}$$

Momentum space noise operators then satisfy

$$\langle G^{\alpha}_{\mathbf{k}}(t)G^{\alpha'}_{\mathbf{k}'}(t')\rangle = 2D^{\alpha\alpha'}_{\mathbf{k}+\mathbf{k}'}\delta(t-t'), \tag{7.37}$$

$$\tag{7.38}$$

with

$$D^{\alpha\alpha'}_{\mathbf{k}+\mathbf{k}'} = \begin{pmatrix} 0 & \frac{\gamma}{2}\,N_A\delta_{\mathbf{k},-\mathbf{k}'} & \frac{\gamma}{2}\langle S^{+}_{\mathbf{k}+\mathbf{k}'}\rangle \\ \frac{d}{2}\,N_A\delta_{\mathbf{k},-\mathbf{k}'} & 0 & -\frac{d}{2}\langle S^{-}_{\mathbf{k}+\mathbf{k}'}\rangle \\ -\frac{d}{2}\langle S^{+}_{\mathbf{k}+\mathbf{k}'}\rangle & \frac{\gamma}{2}\langle S^{-}_{\mathbf{k}+\mathbf{k}'}\rangle & \frac{\Gamma}{2}\left(\frac{N_A}{2}\delta_{\mathbf{k},-\mathbf{k}'} - \mathcal{D}\langle S^{z}_{\mathbf{k}+\mathbf{k}'}\rangle\right) \end{pmatrix}. \tag{7.39}$$

Before proceeding with our discussion, it is worth pointing out that what we have introduced so far is a minimal quantum model to describe condensation in a spatially extended geometry. Depending on the specific system under investigation, other terms might be needed, for instance dephasing of the emitter under the effect of a sort of collisional broadening, or several species of emitters with different resonance frequencies ν_i so to account for more complex gain spectra.

In our formalism, dephasing corresponds to terms of the form

$$\dot{\rho} = \frac{\Gamma_{\mathrm{coll}}}{2}\left(4S^{z}\rho S^{z} - \rho\right) \tag{7.40}$$

in the master equation [337], $\Gamma_{\rm coll}$ being the contribution of the dephasing to the dipole relaxation rate. In the quantum Langevin formalism, these processes give additional deterministic terms

$$\begin{cases} \frac{dS^+}{dt}\Big|_{\rm coll} = -\Gamma_{\rm coll} S^+ + G^+_{\rm coll}, \\ \frac{dS^z}{dt}\Big|_{\rm coll} = 0, \end{cases} \tag{7.41}$$

and an additional contribution to the noise:

$$\begin{cases} \langle G^+_{\rm coll}(t) G^-_{\rm coll}(t')\rangle = 2\Gamma_{\rm coll}\left(\frac{1}{2} + \langle S^z\rangle\right)\delta(t-t'), \\ \langle G^-_{\rm coll}(t) G^+_{\rm coll}(t')\rangle = 2\Gamma_{\rm coll}\left(\frac{1}{2} - \langle S^z\rangle\right)\delta(t-t'). \end{cases} \tag{7.42}$$

We have checked that including such terms does not introduce any qualitatively new feature in the model.

7.2 Mean-field theory

As a first step in our study of non-equilibrium condensation effects, we study the mean-field solution to the quantum Langevin equations. This amounts to neglecting the quantum noise terms in (7.34)-(7.36) and replacing each operator with its expectation value. This study is the simplest in momentum representation, where the mean-field motion equations for $\beta^*_{\mathbf{k}} = \langle \hat{b}^\dagger_{\mathbf{k}}\rangle$ and $\sigma^\alpha_{\mathbf{k}} = \langle S^\alpha_{\mathbf{k}}\rangle$ have the form

$$\dot\sigma^z_{\mathbf{k}} = \Gamma\left(\delta_{\mathbf{k},0} N_A \frac{\mathcal{D}}{2} - \sigma^z_{\mathbf{k}}\right) + \frac{g}{\sqrt{V}}\sum_{\mathbf{q}}\left(\sigma^+_{\mathbf{k}-\mathbf{q}}\beta_{\mathbf{q}} + \beta^*_{\mathbf{q}}\sigma^-_{\mathbf{k}+\mathbf{q}}\right), \tag{7.43}$$

$$\dot\sigma^+_{\mathbf{k}} = \left(i\nu - \frac{\Gamma}{2}\right)\sigma^+_{\mathbf{k}} - 2\frac{g}{\sqrt{V}}\sum_{\mathbf{q}}\beta^*_{\mathbf{q}}\sigma^z_{\mathbf{k}+\mathbf{q}}, \tag{7.44}$$

$$\dot\beta^*_{\mathbf{k}} = \left(i\omega_{\mathbf{k}} - \frac{\kappa}{2}\right)\beta^*_{\mathbf{k}} - \frac{g}{\sqrt{V}}\sigma^+_{-\mathbf{k}} + \frac{i\lambda}{V}\sum_{\mathbf{q}\mathbf{q}'}\beta^*_{\mathbf{q}+\mathbf{q}'}\beta^*_{\mathbf{k}-\mathbf{q}'}\beta_{\mathbf{q}}, \tag{7.45}$$

very similar to the ones of the semi-classical theory of lasers [338].

7.2.1 Stationary state: Bose condensation

While a trivial solution with all $\beta^*_{\mathbf{k}} = \sigma^+_{\mathbf{k}} = 0$ is always present, for some values of the parameters to be specified below, this solution becomes dynamically unstable and is replaced by other *condensed* solutions with a non vanishing field amplitude. Inspired by experiments, we focus our attention on the case where condensation occurs on the $\mathbf{k} = 0$ state. This corresponds to inserting the ansatz

$$\begin{cases} \beta^*_{\mathbf{k}}(t) = \delta_{\mathbf{k}0}\sqrt{V}\,\beta^*_0\,{\rm e}^{i\omega t}, \\ \sigma^+_{\mathbf{k}}(t) = \delta_{\mathbf{k}0}\,V\,\sigma^+_0 {\rm e}^{i\omega t}, \\ \sigma^z_{\mathbf{k}}(t) = \delta_{\mathbf{k}0}\,V\,\sigma^z_0, \end{cases} \tag{7.46}$$

into the mean-field equations, with the amplitudes β^*_0 and σ^+_0, the population inversion σ^z_0 and the frequency ω to be determined in a self consistent way.

In the $\lambda = 0$ case where direct photon-photon interactions vanish, a direct analytical solution of the mean-field equations gives

$$\omega = \frac{\frac{\nu}{\Gamma} + \frac{\omega_0}{\kappa}}{\frac{1}{\Gamma} + \frac{1}{\kappa}} = \omega_0 + \frac{\kappa}{2}\delta, \tag{7.47}$$

where $\delta = 2(\nu - \omega_0)/(\Gamma + \kappa)$ is the dimensionless detuning: the frequency ω is therefore equal to an average of the bare field and dipole frequencies, weighted with their bare lifetimes. Analogously, we find for the field and emitter observables,

$$|\beta_0|^2 = \frac{\Gamma}{\kappa}\left[n_A\frac{\mathcal{D}}{2} - \frac{\Gamma\kappa}{8g^2}\left(1+\delta^2\right)\right], \tag{7.48}$$

$$\sigma_0^z = \frac{\Gamma\kappa}{8g^2}\left(1+\delta^2\right), \tag{7.49}$$

$$\sigma_0^+ = -\frac{\kappa}{2g}\left(1+i\delta\right)\beta_0^*. \tag{7.50}$$

The condensation threshold is clearly visible in these results: for $\mathcal{D}/\Gamma < \kappa(1+\delta^2)/4g^2 n_A$, the right-hand side of (7.48) is negative, so only the trivial β_0 solution is possible. For $\mathcal{D}/\Gamma > \kappa(1+\delta^2)/4g^2 n_A$, a condensed solution appears with a finite field intensity (7.48) and a corresponding emitter dipole moment proportional to (7.50). Remind that both $\mathcal{D} = (d-\gamma)/(d+\gamma)$ and $\Gamma = d + \gamma = \gamma(1+x)$ are here function of the pumping rate.

For finite values of λ, a similar derivation can be carried out. For the frequency, it gives

$$\omega = \frac{\frac{\nu}{\Gamma} + \frac{1}{\kappa}\left(\omega_0 + \lambda|\beta_0|^2\right)}{\frac{1}{\Gamma} + \frac{1}{\kappa}} = \omega_0 + \lambda|\beta_0|^2 + \frac{\kappa}{2}\delta_\lambda, \tag{7.51}$$

where the dimensionless detuning $\delta_\lambda = 2\left(\nu - \omega_0 - \lambda|\beta_0|^2\right)/\left(\Gamma + \kappa\right)$ now involves also the nonlinear frequency shift of the field mode. For the field and the emitter observables, it gives:

$$|\beta_0|^2 = \frac{\Gamma}{\kappa}\left[n_A\frac{\mathcal{D}}{2} - \frac{\Gamma\kappa}{8g^2}\left(1+\delta_\lambda^2\right)\right] \tag{7.52}$$

$$\sigma_0^z = \frac{\Gamma\kappa}{8g^2}\left(1+\delta_\lambda^2\right) \tag{7.53}$$

$$\sigma_0^+ = -\frac{\kappa}{2g}\left(1+i\delta_\lambda\right)\beta_0^*. \tag{7.54}$$

7.2.2 Physical discussion

The most remarkable feature of the mean-field equations is the spontaneous symmetry breaking phenomenon at the condensation threshold. The mean-field equations (7.43)-(7.45) are symmetric under the U(1) transformation $(\beta_{\mathbf{k}}^*, \sigma_{\mathbf{k}}^+) \to (\mathrm{e}^{i\varphi}\beta_{\mathbf{k}}^*, \mathrm{e}^{i\varphi}\sigma_{\mathbf{k}}^+)$ with arbitrary global phase φ. While for all values of the parameters there is a trivial $\beta_0 = \sigma_0^+ = 0$ solution which fulfils this symmetry, any non-trivial solution has to choose a specific phase for β_0 and σ_0^+, only their modulus being fixed by (7.48) or (7.52): as a result, the U(1) symmetry is *spontaneously broken*. In actual experiments, this phase is randomly chosen. Note that since the symmetry transformation does not involve σ_0^z, its mean-field value can always be non-zero.

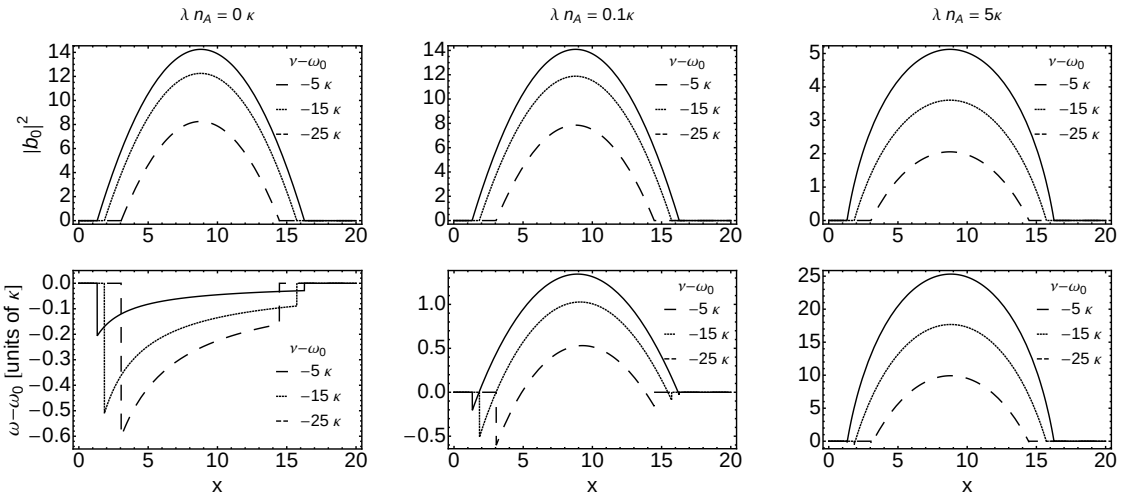

Figure 7.1: Intensity of the field (upper panels) and oscillation frequency of the condensate (lower panels) as a function of the pumping parameter $x = d/\gamma$. Both quantities are shown for different values of self-interaction λ and natural detuning $\nu - \omega_0$. In all panels, $\gamma = 10\kappa$ and $g\sqrt{n_A} = 7\kappa$.

The behaviour of the field intensity $|\beta_0|^2$ and of the oscillation frequency ω is plotted in Fig.7.1 as a function of the pumping strength $x = d/\gamma$ for different (negative) values of the natural field-emitter detuning $\nu - \omega_0 < 0$ (different curves) and different values of the (positive) nonlinear coupling $\lambda > 0$ (different panels). In all cases, two thresholds are well visible: the lower one corresponds to the standard switch-on of laser operation for sufficiently large pump strength. The upper one is a consequence of our specific model and is due to the fact that the gain offered by the emitters is suppressed when the effective emitter linewidth $\Gamma = d + \gamma = \gamma(1 + x)$ appearing in (7.23) is very much broadened by the pumping term d. As usual, whenever a non-trivial $\beta_0 \neq 0$ condensate solution is available, the trivial solution becomes dynamically unstable. For all cases shown in this figure, the order parameter β_0 grows continuously from zero, so the condensation resembles a second-order phase transition.

The behavior of the oscillation frequency shown in the lower panels of Fig.7.1 is determined by a complex interplay of the bare frequencies of the cavity and of the emitter, weighted by their respective linewidths and shifted by the nonlinear interaction energy λ according to (7.51).

The situation for positive detuning $\nu - \omega_0 > 0$ is more complicate and a complete analysis of the rich phenomenology goes beyond the scope of this Chapter. Not only the order parameter as a function of pumping strength can be discontinuous [339] and bistable, but also the spatial shape of the condensate can develop a complicate structure. As the gain is maximum on a **k**-space ring of modes at a finite k, the choice of the specific combination of modes is determined by complex mechanisms involving the interplay of pumping and dissipation, but also the geometrical details of the system beyond the idealised spatially homogeneous approximation. This complex physics is typical of non-equilibrium systems where no minimal free-energy criterion is available to determine the steady

state of the system and is closely related to pattern formation in nonlinear dynamical systems [340]. First experimental evidence of condensation in spatially non-trivial modes was reported in [341] and discussed in [294]. More complicate spatial features were investigated in [329, 342].

7.3 Quantum fluctuations

7.3.1 Linearised theory of small fluctuations

The mean-field steady-state solution obtained in the previous Section is the starting point for a linearised theory of fluctuations. In the spirit of Bogoliubov and the spin wave approximations, we can linearise Eqs.(7.34)-(7.36) around the steady-state by performing the operator replacement:

$$\begin{cases} \hat{b}^\dagger_{\mathbf{k}} = \left(\delta_{\mathbf{k}0}\sqrt{V}\,\beta_0^* + \delta\hat{b}^\dagger_{\mathbf{k}}\right)\mathrm{e}^{i\omega t}, \\ S^+_{\mathbf{k}} = \left(\delta_{\mathbf{k}0}\,V\,\sigma_0^+ + \delta S^+_{\mathbf{k}}\right)\mathrm{e}^{i\omega t}, \\ S^z_{\mathbf{k}} = \delta_{\mathbf{k}0}\,V\,\sigma_0^z + \delta S^z_{\mathbf{k}}: \end{cases} \tag{7.55}$$

β_0^*, σ_0^+ and σ_0^z are here the mean-field steady-states as defined in (7.52)-(7.54) with a frequency ω determined by (7.51). Fluctuations around the mean-field are described by the $\delta\hat{b}^\dagger_{\mathbf{k}}$, $\delta S^+_{\mathbf{k}}$ and $\delta S^z_{\mathbf{k}}$ operators which inherit the commutation rules from the original $\hat{b}^\dagger_{\mathbf{k}}$, $S^+_{\mathbf{k}}$ and $S^z_{\mathbf{k}}$ operators.

Substituting the previous expressions into the motion equations (7.34)-(7.36) and neglecting terms of second or higher order in the fluctuation operators, we obtain a set of coupled linear equations

$$\frac{d\mathbf{v}_{\mathbf{k}}}{dt} = \mathbb{A}_{\mathbf{k}}\mathbf{v}_{\mathbf{k}} + \widetilde{\mathbf{F}}_{\mathbf{k}}, \tag{7.56}$$

for the (rescaled) fluctuation vector

$$\mathbf{v}^t_{\mathbf{k}} = (\delta\widetilde{\hat{b}}^\dagger_{-\mathbf{k}}, \delta\widetilde{\hat{b}}_{\mathbf{k}}, \delta S^+_{\mathbf{k}}, \delta S^-_{\mathbf{k}}, \delta S^z_{\mathbf{k}}), \tag{7.57}$$

with a quantum noise vector

$$\widetilde{\mathbf{F}}^t_{\mathbf{k}} = (\widetilde{F}^\dagger_{-\mathbf{k}}, \widetilde{F}_{\mathbf{k}}, \widetilde{G}^+_{\mathbf{k}}, \widetilde{G}^-_{\mathbf{k}}, \widetilde{G}^z_{\mathbf{k}}). \tag{7.58}$$

For notational convenience, we have used the rescaled quantities $\delta\widetilde{\hat{b}}^\dagger_{\mathbf{k}} = \sqrt{V}\delta\hat{b}^\dagger_{\mathbf{k}}$ with rescaled noise terms $\widetilde{F}^\dagger_{\mathbf{k}} = \sqrt{V}\mathrm{e}^{-i\omega t}F^\dagger_{\mathbf{k}}$ and $\widetilde{G}^+_{\mathbf{k}} = \mathrm{e}^{-i\omega t}G^+_{\mathbf{k}}$ and $\widetilde{G}^z_{\mathbf{k}} = G^z_{\mathbf{k}}$. The equations for the Hermitian conjugate quantities $\delta S^-_{\mathbf{k}}$ and $\delta\hat{b}_{\mathbf{k}}$ follow straightforwardly from $\delta S^-_{-\mathbf{k}} = (\delta S^+_{\mathbf{k}})^\dagger$ and $\delta\hat{b}_{\mathbf{k}} = (\delta\hat{b}^\dagger_{-\mathbf{k}})^\dagger$.

Defining the shorthands $z_\lambda = 1 + i\delta_\lambda$ and $\epsilon_{\mathbf{k}} = k^2/2m$, the Bogoliubov matrix $\mathbb{A}_{\mathbf{k}}$ is equal to

$$\mathbb{A}_{\mathbf{k}} = \begin{pmatrix} -\frac{\kappa}{2}z_\lambda + i\epsilon_{\mathbf{k}} + i\lambda|\beta_0|^2 & i\lambda(\beta_0^*)^2 & -g & 0 & 0 \\ -i\lambda\beta_0^2 & -\frac{\kappa}{2}z_\lambda^* - i\epsilon_{\mathbf{k}} - i\lambda|\beta_0|^2 & 0 & -g & 0 \\ -2g\sigma_0^z & 0 & -\frac{\Gamma}{2}z_\lambda^* & 0 & -2g\beta_0^* \\ 0 & -2g\sigma_0^z & 0 & -\frac{\Gamma}{2}z_\lambda & -2g\beta_0 \\ g\sigma_0^- & g\sigma_0^+ & g\beta_0 & g\beta_0^* & -\Gamma \end{pmatrix}. \tag{7.59}$$

Evaluation of the noise correlation matrix requires a bit more care as the emitter noise depends on the emitter operators themselves.

Inserting into (7.39) the steady-state value of the emitter operators, we have that:

$$\langle \widetilde{G}^{\alpha}_{\mathbf{k}} \widetilde{G}^{\alpha'}_{\mathbf{k}'} \rangle = 2D^{\alpha\alpha'}_{\mathbf{k}+\mathbf{k}'}\, \delta(t-t')\delta_{\mathbf{k}+\mathbf{k}',0} \propto N_A : \tag{7.60}$$

as in this equation the emitter noise terms $G^{\alpha}_{\mathbf{k}} \propto \sqrt{N_A}$ are of the same order as the other terms in the linearised equations, it is legitimate to replace the spin operators in the diffusion coefficients with their mean field values. Note that the $\delta_{\mathbf{k}+\mathbf{k}',0}$ coefficient in (7.60) is a consequence of the assumed ordered arrangement of the emitters: Had we considered a disordered configuration, the zero value for $\mathbf{k}+\mathbf{k}' \neq 0$ would be replaced by something proportional to $\sqrt{N_A}$, still negligible with respect to the value proportional to N_A of the $\mathbf{k}+\mathbf{k}'=0$ term.

The correlation matrix of $\widetilde{\mathbf{F}}_{\mathbf{k}}$ is

$$\langle \widetilde{\mathbf{F}}_{\mathbf{k}}(t) \widetilde{\mathbf{F}}^{\dagger}_{\mathbf{k}'}(t') \rangle = \mathbb{D}\delta(t-t')\delta_{\mathbf{k},\mathbf{k}'} \tag{7.61}$$

with

$$\mathbb{D} = V \begin{pmatrix} 0 & 0 & 0 & 0 & 0 \\ 0 & \kappa & 0 & 0 & 0 \\ 0 & 0 & d\, n_A & 0 & -d\sigma_0^{+} \\ 0 & 0 & 0 & \gamma\, n_A & \gamma\sigma_0^{-} \\ 0 & 0 & -d\sigma_0^{-} & \gamma\sigma_0^{+} & \Gamma\left(\frac{n_A}{2} - \mathcal{D}\sigma_0^{z}\right) \end{pmatrix}. \tag{7.62}$$

As a final remark on the linearisation procedure, let us emphasize how our approximations are controlled by the total number of atoms N_A. Assume the scaling

$$S^{\alpha}_{\mathbf{k}=0} \sim N_A, \quad \hat{b}_{\mathbf{k}=0} \sim \sqrt{N_A}, \quad D^{\alpha\alpha'}_{\mathbf{k}=0} \sim N_A, \tag{7.63}$$

and

$$S^{\alpha}_{\mathbf{k}\neq 0} \sim \sqrt{N_A}, \quad \hat{b}_{\mathbf{k}\neq 0} \sim 1, \quad D^{\alpha\alpha'}_{\mathbf{k}\neq 0} \sim \sqrt{N_A}, \tag{7.64}$$

together with $g \sim 1/\sqrt{n_A}$ the dependence on N_A of each term in Eqs. (7.34)-(7.36) can be made explicit. Then, in the thermodynamical limit $N_A \to +\infty$, retaining the leading order in N_A from such equations is equivalent to the perform mean-field approximation of Sec. 7.2. If the next-to-leading order is also retained, the linearised Bogoliubov theory is recovered.

In analogy with the systematic expansion of equilibrium Bogoliubov theory in powers of the dilution parameter [343], we can make use of these considerations to define a systematic *mean-field* limit for our non-equilibrium system. To this purpose, it is useful to consider the real-space form of the quantum Langevin equations (7.27-7.29). If we let the atomic density and the photon density $|\phi(\mathbf{x})|^2 \sim S^{\alpha}(\mathbf{x}) \sim n_A \to \infty$ at constant $g\sqrt{n_A} \sim g|\phi(\mathbf{x})|$ and $\lambda|\phi(\mathbf{x})|^2$, the mean-field equations are not affected [in particular, their steady-states (7.52-7.54)], while the relative importance of the noise terms in the quantum Langevin and of the commutators tends to zero. As a result, the relative magnitude of quantum fluctuation expectation values vs. mean-field terms scale as $1/n_A$ in the mean-field limit.

7.3.2 The collective Bogoliubov modes

A first step to physically understand the consequences of fluctuations is to study the dispersion of the eigenvalues $\lambda^{\mathrm{Bog}}_{\mathbf{k}}$ of $\mathbb{A}_{\mathbf{k}}$ as a function of k, which gives the generalised Bogoliubov dispersion of excitations on top of the non-equilibrium condensate.

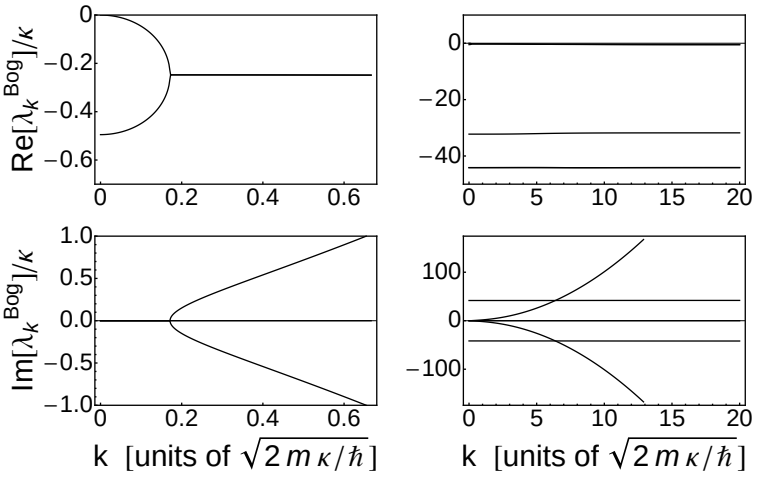

Figure 7.1: Dispersion $\lambda_k^{\rm Bog}$ of the collective modes as predicted by the eigenvalues of the Bogoliubov matrix $\mathbb{A}_{\mathbf{k}}$ in the interacting case with $\lambda n_A = 0.1\kappa$ and $\nu - \omega_0 = -10\kappa$. Left panels show magnified views of the low-$\mathbf{k}$ region of right panels. System parameters: $\gamma = 100\kappa$, $g\sqrt{n_A} = 25$ and $x = 5$.

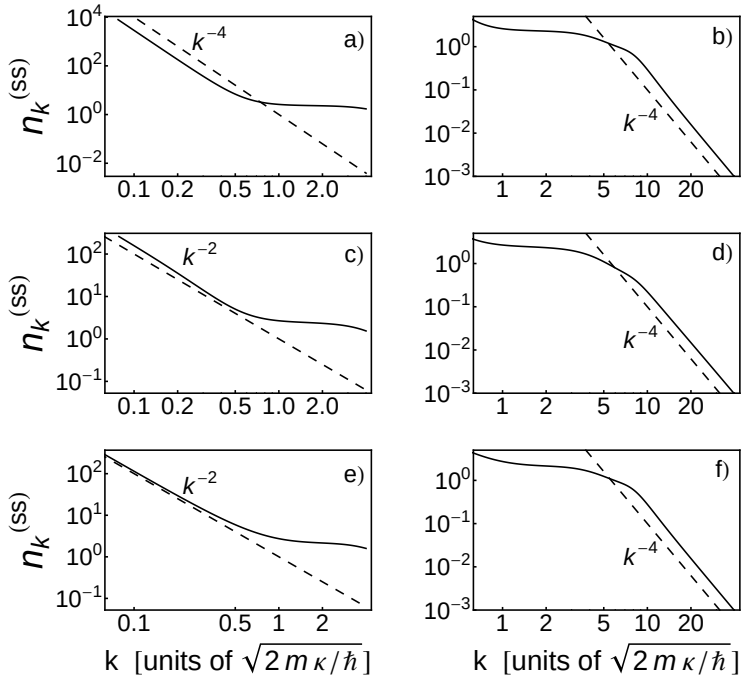

Figure 7.2: Steady state momentum distribution. Left panels show magnified views of the low-$\mathbf{k}$ region of right panels. (a,b) non-interacting case $\lambda n_A = \nu - \omega_0 = 0$. (c,d) $\lambda n_A = 0$, $\nu - \omega_0 = -10\kappa$. (e,f) $\lambda n_A = 0.1\kappa$, $\nu - \omega_0 = 0$. System parameters: $\gamma = 100\kappa$, $g\sqrt{n_A} = 25$ and $x = 5$.

An example of dispersion is shown in Fig.7.1: the upper panels show the real part of the dispersion $\mathrm{Re}[\lambda_k^{\mathbf{Bog}}]$ (describing the damping/growth rate of the mode) and the lower panels show the imaginary part $\mathrm{Im}[\lambda_k^{\mathrm{Bog}}]$ (describing the oscillation frequency of the mode). The left column give magnified views of the same dispersion shown on the right column.

As expected there is a Goldstone mode corresponding to the spontaneously broken U(1) symmetry, whose frequency tends to 0 in both real and imaginary parts as $k \to 0$. As typical in non-equilibrium systems [340], this mode is however diffusive rather than sonic, that is $\mathrm{Im}[\lambda_k^{\mathrm{Bog}}] = 0$ for a finite range around $k = 0$ and the real part starts from zero as $\mathrm{Re}[\lambda_k^{\mathrm{Bog}}] \simeq -\zeta k^2$.

At higher momenta, the diffusive Goldstone mode transform itself into a single-particle cavity photon mode with a parabolic dispersion. Between the two regimes, for $\lambda > 0$ or a finite cavity-emitter detuning δ, there is a sonic-like dispersion of the $\mathrm{Im}[\lambda_k^{\mathrm{Bog}}] \approx c_s|k|$ form (see Figs.7.1): for $\lambda > 0$, this is a standard feature of the Bogoliubov dispersion of interacting photons/polaritons [267]. For a finite δ, it follows from the intensity-dependence of the refractive index of detuned two-level systems [337]. A connection with the Gross-Pitaevskii formulation of [299] will be given at the end of Sec.7.4.

In the larger view displayed on the right column, in addition to the Goldstone mode we see two other, almost dispersionless excitation modes. As their origin is mostly due to emitter degrees of freedom, they could not be captured by the Gross-Pitaevskii approach of [299]. Their splitting is related to the Rabi frequency of the optical dressing of the atoms due to the coherent field in the cavity corresponding to the condensate and they are visible in the emitter emission spectrum as the external sidebands of the so-called Mollow triplet of resonance fluorescence [337].

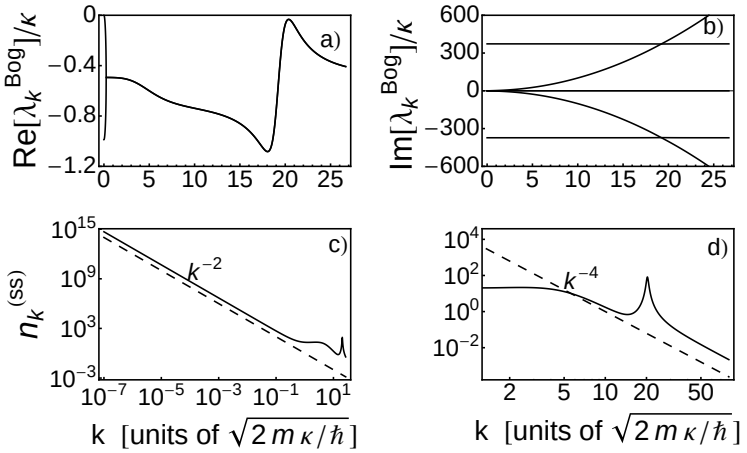

Figure 7.3: Imaginary (a) and real (b) part of the dispersion of the collective modes and steady state momentum distribution (c)-(d) in the vicinity of the Mollow instability onset. (c) shows a magnified view of the low-$\mathbf{k}$ region of (d). System parameters: $\gamma = 10\kappa$, $g\sqrt{n_A} = 42\kappa$, $x = 5$, $\lambda n_A = 0.1\kappa$, $\nu - \omega_0 = 0$.

The effect of these additional modes is more evident in Fig.7.3, where the chosen parameters are close to a secondary instability. The finite instability wavevector is located at the point where

the cavity field dispersion crosses the ones of the dispersionless modes: in this neighborhood, the real part of the dispersion $\mathrm{Re}[\lambda_{\mathbf{k}}^{\mathrm{Bog}}]$ approaches 0 from below. Should $\mathrm{Re}[\lambda_{\mathbf{k}}^{\mathrm{Bog}}]$ go above 0, our ansatz with a uniform condensate localised in the $\mathbf{k} = 0$ mode would no longer be valid and more complicate condensate shapes with spatial modulation should be considered [329, 344–346], analogous to secondary instabilities in pattern formation theory [340]. Physically, this *Mollow instability* can be easily interpreted in terms of the well-known optical gain offered by a two-level emitter driven by a strong coherent beam and probed by a weak probe beam detuned by approximately the Rabi frequency of the dressing [337].

7.3.3 Momentum distribution

From the quantum Langevin equation (7.56), it is straightforward to extract predictions for one-time physical observables. As a most remarkable example, here we shall concentrate our attention on the steady-state momentum distribution of the cavity field,

$$n_{\mathbf{k}}^{s} = \langle \hat{b}_{\mathbf{k}}^{\dagger}\, \hat{b}_{\mathbf{k}} \rangle = \langle \delta\hat{b}_{\mathbf{k}}^{\dagger}\, \delta\hat{b}_{\mathbf{k}} \rangle. \tag{7.65}$$

On one hand, in contrast to the mean-field approximation where the cavity field is concentrated in the $\mathbf{k} = 0$ mode, this observable is a sensitive probe of fluctuations. On the other hand, it is an experimentally accessible quantity, easily measured from the far-field angular distribution of emitted light. By Fourier transform, it is directly related to the two-points, one-time coherence function of the cavity field, a quantity which is of widespread use in experiments [266, 347–349].

Grouping in the $\mathbb{V}_{\mathbf{k}} = \langle \mathbf{v}_{\mathbf{k}}^{s} \mathbf{v}^{s\,\dagger}_{\mathbf{k}} \rangle$ variance matrix the steady-state variances of all operator pairs, from a straightforward integration of the quantum Langevin equations [350], we obtain a Lyapunov equation:

$$\mathbb{A}_{\mathbf{k}} \mathbb{V}_{\mathbf{k}} + \mathbb{V}_{\mathbf{k}} \mathbb{A}_{\mathbf{k}}^{\dagger} = -\mathbb{D} \tag{7.66}$$

from which standard linear algebra methods allow to extract the variance matrix $\mathbb{V}_{\mathbf{k}}$.

While no simple analytical form is available for $n_{\mathbf{k}}^{s}$, plots of its behaviour are given in the bottom panels of Fig. 7.2 for several most relevant cases. For small k, the momentum distribution follows the same $1/k^2$ behaviour as equilibrium systems provided photons are effectively interacting, that is either $\lambda > 0$ or $\delta \neq 0$. In the $\lambda = \delta = 0$ case, the situation is more complicate and the distribution appears to diverge as $1/k^4$. Both these results are in agreement with the predictions of the stochastic Gross-Pitaevskii equation in [312]. However, as it was noted in [351], great care has to be paid when applying the linearised Bogoliubov-like formalism to low-k modes in non-equilibrium, as the effects beyond linearisation can play a dominant role.

At large k, the momentum distribution always decays to zero as $1/k^4$. The large-k decay qualitatively recovers the prediction we guessed in [312] from a phenomenological stochastic Gross-Pitaevskii equation with a frequency-dependent pumping. The specific $1/k^4$ law is a consequence of our choice of monochromatic emitters, whose amplification spectrum decays as $1/(\omega - \nu)^2$: other choices of the emitter distribution would lead to correspondingly different high-momentum tails of $n_{\mathbf{k}}$. The *ab initio* confirmation of this large-k decay of $n_{\mathbf{k}}$ is one of the main results of this Chapter, as it shows that thermal-like momentum distributions can be found also in models where the quasi-particles are not interacting at all and therefore can not get thermalised by collisional processes. A similar feature was

experimentally observed in [300] using a VCSEL device in the weak coupling regime where photons are practically non-interacting.

The intermediate-k region shows a quite structureless plateau connecting the low-k and high-k regimes. The most interesting feature in this window is the peak that appears at the crossing point of the Goldstone mode and the dispersionless branch when the Mollow instability is approached, see Fig.7.4. As usual, the peak height diverges at the onset of the instability.

7.3.4 Photo-luminescence spectrum

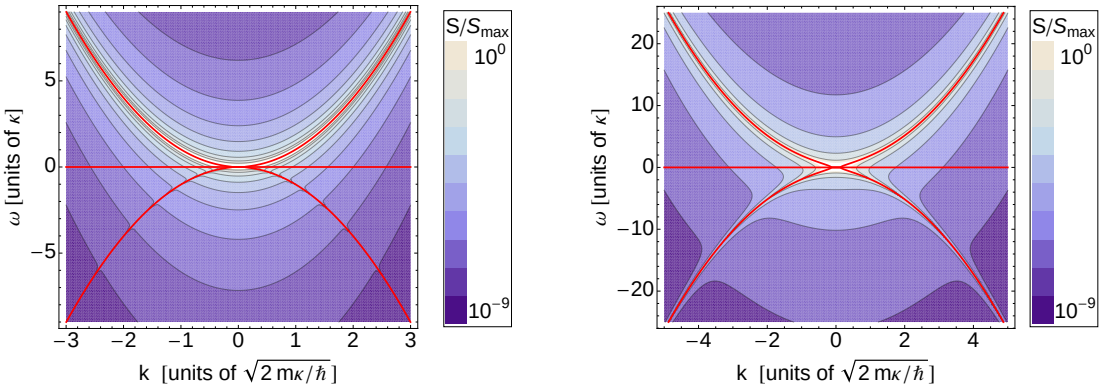

Figure 7.4: Normalised momentum- and frequency-resolved spectrum of the photoluminescence from the cavity. Left panel: detuned $\nu - \omega_0 = -35\kappa$ case with $\lambda n_A = 0$. Right panel: resonant cavity $\nu - \omega_0 = 0$ with photon-photon interactions $\lambda n_A = 0.1\kappa$. Other system parameters: $\gamma = 10\kappa$, $g\sqrt{n_A} = 7\kappa$, $x = 7$.

In addition to the one-time observables discussed in the previous Section, the quantum Langevin equations also allow for a straightforward evaluation of two-time observables. In particular, we shall concentrate here in the photoluminescence spectrum,

$$S_{\mathbf{k}}(\omega) = \int \frac{dt}{2\pi}\, e^{-i\omega t} \left\langle \hat{b}^{\dagger}_{\mathbf{k}}(t)\, \hat{b}_{\mathbf{k}}(0) \right\rangle \tag{7.67}$$

which is accessible from a frequency- and angle-resolved measurement of the emission from the cavity. A detailed study of this quantity in an equilibrium context can be found in [352]. A non-equilibrium calculation using linearised Keldysh techniques was reported in [298].

In our quantum Langevin approach [350], this spectrum is directly obtained as the top-left element of the matrix

$$\mathbb{S}_{\mathbf{k}}(\omega) = \frac{1}{2\pi}(\mathbb{A}_{\mathbf{k}} - i\omega)^{-1}\mathbb{D}(\mathbb{A}^{\dagger}_{\mathbf{k}} + i\omega)^{-1} : \tag{7.68}$$

the resonant denominators in the right-hand side of this equation shows that the photoluminescence spectrum is peaked along the real part of the Bogoliubov dispersion, while the linewidth of the peaks is set by the imaginary part.

Among the most interesting and non-trivial examples, we show in Fig.7.4 the photoluminescence spectrum for two cases of a negative detuning $\delta < 0$ (left) and of finite photon-photon interactions $\lambda > 0$ (right): in both cases, photons are effectively interacting and the Bogoliubov transformation is expected to give spectral weight to the negative "ghost" branch of the Goldstone mode as well [353]. While this feature is clearly visible in the central panel, the effective interaction in the left panel is too weak to give an appreciable effect on this scale: the emitter-cavity detuning that is required for this purpose is in fact much larger than the amplification bandwidth of the emitters and therefore hardly compatible with condensation.

At generic wavevectors and frequencies, the cavity luminescence from the dispersionless branches is typically suppressed by the detuning from the cavity mode. The only exception are the crossing points with the cavity mode, where clear peaks can be observed thanks to the resonance of the upper sideband of the Mollow triplet with the cavity mode (not shown).

7.4 The Stochastic Gross-Pitaevskii equation

In the previous Sections we have developed a microscopic model of condensation from which we have obtained predictions for some most interesting observable quantities. In this final Section, we are going to discuss how our model can be reduced under suitable approximations to a simpler quantum Langevin equation for the cavity field only. In particular, we shall concentrate on the good cavity limit $\Gamma/\kappa \gg 1$, where the dynamics of the cavity field occurs on a much faster time scale as compared to the one of the emitters, which can therefore be adiabatically eliminated. Throughout this last section, we will sacrifice mathematical rigour in favor of physical intuition.

7.4.1 Adiabatic elimination

Expressing the fields in the rotating frame as:

$$\phi^\dagger = \psi^\dagger \mathrm{e}^{i\omega t}, \qquad S^+ = \mathcal{S}^+ \mathrm{e}^{i\omega t}, \qquad S^z = \mathcal{S}^z, \tag{7.69}$$

the real-space equations of motion (7.27)-(7.29) can be rewritten as

$$\frac{\partial \mathcal{S}^z}{\partial t} = \Gamma\left(n_A \frac{\mathcal{D}}{2} - \mathcal{S}^z\right) + g\left(\mathcal{S}^+\psi + \psi^\dagger \mathcal{S}^-\right) + G^z, \tag{7.70}$$

$$\frac{\partial \mathcal{S}^+}{\partial t} = -\frac{\Gamma}{2}(1 - i\delta)\,\mathcal{S}^+ - 2g\,\psi^\dagger \mathcal{S}^z + \widetilde{G}^+, \tag{7.71}$$

$$\frac{\partial \psi^\dagger}{\partial t} = -\frac{\kappa}{2}(1 + i\delta)\,\psi^\dagger - i\frac{\nabla^2}{2m}\psi^\dagger - g\mathcal{S}^+ + i\lambda\psi^\dagger\psi^\dagger\psi + \widetilde{F}^\dagger, \tag{7.72}$$

where $\widetilde{G}^+ = \mathrm{e}^{-i\omega t}G^+$ and $\widetilde{F}^\dagger = \mathrm{e}^{-i\omega t}F^\dagger$. In the spirit of [354], the limit $\sigma \to +\infty$ can be taken provided that the quantities $g\sqrt{n_A}/\Gamma$, δ, $\langle \widetilde{G}^\alpha \widetilde{G}^{\alpha'}\rangle / n_A^2\Gamma^2$ remain finite and that the average $\lambda\langle\psi^\dagger\psi\rangle$ remains negligible with respect to Γ.

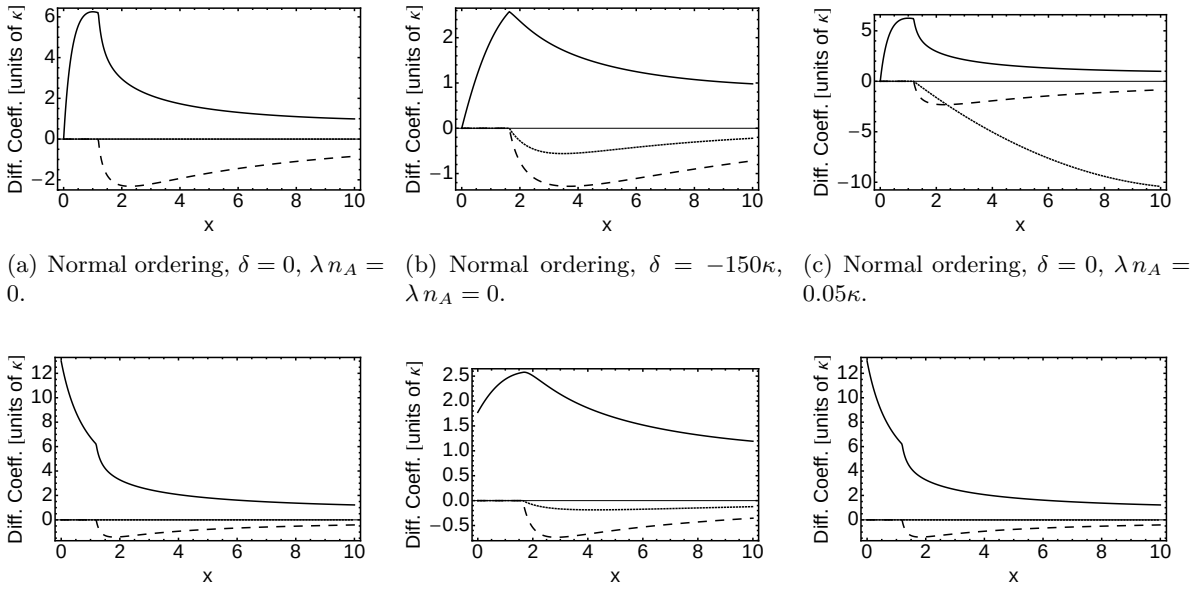

(a) Normal ordering, $\delta = 0$, $\lambda n_A = 0$.

(b) Normal ordering, $\delta = -150\kappa$, $\lambda n_A = 0$.

(c) Normal ordering, $\delta = 0$, $\lambda n_A = 0.05\kappa$.

(d) Wigner ordering, $\delta = 0$, $\lambda n_A = 0$.

(e) Wigner ordering, $\delta = -150\kappa$, $\lambda n_A = 0$.

(f) Wigner ordering, $\delta = 0$, $\lambda n_A = 0.05\kappa$.

Figure 7.1: Diffusion coefficients $D_{\phi\phi^*}$ (solid lines), $\mathrm{Re}[D_{\phi\phi}]$ (dashed lines) and $\mathrm{Im}[D_{\phi\phi}]$ (dotted lines) appearing in the SGPE for a field ψ equal to the mean-field steady state. The quantities are plotted as a function of the pumping parameter $x = d/\gamma$ for different regimes of photon-photon interactions (left to right). The top (bottom) row refers to the SGPE in the normal (Wigner) ordering case. In all panels, we have taken $\gamma = 100\kappa$ and $g\sqrt{n_A} = 25\kappa$.

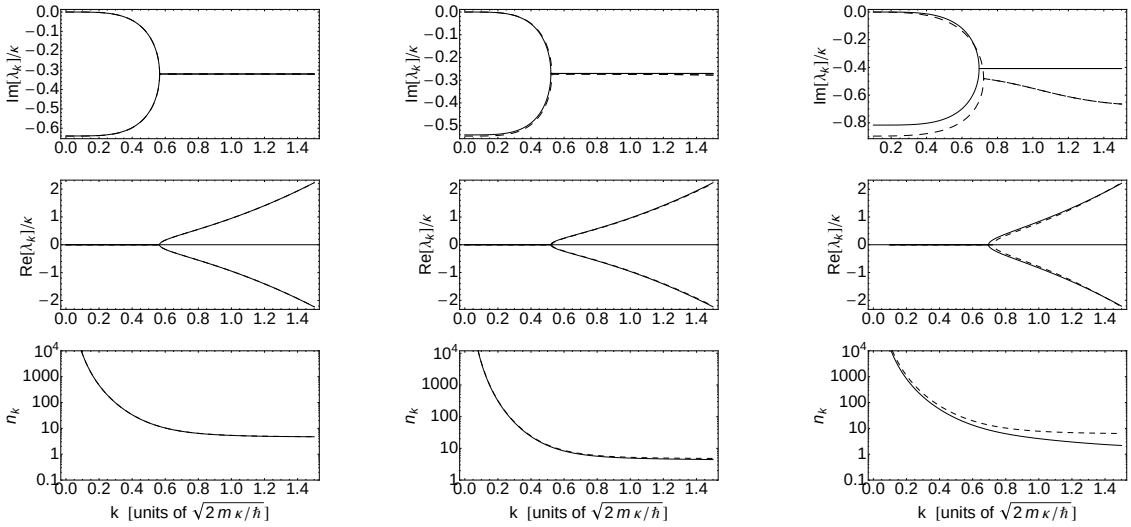

(a) $\gamma = 100\kappa$, $g\sqrt{n_A} = 25\kappa$. (b) $\gamma = 10\kappa$, $g\sqrt{n_A} = 7\kappa$. (c) $\gamma = 1\kappa$, $g\sqrt{n_A} = 2.5\kappa$.

Figure 7.2: Comparison between SGPE the full model. First row and second row: eigenvalues of the Bogoliubov matrix in functions of the momentum; solid lines refers to SGPE quantities, dashed ones to the full model. Last row: Momentum distributions. In all panels, $\lambda n_A = \nu - \omega_0 = 0$, $x = 2$.

While rigorous ways to perform adiabatic elimination for ordinary differential equations exist, the situation is more complicate for our stochastic and quantum case. In what follows we shall then follow a heuristic path inspired from laser theory [331, 355] whose validity can be checked *a posteriori* by comparing its predictions with the full model in the linearised case; a brief discussion of a simplified but illustrative example is given in the Appendix. A rigorous derivation of the whole approach is of course needed, but goes far beyond the scope of the present Chapter.

As a first step, we note that time derivatives of the spin densities can be dropped from the equations as they are negligible for large Γ. The spin operators can therefore be expressed in terms of the cavity field using the equations:

$$0 = \Gamma\left(n_A\frac{\mathcal{D}}{2} - \mathcal{S}^z\right) + g\left(\mathcal{S}^+\psi + \psi^\dagger\mathcal{S}^-\right) + G^z, \tag{7.73}$$

$$0 = -\frac{\Gamma}{2}(1 - i\delta)\,\mathcal{S}^+ - 2g\,\psi^\dagger\mathcal{S}^z + \widetilde{G}^+, \tag{7.74}$$

$$0 = -\frac{\Gamma}{2}(1 + i\delta)\,\mathcal{S}^- - 2g\,\mathcal{S}^z\psi + \widetilde{G}^-. \tag{7.75}$$

From (7.74) and (7.75), $\mathcal{S}^+$ and $\mathcal{S}^-$ can be expressed in terms of $\mathcal{S}^z$ as

$$S^+ = \frac{2}{\Gamma(1 - i\delta)}\left(-2g\psi^\dagger\mathcal{S}^z + \widetilde{G}^+\right), \tag{7.76}$$

$$S^- = \frac{2}{\Gamma(1 + i\delta)}\left(-2g\mathcal{S}^z\psi + \widetilde{G}^-\right), \tag{7.77}$$

and hence inserted in (7.73), which reads:

$$\mathcal{S}^z = n_A \frac{\mathcal{D}}{2} - \frac{8g^2}{\Gamma^2(1+\delta^2)} \psi^\dagger \mathcal{S}^z \psi + \mathbb{G}^z, \tag{7.78}$$

where

$$\mathbb{G}^z = \frac{2g}{\Gamma^2(1-i\delta)} \widetilde{G}^+ \psi + \frac{2g}{\Gamma^2(1+i\delta)} \psi^\dagger \widetilde{G}^- + \frac{1}{\Gamma} G^z. \tag{7.79}$$

While equal-time spin and cavity operators commute in the full theory, this is no longer true after the elimination, as it was noticed in [355]. An ambiguity therefore arises when writing (7.74) and (7.75). In the following, inspired by [356], we heuristically propose to choose the generalised normal ordering, $\psi^\dagger \mathcal{S}^+ \mathcal{S}^z \mathcal{S}^- \psi$. This issue is important when solving Eq. (7.78) for $\mathcal{S}^z$, which can be done by formally iterating on $\mathcal{S}^z$:

$$\begin{aligned} \mathcal{S}^z &= n_A \frac{\mathcal{D}}{2} \sum_{m=0}^{+\infty} \frac{(-1)^m}{n_s^m} \left(\psi^\dagger\right)^m \psi^m + \sum_{m=0}^{+\infty} \frac{(-1)^m}{n_s^m} \left(\psi^\dagger\right)^m \mathbb{G}^z \psi^m \\ &= n_A \frac{\mathcal{D}}{2} : \frac{1}{1+\frac{\psi^\dagger\psi}{n_s}} : + : \frac{1}{1+\frac{\psi^\dagger\psi}{n_s}} \mathbb{G}^z :, \end{aligned} \tag{7.80}$$

where columns denote normal ordering and the saturation density is defined as

$$n_s = \frac{\Gamma^2}{8g^2}(1+\delta^2). \tag{7.81}$$

The explicit expression for $\mathcal{S}^z$ can be inserted back in (7.76) to obtain the expression for $\mathcal{S}^+$ and $\mathcal{S}^-$, which can be finally substituted in (7.72) to give a quantum stochastic Gross-Pitaevskii equation

$$\frac{\partial \psi^\dagger}{\partial t} = -\frac{\kappa}{2}(1+i\delta)\psi^\dagger - i\frac{\nabla^2}{2m}\psi^\dagger + \psi^\dagger : \frac{P_0(1+i\delta)}{1+\frac{\psi^\dagger\psi}{n_s}} : + i\lambda \psi^\dagger\psi^\dagger\psi + \mathbb{F}^\dagger, \tag{7.82}$$

where the pumping coefficient has the form

$$P_0 = \frac{2g^2 n_A \mathcal{D}}{\Gamma(1+\delta^2)}, \tag{7.83}$$

and $\mathbb{F}^\dagger$ is a new effective noise operator given by

$$\mathbb{F}^\dagger = \widetilde{F}^\dagger - \frac{2g}{\Gamma(1-i\delta)} \widetilde{G}^+ + \frac{4g^2}{\Gamma(1-i\delta)} : \psi^\dagger \frac{1}{1+\frac{\psi^\dagger\psi}{n_s}} \mathbb{G}^z : . \tag{7.84}$$

The diffusion matrix of the noise $\mathbb{F}^\dagger$ depends on the field state ψ and $\psi^\dagger$ and can be written in the form

$$\begin{pmatrix} \langle \mathbb{F}^\dagger(\mathbf{x},t)\mathbb{F}(\mathbf{x}',t')\rangle & \langle \mathbb{F}^\dagger(\mathbf{x},t)\mathbb{F}^\dagger(\mathbf{x}',t')\rangle \\ \langle \mathbb{F}(\mathbf{x},t)\mathbb{F}(\mathbf{x}',t')\rangle & \langle \mathbb{F}(\mathbf{x},t)\mathbb{F}^\dagger(\mathbf{x}',t')\rangle \end{pmatrix} = \begin{pmatrix} A & C^* \\ C & B \end{pmatrix}, \tag{7.85}$$

where A, B, C are functions of ψ and $\psi^\dagger$. Note in particular the non-zero C term in the non-diagonal positions, which originates from the contribution of the emitter noise operators G^α ($\alpha = +, -, z$) to the resulting noise $\mathbb{F}$.

7.4.2 Normally-ordered c-number representation

A useful technique to obtain physical predictions from the operator-valued stochastic Gross-Pitaevskii (7.82), is to represent it in terms of an equivalent c-number equation. In doing this, we follow the procedure explained in [357]. As one typically does for phase-space representations [256], the first step is to choose an ordering prescription for the operator products according to which all quantities of the theory have to be consistently expressed.

A first choice is to assume normal ordering. In this case, the operator-valued SGPE (7.82) gets projected onto the c-number Ito SGPE

$$i\mathrm{d}\psi = \left[\omega_0 - \frac{\nabla^2}{2m} + \lambda|\psi|^2 + \frac{P_0\delta}{1+\frac{|\psi|^2}{n_s}} + i\left(\frac{P_0}{1+\frac{|\psi|^2}{n_s}} - \frac{\kappa}{2}\right)\right]\psi\,\mathrm{d}t + \mathrm{d}W. \tag{7.86}$$

A similar equation was derived in the early theory of laser [358]. The second order momenta of the noise have local spatial and temporal correlations

$$\left\langle \mathrm{d}W(\mathbf{x},t)\mathrm{d}W^*(\mathbf{x}',t)\right\rangle = 2D_{\psi\psi^*}(\mathbf{x})\,\delta^{(d)}(\mathbf{x}-\mathbf{x}')\mathrm{d}t, \tag{7.87}$$

$$\left\langle \mathrm{d}W(\mathbf{x},t)\mathrm{d}W(\mathbf{x}',t)\right\rangle = 2D_{\psi\psi}(\mathbf{x})\,\delta^{(d)}(\mathbf{x}-\mathbf{x}')\mathrm{d}t \tag{7.88}$$

and their variances $D_{\psi\psi^*}(\mathbf{x})$ and $D_{\psi\psi}(\mathbf{x})$ depend locally on the field $\psi(\mathbf{x})$. Their value can be determined by imposing that the motion equation for the second moments of the field determined by the c-number equation (7.86) must be equal to the ones obtained from the operatorial equation (7.82) in the normal ordered form. Using this prescription, we obtain:

$$\begin{cases} 2D_{\psi\psi^*} = A, \\ 2D_{\psi\psi} = C - \frac{P_0(1-i\delta)}{\left(1+\frac{|\psi|^2}{n_s}\right)^2}\frac{\psi^2}{n_s} - i\lambda\psi^2. \end{cases} \tag{7.89}$$

As expected from the U(1) symmetry of the original problem, both C and the normal ordering terms in (7.89) are all proportional to ψ^2. The dependence of the diffusion coefficients on the pumping parameter $x = d/\gamma$ are plotted in Fig. 7.1 for the mean-field steady state. Remarkably, while $D_{\psi^*\psi}$ and $\mathrm{Re}[D_{\psi\psi}]$ depend very slowly on x and are not much affected by the presence of detuning or self-interaction, the imaginary part $\mathrm{Im}[D_{\psi\psi}]$ crucially depends on these parameters. Note that the possibility of a non-vanishing $D_{\psi\psi}$ variance was overlooked in the phenomenological discussion that we published in [312] and has not been taken into account in [271, 278, 351].

Due to the saturable pumping term in the SGPE, higher-order momenta of the noise are present beyond the usual Gaussian noise. Their correlation can be extracted by considering the equation of motion for higher-order operator products. Inspired by the so-called truncated Wigner scheme [267, 327], one can expect that their contribution is actually negligible in the mean-field limit discussed in Sec.7.3.

7.4.3 Comparison with full calculation

As a check of the validity of this reformulation, in Fig.7.2 we compare the predictions of the SGPE for the dispersion of the collective Bogoliubov modes (upper and central row) and for the momentum distribution (lower row) with the predictions of the full model as derived in Sec.7.3.

The Bogoliubov dispersion is obtained by linearising the deterministic part of the SGPE equation (7.86) around the steady-state. a straightforward calculation gives a dispersion analogous to the one originally obtained in [299],

$$\omega_{\mathbf{k}}^{\pm} = -\Gamma_p \pm \sqrt{\Gamma_p^2 - E_{\mathbf{k}}^2} \tag{7.90}$$

with the damping parameter $\Gamma_p = \kappa(2P_0 - \kappa)/4P_0$ and the equilibrium Bogoliubov dispersion $E_{\mathbf{k}} = \sqrt{\epsilon_{\mathbf{k}}(\epsilon_{\mathbf{k}} + 2\lambda_{\rm eff}|\beta_0|^2)}$. In this latter, note that the effective nonlinear term

$$\lambda_{\rm eff} = \lambda - \frac{\kappa}{2}\frac{\delta}{n_s + |\beta_0|^2}, \tag{7.91}$$

contains two contribution: the former results from the direct photon-photon interaction λ, the latter describes the effective Kerr optical nonlinearity due to saturation of the emitters [337].

The momentum distribution shown in the bottom row is instead obtained by reintroducing the noise terms in the linearised equation and then making a small noise expansion: average of fluctuation operators like $n_{\mathbf{k}}^s$ are written as a linear function of the noise variances $D_{\psi^*\psi}$ and $D_{\psi\psi}$.

In the three columns of Fig.7.2, we show the result of the comparison for different system parameters: as one moves deeper in the good cavity limit (left panels), the agreement becomes very good, while significant discrepancies are expected outside this limit (right panels). As expected, the adiabatic elimination procedure for the momentum distribution is only valid at sufficiently low k when the cavity field detuning is small as compared to the atomic linewidth: breakdown of this condition is indeed visible in the bottom-right panel, where a clear qualitative deviation appears at large k. In particular, the adiabatic elimination of the emitters in the SGPE loses track of frequency dependence amplification and therefore is not able to recover the large k behaviour of the momentum distribution. Note also that the quantitative agreement visible in the figure crucially relies on the correct inclusion of the $D_{\psi\psi}$ variance.

In spite of its accurate predictions illustrated in Fig.7.2, the stochastic equation (7.86) is only meaningful at a linearised level. A closer look at the top row of Fig.7.1 shows in fact that $|D_{\psi\psi}|$ is not always lower or equal to $D_{\psi\psi^*}$, as it is expected from the Cauchy-Schwartz inequality for a generic Ito stochastic equation [350]. While at the linearised level one can forget this fact and formally solve the linear stochastic equation irrespectively on the positivity of the noise variance, this is no longer possible when one wishes to describe the nonlinear dynamics stemming from large fluctuations, e.g. in the vicinity of the critical point for condensation. This feature, often neglected in laser theory [331], is particularly visible in the interacting case for $\lambda \neq 0$ or $\delta \neq 0$. Techniques for numerically solving (generalised) stochastic differential equations with non-positive-definite noise were proposed, the best known example being the so-called Positive-P representation which however keeps suffering from other difficulties [256].

7.4.4 Symmetrically-ordered c-number representation

Another possible way-out is to make a different choice for the ordering of operators when performing the projection of the operator-valued SGPE (7.82) onto the c-number SGPE, e.g. the symmetric ordering of Wigner representation where c-number averages correspond to symmetrically ordered quantities. In this case, the variance matrix of the noise is indeed positive definite (see bottom row of

Fig.7.1), but several other difficulties appear [256, 267]. Firstly, the normal ordered saturation term in Eq. (7.82) cannot be easily symmetrised, which complicates writing of the deterministic part of the stochastic equation. Secondly, the symmetrisation of any non-linear term in (7.82) produces terms proportional to the commutator $[\psi(\mathbf{x}), \psi^\dagger(\mathbf{x})]$, which is a UV divergent quantity. Finally, any non linear term in (7.82) will generate a noise with non-vanishing third order momenta, e.g. $\langle \mathrm{d}W^2 \mathrm{d}W^* \rangle \propto \mathrm{d}t$.

The first two problems can be overcome: the saturation term can be approximated truncating the power expansion to some order, so that symmetrisation becomes viable. A finite expression for the field commutator is available if one discretises the field on a lattice, which corresponds to broadening the delta-function according to the smallest accessible length-scale of the system. The third problem poses a more challenging task, as noise with such features is extremely difficult to treat. Solutions have been proposed [359, 360] but never implemented into the simulation of large systems. Note that this is a well-known issue in the theory of phase-space representation of quantum fields, where interaction terms generate third-order derivatives in the equation for the Wigner function, spoiling its interpretation as a Fokker-Planck equation [256, 361]. As already mentioned, truncated-Wigner simulations where these terms are neglected are expected to be correct in the mean-field limit and have been used in simulations of polariton condensation in [327].

7.5 Concluding remarks

In this Chapter, we have built on top of laser theory to develop a quantum field model of non-equilibrium Bose-Einstein condensation of photons/polaritons in planar microcavity devices. The system under examination consists of a spatially extended cavity mode coupled to a continuous distribution of externally pumped two-level emitters and is described in terms of quantum Langevin equations. In our view, this is a minimal model that is able to describe non-equilibrium condensation simultaneously including at a quantum level the spatial dynamics of the cavity field, a saturation mechanism, and some frequency-dependence of the gain. We expect that such a model may become an essential tool in view of full numerical simulations of the non-equilibrium phase transition.

As a first example of application of our theory, we have worked out the main characteristics of quantum fluctuations around the condensate state. Our calculations confirm the non-equilibrium features that were anticipated by previous theories and/or observed in the experiments: in particular, the collective Bogoliubov modes include a Goldstone branch with diffusive properties, photoluminescence is visible on both upper and lower branches of the Bogoliubov spectrum, and the momentum distribution shows a large-k decrease even in the absence of any collisional thermalisation mechanism. This result provides a theoretical explanation to the experimental observation [300] that a condensate can exhibit thermal-like features in the momentum distribution even in the absence of thermalising collisions. Given the qualitatively different shape of the collective excitation dispersion, we expect that a decisive insight in the equilibrium vs. non-equilibrium nature of a condensation process can be obtained by measuring dispersions from the luminescence spectra or via pump-and-probe spectroscopy [352, 353, 362, 363].

In the good-cavity limit, we propose a reformulation of our theory in terms of a stochastic Gross-Pitaevskii equation. In addition to contributing to the justification of a widely used model of non-equilibrium statistical mechanics, this connection allows to relate the phenomenological parameters of the SGPE to a more fundamental theory. In particular, it turns out that the noise term originates

from a complex interplay between pumping and interactions and, in some cases, can even exhibit a multiplicative dependence on the field. This unexpected fact may turn out to have important consequences on the critical properties. To reliably simulate this physics in large systems, further work is needed to overcome subtle issues related to the peculiar statistics of the noise terms.

Appendix

7.A Adiabatic elimination

In this Appendix we will work out a simple example to give a more solid ground to the adiabatic elimination of Sec. 7.4. Let us consider the following simple Ito equations

$$\begin{cases} \mathrm{d}x = (-\gamma\, x - g\, y)\mathrm{d}t + \mathrm{d}W_x, \\ \mathrm{d}y = (-\Gamma\, y - g\, x)\mathrm{d}t + \mathrm{d}W_y. \end{cases} \tag{7.92}$$

Assuming to be interested in the slow function $x(t)$ in the limit of $\Gamma \gg \gamma, g$, one can formally explicit

$$y(t) = -g \int_{-\infty}^{t} \mathrm{d}t'\, \mathrm{e}^{-\Gamma(t-t')} x(t') + \int_{-\infty}^{t} \mathrm{e}^{-\Gamma(t-t')} \mathrm{d}W_y(t') \tag{7.93}$$

and substitute its expression in the equation for x, to obtain

$$\mathrm{d}x = \left[-\gamma x + g^2 \int_{-\infty}^{t} \mathrm{d}t'\, \mathrm{e}^{-\Gamma(t-t')} x(t') \right] \mathrm{d}t + \mathrm{d}\widetilde{W}_x, \tag{7.94}$$

where we considered the initial time $t_0 = -\infty$ and

$$\mathrm{d}\widetilde{W}_x = \mathrm{d}W_x - g \int_{-\infty}^{t} \mathrm{e}^{-\Gamma(t-t')} \mathrm{d}W_y(t'). \tag{7.95}$$

Eq. (7.94) is exact and notice that $\mathrm{d}\widetilde{W}_x$ now has a frequency-dependent spectrum. If $\gamma \ll \Gamma$, the kernel $\exp[-\Gamma|t|]$ has a support which is much smaller than the time-scale on which $x(t)$ varies appreciably . Therefore one can approximate it as a delta-function

$$\frac{\Gamma}{2} \mathrm{e}^{-\Gamma|t|} \simeq \delta(t), \tag{7.96}$$

and (7.94), (7.95) become

$$\begin{cases} \mathrm{d}x = -\left(\gamma - \frac{g^2}{\Gamma}\right) x\, \mathrm{d}t + \mathrm{d}\widetilde{W}_x, \\ \mathrm{d}\widetilde{W}_x = \mathrm{d}W_x - \frac{g}{\Gamma} \mathrm{d}W_y. \end{cases} \tag{7.97}$$

This equations are the same we would have obtained simply dropping the temporal derivative dy/dt in (7.92), as we did in Sec. 7.4.

Chapter 8

FDT for photonic systems

Abstract

We propose a quantitative criterion to experimentally assess the equilibrium vs. non-equilibrium nature of a specific condensation process, based on fluctuation-dissipation relations. The power of this criterion is illustrated on two models which show very different behaviors.

8.1 Fluctuation-dissipation relations

Thermodynamical equilibrium is not only a property of the *state* of a system, but also of its *dynamics*. A remarkable consequence of equilibrium which involves dynamical quantities is the so-called fluctuation-dissipation theorem (FDT) [181] which provides a relationship between the linear response of a system to an external perturbation of frequency ω and the thermal fluctuations of the same system at the same frequency ω. FDT relations hold for generic pairs of operators $\hat{A}$ and $\hat{B}$ (which will be assumed to be bosonic): by introducing the two functions

$$C_{AB}(t-t') = \frac{1}{2}\left\langle \left\{ \hat{A}(t), \hat{B}(t') \right\} \right\rangle \quad \text{and} \quad \chi''_{AB}(t-t') = \frac{1}{2}\left\langle \left[\hat{A}(t), \hat{B}(t') \right] \right\rangle, \tag{8.1}$$

where the time dependence of the operator corresponds to their Heisenberg evolution under the system Hamiltonian H and the average $\langle \dots \rangle$ is taken in a thermal equilibrium state at temperature T with density matrix $\rho \propto \exp(-H/k_B T)$. In such a state, these correlations depend only on the time difference $t - t'$ and we can define their Fourier transforms $C_{AB}(\omega)$ and $\chi''_{AB}(\omega)$. The explicit form of the FDT then reads [181]:

$$C_{AB}(\omega) = \coth\left(\frac{\omega}{2k_B T}\right) \chi''_{AB}(\omega). \tag{8.2}$$

In order to understand the physical content of this relation, note that $\chi''_{AB}(\mathbf{k}, \omega)$ on the r.h.s. of this relation is directly related to the imaginary part of the response function $\chi_{AB}(\omega)$ of the system which quantifies the energy it absorbs from the weak perturbation [364], i.e. $\chi''_{AB}(\omega) = -\mathrm{Im}[\chi_{AB}(\omega)]$. As usual, $\chi_{AB}(\omega)$ is defined as the Fourier transform of the linear response susceptibility $\chi_{AB}(t) =$

$-2i\theta(t)\,\chi''_{AB}(t)$. We also recall that an alternative, fully equivalent formulation of the FDT (8.2) is provided by the so-called Kubo-Martin-Schwinger (KMS) condition [365, 366], which in our example reads

$$S_{AB}(-\omega) = \mathrm{e}^{-\beta\omega} S_{BA}(\omega), \tag{8.3}$$

where $S_{AB}(t) = \langle \hat{A}(t)\hat{B}\rangle$ and $S_{BA}(t) = \langle \hat{B}(t)\hat{A}\rangle$.

The FDT has quite often been used in order to probe the effective thermalization of a system and to characterize the eventual departure from equilibrium [182, 183, 185]. In particular, given a pair of correlation functions, one can always define from (8.3) an effective temperature $T_{\rm eff}$ such that the functions satisfy a FDT: if the system is really at equilibrium, $T_{\rm eff}$ has a constant value independently of ω and of the specific choice of $\hat{A}$ and $\hat{B}$. On the other hand, if the system is out of equilibrium $T_{\rm eff}$ will generically develop a non-trivial dependence on ω, and its value will depend on the choice of $\hat{A}$ and $\hat{B}$.

8.2 Application to photon/polariton condensates

Applying these ideas to the photon/polariton condensates discussed in the previous Section provides a quantitative criterion to assess the equilibrium or non-equilibrium nature of the condensate: the protocol we propose consists in measuring different correlation and response functions and in checking if they satisfy the FDT. To this end, we will focus on the correlation involving the creation and the annihilation operators $\hat{b}^\dagger_{\mathbf{k}}$ and $\hat{b}_{\mathbf{k}}$, i.e., we choose $\hat{A} = \hat{b}_{\mathbf{k}}$ and $\hat{B} = \hat{b}^\dagger_{\mathbf{k}}$: accordingly, the functions S, χ'' and C introduced in the previous section will depend also on the momentum $\mathbf{k}$. With this choice, the correlation function $S_{b^\dagger b}$ can be related to the angle- and frequency-resolved photoluminescence intensity $\mathcal{S}(\mathbf{k},\omega)$ coming from the non-condensed particles via $\mathcal{S}(\mathbf{k},\omega+\omega_{BEC}) = S_{b^\dagger b}(\mathbf{k},-\omega)$, where the condensate emission frequency ω_{BEC} plays the role of the chemical potential μ in the non-equilibrium context. On the other hand, $\chi''_{bb^\dagger}(\mathbf{k},\omega)$ is related to the imaginary part of the linear response to an external monochromatic field with momentum $\mathbf{k}$ and frequency $\omega+\omega_{BEC}$. To be more specific, let us assume a two-sided cavity illuminated by an external classical field $E^{\rm inc}_{\mathbf{k}}(t)$ incident from the left. This field couples to the intra-cavity bosons through the Hamiltonian [267, 367]

$$H_{\rm pump} = i\int \frac{\mathrm{d}^d k}{(2\pi)^d}\,\left[\eta^{\rm l}_{\mathbf{k}} E^{\rm inc}_{\mathbf{k}}(t) b^\dagger_{\mathbf{k}} - \eta^{\rm l*}_{\mathbf{k}} E^{\rm inc*}_{\mathbf{k}}(t) b_{\mathbf{k}}\right], \tag{8.4}$$

where $\eta^{\rm l}_{\mathbf{k}}$ ($\eta^{\rm r}_{\mathbf{k}}$) is the transmission amplitude of the left (right) mirror of the cavity. In the steady state the intra-cavity field vanishes $\langle b_{\mathbf{k}}\rangle_{\rm eq} = 0$ and the incident classical field induces a perturbation $\langle b_{\mathbf{k}}(\omega)\rangle = i\eta^{\rm l}_{\mathbf{k}}\,\chi_{bb^\dagger}(\mathbf{k},\omega)\,E^{\rm inc}_{\mathbf{k}}(\omega)$, where $b_{\mathbf{k}}(\omega) = \int \mathrm{d}t\, b_{\mathbf{k}}(t)\mathrm{e}^{i\omega t}$. From the boundary conditions at the two mirrors, the reflected and transmitted fields can be related to the intra-cavity field [267, 367] as:

$$E^{\rm refl}_{\mathbf{k}}(\omega) = \left[1 - i|\eta^{\rm l}_{\mathbf{k}}|^2\,\chi_{bb^\dagger}(\mathbf{k},\omega)\right] E^{\rm inc}_{\mathbf{k}}(\omega), \tag{8.5}$$

$$E^{\rm tr}_{\mathbf{k}}(\omega) = -i\eta^{\rm r*}_{\mathbf{k}}\,\eta^{\rm l}_{\mathbf{k}}\,\chi_{bb^\dagger}(\mathbf{k},\omega)\,E^{\rm inc}_{\mathbf{k}}(\omega). \tag{8.6}$$

Accordingly, from a measurement of the reflected or transmitted fields it is possible to reconstruct the response function $\chi''_{bb^\dagger}(k,\omega)$ through the formula

$$\chi''_{bb^\dagger}(\mathbf{k},\omega) = \frac{1}{|\eta^{\rm l}_{\mathbf{k}}|^2}\left(1 - \mathrm{Re}\left[\frac{E^{\rm refl}_{\mathbf{k}}(\omega)}{E^{\rm inc}_{\mathbf{k}}(\omega)}\right]\right) = -\frac{1}{|\eta^{\rm l}_{\mathbf{k}}|^2}\mathrm{Re}\left[\frac{\eta^{\rm l*}_{\mathbf{k}}}{\eta^{\rm r*}_{\mathbf{k}}}\frac{E^{\rm tr}_{\mathbf{k}}(\omega)}{E^{\rm inc}_{\mathbf{k}}(\omega)}\right], \tag{8.7}$$

where both the amplitude and the phase of $E^{\rm refl}_{\mathbf{k}}$ and $E^{\rm tr}_{\mathbf{k}}$ can be measured with standard optical tools and the coefficients $\eta^{\rm l,r}_{\mathbf{k}}$ can be extracted from reflection and transmission measurements on the unloaded cavity.

At equilibrium, these quantities are related to the angle- and frequency-resolved luminescence spectrum $\mathcal{S}$ by the FDT

$$\chi''_{bb^\dagger}(\mathbf{k},\omega) = \frac{1-\mathrm{e}^{-\beta\omega}}{2}\, S_{bb^\dagger}(\mathbf{k},\omega) = \frac{e^{\beta\omega}-1}{2}\, \mathcal{S}(\omega_{BEC}+\omega,\mathbf{k})\,: \tag{8.8}$$

as both sides of this equation are experimentally measurable, any discrepancy is a detectable signature of a non-equilibrium condition.

As a further verification, the interested reader may check that this FDT is satisfied for an empty cavity which is illuminated from both sides by thermal radiation at the same temperature.

8.3 Application to some models of photon/polariton BEC

In this Section, we will illustrate the behavior of the FDT for two simple models of photon/polariton BEC. In doing this, one has to keep in mind that some of the approaches usually used for describing open quantum systems are intrinsically unable to correctly reproduce the FDT, so one must be careful not to mistake an equilibrium system for a non-equilibrium one just because of the approximations made in the theoretical model. In particular, every quantum master equation governed by a Lindblad super-operator always violates the FDT [7, 368, 369], even if the stationary solution has the form of a thermal density matrix: the reason of this pathology lies in the Markovian approximation, which is inherent in the master equations [256].

8.3.1 Quantum Langevin model

In Chapter 7 we proposed a simple model of non-equilibrium condensation based on a generalized laser model. The idea is to model the complex scattering processes responsible for condensation in terms of a spatially uniform distribution of population-inverted two-level atoms, which can emit light into the cavity mode. Once the population inversion is large enough, laser operation will occur into the cavity. The dynamics of quantum fluctuations on top of the coherent laser emission is then described by means of quantum Langevin equations for the non-condensed mode amplitudes.

In order to check the effective lack of thermalization of the system, in Fig. 8.1 we study the ω and $\mathbf{k}$ dependence of the effective inverse temperature $\beta_{\rm eff}$, as extracted from the KMS relation (8.3) using the quantum Langevin prediction for the correlation functions. The resulting $\beta_{\rm eff}(\mathbf{k},\omega)$ strongly depends on both ω and $\mathbf{k}$ and becomes even negative in some regions: all these features are a clear signature of a very non-equilibrium condition.

8.3.2 Non-Markovian toy model

The situation is much more intriguing for the model recently proposed in Refs. [334, 370] for studying the photon BEC experiments of Ref. [289]: clear signatures of a thermal distribution of the non-condensed cloud were observed as soon as the thermalization rate under the effect of repeated

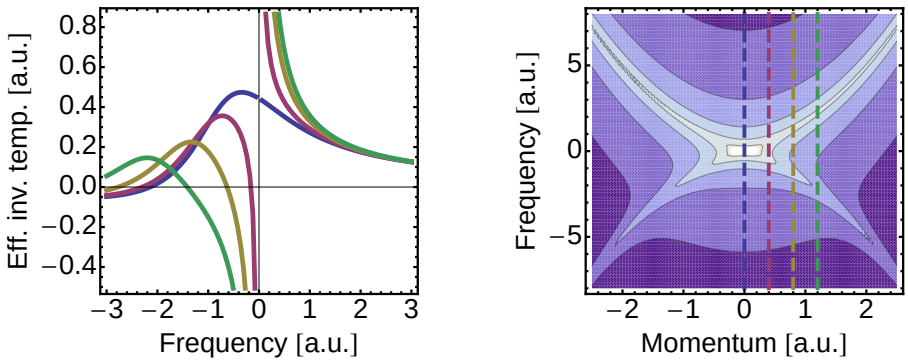

Figure 8.1: Left panel: Effective inverse temperatures vs frequency for the model of Chapter 7. The various curves correspond to different values of the in-plane momenta $\mathbf{k}$. Right panel: Angle- and frequency-resolved photoluminescence intensity $\mathcal{S}(\mathbf{k}, \omega_{BEC} + \omega)$ from Ref. [5]. The dashed vertical lines correspond to the in-plane momenta considered in the left panel.

absorption and emission cycles by the dye molecules becomes comparable to the photon loss rate. On the other hand, when thermalization is too slow, the thermal-like features disappear and the system reproduces the non-equilibrium physics of a laser.

In order to investigate how this crossover affects the FDT, we introduce a non-Markovian toy model which extends the theory of Refs. [334, 370] and avoids spurious effects due to the Markov approximation. For simplicity, we consider a single non-condensed mode of frequency ω_c described by operators $\hat{b}, \hat{b}^\dagger$. The frequency-dependent absorption and amplification by the dye molecules is modeled by two distinct baths of harmonic oscillators $\hat{a}_n, \hat{a}_n^\dagger$ and $\hat{c}_n, \hat{c}_n^\dagger$ with frequencies ω_n^- and ω_n^+, respectively:

$$H = \omega_c \hat{b}^\dagger \hat{b} + \sum_n (\omega_n^- \hat{a}_n^\dagger \hat{a}_n + \omega_n^+ \hat{c}_n^\dagger \hat{c}_n) + \sum_n \left(\eta_n^- \hat{b} \hat{a}_n^\dagger + \eta_n^+ \hat{b}^\dagger \hat{c}_n^\dagger + \text{H.c.} \right). \tag{8.9}$$

The baths take into account the two processes pictorially represented in the left panel of Fig. 8.2, in which the photon absorption and emission processes are associated with the creation/destruction of ro-vibrational phonons. An analogous absorbing bath is used to model cavity losses due to the imperfect mirrors.

According to the usual quantum-Langevin theory [256], we solve the Heisenberg equations of motions for $\hat{a}_n, \hat{a}_n^\dagger$ and $\hat{c}_n, \hat{c}_n^\dagger$ and replace the formal solution into the Heisenberg equation for $\hat{b}$, which eventually takes the simple form

$$\frac{\mathrm{d}\hat{b}}{\mathrm{d}t} = -\left(i\omega_c + \frac{\kappa}{2} \right) \hat{b} - \int_{-\infty}^{+\infty} \mathrm{d}t' \, [\Gamma^-(t-t') - \Gamma^+(t-t')] \hat{b}(t') + F, \tag{8.10}$$

where κ is the decay rate of the cavity photon, $F = F^\kappa + F^- + F^+$ is the total noise operator and the memory kernels $\Gamma^\pm$ are defined as $\Gamma^\pm(t) = \theta(t) \int_{-\infty}^{+\infty} \mathrm{d}\omega \, \rho^\pm(\omega) \mathrm{e}^{\pm i\omega t}/(2\pi)$, in terms of the absorption and emission spectral functions $\rho^\pm(\omega) = 2\pi \sum_n |\eta_n^\pm|^2 \delta(\omega - \omega_n^\pm)$.

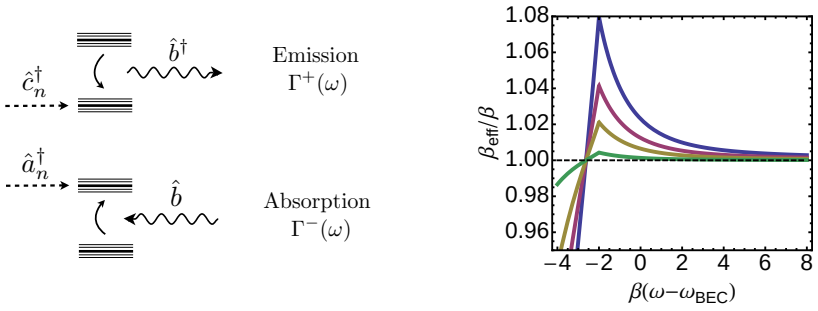

Figure 8.2: Left panel: Sketch of the energy levels under consideration. Right panel: Effective inverse temperatures $\beta_{\rm eff}$ for $\beta(\omega_{BEC}-\bar{\omega})=2$ and for different values of $\kappa/\gamma^-=0.2$ (blue), 0.1 (red), 0.05 (yellow), 0.01 (green).

Given the form of the bath-system coupling (8.9) and of the memory kernels $\Gamma^\pm(t)$, absorption (viz. amplification) of a photon at ω_c is proportional to $\rho^-(\omega)$ (viz. $\rho^+(-\omega)$). The Kennard-Stepanov (KS) relation between the absorption and emission spectra from molecules in thermal contact with an environment at inverse temperature β then translates into

$$\rho^+(-\omega)=\mathcal{C}\,\mathrm{e}^{-\beta\omega}\rho^-(\omega), \tag{8.11}$$

the constant $\mathcal{C}$ depending on the pumping conditions, e.g. on the fraction of molecules in the ground and excited electronic states. In what follows, we assume all baths to be initially in their vacuum state, so as to model irreversible absorption and emission processes. In this regime, the structure factors read:

$$S_{b^\dagger b}(-\omega)=\frac{\rho^+(-\omega)}{[\omega-\Sigma(\omega)]^2+\Gamma_T^2(\omega)},\quad S_{bb^\dagger}(\omega)=\frac{\kappa+\rho^-(\omega)}{[\omega-\Sigma(\omega)]^2+\Gamma_T^2(\omega)}, \tag{8.12}$$

where $\Sigma(\omega)=\omega_c-\mathrm{Im}[\Gamma^-(\omega)]+\mathrm{Im}[\Gamma^+(\omega)]$ takes into account the Lamb-shift induced by the baths and the total relaxation rate is $\Gamma_T(\omega)=\kappa/2+\mathrm{Re}[\Gamma^-(\omega)]-\mathrm{Re}[\Gamma^+(\omega)]>0$. For concreteness, we choose the forms

$$\rho^-(\omega) = \gamma^-\{[n(\omega-\bar{\omega})+1]\,\theta(\omega-\bar{\omega})+n(\bar{\omega}-\omega)\,\theta(\bar{\omega}-\omega)\}, \tag{8.13}$$
$$\rho^+(-\omega) = \gamma^+\{n(\omega-\bar{\omega})\,\theta(\omega-\bar{\omega})+[n(\bar{\omega}-\omega)+1]\,\theta(\bar{\omega}-\omega)\}, \tag{8.14}$$

modelling phonon-assisted absorption on a molecular line at $\bar{\omega}$, with $\gamma^\pm$ proportional to the molecular population in the ground and excited states and $n(\omega)=[\exp(\beta\omega)-1]^{-1}$. It is straightforward to check that these forms of $\rho^\pm$ indeed satisfy the KS relation (8.11) with $\mathcal{C}=e^{\beta\bar{\omega}}\gamma^+/\gamma^-$. Dynamical stability of the condensate imposes the further condition $\kappa+\rho^-(\omega_{BEC})=\rho^+(-\omega_{BEC})$, which translates into $\mathcal{C}=e^{\beta\omega_{BEC}}[1+\kappa/\rho^-(\omega_{BEC})]$.

As discussed in Sec.8.1, the frequencies appearing in the KMS condition (8.3) are measured from the chemical potential. Even with this rescaling, it is immediate to see that the structure factors do

not generally satisfy the KMS condition (8.3) signalling a non-equilibrium behavior. However, in the plots shown in the right panel of Fig. 8.2 of the KMS effective inverse temperature

$$\beta_{\rm eff}(\omega) = \frac{\log\left(\frac{\kappa+\rho^-(\omega)}{\rho^+(-\omega)}\right)}{\omega-\omega_{BEC}} = \beta + \frac{1}{\omega-\omega_{BEC}}\log\left[\frac{1+\kappa/\rho^-(\omega)}{1+\kappa/\rho^-(\omega_{BEC})}\right] \tag{8.15}$$

one easily sees that an effective equilibrium at β is recovered for $\kappa \ll \gamma^-$, where the KS relation (8.11) makes the KMS condition to be trivially fulfilled. Physically, if the repeated absorption and emission cycles by the molecules are much faster than cavity losses, the KS condition imposes a full thermal equilibrium condition in the photon gas.

8.4 Concluding remarks

We have proposed and characterized a quantitative criterion to experimentally assess the equilibrium vs. non-equilibrium nature of a condensate. This criterion has been applied to a strongly non-equilibrium model of condensation inspired by the semi-classical theory of laser and to a simple non-Markovian model of the photon BEC: provided photons undergo repeated absorption-emission cycles before being lost, the photon gas can inherit the thermal condition of the dye molecules. With respect to static properties, such as the momentum distribution, considered so far in experiments, our criterion based on fluctuation-dissipation relations imposes stringent conditions also on the dynamical properties of the gas: its experimental implementation appears feasible with state-of-the-art technology and it would give a conclusive evidence of thermal equilibrium in the gas.

Chapter 9

Thermodynamic Equilibrium as a Symmetry

Abstract

Extended quantum systems can be theoretically described in terms of the Schwinger-Keldysh functional integral formalism, whose action conveniently describes both dynamical and static properties. We show here that in thermal equilibrium, defined by the validity of fluctuation-dissipation relations, the action of a quantum system is invariant under a certain symmetry transformation and thus it is distinguished from generic systems. In turn, the fluctuation-dissipation relations can be derived as the Ward-Takahashi identities associated with this symmetry. Accordingly, the latter provides an efficient test for the onset of thermodynamic equilibrium and it makes checking the validity of fluctuation-dissipation relations unnecessary. In the classical limit, this symmetry reduces to the well-known one which characterizes equilibrium in the stochastic dynamics of classical systems coupled to thermal baths, described by Langevin equations.

9.1 Introduction

In this Chapter we consider the following operative definition of thermal equilibrium: a system is in thermal equilibrium at a certain temperature T if expectation values of arbitrary products of operators, evaluated at different times, are connected by quantum fluctuation-dissipation relations (FDRs) involving the temperature T. These FDRs were shown [371–373] to be equivalent to a combination of the quantum-mechanical time-reversal transformation [374] and the Kubo-Martin-Schwinger (KMS) condition [365, 366]. Heuristically, the latter condition expresses the fact that the Hamiltonian ruling the time evolution of a system is the same as that one determining the density matrix of the canonical ensemble which characterizes the system when it is weakly coupled to a thermal bath. In both the generalized FDRs and the KMS condition the temperature actually appears as a parameter.

From the theoretical point of view, static and dynamical properties of statistical systems (both classical and quantum) are often conveniently studied in terms of dynamical functionals, which are used

in order to generate expectation values of physical observables in the form of functional integrals over a suitable set of fields. Then, it is natural to address the issue of the possible equilibrium character of the stationary state by investigating the properties of the corresponding dynamical functional. In the case of classical statistical systems evolving under the effect of an external stochastic noise of thermal origin, this issue has been discussed to a certain level of detail in the past [118, 236, 239, 375–377] and, in fact, it was found that the dynamical functional acquires a specific symmetry in thermodynamic equilibrium. As in the case of the FDRs and the KMS condition, the (inverse) temperature $\beta = 1/T$ enters as a parameter in this symmetry transformation. Remarkably, classical FDRs can be derived as a consequence of this symmetry. For quantum systems, instead, we are not aware of any analogous derivation based on the symmetries of the corresponding dynamical functional, which takes the form of a Schwinger-Keldysh action (see, e.g., Refs. [214, 215, 378–383]).

The aim of the present Chapter is to fill in this gap by showing that also the Schwinger-Keldysh dynamical functional of a quantum system in thermal equilibrium is characterized by a specific symmetry, i.e., it is invariant under a certain transformation $\mathcal{T}_\beta$. This symmetry may be considered as the generalization of the classical one mentioned above, to which it reduces in a suitable classical limit [384]. In addition, $\mathcal{T}_\beta$ can be written as a composition of the quantum-mechanical time reversal expressed within the Schwinger-Keldysh formalism — reflecting a property of the generator of dynamics — and of the transformation which implements the KMS conditions, associated with a property of the state in question. The existence of this symmetry was already noticed in Ref. [384] for mesoscopic quantum devices, where it was used to derive fluctuation relations for particle transport across them. However, to our knowledge, the connection between this symmetry and the presence of equilibrium conditions has not yet been established.

The rest of the presentation is organized as follows: the key results of this Chapter are anticipated and summarized in Sec. 9.2; in Sec. 9.3 we specify the symmetry transformation $\mathcal{T}_\beta$, provide its various representations, and list a number of properties which are then detailed in Sec. 9.4. In particular, we discuss the invariance of unitary time evolution in Sec. 9.4.1, while in Sec. 9.4.2 we consider possible dissipative terms which are invariant under $\mathcal{T}_\beta$. We discuss how the quantum symmetry reduces in the limit $\hbar \to 0$ to the one known in classical stochastic systems in Sec. 9.4.3. As we discuss in Sec. 9.5, the symmetry can be interpreted as a practical implementation of the KMS condition on the Schwinger-Keldysh functional integral. Finally, Sec. 9.6 presents applications of the equilibrium symmetry: in Sec. 9.6.1 we derive the FDR for two-point functions while in Sec. 9.6.2 we show that the steady states of a quantum master equation explicitly violate the symmetry. The case of a system driven out of equilibrium by a coupling with two baths at different temperature and chemical potential is considered in Sec. 9.6.3; Sec. 9.6.4 briefly touches upon a number of other applications of the symmetry.

9.2 Key results

The invariance under $\mathcal{T}_\beta$ of the Schwinger-Keldysh action is a sufficient and necessary condition for a system to be in thermal equilibrium. As mentioned in Sec. 9.1, we consider a system to be in thermal equilibrium if all the FDRs are satisfied with the same temperature $T = \beta^{-1}$ or, equivalently [371–373], if the KMS condition (combined with time reversal) is satisfied. In Sec. 9.5, we show that these conditions imply the thermal symmetry $\mathcal{T}_\beta$ of the Schwinger-Keldysh action corresponding to the stationary state of the system. Conversely, the fluctuation-dissipation

relations can be derived as consequences of the symmetry, proving their equivalence.

A different perspective: thermal equilibrium as a symmetry. A key conceptual step forward we take in this Chapter is to provide a compact formulation of thermal equilibrium conditions of a quantum system — i.e., the KMS condition (or, alternatively, of the equivalent hierarchy of FDRs) — in terms of a single symmetry $\mathcal{T}_\beta$, which can be considered as the fundamental property of quantum systems in thermal equilibrium. This perspective is especially fruitful within the field-theoretical formalism, where various tools have been developed to work out the consequences of the symmetries of the action of a given system. In this context, for example, the hierarchy of generalized quantum FDRs can be derived straightforwardly as the Ward-Takahashi identities associated with the thermal symmetry (see Secs. 9.5 and 9.6.1). In addition, the Schwinger-Keldysh formalism provides a convenient framework to take advantage of very powerful and efficient renormalization-group techniques for studying the possible emergence of collective behaviors and for monitoring how the effective description of a statistical system depends on the length and time scale at which it is analyzed. The possible scale dependence of the restoration/violation of the equilibrium symmetry could shed light on the mechanism underlying the thermalization of extended systems.

As we mentioned above, the idea of viewing thermal equilibrium as a symmetry is certainly not new. However, while previous studies were primarily concerned with classical statistical physics [118, 236, 239, 375–377], here we generalize this idea to the quantum case.

Unification of the quantum and classical description of equilibrium systems. As pointed out in Ref. [384], the equilibrium symmetry reduces, in the classical limit, to a known symmetry which characterizes thermal equilibrium in open classical systems [118, 236, 239, 375–377]. In Sec. 9.4.3 we review the classical limit of the Schwinger-Keldysh action for a system coupled to a thermal bath [214, 215] and we discuss in detail how the classical equilibrium symmetry is correspondingly recovered. The comparison with the classical symmetry highlights some remarkable differences with the quantum case: in fact, in classical systems, thermal equilibrium can be regarded as a consequence of detailed balance, which, in turn, is related to the property of microreversibility of the underlying microscopic dynamics. In fact, the classical equilibrium symmetry is derived by requiring the dynamical functional to satisfy these properties [118, 239, 376]. For quantum system, instead, an analogous satisfactory definition of detailed balance and microreversibility is seemingly still missing, leaving open the important question about the very nature of thermal equilibrium of quantum systems.

Efficient check for the presence of thermodynamic equilibrium conditions. The symmetry is of great practical value, as it reduces answering the question about the possible presence of thermodynamic equilibrium to verifying a symmetry of the Schwinger-Keldysh action instead of having to check explicitly the validity of all FDRs. In particular, we show in Sec. 9.6.2 that the Markovian quantum dynamics described by a Lindblad master equation [385, 386] explicitly violates the symmetry. This reflects the driven nature of the system: indeed, the Lindblad equation may be viewed as resulting from the coarse graining of the evolution of an underlying time-dependent system-bath Hamiltonian, with a time dependence dictated by coherent external driving fields.

Moreover, in Sec. 9.6.3 we consider a bosonic mode coupled to two baths at different temperatures and chemical potentials: in this case, the resulting net fluxes of energy or particles drive the system

out of equilibrium with a consequent violation of the symmetry.

A new perspective on the construction of the Schwinger-Keldysh action. At the conceptual level, the existence of the symmetry provides a new perspective on the construction of Schwinger-Keldysh functional integrals. In particular, as customary in quantum field theories, one may consider the symmetry as the fundamental principle: indeed, it is explicitly present for any time-independent (time-translation invariant) Hamiltonian which generates the dynamics of a system at the microscopic scale. Then, requiring the symmetry to hold for the full effective Keldysh action at a different scale fixes the admissible dissipative terms so as to satisfy FDRs between response and correlation functions of arbitrary order; translating back into the operator language, this provides a concrete hint why stationary density matrices of the form $\rho \sim e^{-\beta H}$ are favored over arbitrary functions $\rho(H)$ for the description of static correlation functions.

9.3 Symmetry transformation

As we anticipated above, a convenient framework for the theoretical description of the time evolution of interacting quantum many-body systems is provided by the Schwinger-Keldysh functional integral formalism [214, 215]. In fact, it offers full flexibility in describing both non-equilibrium dynamics and equilibrium as well as non-equilibrium stationary states, which is out of reach of the finite-temperature Matsubara technique [387]. In addition, it is amenable to the well-established toolbox of quantum field theory. The simplest way to illustrate the basic ingredients of the Schwinger-Keldysh formalism is to consider the functional integral representation of the so-called Schwinger-Keldysh partition function Z. For a system with unitary dynamics generated by the Hamiltonian H and initialized in a state described by a density matrix ρ_0, this function is given by $Z = \mathrm{tr}\left(e^{-iHt}\rho_0 e^{iHt}\right)$. (Note that, as it stands, $Z = 1$; however, it is convenient to focus on its structure independently of its actual value.) In this expression, time evolution is interpreted as occurring along a closed path: starting in the state described by ρ_0, the exponential e^{-iHt} to the left of ρ_0 corresponds to a "forward" evolution up to the time t, while the exponential e^{iHt} to its right corresponds to an evolution going "backward" in time. The trace $\mathrm{tr}\,(\cdots)$ connects, at time t, the forward with the backward branch of the time path and therefore it produces a closed-time-path integral. Along each of these two branches, the temporal evolution can be represented in a standard way as a functional integral of an exponential weight e^{iS} over suitably introduced (generally complex) integration variables, i.e., fields, $\psi_+(t, \mathbf{x})$ and $\psi_-(t, \mathbf{x})$ on the forward and backward branches, respectively. These fields are associated with the two sets of coherent states suitably introduced as resolutions of the identity in-between two consecutive infinitesimal time evolutions in the Trotter decomposition of the unitary temporal evolution along the two branches [214, 215]. The resulting Schwinger-Keldysh action S is a functional of $\psi_\pm(t, \mathbf{x})$ and it is generally obtained as a temporal integral along the close path in time of a Lagrangian density. (Explicit forms of S will be discussed further below, but they are not relevant for the present discussion.) By introducing different (time-dependent) sources $J_\pm$ for the fields $\psi_\pm$ on the two branches, the partition function $Z[J_+, J_-]$ is no longer identically equal to 1 and its functional derivatives can be used in order to generate various time-dependent correlation functions (see, e.g., Refs. [214, 215, 383]).

As we show further below in Sec. 9.4, a system is in thermodynamic equilibrium at a temperature

$T = 1/\beta$, if the corresponding Schwinger-Keldysh action is invariant under a certain transformation $\mathcal{T}_\beta$ which acts on the fields along the closed time path. In order to specify the form of $\mathcal{T}_\beta$, we focus on the dynamics of a single complex bosonic field which is sufficiently simple but general enough to illustrate conveniently all the basic ideas. In this case, the transformation $\mathcal{T}_\beta$ turns out to be composed of a complex conjugation [1] of the field components ψ_σ with $\sigma = \pm$, an inversion of the sign of the time variable, and a translation of the time variable into the complex plane by an amount $i\sigma\beta/2$, i.e.,

$$\begin{aligned} \mathcal{T}_\beta \psi_\sigma(t, \mathbf{x}) &= \psi^*_\sigma(-t + i\sigma\beta/2, \mathbf{x}), \\ \mathcal{T}_\beta \psi^*_\sigma(t, \mathbf{x}) &= \psi_\sigma(-t + i\sigma\beta/2, \mathbf{x}). \end{aligned} \tag{9.1}$$

For convenience and future reference we provide an alternative compact representation of the action of $\mathcal{T}_\beta$ both in the time and real space domain $(t, \mathbf{x})$ as well as in the frequency-momentum domain $(\omega, \mathbf{q})$. The convention for the Fourier transforms of the fields, conveniently collected into two spinors $\Psi_\sigma(t, \mathbf{x}) = (\psi_\sigma(t, \mathbf{x}), \psi^*_\sigma(t, \mathbf{x}))^T$, is the following:

$$\Psi_\sigma(t, \mathbf{x}) = \int \frac{\mathrm{d}^d \mathbf{q}}{(2\pi)^d} \int_{-\infty}^{+\infty} \frac{\mathrm{d}\omega}{2\pi}\, e^{i(\mathbf{q}\cdot\mathbf{x} - \omega t)} \Psi_\sigma(\omega, \mathbf{q}). \tag{9.2}$$

In this relation, d is the spatial dimensionality of the system, and the field spinors in the frequency-momentum domain are defined as $\Psi_\sigma(\omega, \mathbf{q}) = (\psi_\sigma(\omega, \mathbf{q}), \psi^*_\sigma(-\omega, -\mathbf{q}))^T$. Accordingly, we can write the symmetry transformation $\mathcal{T}_\beta$ in the form

$$\begin{aligned} \mathcal{T}_\beta \Psi_\sigma(t, \mathbf{x}) &= \Psi^*_\sigma(-t + i\sigma\beta/2, \mathbf{x}) = \sigma_x \Psi_\sigma(-t + i\sigma\beta/2, \mathbf{x}), \\ \mathcal{T}_\beta \Psi_\sigma(\omega, \mathbf{q}) &= e^{-\sigma\beta\omega/2} \Psi^*_\sigma(\omega, -\mathbf{q}) = e^{-\sigma\beta\omega/2} \sigma_x \Psi_\sigma(-\omega, \mathbf{q}), \end{aligned} \tag{9.3}$$

where we introduced the Pauli matrix $\sigma_x = \left(\begin{smallmatrix} 0 & 1 \\ 1 & 0 \end{smallmatrix}\right)$. The transformation in real time requires evaluating the fields for complex values of the time argument, which in principle is not defined; however, the complementary representation in Fourier space indicates how this can be done in practice. In fact, in frequency space, the shift of time by an imaginary part $i\sigma\beta/2$ amounts to a multiplication by a prefactor $e^{-\sigma\beta\omega/2}$.

As usual within the Schwinger-Keldysh formalism, it is convenient to introduce what are known as *classical* and *quantum* fields. These are defined as the symmetric and antisymmetric combinations, respectively, of fields on the forward and backward branches:

$$\phi_c = \frac{1}{\sqrt{2}} (\psi_+ + \psi_-), \quad \phi_q = \frac{1}{\sqrt{2}} (\psi_+ - \psi_-). \tag{9.4}$$

Combining these fields into spinors $\Phi_\nu(\omega, \mathbf{q}) = (\phi_\nu(\omega, \mathbf{q}), \phi^*_\nu(-\omega, -\mathbf{q}))^T$ — where the index $\nu = c, q$ distinguishes classical and quantum fields — the transformation $\mathcal{T}_\beta$ takes the following form, which we report here for future reference:

$$\begin{aligned} \mathcal{T}_\beta \Phi_c(\omega, \mathbf{q}) &= \sigma_x \left(\cosh(\beta\omega/2) \Phi_c(-\omega, \mathbf{q}) - \sinh(\beta\omega/2) \Phi_q(-\omega, \mathbf{q})\right), \\ \mathcal{T}_\beta \Phi_q(\omega, \mathbf{q}) &= \sigma_x \left(-\sinh(\beta\omega/2) \Phi_c(-\omega, \mathbf{q}) + \cosh(\beta\omega/2) \Phi_q(-\omega, \mathbf{q})\right). \end{aligned} \tag{9.5}$$

[1] In Ref. [384], the symmetry is stated in terms of the real phase variables of complex fields. Then, the complex conjugation in Eq. (9.1) should be replaced by a change of sign.

We anticipate and summarize here a number of properties of the equilibrium transformation $\mathcal{T}_\beta$ which are going to be discussed in detail in Secs. 9.4 and 9.5:

1. The transformation is linear, discrete and involutive, i.e., $\mathcal{T}_\beta^2 = \mathbb{1}$. The last property follows straightforwardly from Eqs. (9.1) or (9.3). Concerning linearity, note in particular that the complex conjugation in Eq. (9.1) affects only the field variables, i.e., $\mathcal{T}_\beta \lambda \psi_\sigma(t, \mathbf{x}) = \lambda \psi_\sigma^*(-t + i\sigma\beta/2, \mathbf{x})$ for $\lambda \in \mathbb{C}$ (see Sec. 9.5.2).

2. $\mathcal{T}_\beta$ can be written as a a composition $\mathcal{T}_\beta = \mathsf{T} \circ \mathcal{K}_\beta$ of a time-reversal transformation T and an additional transformation $\mathcal{K}_\beta$, which we will identify in Sec. 9.5.3 as the implementation of the KMS condition within the Schwinger-Keldysh functional integral formalism.

3. $\mathcal{T}_\beta$ is not uniquely defined, due to a certain freedom in implementing the time-reversal transformation within the Schwinger-Keldysh functional integral formalism, as discussed in Sec. 9.5.2. However, without loss of generality, we stick to the definition provided by Eq. (9.1) and we comment on the alternative forms in Sec. 9.5.2.

4. The transformation $\mathcal{T}_\beta$ leaves the functional measure invariant, i.e., the absolute value of the Jacobian determinant associated with $\mathcal{T}_\beta$ is equal to one, as discussed in Sec. 9.5.4 and shown in App. 9.D.

5. The various forms of the transformation $\mathcal{T}_\beta$ presented above apply to the case of a system of bosons with vanishing chemical potential μ. In the presence of $\mu \neq 0$, Eq. (9.1) becomes

$$\begin{aligned} \mathcal{T}_{\beta,\mu} \psi_\sigma(t, \mathbf{x}) &= e^{\sigma\beta\mu/2} \psi_\sigma^*(-t + i\sigma\beta/2, \mathbf{x}), \\ \mathcal{T}_{\beta,\mu} \psi_\sigma^*(t, \mathbf{x}) &= e^{-\sigma\beta\mu/2} \psi_\sigma(-t + i\sigma\beta/2, \mathbf{x}), \end{aligned} \tag{9.6}$$

   with a consequent modification of Eq. (9.3), which can be easily worked out. After a transformation to the basis of classical and quantum fields according to Eq. (9.4), this modification amounts to shifting the frequency ω in the arguments of the hyperbolic functions in Eq. (9.5), i.e., to $\omega \to \omega - \mu$.

6. In taking the Fourier transforms in Eqs. (9.3) and (9.5) one implicitly assumes that the initial state of the system was prepared at time $t = -\infty$, while its evolution extends to $t = \infty$. In the following we will work under this assumption, commenting briefly on the role of an initial condition imposed at a finite time in Sec. 9.4.3.

9.4 Invariance of the Schwinger-Keldysh action

As we demonstrate further below, a system is in thermodynamic equilibrium if its Schwinger-Keldysh action S is invariant under the transformation $\mathcal{T}_\beta$, i.e.,

$$S[\Psi] = \tilde{S}[\mathcal{T}_\beta \Psi], \tag{9.7}$$

where, for convenience of notation, $\Psi = \left(\psi_+, \psi_+^*, \psi_-, \psi_-^*\right)^T$ collects all the fields introduced in the previous section into a single vector. The tilde in $\tilde{S}$ indicates that all the parameters in S which

are related to external fields have to be replaced by their corresponding time-reversed values (e.g., the signs of magnetic fields have to be inverted), while in the absence of these fields the tilde may be dropped. According to the construction of the Schwinger-Keldysh functional integral outlined at the beginning of the previous section, the action corresponding to the unitary dynamics of a closed system is completely determined by its Hamiltonian H. The initial state ρ_0 of the dynamics enters the functional integral as a boundary condition: if the system was prepared in the state ρ_0 at the time $t = 0$, the matrix element $\langle\psi_{+,0}|\rho_0|\psi_{-,0}\rangle$, where $|\psi_{\pm,0}\rangle$ are coherent states, determines the (complex) weight of field configurations at the initial time with $\psi_\pm(0,\mathbf{x}) = \psi_{\pm,0}(\mathbf{x})$. In Sec. 9.4.1, we demonstrate the invariance of the Schwinger-Keldysh action associated with a time-independent Hamiltonian dynamics under the transformation $\mathcal{T}_\beta$. In particular, this invariance holds for *for any value of* β. Interestingly enough, the Schwinger-Keldysh action associated with a Hamiltonian of a simple non-interacting system — which can be diagonalized in terms of single-particle states — turns out to be invariant under an enhanced version of this transformation, involving possibly different values of β for each of the single-particle states (see Sec. 9.4.1). A constraint on the value of β, however, comes from the inclusion of the boundary condition for the functional integral which specifies the initial state ρ_0. Here we are interested in the stationary state of the system, which is generically reached a long time after its preparation in the state ρ_0. Hence, we assume that this was done in the distant past, i.e., at $t = -\infty$, and that the evolution of the system extends to $t = +\infty$ (cf. point 6 in Sec. 9.3). In the construction of the Schwinger-Keldysh functional integral for a system in thermodynamic equilibrium [214,215], a convenient alternative approach for specifying the appropriate boundary conditions corresponding to the initial equilibrium state ρ_0 of the system, consists in adding infinitesimal dissipative contributions to the action. Usually [214,215], the form of these contributions is determined by the requirement that the Green's functions of the system are thermal with a specific temperature $T = 1/\beta$, i.e., that they obey a fluctuation-dissipation relation; once these terms are included, any reference to ρ_0 may be omitted. We demonstrate in Sec. 9.4.2, that these dissipative contributions are invariant under $\mathcal{T}_\beta$ with exactly the same β. Hence, the thermal symmetry provides a different perspective on the construction of the Schwinger-Keldysh functional integral for a system in thermal equilibrium: while the unitary contributions are fixed by the Hamiltonian of the system, the requirement of invariance under the symmetry transformation $\mathcal{T}_\beta$ can be taken as the fundamental principle for specifying the structure of the dissipative terms which can occur in the action if the system is in thermodynamic equilibrium at temperature $T = 1/\beta$. We emphasize that only the simultaneous presence in the Schwinger-Keldysh action of both the Hamiltonian and the dissipative contributions yields a well-defined functional integral: the dissipative terms in the microscopic action are taken to be infinitesimally small as for an isolated system, where they merely act as a regularization which renders the functional integral finite and ensures that the bare response and correlation functions satisfy a FDR; on the other hand, if the isolated system is composed of a small subsystem of interest and a remainder which can be considered as a bath, then finite dissipative contributions emerge in the Schwinger-Keldysh action of the subsystem after the bath has been integrated out. This scenario is considered in Secs. 9.4.3 and 9.6.2. Moreover, the system can act as its own bath: in fact, one expects the effective action for the low-frequency and long-wavelength dynamics of the system to contain dissipative contributions which are due to the coupling to high-frequency fluctuations. In Sec. 9.4.2 we explicitly construct dissipative terms which comply with the thermal symmetry $\mathcal{T}_\beta$. In particular, we find that the noise components associated with these dissipative terms must necessarily have the

form of the equilibrium Bose-Einstein distribution function, as appropriate for the bosonic fields which we are presently focussing on.

9.4.1 Invariance of Hamiltonian dynamics

The Schwinger-Keldysh action S associated with the dynamics generated by a time-independent Hamiltonian H can be written as the sum of a "dynamical" and a "Hamiltonian" part, $S_{\rm dyn}$ and $S_{\mathcal{H}}$, respectively,

$$S = S_{\rm dyn} + S_{\mathcal{H}}, \tag{9.8}$$

$$S_{\rm dyn} = \frac{1}{2}\int_{t,\mathbf{x}} \left(\Psi_+^\dagger i\sigma_z \partial_t \Psi_+ - \Psi_-^\dagger i\sigma_z \partial_t \Psi_- \right), \tag{9.9}$$

$$S_{\mathcal{H}} = -\int_t \left(\mathcal{H}_+ - \mathcal{H}_- \right), \tag{9.10}$$

where we used the shorthand $\int_t \equiv \int_{-\infty}^{\infty} \mathrm{d}t$, $\int_{\mathbf{x}} \equiv \int \mathrm{d}^d\mathbf{x}$, while $\sigma_z = \left(\begin{smallmatrix} 1 & 0 \\ 0 & -1 \end{smallmatrix}\right)$ is the Pauli matrix. This structure of the Schwinger-Keldysh action results from the construction of the functional integral outlined at the beginning of Sec. 9.3. In particular, the Hamiltonians $\mathcal{H}_\pm$ are matrix elements of the Hamiltonian operator H in the basis of coherent states $|\psi_\pm\rangle$, i.e., $\mathcal{H}_\sigma = \langle\psi_\sigma|H|\psi_\sigma\rangle / \langle\psi_\sigma|\psi_\sigma\rangle$, where the amplitudes $\psi_\pm$ of the coherent states are just the integration variables in the functional integral [214, 215]. Henceforth we focus on the case of a bosonic many-body system with contact interaction, i.e., with Hamiltonians in Eq. (9.10) given by

$$\mathcal{H}_\sigma = \int_{\mathbf{x}} \left(\frac{1}{2m} |\nabla\psi_\sigma|^2 + \tau |\psi_\sigma|^2 + \lambda |\psi_\sigma|^4 \right). \tag{9.11}$$

Here m is the mass of bosons, τ the chemical potential, and λ parametrizes the strength of the s-wave two-body interaction. We consider this case because it is sufficiently general for the purpose of illustrating all basic concepts associated with the thermal symmetry and, in addition, in the classical limit it allows a direct comparison with classical stochastic models [232, 388], where $\phi_c = (\psi_+ + \psi_-)/\sqrt{2}$ plays the role of a bosonic order parameter field. This point is elaborated in Sec. 9.4.3.

Below we show that the invariance of the Schwinger-Keldysh action S under $\mathcal{T}_\beta$ is intimately related to the structure of the action, i.e., to the fact that it can be written as the sum of two terms containing, separately, only fields on the forward and backward branches.

Dynamical term

To begin with, we show that the dynamical contribution $S_{\rm dyn}$ to the Schwinger-Keldysh action S given in Eq. (9.9), is invariant under $\mathcal{T}_\beta$, i.e., that $S_{\rm dyn}[\mathcal{T}_\beta\Phi] = S_{\rm dyn}[\Phi]$. To this end, it is convenient to express the original fields $\{\psi_\pm, \psi_\pm^*\}$ in the so-called Keldysh basis, which is formed by the classical and quantum components $\{\phi_{c,q}, \phi_{c,q}^*\}$ introduced in Eq. (9.4). For the sake of brevity, we arrange these fields into the multiplet $\Phi = \left(\phi_c, \phi_c^*, \phi_q, \phi_q^*\right)^T$. Rewriting $S_{\rm dyn}$ in these terms and in the frequency-

momentum space, we obtain ($\int_{\omega,\mathbf{q}} \equiv \int \mathrm{d}\omega\, \mathrm{d}^d\mathbf{q}/(2\pi)^{d+1}$)

$$S_{\mathrm{dyn}}[\mathcal{T}_\beta\Phi] = \int_{\omega,\mathbf{q}} \omega \Big[\cosh^2(\beta\omega/2)\Phi_q^\dagger(\omega,\mathbf{q})\sigma_z\Phi_c(\omega,\mathbf{q}) - \sinh^2(\beta\omega/2)\Phi_c^\dagger(\omega,\mathbf{q})\sigma_z\Phi_q(\omega,\mathbf{q}) + \sinh(\beta\omega/2)\cosh(\beta\omega/2) \times \Big(\Phi_c^\dagger(\omega,\mathbf{q})\sigma_z\Phi_c^\dagger(\omega,\mathbf{q}) - \Phi_q^\dagger(\omega,\mathbf{q})\Phi_q(\omega,\mathbf{q})\Big)\Big]. \quad (9.12)$$

The combination $\Phi_\nu^\dagger(\omega,\mathbf{q})\sigma_z\Phi_\nu(\omega,\mathbf{q}) = \phi_\nu^*(\omega,\mathbf{q})\phi_\nu(\omega,\mathbf{q}) - \phi_\nu(-\omega,-\mathbf{q})\phi_\nu^*(-\omega,-\mathbf{q})$ with $\nu = c,q$ is an odd function of $(\omega,\mathbf{q})$, whereas $\omega\cosh(\beta\omega/2)\sinh(\beta\omega/2)$ is even, and therefore the integral over the product of these terms vanishes. Then, with some simple algebraic manipulation, the first line in Eq. (9.12) is recognised to be nothing but $S_{\mathrm{dyn}}[\Phi]$, from which the invariance of S_{dyn} follows straightforwardly. Note that this property holds independently of the value of the parameter β in the transformation $\mathcal{T}_\beta$.

Hamiltonian contribution

We consider now the transformation of the Hamiltonian contribution $S_\mathcal{H}$ in Eq. (9.10) under $\mathcal{T}_\beta$. First, we argue that the strictly local terms (i.e., those which do not involve spatial derivatives) in the Hamiltonian (9.11) are invariant under $\mathcal{T}_\beta$; then, we extend the argument to the case of quasilocal terms such as the kinetic energy contribution $\propto |\nabla\psi_\pm|^2$ or non-local interactions. Consider a contribution to $S_\mathcal{H}$ of the form

$$\mathcal{V}[\Psi] = \int_{t,\mathbf{x}} \left(v_+(t,\mathbf{x}) - v_-(t,\mathbf{x})\right), \quad (9.13)$$

where $v_\sigma(t,\mathbf{x}) = (\psi_\sigma^*(t,\mathbf{x})\psi_\sigma(t,\mathbf{x}))^N$ is a generic local contribution to the Hamiltonian $\mathcal{H}_\sigma$ and N is an integer. In particular, for $N=1$ we obtain the term proportional to the chemical potential in Eq. (9.11), while for $N=2$, $\mathcal{V}[\Psi]$ is just the contact interaction. Since $v_\sigma(t,\mathbf{x})$ is real, under the transformation $\mathcal{T}_\beta$ [see Eq. (9.6)] only its time argument is shifted according to $\mathcal{T}_\beta v_\sigma(t,\mathbf{x}) = v_\sigma(-t+i\sigma\beta/2,\mathbf{x})$ and, taking the Fourier transform with respect to time of this relation, one eventually finds

$$\mathcal{T}_\beta v_\sigma(\omega,\mathbf{x}) = e^{-\sigma\beta\omega/2} v_\sigma(-\omega,\mathbf{x}). \quad (9.14)$$

Accordingly, the vertex (9.13) is invariant under $\mathcal{T}_\beta$: in fact, being local in time, its diagrammatic representation — where the fields $\psi_\sigma(t,\mathbf{x})$ and $\psi_\sigma^*(t,\mathbf{x})$ are represented by ingoing and outgoing lines, respectively — satisfies frequency conservation for in- and outgoing lines, as can be seen by taking the Fourier transform of each of the fields in $v_\sigma(t,\mathbf{x})$ individually. In particular, the frequency ω in Eq. (9.14) corresponds to the difference between the sums of the in- and outgoing frequencies and only the $\omega = 0$ component contributes to Eq. (9.13). (Here we assume that the time integrals in Eqs. (9.9), (9.10), and therefore (9.14) extend over all possible real values, i.e., we focus on the stationary state of the dynamics.) This component, however, is invariant under $\mathcal{T}_\beta$ as follows directly from Eq. (9.14), and hence the same is true for the vertex, for which $\mathcal{V}[\mathcal{T}_\beta\Psi] = \mathcal{V}[\Psi]$.

Clearly, the invariance of the vertex and of the dynamical term in Eq. (9.9) relies on the fact that vertices, which are local in time, obey frequency conservation. (Note that, as before, this invariance holds independently of the value of the parameter β in $\mathcal{T}_\beta$.) Accordingly, one concludes that any contribution to the Hamiltonian, which is local in time and does not explicitly depend on time, is

invariant. In particular, the proof of invariance presented here for the vertex in Eq. (9.13) can be straightforwardly extended to expressions containing spatial derivatives such as the kinetic energy $\propto |\nabla\psi_\pm|^2$ in Eq. (9.11) and even to interactions which are not local in space, as long as they are local in time, as anticipated above. Note, however, that these considerations do not rule out the possible emergence upon renormalization or coarse-graining of terms which are non-local in time, as long as they are invariant under $\mathcal{T}_\beta$. This case is actually discussed further below in Sec. 9.4.2.

Enhanced symmetry for non-interacting systems

The equilibrium transformation $\mathcal{T}_\beta$ presented in Sec. 9.3 involves a single parameter β. While this form is appropriate for the Gibbs ensemble describing the thermal equilibrium state of the interacting many-body system with the Hamiltonian in Eq. (9.11), an enhanced version of the symmetry is realized in non-interacting systems. Since these systems can be diagonalized in terms of single-particle states, they are trivially integrable. Statistically, integrable systems are described by a generalized Gibbs ensemble [31,61,62,68,95,96,109,389,390], constructed from the extensive number of conserved quantities (with possible exceptions, see, e.g., Refs. [95, 96, 389, 390]). In the case of non-interacting systems which we consider here (or, more generally, for any system that can be mapped to a non-interacting one), these integrals of motion are just the occupation numbers of single-particle states. Below we provide an example, in which the Lagrange multipliers associated with these conserved occupations enter as parameters in a generalization of the equilibrium transformation Eq. (9.3): more specifically, these multipliers play the role of effective inverse temperatures of the individual single-particle states. On the other hand, in non-integrable cases, the eigenstates of the Hamiltonian are not single-particle states. Then one generically expects the stationary state of the system to be in thermal equilibrium at a temperature $T = 1/\beta$, which is determined by the initial conditions of the dynamics of the system. Accordingly, the enhanced symmetry that is present in the stationary state of the non-interacting integrable system breaks down and the corresponding Schwinger-Keldysh action is invariant under a single $\mathcal{T}_\beta$, only for that specific value of β. This shows that the transformation $\mathcal{T}_\beta$ can be generalized in order to account for the appearance of a generalized Gibbs ensemble in the trivial case of a system that can be diagonalized in terms of single-particle states. However, the question whether the generalized Gibbs ensemble emerging in the stationary states of generic integrable systems is characterized by a symmetry involving the Lagrangian multipliers associated with the respective integrals of motion as parameters, is beyond the scope of the present Chapter.

As an example, let us consider bosons on a d-dimensional lattice with nearest-neighbour hopping and on-site interaction (i.e., the Bose-Hubbard model [391]), with Hamiltonian

$$\begin{aligned} H &= H_{\rm kin} + H_{\rm int}, \\ H_{\rm kin} &= -t \sum_{\langle \mathbf{l},\mathbf{l}'\rangle} a^\dagger_{\mathbf{l}} a_{\mathbf{l}'}, \\ H_{\rm int} &= \frac{U}{2} \sum_{\mathbf{l}} a^\dagger_{\mathbf{l}} a_{\mathbf{l}} \left(a^\dagger_{\mathbf{l}} a_{\mathbf{l}} - 1 \right), \end{aligned} \tag{9.15}$$

where $a_{\mathbf{l}}$ is the annihilation operator for bosons on the lattice site $\mathbf{l}$, t is the hopping matrix element between site $\mathbf{l}$ and its nearest-neighbours $\mathbf{l}'$, while U determines the strength of on-site interactions.

We first consider the case $U = 0$, which is trivially integrable: the kinetic energy contribution to the Hamiltonian is diagonal in momentum space and the corresponding single-particle eigenstates are the Bloch states. These are labelled by a quasi-momentum $\mathbf{q}$, and in terms of creation and annihilation operators for particles in Bloch states, $a^\dagger_{\mathbf{q}}$ and $a_{\mathbf{q}}$ respectively, the kinetic energy can be written as

$$H_{\text{kin}} = \sum_{\mathbf{q}} \epsilon_{\mathbf{q}} a^\dagger_{\mathbf{q}} a_{\mathbf{q}}. \tag{9.16}$$

Let us now consider a Schwinger-Keldysh functional integral description of the stationary state of the system. Then, the kinetic energy in Eq. (9.16) yields a contribution to the corresponding action which reads

$$S_{\mathcal{H},\text{kin}} = -\int_t \sum_{\mathbf{q}} \epsilon_{\mathbf{q}} \left(\psi^*_{\mathbf{q},+} \psi_{\mathbf{q},+} - \psi^*_{\mathbf{q},-} \psi_{\mathbf{q},-} \right), \tag{9.17}$$

where $\psi_{\mathbf{q},+}$ and $\psi_{\mathbf{q},-}$ are the fields on the forward and backward branches of the closed time path respectively, expressed in the basis of Bloch states. $S_{\mathcal{H},\text{kin}}$ is invariant under the transformation of the fields

$$\mathcal{T}_{\beta_{\mathbf{q}}} \Psi_{\mathbf{q},\sigma}(\omega) = e^{-\sigma \beta_{\mathbf{q}} \omega/2} \Psi^*_{-\mathbf{q},\sigma}(\omega), \tag{9.18}$$

where, as in Eq. (9.3), we arrange the fields in a spinor $\Psi_{\mathbf{q},\sigma}(\omega) = \left(\psi_{\mathbf{q},\sigma}(\omega), \psi^*_{-\mathbf{q},\sigma}(-\omega)\right)^T$. The crucial point is that $\beta_{\mathbf{q}}$ can be chosen to depend on the quantum quasi-momentum $\mathbf{q}$, indicating that to each eigenstate of the system we can assign an individual "temperature" $T_{\mathbf{q}} = 1/\beta_{\mathbf{q}}$ such that the corresponding mean occupation number $n_{\mathbf{q}} = \langle a^\dagger_{\mathbf{q}} a_{\mathbf{q}} \rangle$ is determined by a Bose distribution with precisely this "temperature."

Let us now consider the opposite limit $t = 0$, in which the hopping amplitude t vanishes while the interaction strength U is finite. The interaction energy H_{int} in Eq. (9.15) is diagonal in the basis of Wannier states localized at specific lattice sites and the occupation numbers $\hat{n}_{\mathbf{l}} = a^\dagger_{\mathbf{l}} a_{\mathbf{l}}$ of these sites are conserved, rendering the system integrable. The generalized symmetry transformation appropriate for this case can be obtained from Eq. (9.18) by replacing the quasi-momentum $\mathbf{q}$ by the lattice site index $\mathbf{l}$ and by introducing a set of "local (inverse) temperatures" $T_{\mathbf{l}}$ ($\beta_{\mathbf{l}}$) instead of $T_{\mathbf{q}}$ ($\beta_{\mathbf{q}}$).

In the generic case, when both the hopping t and the interaction U are non-zero, the system is not integrable. Then, neither the generalized transformation Eq. (9.18) nor its variant with local "temperatures" are symmetries of the corresponding Schwinger-Keldysh action, showing that this case eventually admits only one single global temperature, which determines the statistical weight of individual many-body eigenstates of the system.

9.4.2 Dissipative contributions in equilibrium

The functional integral with the action S in Eq. (9.8), as it stands, is not convergent but it can be made so by adding to S an infinitesimally small imaginary (i.e., dissipative) contribution [214, 215]. Within a renormalization-group picture, this *infinitesimal* dissipation may be seen as the "initial value", at a microscopic scale, of *finite* dissipative contributions, which are eventually obtained upon coarse graining the original action S and which result in, e.g., finite lifetimes of excitations of the effective low-energy degrees of freedom. The precise form of the corresponding effective low-energy action and, in particular, of the dissipative contributions which appear therein, is strongly constrained

by the requirement of invariance under $\mathcal{T}_\beta$ of the starting action at the microscopic scale: in fact, terms which violate this symmetry will not be generated upon coarse-graining. In the discussion below we identify those dissipative contributions to the Schwinger-Keldysh action which are invariant under $\mathcal{T}_\beta$. This allows us to anticipate the structure of any low-energy effective action possessing this a symmetry. Note, however, that *finite* dissipative terms may appear even at the microscopic scale because of, e.g., the coupling of the system to an external bath. Below we consider two instances of this case: in Sec. 9.6.2 we show that $\mathcal{T}_\beta$ cannot be a symmetry of the action if the system is coupled to Markovian baths and driven — a situation described by a quantum master equation. Another specific example, in which the equilibrium symmetry is realized, is the particle number non-conserving coupling of the Schwinger-Keldysh action Eq. (9.8) to an ohmic bath. This situation, which we discuss in Sec. 9.4.3, is of particular interest, because its classical limit renders what is known as the dynamical model A [232] with reversible mode couplings (termed model A* in Ref. [388]); this correspondence allows us to establish a connection with the known equilibrium symmetry of the generating functional associated with this classical stochastic dynamics.

Below we discuss dissipative terms of the action invariant under $\mathcal{T}_\beta$, which involve first single particles (being quadratic in the fields of the Schwinger-Keldysh action) in Sec. 9.4.2, and then their interactions in Sec. 9.4.2.

Single-particle sector

Dissipative contributions to the single-particle sector of the Schwinger-Keldysh action which are invariant under $\mathcal{T}_\beta$ take the form

$$S_d = i \int_{\omega,\mathbf{q}} h(\omega,\mathbf{q}) \left(\phi_q^*(\omega,\mathbf{q})\phi_c(\omega,\mathbf{q}) - \phi_q(\omega,\mathbf{q})\phi_c^*(\omega,\mathbf{q}) + 2\coth(\beta\omega/2)\phi_q^*(\omega,\mathbf{q})\phi_q(\omega,\mathbf{q}) \right), \qquad (9.19)$$

with an arbitrary real function $h(\omega,\mathbf{q})$ which transforms under time reversal as $\tilde{h}(\omega,\mathbf{q}) = h(\omega,-\mathbf{q})$. When such dissipative terms are introduced in order to regularize the Schwinger-Keldysh functional integral, a typical choice for $h(\omega,\mathbf{q})$ is $h(\omega,\mathbf{q}) = \epsilon$ [214,215] with $\epsilon \to 0$: this ensures that the Green's functions in the absence of interactions satisfy a fluctuation-dissipation relation (FDR; we postpone the detailed discussion of these relations to Sec. 9.6.1). The FDR for non-interacting Green's functions, together with the invariance of interactions under the transformation $\mathcal{T}_\beta$ shown in Sec. 9.4.1, guarantees that the FDR is satisfied to all orders in perturbation theory [373].

While there are no restrictions on the form of the function $h(\omega,\mathbf{q})$, the hyperbolic cotangent $\coth(\beta\omega/2)$ appearing in the last term of S_d is *uniquely* fixed by the requirement of invariance under $\mathcal{T}_\beta$, as can be verified by following the line of argument presented in Appendix 9.A. In particular, S_d with a certain value of β in the argument of $\coth(\beta\omega/2)$ is invariant under $\mathcal{T}_{\beta'}$ if and only if $\beta' = \beta$. This shows that, remarkably, the appearance of the thermodynamic equilibrium Bose distribution function $n(\omega) = 1/(e^{\beta\omega}-1)$ at a temperature $T = 1/\beta$ in $\coth(\beta\omega/2) = 2n(\omega)+1$, can be traced back to the fact that $\mathcal{T}_\beta$ is a symmetry of the action. Note that for simplicity we considered here only the case of vanishing chemical potential, $\mu = 0$. For finite μ, the frequency ω in the argument of the hyperbolic cotangent in Eq. (9.19) should be shifted according to $\omega \to \omega - \mu$, as we discussed in point 5 in Sec. 9.3.

Dissipative vertices

The dissipative contributions discussed in the previous section are quadratic in the field operators and they naturally occur, e.g., when the system is coupled to a thermal bath by means of an interaction which is linear in those fields. However, this type of coupling necessarily breaks particle number conservation. The number of particles is conserved if instead the system-bath interaction term commutes with the total number of particles of the system, $N = \int_{\mathbf{x}} n(\mathbf{x})$, where $n(\mathbf{x}) = \psi^\dagger(\mathbf{x})\psi(\mathbf{x})$ is the local density. In other words, to ensure particle number conservation, it is necessary that the coupling terms are at least quadratic in the system operators. Accordingly, dissipative *vertices* appear in the Schwinger-Keldysh action after integrating out the bath degrees of freedom: the requirement of invariance of these terms under $\mathcal{T}_\beta$ allows us to infer *a priori* their possible structure. In particular, we find that a frequency-independent number-conserving quartic vertex (i.e., the dissipative counterpart to the two-body interaction $\propto |\psi_\sigma|^4$ in the Hamiltonian (9.11)) is forbidden by the thermal symmetry.

A generic quartic vertex, which conserves the number of particles and which is local in time, can be parameterized as

$$S_d = -i \int_{\omega_1,\ldots,\omega_4} \delta(\omega_1 - \omega_2 + \omega_3 - \omega_4) \times \big[f_1(\omega_1,\omega_2,\omega_3,\omega_4)\psi_+^*(\omega_1)\psi_+(\omega_2)\psi_+^*(\omega_3)\psi_+(\omega_4) \\ + f_2(\omega_1,\omega_2,\omega_3,\omega_4)\psi_-^*(\omega_1)\psi_-(\omega_2)\psi_-^*(\omega_3)\psi_-(\omega_4) + f_3(\omega_1,\omega_2,\omega_3,\omega_4)\psi_+^*(\omega_1)\psi_+(\omega_2)\psi_-^*(\omega_3)\psi_-(\omega_4) \big], \tag{9.20}$$

where $f_{1,2,3}$ are real functions; in order to simplify the notation we do not indicate the (local) spatial dependence of the fields, which is understood together with the corresponding integration in space. Conservation of particle number is ensured by the $U(1)$ invariance $\psi_\pm \mapsto e^{i\alpha_\pm}\psi_\pm$ on each contour separately, with generic phases $\alpha_\pm$, while the overall δ-function on the frequencies guarantees locality in time. Restrictions on the functions $f_{1,2,3}$ in the generic dissipative vertex in Eq. (9.20) follow from the requirements of causality [215], according to which S_d to the action must vanish for $\psi_+ = \psi_-$, and invariance of the dissipative vertex under the equilibrium transformation. These conditions are studied in detail in Appendix 9.B. In particular, we find that they cannot be satisfied if $f_{1,2,3}$ are constant, i.e., do not depend on the frequencies. One particular choice of these functions that is compatible with the constraints is given by

$$\begin{aligned} f_3(\omega_1,\omega_2,\omega_3,\omega_4) &= -4\,(\omega_1-\omega_2)\,(n(\omega_1-\omega_2)+1)\,, \\ f_1(\omega_1,\omega_2,\omega_3,\omega_4) &= f_2(\omega_1,\omega_2,\omega_3,\omega_4) = (\omega_1-\omega_2)\coth(\beta\,(\omega_1-\omega_2)\,/2)\,, \end{aligned} \tag{9.21}$$

with the Bose distribution function $n(\omega)$. It is interesting to note that, in the basis of classical and quantum fields, this corresponds to a generalization of Eq. (9.19) with $h(\omega,\mathbf{q}) = \omega$, in which the fields are replaced by the respective densities defined as $\rho_c = \left(\psi_+^*\psi_+ + \psi_-^*\psi_-\right)/\sqrt{2}$ and $\rho_q = \left(\psi_+^*\psi_+ - \psi_-^*\psi_-\right)/\sqrt{2}$. Another notable property of this solution is that for $\omega_{1,2} \to 0$ we have $f_{1,2}(\omega_1,\omega_2,\omega_3,\omega_4) \to 2T$ and $f_3(\omega_1,\omega_2,\omega_3,\omega_4) \to -4T$, i.e., these limits of vanishing frequencies are finite. This implies that the form of S_d with $f_{1,2,3}$ given by Eq. (9.21) is to some extent universal: indeed, it should be expected to give the leading dissipative contribution to the Schwinger-Keldysh action of any number-conserving system in the low-frequency limit. At higher frequencies, other less universal solutions might also be important and one cannot make a general statement.

9.4.3 Classical limit, detailed balance and microreversibility

A transformation analogous to $\mathcal{T}_\beta$ — which becomes a symmetry in equilibrium — was previously derived for the stochastic evolution of classical statistical systems in contact with an environment, within the response functional formalism [118, 235–239, 313, 375]. This formalism allows one to determine expectation values of relevant quantities as a functional integral with a certain action known as response functional, which can also be derived from a suitable classical limit of the Schwinger-Keldysh action for quantum systems [214, 215]. In these classical systems, the environment acts effectively as a source of stochastic noise over which the expectation values are taken.

Here, we show that the classical limit of $\mathcal{T}_\beta$ [384] yields exactly the transformation which becomes a symmetry when the classical system is at equilibrium [376]. In order to consider this limit within the Schwinger-Keldysh formalism, it is convenient to express the Schwinger-Keldysh action in Eq. (9.8) in terms of the classical and quantum fields ϕ_c and ϕ_q, respectively, defined in Eq. (9.4) and to reinstate Planck's constant according to [214, 215]

$$S \to S/\hbar, \quad \coth(\beta\omega/2) \to \coth(\beta\hbar\omega/2), \quad \phi_q \to \hbar\phi_q. \tag{9.22}$$

Then, the action can be formally expanded in powers of $\hbar$ in order to take the classical limit $\hbar \to 0$ and the classical part of the Schwinger-Keldysh action is given by the contribution which remains for $\hbar = 0$. Note that the limit $\hbar \to 0$ considered here is formally equivalent to approaching criticality in equilibrium at finite temperature $T = \beta^{-1}$, for which $\beta\Delta \to 0$, where Δ is the energy gap, which can be read off from the retarded Green's function (see, e.g., Ref. [245]). This equivalence conforms with the expectation that quantum fluctuations generically play only a subdominant role in determining the critical behavior of quantum systems at finite temperature. In order to see the emergence of a stochastic dynamics driven by incoherent (thermal) noise from a quantum coherent dynamics, we supplement the Schwinger-Keldysh action in Eq. (9.8) (describing the latter) with dissipative terms arising from its coupling to a bath. For simplicity, we assume this bath to be characterized by an ohmic spectral density, while the system is assumed to have the Hamiltonian in Eq. (9.11). Deferring to Sec. 9.6.2 the discussion of the theoretical description of such a system-bath coupling, we anticipate here that the resulting contribution to the Schwinger-Keldysh action can be written as in Eq. (9.63), under the assumption that $\gamma(\omega)\nu(\omega)$ is linear in the frequency, i.e., $\gamma(\omega)\nu(\omega) = 2\kappa\omega$ and by choosing $L_\sigma(\omega) \to \psi_\sigma(\omega, \mathbf{q})$, with the thermal bath acting independently on each momentum mode [214]. Then, in the classical limit $\hbar \to 0$, we find

$$S = \int_{t,\mathbf{x}} \Phi_q^\dagger \left\{ \left[(\sigma_z + i\kappa\mathbb{1})\, i\partial_t + \frac{\nabla^2}{2m} \right] \Phi_c + i2\kappa T \Phi_q \right\} - \lambda \int_{t,\mathbf{x}} \left(\phi_c^{*2} \phi_c \phi_q + \text{c.c.} \right). \tag{9.23}$$

This action has the form of the response functional of the equilibrium dynamical models considered in Ref. [232]: it includes both a linear and a quadratic contribution in the quantum field ϕ_q, but no higher-order terms. After having transformed the quadratic term into a linear one via the introduction of an auxiliary field (which is eventually interpreted as a Gaussian additive noise), this quantum field can be integrated out and one is left with an effective constraint on the dynamics of the classical field ϕ_c, which takes the form of a Langevin equation; here:

$$(i - \kappa)\, \partial_t \phi_c = \left(-\frac{\nabla^2}{2m} + \lambda |\phi_c|^2 \right) \phi_c + \eta, \tag{9.24}$$

where $\eta = \eta(\mathbf{x}, t)$ is a (complex) Gaussian stochastic noise with zero mean $\langle \eta(\mathbf{x}, t) \rangle = 0$ and correlations

$$\langle \eta(\mathbf{x}, t) \eta^*(\mathbf{x}', t') \rangle = \kappa T \delta(t - t') \delta^{(d)}(\mathbf{x} - \mathbf{x}'), \qquad \langle \eta(\mathbf{x}, t) \eta(\mathbf{x}', t') \rangle = 0. \tag{9.25}$$

Equation (9.24) describes the dynamics of the non-conserved (complex scalar) field ϕ_c without additional conserved densities, which is known in the literature as *model A* [232]. However, as can be seen from the complex prefactor $i - \kappa$ of the time derivative on the left-hand side of Eq. (9.24), the dynamics is not purely relaxational as in model A, but it has additional coherent contributions, also known as *reversible mode couplings* [313]. The fact that the simultaneous appearance of dissipative and coherent dynamics can be described by a complex prefactor of the time derivative is specific to thermal equilibrium: in fact, dividing Eq. (9.24) by $i - \kappa$, the reversible and irreversible parts of the resulting Langevin dynamics are not independent of each other and in fact their coupling constants share a common ratio [118,239,350]. Under more general non-equilibrium conditions, however, these reversible and irreversible generators of the dynamics have different microscopic origins and no common ratio generically exists. In the present equilibrium context, however, the action Eq. (9.23) corresponds to *model A** in the notion of Ref. [388], and the form of the classical transformation appropriate for this case which becomes a symmetry in equilibrium was given in Ref. [245]. This transformation emerges as the classical limit of $\mathcal{T}_\beta$ discussed in the previous sections [384]. In fact, for $\beta = T^{-1} \to 0$ and neglecting the contribution of the quantum fields in the transformation of the classical fields (i.e., at the leading order in $\hbar$), Eq. (9.5) becomes

$$\begin{aligned} &\mathcal{T}_\beta \Phi_c(t, \mathbf{x}) = \sigma_x \Phi_c(-t, \mathbf{x}), \\ &\mathcal{T}_\beta \Phi_q(t, \mathbf{x}) = \sigma_x \left(\Phi_q(-t, \mathbf{x}) + \frac{i}{2T} \partial_t \Phi_c(-t, \mathbf{x}) \right), \end{aligned} \tag{9.26}$$

after a transformation back to the time and space domains. Upon identifying the classical field Φ_c with the physical field and Φ_q with the response field $\tilde{\Phi}$, according to $\Phi_q = i\tilde{\Phi}$, Eq. (9.26) takes the form of the classical symmetry introduced in Ref. [376]. Note, however, that the transformation (9.26) is not the only form in which the equilibrium symmetry in the classical context can be expressed. In fact, the transformation of the response field $\tilde{\Phi}$ can also be expressed [118, 239] in terms of a functional derivative of the equilibrium distribution rather than of the time derivative of the classical field $\partial_t \Phi_c$ as in Eq. (9.26). The existence of these different but equivalent transformations might be related to the freedom in the definition of the response field, which is introduced in the theory as an auxiliary variable in order to enforce the dynamical constraint represented by the Langevin equation [118, 195, 239, 313] such as Eq. (9.24). This implies [195] that the related action acquires the so-called Slavnov-Taylor symmetry. As far as we know, the consequences of this symmetry have not been thoroughly investigated in the classical case and its role for quantum dynamics surely represents an intriguing issue for future studies.

We emphasize the fact that the derivation of the symmetry in the classical case involves explicitly the equilibrium probability density [118, 239]. Indeed, the response functional contains an additional contribution from the probability distribution of the value of the fields at the initial time, after which the dynamics is considered. This term generically breaks the time-translational invariance of the theory [118, 239], unless the initial probability distribution is the equilibrium one. Accordingly, when the classical equilibrium symmetry $\mathcal{T}_\beta$ is derived under the assumption of time-translational

invariance, its expression involves also the equilibrium distribution. In the quantum case discussed in the previous sections, instead, time-translational symmetry was implicitly imposed by extending the time integration in the action from $-\infty$ to $+\infty$, which is equivalent to the explicit inclusion of the initial condition (in the form of an initial density matrix) and makes the analysis simpler, though with a less transparent interpretation from the physical standpoint.

Although in classical systems this equilibrium symmetry takes (at least) two different but equivalent forms due to the arbitrariness in the definition of the response functional mentioned above, it can always be traced back to the condition of detailed balance [118,239,376]. Within this context, detailed balance is defined by the requirement that the probability of observing a certain (stochastic) realization of the dynamics of the system equals the probability of observing the time-reversed realization, and therefore it encodes the notion of *microreversibility*. This condition guarantees the existence and validity of fluctuation-dissipation relations, which can be proved on the basis of this symmetry. In addition, detailed balance constrains the form that the response functional can take as well as the one of the equilibrium probability distribution for this stochastic process.

The situation in the quantum case appears to be significantly less clear. In fact, a precise and shared notion of *quantum detailed balance* and *quantum microreversibility* is seemingly lacking. The first attempt to introduce a principle of quantum detailed balance dates back to Ref. [392], where it was derived from a condition of microreversibility in the context of Markovian quantum dynamics described by a Lindblad master equation. The mathematical properties of these conditions were subsequently studied in detail (see, e.g., Refs. [393–397]) and were shown to constrain the form of the Lindblad super-operator in order for it to admit a Gibbs-like stationary density matrix. However, even when this occurs, these operators are not able to reproduce the KMS condition and the fluctuation-dissipation relations because of the underlying Markovian approximation, as we discuss in Sec. 9.6.2.

The notion of microreversibility in quantum systems appears to have received even less attention, as well as its connection with some sort of reversibility expressed in terms of the probability of observing certain "trajectories" and their time-reversed ones. The definition proposed in Ref. [392] (also discussed in Ref. [398]) appears to be a natural generalization of the notion in the classical case, as it relates the correlation of two operators evaluated at two different times with the correlation of the time-reversed ones. However, to our knowledge, the relationship between this condition and thermodynamic equilibrium has never been fully elucidated. Although addressing these issues goes well beyond the scope of the present Chapter, they surely represent an interesting subject for future investigations.

9.5 Equivalence between the symmetry and the KMS condition

In this section we show that the invariance of the Schwinger-Keldysh action of a certain system under $\mathcal{T}_\beta$ (as specified in Sec. 9.4) is equivalent to having multi-time correlation functions of the relevant fields which satisfy the KMS condition [365, 366]. As the latter can be considered as the defining property of thermodynamic equilibrium, this shows that the same applies to the invariance under the equilibrium symmetry.

The KMS condition involves *both* the Hamiltonian generator of dynamics *and* the thermal nature of the density matrix which describes the stationary state of the system: heuristically this condition amounts to requiring that the many-body Hamiltonian which determines the (canonical) population

of the various energy levels is the same as the one which rules the dynamics of the system. The equivalence proved here allows us to think of the problem from a different perspective: taking the invariance under $\mathcal{T}_\beta$ as the fundamental property and observing that any time-independent Hamiltonian respects it, we may require it to hold at any scale, beyond the microscopic one governed by reversible Hamiltonian dynamics alone. In particular, upon coarse graining within a renormalization-group framework, only irreversible dissipative terms which comply with the symmetry (such as those discussed in Sec. 9.4.2) can be generated in stationary state and the hierarchy of correlation functions respect thermal fluctuation-dissipation relations. The validity of KMS conditions (and therefore of the symmetry $\mathcal{T}_\beta$) hinges on the *whole* system being prepared in a canonical density matrix ρ_0. Accordingly, if the system is described by a microcanonical ensemble, the KMS condition holds only in a subsystem of it, which is expected to be described by a canonical reduced density matrix. Equivalently, this means that, in a microcanonical ensemble, only suitable local observables satisfy this condition. In the case of quantum many-body systems evolving from a pure state, an additional restriction on the class of observables emerges due to the fact that, if thermalization occurs as conjectured by the eigenstate thermalization hypothesis (ETH) [36, 37, 62], the microcanonical ensemble is appropriate only if the observable involves the creation and annihilation of a small number of particles (low order correlation functions). This was shown to be also the case for FDRs [38, 43]: however, as pointed out above, the thermal symmetry implies the validity of FDRs involving an arbitrary number of particles, which leads to the conclusion that it does not apply to an isolated system thermalizing via the ETH. In other words, the thermal symmetry implies that the whole density matrix takes the form of a Gibbs ensemble, while in thermalization according to the ETH, only finite subsystems are thermalized by the coupling to the remainder of the system, which acts as a bath. Thus we see how Hamiltonian dynamics favors thermal stationary states (with density matrix ρ proportional to $e^{-\beta H}$) over arbitrary functionals $\rho = \rho(H)$. One explicit technical advantage of this perspective based on symmetry is that it allows us to utilize the toolbox of quantum field theory straightforwardly and to study the implications of $\mathcal{T}_\beta$ being a symmetry; this is exemplified here by considering the associated Ward-Takahashi identities and by showing the absence of this symmetry in dynamics described by Markovian quantum master equations in Sec. 9.6.2. We also note that the presence of this symmetry provides a criterion for assessing the equilibrium nature of a certain dynamics by inspecting only the dynamic action functional, instead of the whole hierarchy of fluctuation-dissipation relations. In addition, this symmetry may be present in the actions of open systems with both reversible and dissipative terms.

In the following, we consider a quantum system with unitary dynamics generated by the (time-independent) Hamiltonian H, which is in thermal equilibrium at temperature $T = \beta^{-1}$ and therefore has a density matrix $\rho = e^{-\beta H}/\operatorname{tr} e^{-\beta H}$. The KMS condition relies on the observation that for an operator in the Heisenberg representation $A(t) = e^{iHt} A e^{-iHt}$, one has

$$A(t)\rho = \rho A(t - i\beta) \tag{9.27}$$

(for simplicity we do not include here a chemical potential but at the end of the discussion we indicate how to account for it).This identity effectively corresponds, up to a translation of the time by an imaginary amount, to exchanging the order of the density matrix and of the operator A and therefore, when Eq. (9.27) is applied to a multi-time correlation function, it inverts the time order of the involved times, which can be subsequently restored by means of the quantum-mechanical time-reversal operation. Hence, the quantum-mechanical time reversal naturally appears as an element of

the equilibrium symmetry $\mathcal{T}_\beta$, while external fields have to be transformed accordingly, as indicated in Eq. (9.7). The application of time reversal yields a representation of the KMS condition which can be readily translated into the Schwinger-Keldysh formalism, as was noted in Refs. [371–373]. In particular, it results in an infinite hierarchy of generalized multi-time quantum fluctuations-dissipation relations which include the usual FDR for two-time correlation and response functions of the bosonic fields as a special case (see Ref. [373] and Sec. 9.6.1). One of the main points of this Chapter is that these FDRs can also be regarded as the Ward-Takahashi identities associated with the invariance of the Schwinger-Keldysh action S under the discrete symmetry [2] $\mathcal{T}_\beta$ and that, conversely, the full hierarchy of FDRs implies the invariance of S under $\mathcal{T}_\beta$.

The argument outlined below, which shows the equivalence between the KMS condition and the thermal symmetry, involves several steps: as a preliminary we review in Secs. 9.5.1 and 9.5.2 how time-ordered and anti-time-ordered correlation functions can be expressed using the Schwinger-Keldysh technique and we specify how these correlation functions transform under quantum mechanical time reversal. We apply these results to the KMS condition in Sec. 9.5.3: first we discuss its generalization to multi-time correlation functions and then we translate such a generalization into the Schwinger-Keldysh formalism. This part proceeds mainly along the lines of Ref. [373], with some technical differences. Finally, we establish the equivalence between the resulting hierarchy of FDRs and the thermal symmetry at the end of Sec. 9.5.3.

9.5.1 Multi-time correlation functions in the Schwinger-Keldysh formalism

Two-time correlation functions. Let us first consider a two-time correlation function

$$\langle A(t_A)B(t_B)\rangle \equiv \mathrm{tr}\,(A(t_A)B(t_B)\rho) \tag{9.28}$$

between two generic operators A and B (in the following we are particularly interested in considering the case in which A and B are the field operators $\psi(\mathbf{x})$ or $\psi^\dagger(\mathbf{x})$ at positions $\mathbf{x}=\mathbf{x}_A$ and $\mathbf{x}=\mathbf{x}_B$) evaluated at different times t_A and t_B, respectively, in a quantum state described by the density matrix ρ. We assume that the dynamics of the system is unitary and generated by the Hamiltonian H. Then, the Heisenberg operator A at time t_A is related to the Schrödinger operator at a certain initial time $t_i < t_A$ via

$$A(t_A) = e^{iH(t_A-t_i)}Ae^{-iH(t_A-t_i)}, \tag{9.29}$$

with an analogous relation for B.

The two-time correlation function can be represented within the Schwinger-Keldysh formalism as

$$\begin{aligned}\langle A(t_A)B(t_B)\rangle &= \langle A_-(t_A)B_+(t_B)\rangle \\ &\equiv \int \mathcal{D}[\Psi]A_-(t_A)B_+(t_B)e^{iS[\Psi]},\end{aligned} \tag{9.30}$$

irrespective of the relative order of the times t_A and t_B. Here, the functional integral is taken over the fields $\Psi = \left(\psi_+, \psi_+^*, \psi_-, \psi_-^*\right)^T$, and the exponential weight with which a specific field configuration

[2] Here we used the notion of "Ward-Takahashi identity" in the slightly generalized sense which encompasses the case of identities between correlation functions resulting from discrete symmetries (such as Eq. (9.3) in Sec. 9.5.4, which leads to, c.f., Eqs. (9.46) and (9.47)) beyond the usual case of continuous symmetries [195].

contributes to the integral is determined by the Schwinger-Keldysh action $S[\Psi]$. In the following, by $O_{+/-}$ we indicate that a certain operator O has been evaluated in terms of the fields $\psi_\pm$ defined on the forward/backward branch of the temporal contour associated with the Schwinger-Keldysh formalism (see, e.g., Refs. [214, 215]).

Multi-time correlation functions. We define multi-time correlation functions in terms of time-ordered and anti-time-ordered products of operators

$$\begin{aligned} A(t_{A,1},\dots,t_{A,N}) &= a_1(t_{A,1})a_2(t_{A,2})\cdots a_N(t_{A,N}),\\ B(t_{B,1},\dots,t_{B,M}) &= b_M(t_{B,M})b_{M-1}(t_{B,M-1})\cdots b_1(t_{B,1}), \end{aligned} \tag{9.31}$$

for $t_i < t_{A,1} < \cdots < t_{A,N} < t_f$ and $t_i < t_{B,1} < \cdots < t_{B,M} < t_f$. Here, $\{a_n, b_m\}_{m,n}$ are bosonic field operators. The specific sequence of time arguments in A and B (increasing and decreasing from left to right, respectively) leads to a time-ordering on the Schwinger-Keldysh contour: indeed, the multi-time correlation function can be expressed as a Schwinger-Keldysh functional integral in the form

$$\langle A(t_{A,1},\dots,t_{A,N})B(t_{B,1},\dots,t_{B,M})\rangle = \langle B_+(t_{B,1},\dots,t_{B,M})A_-(t_{A,1},\dots,t_{A,N})\rangle. \tag{9.32}$$

Anti-time-ordered correlation functions. Not only time-ordered correlation functions such as Eq. (9.32) can be expressed in terms of functional integrals, but also correlation functions which are anti-time-ordered and which, e.g., are obtained by exchanging the positions of $A(t_{A,1},\dots,t_{A,N})$ and $B(t_{B,1},\dots,t_{B,M})$ on the l.h.s. of Eq. (9.32). The construction of the corresponding functional integral can be accomplished with a few straightforward modifications to the procedure summarized in Appendix 9.C (and presented, e.g., in Refs. [214,215]). In a stationary state one has $[\rho, H] = 0$ and all the Heisenberg operators on the l.h.s. of Eq. (9.32) can be related to the Schrödinger operators at a later time t_f. Then one finds

$$\langle B(t_{B,1},\dots,t_{B,M})A(t_{A,1},\dots,t_{A,N})\rangle = \langle A_+(t_{A,1},\dots,t_{A,N})B_-(t_{B,1},\dots,t_{B,M})\rangle_{S_b}, \tag{9.33}$$

where the action S_b describes the backward evolution and it is related to the action S which enters the forward evolution in Eq. (9.32) simply by a global change of sign $S_b = -S$.

9.5.2 Quantum-mechanical time reversal

In this section we first recall some properties of the quantum-mechanical time reversal operation T [374] and then discuss its implementation within the Schwinger-Keldysh formalism. T is an antiunitary operator, i.e., it is antilinear (such that $\mathsf{T}\lambda|\psi\rangle = \lambda^*\mathsf{T}|\psi\rangle$ for $\lambda \in \mathbb{C}$) and unitary ($\mathsf{T}^\dagger = \mathsf{T}^{-1}$). Scalar products transform under antiunitary transformations into their complex conjugates, i.e., $\langle\psi|A|\phi\rangle = \langle\tilde{\psi}|\tilde{A}|\tilde{\phi}\rangle^*$, where we denote by $|\tilde{\psi}\rangle = \mathsf{T}|\psi\rangle$ and $\tilde{A} = \mathsf{T}A\mathsf{T}^\dagger$ the state and the Schrödinger operator obtained from the state $|\psi\rangle$ and the operator A, respectively, after time reversal. Accordingly, expressing the trace of an operator in a certain basis $\{|\psi_n\rangle\}_n$, one finds

$$\mathrm{tr}\, A = \sum_n \langle\psi_n|A|\psi_n\rangle = \sum_n \langle\tilde{\psi}_n|\tilde{A}|\tilde{\psi}_n\rangle^* = (\mathrm{tr}\,\tilde{A})^*. \tag{9.34}$$

In the last equality we used the fact that, due to the unitarity of T, also the time-reversed set $\{|\tilde{\psi}_n\rangle\}_n$ forms a basis. For future convenience, we shall define the Heisenberg representation of time-reversed operators such that it coincides with the Schrödinger one at time $-t_f$, i.e., we set

$$\tilde{A}(t_A) = e^{i\tilde{H}(t_A+t_f)}\,\tilde{A}e^{-i\tilde{H}(t_A+t_f)}. \tag{9.35}$$

Note that this is distinct from the Heisenberg representation defined in Eq. (9.29), which coincides with the Schrödinger one only at time t_i. In order to simplify the notation, we shall not distinguish these two different Heisenberg representations, assuming implicitly that the latter and the former are used, respectively, for operators and their time-reversed ones, such that $A(t_i) = A$ while $\tilde{A}(-t_f) = \tilde{A}$.

Let us now study the effect of time reversal on the generic multi-time correlation function in Eq. (9.32). Due to translational invariance in time, the time arguments of the operators A and B can be shifted by $t_i - t_f$ without affecting the correlation function. Then, by using Eqs. (9.34) and (9.35), one has

$$\begin{aligned}\langle A(t_{A,1},\ldots,t_{A,N})B(t_{B,1},\ldots,t_{B,M})\rangle &= \langle \tilde{A}(-t_{A,1},\ldots,-t_{A,N})\tilde{B}(-t_{B,1},\ldots,-t_{B,M})\rangle^*_{\tilde{\rho}} \\ &= \langle \tilde{B}^\dagger(-t_{B,1},\ldots,-t_{B,M})\tilde{A}^\dagger(-t_{A,1},\ldots,-t_{A,N})\rangle_{\tilde{\rho}},\end{aligned} \tag{9.36}$$

where the subscript in $\langle\cdots\rangle_{\tilde{\rho}}$ indicates that the expectation value is taken with respect to the time-reversed density operator $\tilde{\rho} \equiv \mathsf{T}\rho\mathsf{T}^\dagger$, which is time-independent. The expectation value on the r.h.s. of Eq. (9.36) is anti-time ordered and therefore it can be rewritten as a Schwinger-Keldysh functional integral by using Eq. (9.33). The l.h.s., instead, is time-ordered and therefore it can be expressed as in Eq. (9.32), such that Eq. (9.36) becomes

$$\langle B_+(t_{B,1},\ldots,t_{B,M})A_-(t_{A,1},\ldots,t_{A,N})\rangle = \langle \tilde{A}^*_+(-t_{A,1},\ldots,-t_{A,N})\tilde{B}^*_-(-t_{B,1},\ldots,-t_{B,M})\rangle_{\tilde{S}_b}, \tag{9.37}$$

where the subscript b in $\tilde{S}_b$ indicates that the sign of the action which describes the Hamiltonian evolution on the r.h.s. of this relation has been reversed, as explained below Eq. (9.33). The time-reversed action $\tilde{S}$ differs from the action S associated with H which enters (implicitly, cf. Eq. (9.30)) Eq. (9.32) because in $\tilde{S}$ the time evolution is generated by $\tilde{H}$, the initial state is the time-reversed density matrix $\tilde{\rho}$, and the integration over time extends from $-t_f$ to $-t_i$. This latter difference becomes inconsequential as $t_i \to -\infty$ and $t_f \to \infty$.

Let us now consider the case in which A and B are products of the bosonic field operators ψ and $\psi^\dagger$, such that $A_\pm$ and $B_\pm$ involve the corresponding products of $\psi_\pm$ and their complex conjugates. As there are no further restrictions on A and B, the l.h.s. of Eq. (9.37) can be generically indicated as $\langle\mathcal{O}[\Psi]\rangle$, where $\mathcal{O}[\Psi]$ is the product of various fields on the Schwinger-Keldysh contour corresponding to $B_+(\ldots)A_-(\ldots)$ which, according to the notation introduced in Sec. 9.3, are collectively indicated by $\Psi = \left(\psi_+, \psi^*_+, \psi_-, \psi^*_-\right)^T$. With this shorthand notation, Eq. (9.37) can be cast in the form

$$\langle\mathcal{O}[\Psi]\rangle = \langle\mathcal{O}[\mathsf{T}\Psi]\rangle_{\tilde{S}_b}, \tag{9.38}$$

where the transformation

$$\mathsf{T}\Psi_\sigma(t,\mathbf{x}) = \Psi^*_{-\sigma}(-t,\mathbf{x}), \tag{9.39}$$

implements the quantum-mechanical time reversal within the Schwinger-Keldysh formalism. (With a slight abuse of notation, the same symbol T is used to indicate here both the quantum-mechanical

time-reversal operator introduced above and the transformation of fields on the Schwinger-Keldysh contour in Eqs. (9.38) and (9.39).) In Eq. (9.39) we took into account that the bosonic field operators in the Schrödinger picture and in the real-space representation are time-reversal invariant, i.e., $\tilde{\psi}(\mathbf{x}) = \mathsf{T}\psi(\mathbf{x})\mathsf{T}^\dagger = \psi(\mathbf{x})$, which allows us to drop the tilde on the transformed field on the r.h.s. of Eq. (9.39). However, we note that in the last line of Eq. (9.36) the Hermitean adjoint operators of those on the l.h.s. appear and this is the reason why both the r.h.s. of Eq. (9.37) and the transformation prescription Eq. (9.39) involve complex conjugation of the fields. Note that the time-reversal transformation in Eq. (9.39) is actually linear, i.e., the complex conjugation affects only the fields variables and not possible complex prefactors. This follows again from the last line of Eq. (9.36): the combination of two antilinear transformations (time reversal and Hermitean conjugation) results into a linear one.

Let us mention that while Eq. (9.37) follows from the second line of Eq. (9.36), one could have equivalently taken its first line as the starting point for deriving a Schwinger-Keldysh time-reversal transformation. Then one would have been lead to a different implementation T' of time reversal:

$$\mathsf{T}'\Psi_\sigma(t,\mathbf{x}) = \Psi_\sigma(-t,\mathbf{x}), \tag{9.40}$$

with an additional overall complex conjugation of the correlation function. In some sense, the transformation T' is closer to the common way of representing the quantum-mechanical time reversal than T is, as it amounts to a mapping $t \mapsto -t$ and $i \mapsto -i$ [374]. For our purposes, however, T is of main interest, since it is part of the equilibrium transformation as we describe below.

We finally note that an alternative implementation of the time-reversal transformation is based on the observation that the forward and backward branches of the closed-time path integral are actually equivalent if the dynamics of a system is time-reversal invariant (TRI) [215]. More specifically, this means that the Schwinger-Keldysh action is invariant — up to a global change of sign — upon exchanging the corresponding fields, i.e., $S[\psi_+,\psi_-] = -S[\psi_-,\psi_+]$. This transformation is partly recovered in Eqs. (9.38) and (9.39): in fact, T in Eq. (9.39) involves an exchange of the contour indices, while the corresponding global change of sign in the action is indicated on the r.h.s. of Eq. (9.38) by the subscript $\tilde{S}_b$ (cf. the definition of S_b below Eq. (9.33)). However, the time reversal transformation T in Eq. (9.39) — derived from the quantum-mechanical time-reversal operation — additionally involves both complex conjugation and the time inversion $t \mapsto -t$.

9.5.3 KMS condition and generalized fluctuation-dissipation relations

The discussion of the previous sections about multi-time correlation functions and the time-reversal transformation provides the basis for the formulation of the KMS condition for multi-time correlation functions and of its representation in terms of Schwinger-Keldysh functional integrals. For the specific case of a four-time correlation function, the KMS condition is pictorially illustrated in Fig. 9.1. As described in the caption, panel (a) summarizes the convention as far as the forward/backward contours are concerned. Panel (b), instead, refers to the KMS condition which, as anticipated after Eq. (9.27), involves a contour exchange of the multi-time operators A and B. This exchange is the reason why the arrows in the second equality in Fig. 9.1 (b) are reversed, since both A and B turn out to be anti-time ordered when moved to the opposite contour. The appropriate time-ordering can be restored by means of the quantum-mechanical time reversal transformation introduced in Sec. 9.5.2, as indicated by the third equality in the figure. This is a crucial step, because only time-ordered correlation functions

can be directly translated into the functional integral by means of the usual Trotter decomposition, which makes the time-reversal transformation indispensable in the construction. However, this does not mean that properties related to equilibrium conditions such as fluctuation-dissipation relations are fulfilled only if the Hamiltonian is invariant under the time-reversal transformation. Indeed, it turns out that multi-time FDRs always involve both the Hamiltonian and its time-reversed counterpart [373], while as we show in Sec. 9.6.1 the FDR for two-time functions can be stated without reference to the time-reversed Hamiltonian, even if the Hamiltonian is not TRI.

The KMS condition for a two-time function reads [3]

$$\langle A(t_A)B(t_B)\rangle = \langle B(t_B - i\beta/2)A(t_A + i\beta/2)\rangle. \tag{9.41}$$

This relation can be proven by writing down explicitly the expectation value on the l.h.s. with $\rho = e^{-\beta H}/\operatorname{tr} e^{-\beta H}$ and by inserting the definition of the Heisenberg operators reported in Eq. (9.29). The generalization of this procedure to the case of multi-time correlation functions is straightforward and yields

$$\langle A(t_{A,1},\ldots,t_{A,N})B(t_{B,1},\ldots,t_{B,M})\rangle = \langle B(t_{B,1}-i\beta/2,\ldots,t_{B,M}-i\beta/2)\times A(t_{A,1}+i\beta/2,\ldots,t_{A,N}+i\beta/2)\rangle. \tag{9.42}$$

The real parts of the time variables on the r.h.s. of this equation are such that the corresponding product of operators is anti-time-ordered (see Fig. 9.1). According to their definition in Eq. (9.31), A and B correspond to products of operators with, respectively, decreasing and increasing time arguments from right to left. Consequently, Eq. (9.42) can be expressed as a functional integral by using Eqs. (9.32) and (9.33) on the l.h.s. and r.h.s., respectively. The presence of an imaginary part in the time arguments of Eq. (9.42) does not constitute a problem: in fact, the functional integral along the vertical parts of the time path in Fig. 9.1 can be constructed by the same method as the horizontal parts, which is summarized in Sec. 9.5.1. Hence, we find

$$\begin{aligned}\langle B_+(t_{B,1},\ldots,t_{B,M})A_-(t_{A,1},\ldots,t_{A,N})\rangle \\ = \langle A_+(t_{A,1}+i\beta/2,\ldots,t_{A,N}+i\beta/2) \\ \times B_-(t_{B,1}-i\beta/2,\ldots,t_{B,M}-i\beta/2)\rangle_{S_b}.\end{aligned} \tag{9.43}$$

As we did in Eq. (9.38) for the case of quantum-mechanical time-reversal, we may rewrite this equation in the form

$$\langle \mathcal{O}[\Psi]\rangle = \langle \mathcal{O}[\mathcal{K}_\beta\Psi]\rangle_{S_b}, \tag{9.44}$$

where we define

$$\mathcal{K}_\beta\Psi_\sigma(t) = \Psi_{-\sigma}(t - i\sigma\beta/2). \tag{9.45}$$

[3] We note that this condition is usually expressed in the form

$$\langle A(t_A)B(t_B)\rangle = \langle B(t_B)A(t_A + i\beta)\rangle.$$

However, an equilibrium state is also stationary and therefore both time arguments on the r.h.s. can be translated by $-i\beta/2$ which leads immediately to Eq. (9.41). Here we are assuming that the analytic continuation of real-time correlation functions into the complex plane is possible and unambiguous.

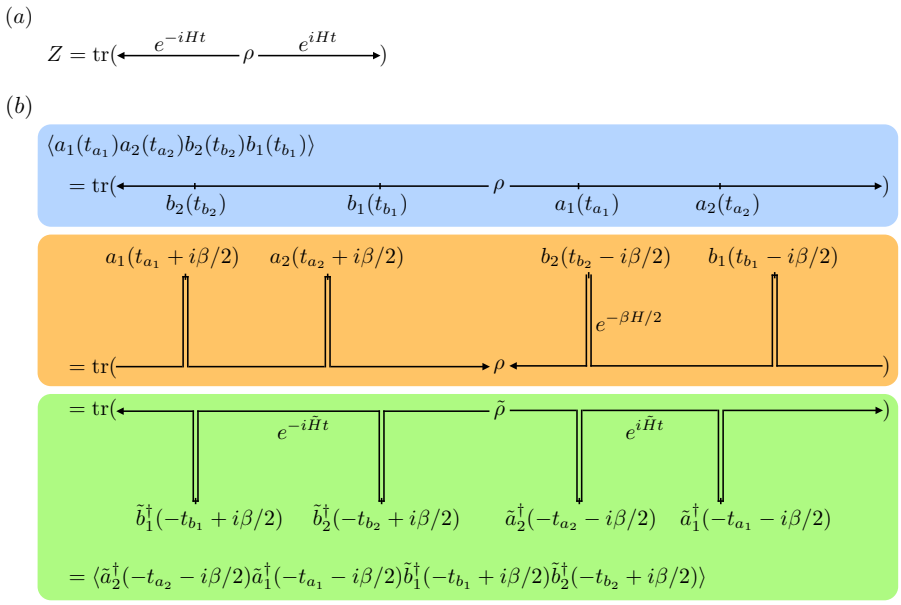

Figure 9.1: (a) Schematic representation of the Schwinger-Keldysh partition function [214, 215]. The time evolution of the density matrix $\rho(t) = e^{-iHt}\rho e^{iHt}$ can be represented by introducing two time lines to the left and right of ρ. These time lines correspond to the $+$ and $-$ parts of the Schwinger-Keldysh contour, respectively. (b) Schematic representation of the KMS condition for a four-time correlation function $\langle a_1(t_{a,1}) a_2(t_{a,2}) b_2(t_{b,2}) b_1(t_{b,1}) \rangle$ with $t_{a,1} < t_{a,2}$ and $t_{b,1} < t_{b,2}$, where $a_{1,2}$ and $b_{1,2}$ are bosonic field operators. As illustrated by the first equality (light blue box), this correlation function is properly time-ordered and therefore it can be directly represented within the Schwinger-Keldysh formalism with the operators $a_{1,2}$ and $b_{1,2}$ evaluated along the $-$ and $+$ contours, respectively. The thermal density matrix $\rho = e^{-\beta H}/\operatorname{tr} e^{-\beta H}$ can be first split into the products of $e^{-\beta H/2} \times e^{-\beta H/2}$ and then these two factors can be moved in opposite directions along the two time lines, with the effect of adding $+i\beta/2$ and $-i\beta/2$ to the time arguments of $a_{1,2}$ and $b_{1,2}$, respectively. After these two factors have been moved to the end of the timelines, due to the cyclic property of the trace, they combine as represented by the second equality (orange box), where the time lines now take detours into the complex plane and the overall time order is effectively reversed as indicated by the arrows, which converge towards ρ instead of departing from it as in the case of sketch (a) or of the first equality of sketch (b). The original time ordering can be then restored by means of the time-reversal operation T, upon application of which operators are replaced by time-reversal transformed ones, $\tilde{\rho} = \mathsf{T}\rho\mathsf{T}^\dagger$ etc., and the signs of time variables are reversed. In addition, due to the anti-unitarity of T one has to take the Hermitian adjoint of the expression inside the trace. As a result, the order of operators is inverted and one obtains the third equality (green box) which is again properly time ordered. This construction can be generalized to arbitrary correlation functions, leading to Eq. (9.46).

This transformation $\mathcal{K}_\beta$ can be combined with the quantum mechanical time reversal T defined in Eq. (9.39) in order to express the equilibrium transformation $\mathcal{T}_\beta$ as $\mathcal{T}_\beta = \mathsf{T} \circ \mathcal{K}_\beta$. [4] By using Eq. (9.38) on the r.h.s. of Eq. (9.44), one concludes that the KMS condition implies

$$\langle \mathcal{O}[\Psi] \rangle = \langle \mathcal{O}[\mathcal{T}_\beta \Psi] \rangle_{\tilde{S}}, \tag{9.46}$$

which indeed provides a generalized FDR for the correlation function $\langle \mathcal{O}[\Psi] \rangle$ [373]. For various choices of the observable $\mathcal{O}[\Psi]$ we obtain the full hierarchy of multi-time FDRs, which contains as a special case the usual FDR for two-time functions (see Sec. 9.6.1). Before demonstrating that this hierarchy is actually equivalent to the invariance of the Schwinger-Keldysh action as expressed by Eq. (9.7), several remarks are in order:

1. Although by means of the time-reversal transformation T we were able to restore the time ordering in Eq. (9.43), Eq. (9.46) still involves the time-reversed action $\tilde{S}$ and not the original action S. However, in practice it will typically be clear how $\tilde{S}$ can be obtained from S, e.g., by reversing the signs of external magnetic fields. In the absence of fields which break time-reversal invariance the tilde in Eq. (9.46) may be dropped, i.e., $\tilde{S} = S$.

2. Equation (9.46) provides a generalized FDR expressed in terms of products $\mathcal{O}[\Psi]$ of fields on the forward and backward branches, which we collected in the four-component vector $\Psi = \left(\psi_+, \psi_+^*, \psi_-, \psi_-^*\right)^T$. A more familiar formulation of FDRs is provided in terms of classical and quantum fields (Φ_c and Φ_q, see Eq. (9.4)), which allow one to identify correlations functions (i.e., expectation values involving only classical fields) and response functions or susceptibilities (expectation values involving both classical and quantum fields). FDRs provide relations between correlation and response functions. In order to express the KMS condition in Eq. (9.46) in terms of the classical and quantum fields Φ_c and Φ_q (or, alternatively, of $\Phi = \left(\phi_c, \phi_c^*, \phi_q, \phi_q^*\right)^T$), we note that they are linearly related to Ψ_+ and Ψ_- and therefore a generic product $\mathcal{O}[\Phi]$ of such fields can be expressed as a linear combination (with real coefficients) of products $\mathcal{O}_i[\Psi]$. According to Eq. (9.46), the expectation value of such a combination and therefore $\langle \mathcal{O}[\Phi] \rangle$ can be expressed as on its r.h.s. in terms of the same linear combination of $\langle \mathcal{O}_i[\mathcal{T}_\beta \Psi] \rangle_{\tilde{S}}$; since the transformation $\mathcal{T}_\beta$ is linear, it immediately follows that this linear combination is nothing but $\langle \mathcal{O}[\mathcal{T}_\beta \Phi] \rangle_{\tilde{S}}$, where the explicit form of the transformation of the components of the field Φ under $\mathcal{T}_\beta$ is reported in Eq. (9.5). The KMS condition then becomes

$$\langle \mathcal{O}[\Phi] \rangle = \langle \mathcal{O}[\mathcal{T}_\beta \Phi] \rangle_{\tilde{S}}. \tag{9.47}$$

   In Sec. 9.6.1, on the basis of Eq. (9.47), we derive the typical form of the FDR, which involves the correlation function of two classical fields and the susceptibility expressed as a correlation between one quantum and one classical field.

3. In the grand canonical ensemble with density matrix $\rho = e^{-\beta(H-\mu N)} / \operatorname{tr} e^{-\beta(H-\mu N)}$, where $N = \int_{\mathbf{x}} \psi^\dagger(\mathbf{x}) \psi(\mathbf{x})$ is the particle number operator, the KMS condition Eq. (9.42) has to be generalized. In order to derive it, we split again the density matrix into a product $e^{-\beta(H-\mu N)/2} \times e^{-\beta(H-\mu N)/2}$

[4] It is straightforward to verify that the transformation T is not modified in the presence of complex time arguments.

(cf. the caption of Fig. 9.1). Then, moving one of the two factors through each of the blocks of operators A and B as in the second (orange) box in panel *(b)* of Fig. 9.1 has not only the effect of adding $+i\beta/2$ and $-i\beta/2$ to the time arguments of the field operators in A and B respectively, as in the case $\mu = 0$; taking into account the canonical commutation relations, additional factors appears due to the fact that

$$\begin{aligned} e^{\sigma\beta\mu N/2}\psi(\mathbf{x})e^{-\sigma\beta\mu N/2} &= e^{-\sigma\beta\mu/2}\psi(\mathbf{x}), \\ e^{\sigma\beta\mu N/2}\psi^\dagger(\mathbf{x})e^{-\sigma\beta\mu N/2} &= e^{\sigma\beta\mu/2}\psi^\dagger(\mathbf{x}), \end{aligned} \tag{9.48}$$

where $\sigma = +1$ and -1 for operators which are part of the time-ordered and anti-time-ordered blocks of operators A and B, respectively. The factors $e^{\pm\sigma\beta\mu/2}$ can be taken out of the expectation value in Eq. (9.42) (corresponding to the trace in Fig. 9.1 *(b)*) and do not affect the restoration of time order by means of the time-reversal transformation, which is illustrated in the last (green) box in panel *(b)* of Fig. 9.1. Therefore, on the r.h.s. of Eq. (9.46) they would appear as prefactors, which are absorbed in the modified transformation given in Eq. (9.6).

9.5.4 From the KMS condition to a symmetry of the Schwinger-Keldysh action

In the previous section we showed that the KMS condition within the Schwinger-Keldysh functional integral formalism takes the form of Eq. (9.46) (with $\mathcal{T}_\beta$ given by either Eq. (9.3) or (9.6)). Here we argue further that the latter relation is equivalent to requiring the invariance of the Schwinger-Keldysh action under the equilibrium symmetry $\mathcal{T}_\beta$. To this end, we express the expectation values on the left and right hand sides of Eq. (9.46) as the functional integrals

$$\langle \mathcal{O}[\Psi] \rangle = \int \mathcal{D}[\Psi]\mathcal{O}[\Psi]e^{iS[\Psi]} \tag{9.49}$$

and

$$\langle \mathcal{O}[\mathcal{T}_\beta\Psi] \rangle_{\tilde{S}} = \int \mathcal{D}[\Psi]\mathcal{O}[\mathcal{T}_\beta\Psi]e^{i\tilde{S}[\Psi]}, \tag{9.50}$$

respectively. Performing a change of integration variables $\Psi \to \mathcal{T}_\beta\Psi$ in the last expression, the argument of $\mathcal{O}$ simplifies because $\mathcal{T}_\beta\Psi \to \mathcal{T}_\beta^2\Psi = \Psi$, since $\mathcal{T}_\beta$ is involutive (see Sec. 9.3). In addition, we show in Appendix 9.D that the absolute value of the determinant of the Jacobian $\mathcal{J} = \delta(\mathcal{T}_\beta\Psi)/\delta\Psi$ associated with $\mathcal{T}_\beta$ equals one, i.e., $|\mathrm{Det}\,\mathcal{J}| = 1$, and therefore the integration measure is not affected by the change of variable. Accordingly, one has

$$\langle \mathcal{O}[\mathcal{T}_\beta\Psi] \rangle_{\tilde{S}} = \int \mathcal{D}[\Psi]\mathcal{O}[\Psi]e^{i\tilde{S}[\mathcal{T}_\beta\Psi]}, \tag{9.51}$$

and by comparing this expression to Eq. (9.49) a *sufficient* condition for their equality is indeed Eq. (9.7), which expresses the invariance of the Schwinger-Keldysh action under the equilibrium transformation. Since the observable $\mathcal{O}[\Psi]$ in Eqs. (9.46), (9.49), and (9.51) is arbitrary, the condition is also *necessary*, which proves that Eqs. (9.7) and (9.46) (and, consequently, the KMS condition) are equivalent.

9.6 Examples

In this section we discuss some concrete examples of how the invariance of a certain Schwinger-Keldysh action under the equilibrium transformation $\mathcal{T}_\beta$ can be used in practice. First we show that Eq. (9.46) (or, equivalently, Eq. (9.47)) contains as a special case the quantum FDR which establishes a relationship between the two-time correlation function of the field ϕ_c (see Eq. (9.4)) and its response to an external perturbation which couples linearly to it. This was also noted in Ref. [373]; however, the conceptual advance done here consists in realizing that the FDR can be regarded as a Ward-Takahashi identity associated with the equilibrium symmetry. In Sec. 9.6.2, instead, we elaborate on the non-equilibrium nature of Markovian dynamics described by a quantum master equation (of the Lindblad form), which is seen to violate explicitly the equilibrium symmetry.

The case of a system which is driven out of equilibrium by a coupling to different baths is considered in Sec. 9.6.3. In particular, we discuss a single bosonic mode coupled to two baths at different temperatures and chemical potentials. Finally, in Sec. 9.6.4 we briefly list a number of additional applications of the symmetry. Some of those have been put into practice in the context of classical dynamical systems, and could be generalized to the quantum case with the aid of the symmetry transformation discussed in the present Chapter.

9.6.1 Fluctuation-dissipation relation for two-time functions

Considering the invariance of the Schwinger-Keldysh action under $\mathcal{T}_\beta$ in Eq. (9.5) as the defining property of thermodynamic equilibrium, the generalized FDR in Eq. (9.47) (which, as discussed above, is nothing but the Ward-Takahashi identity associated with the symmetry), emerges as a *consequence* of equilibrium conditions. Then, from the generalized FDR in Eq. (9.47), the FDR for two-time functions [214, 215] can indeed be derived as a special case. The latter reads

$$\begin{aligned} G^K(\omega,\mathbf{q}) &= \big(G^R(\omega,\mathbf{q}) - G^A(\omega,\mathbf{q})\big)\coth(\beta\omega/2) \\ &= i\,2\Im G^R(\omega,\mathbf{q})\coth(\beta\omega/2), \end{aligned} \tag{9.52}$$

where the Keldysh, retarded, and advanced Green's functions G^K, G^R, and G^A, respectively, are related to expectation values of classical and quantum fields via

$$\begin{aligned} iG^K(\omega,\mathbf{q})\,(2\pi)^{d+1}\,\delta(\omega-\omega')\delta^{(d)}(\mathbf{q}-\mathbf{q}') &= \langle\phi_c(\omega,\mathbf{q})\phi_c^*(\omega',\mathbf{q}')\rangle, \\ iG^R(\omega,\mathbf{q})\,(2\pi)^{d+1}\,\delta(\omega-\omega')\delta^{(d)}(\mathbf{q}-\mathbf{q}') &= \langle\phi_c(\omega,\mathbf{q})\phi_q^*(\omega',\mathbf{q}')\rangle, \\ iG^A(\omega,\mathbf{q})\,(2\pi)^{d+1}\,\delta(\omega-\omega')\delta^{(d)}(\mathbf{q}-\mathbf{q}') &= \langle\phi_q(\omega,\mathbf{q})\phi_c^*(\omega',\mathbf{q}')\rangle. \end{aligned} \tag{9.53}$$

Here we are assuming translational invariance in both time and space, which is reflected in the appearance of frequency- and momentum-conserving δ-functions in the previous expressions. The FDR valid in classical systems [376, 377] can be recovered from the quantum FDR Eq. (9.52) by taking the classical limit as described in Sec. 9.4.3. Contrary to what one might suspect at a first glance from the appearance of the time-reversed action $\tilde{S}$ in the generalized FDR in Eq. (9.47), the derivation of the FDR for two-time functions we present below is valid *irrespective* of whether the action contains external fields which break TRI or not.

Let us consider the identity Eq. (9.47) for specific choices of the functional $\mathcal{O}[\Phi]$. In particular, by taking $\mathcal{O}$ to be equal to $\phi_q\phi_q^*$, the expectation value on the l.h.s. of Eq. (9.47) has to vanish due to causality [215] and therefore

$$0 = \langle \phi_q(\omega, \mathbf{q})\phi_q^*(\omega', \mathbf{q}')\rangle = \langle \mathcal{T}_\beta\phi_q(\omega, -\mathbf{q})\mathcal{T}_\beta\phi_q^*(\omega', -\mathbf{q}')\rangle_{\tilde{S}}. \tag{9.54}$$

Upon inserting the expression of the fields transformed according to Eq. (9.5), one readily finds the FDR

$$G^K_{\tilde{S}}(\omega, \mathbf{q}) = \Big(G^R_{\tilde{S}}(\omega, \mathbf{q}) - G^A_{\tilde{S}}(\omega, \mathbf{q})\Big)\coth(\beta\omega/2) \tag{9.55}$$

with the time-reversed action $\tilde{S}$. By setting, instead, $\mathcal{O}$ equal to the product of two classical fields, the l.h.s. of Eq. (9.47) renders the Keldysh Green's function G^K in Eq. (9.53); by using the explicit form of $\mathcal{T}_\beta$ in Eq. (9.5) and the FDR derived above, the r.h.s. of that equation coincides with $G^K_{\tilde{S}}$ and therefore one concludes that

$$G^K_{\tilde{S}}(\omega, \mathbf{q}) = G^K(\omega, -\mathbf{q}), \tag{9.56}$$

which expresses the transformation behavior of the Keldysh Green's function under time reversal of the Hamiltonian. Finally, by replacing $\mathcal{O}[\Phi]$ in Eq. (9.47) with the product $\phi_c(\omega, \mathbf{q})\phi_q^*(\omega', \mathbf{q})$ of one classical and one quantum field, the l.h.s. renders by definition the retarded Green's function G^R while the r.h.s. can be worked out as explained above. Taking into account Eq. (9.55), one can eliminate the Keldysh Green's function G^K appearing on the r.h.s. in favor of the retarded and advanced Green's functions G^R and G^A, respectively, and eventually finds

$$G^R_{\tilde{S}}(\omega, \mathbf{q}) = G^R(\omega, -\mathbf{q}). \tag{9.57}$$

This relation, together with its complex conjugate (which relates the advanced Green's functions calculated from the original and time-reversed Hamiltonians, respectively) and Eqs. (9.56) and (9.55), yields the FDR (9.52).

9.6.2 Non-equilibrium nature of steady states of quantum master equations

In classical statistical physics, the coupling of a system to a thermal bath and the resulting relaxation to thermodynamic equilibrium are commonly modelled in terms of Markovian stochastic processes, which can be described, e.g., by suitable Langevin equations with Gaussian white noise [313]. The Markovian dynamics of a *quantum* system, on the other hand, is described by a quantum master equation in the Lindblad form [385,386] (or by an equivalent Schwinger-Keldysh functional integral). Under specific conditions on the structure of the Lindblad operator [256,397], the stationary state of this dynamics is described by a thermal Gibbs distribution, such that all *static* properties (equal-time correlation functions) are indistinguishable from those in thermodynamic equilibrium. In spite of this fact, however, *dynamical* signatures of thermodynamic equilibrium such as the KMS condition (see Sec. 9.5.3) and the FDR (see Sec. 9.6.1) are violated [368,369]. This violation can be traced back to the fact that the Markovian and rotating wave approximations, which are done in deriving this quantum master equation causes an *explicit* breaking of the equilibrium symmetry as we show in this section — i.e., although the system is coupled to a bath in thermodynamic equilibrium, the system itself does not reach equilibrium. Physically, this can be understood by noting that the microscopic dynamics

underlying an approximate Markovian behavior in this case is indeed driven. A typical example in the context of quantum optics is an atom with two relevant energy levels separated by a level spacing ω_0 and subject to an external driving laser with frequency ν detuned from resonance by an amount $\Delta = \nu - \omega_0 \ll \omega_0$. Transitions between the ground and the excited state are made possible only by the driving laser, and the energy scale which controls the validity of the Markov approximation in the dynamics of the two-level system is set by ω_0. The excited state is assumed to be unstable and it can undergo spontaneous decay by emitting a photon to the radiation field, which acts as a reservoir. This illustrates the combined driven and dissipative nature of such quantum optical systems.

In order to investigate in more detail the effect of the Markovian approximation typically done in the driven context on the validity of the equilibrium symmetry $\mathcal{T}_\beta$, we consider a system with a certain action S whose degrees of freedom are linearly coupled to those of a thermal bath. By integrating out the latter degrees of freedom, a dissipative contribution to the original action is generated. In order to simplify the discussion, we assume that the bath consists of non-interacting harmonic oscillators $b_{\mu,\sigma}(t)$, labelled by an index μ (with σ referring to the branch of the Schwinger-Keldysh contour), with proper frequency ω_μ, which are in thermodynamic equilibrium at a temperature $T = 1/\beta$. The Schwinger-Keldysh action of the bath is then given by

$$S_b = \sum_\mu \int_{t,t'} \left(b^*_{\mu,+}(t), b^*_{\mu,-}(t)\right) \begin{pmatrix} G^{++}_\mu(t,t') & G^{+-}_\mu(t,t') \\ G^{-+}_\mu(t,t') & G^{--}_\mu(t,t') \end{pmatrix}^{-1} \begin{pmatrix} b_{\mu,+}(t') \\ b_{\mu,-}(t') \end{pmatrix}, \tag{9.58}$$

where the Green's functions $iG^{\sigma\sigma'}_\mu(t,t') = \langle b_{\mu,\sigma}(t) b^*_{\mu,\sigma'}(t')\rangle$ for the oscillators of the bath are fixed by requiring it to be in equilibrium and therefore they read [214, 215]

$$\begin{aligned} G^{+-}_\mu(t,t') &= -in(\omega_\mu) e^{-i\omega_\mu(t-t')}, \\ G^{-+}_\mu(t,t') &= -i\left(n(\omega_\mu)+1\right) e^{-i\omega_\mu(t-t')}, \\ G^{++}_\mu(t,t') &= \theta(t-t') G^{-+}_\mu(t,t') + \theta(t'-t) G^{+-}_\mu(t,t'), \\ G^{--}_\mu(t,t') &= \theta(t'-t) G^{-+}_\mu(t,t') + \theta(t-t') G^{+-}_\mu(t,t'). \end{aligned} \tag{9.59}$$

Here $n(\omega) = 1/\left(e^{\beta\omega}-1\right)$ is the Bose distribution function and $\theta(t)$ denotes the Heaviside step function, which is defined as

$$\theta(t) = \begin{cases} 1, & t \geq 0, \\ 0, & t < 0. \end{cases} \tag{9.60}$$

The coupling S_{sb} between the system and the bath is assumed to be linear in the bath variables and has a strength $\sqrt{\gamma_\mu}$,

$$S_{sb} = \sum_\mu \sqrt{\gamma_\mu} \int_t \left(L^*_+(t) b_{\mu,+}(t) + L_+(t) b^*_{\mu,+}(t) - L^*_-(t) b_{\mu,-}(t) - L_-(t) b^*_{\mu,-}(t)\right). \tag{9.61}$$

Here $L_\pm(t)$ are associated with the quantum jump or Lindblad operators, which we assume to be quasilocal polynomials of the system's bosonic fields $\{\psi_\pm, \psi^*_\pm\}$ resulting from normally ordered operators in a second quantized description (e.g., the simplest choice would be $L_\pm(t) = \psi_\pm(t, \mathbf{x})$). In order to simplify the notation, we do not indicate here the spatial dependence of the fields (both of

the system and of the bath), which is understood together with the corresponding integration over space. We assume the harmonic oscillators which constitute the bath to be spatially uncorrelated. The Schwinger-Keldysh functional integral with total action $S + S_b + S_{sb}$ involving both system and bath degrees of freedom is quadratic in the latter and, therefore, the bath can be integrated out. The resulting contribution is

$$S' = -\int_{\omega_0-\vartheta}^{\omega_0+\vartheta} \mathrm{d}\omega\, \gamma(\omega)\nu(\omega) \int_{t,t'} \big(L_+^*(t), -L_-^*(t)\big) \begin{pmatrix} G_\omega^{++}(t,t') & G_\omega^{+-}(t,t') \\ G_\omega^{-+}(t,t') & G_\omega^{--}(t,t') \end{pmatrix} \begin{pmatrix} L_+(t') \\ -L_-(t') \end{pmatrix}, \tag{9.62}$$

which eventually sums to S. In deriving this action, we made the additional assumption that the bath modes $\{\omega_\mu\}_\mu$ form a dense continuum with a spectral density $\nu(\omega) = \sum_\mu \delta(\omega - \omega_\mu)$, centered around a frequency ω_0, with a bandwidth ϑ (see further below for its interpretation). Then, sums of the form $\sum_\mu \gamma_\mu \cdots$ can be approximated as integrals over frequencies $\int_{\omega_0-\vartheta}^{\omega_0+\vartheta} \mathrm{d}\omega\, \gamma(\omega)\nu(\omega)\cdots$, where $\gamma(\omega)$ describes the frequency distribution of the oscillator strengths. Inserting the explicit expressions (9.59) for the bath Green's functions into Eq. (9.62), we obtain

$$\begin{aligned} S' = -i \int_{\omega_0-\vartheta}^{\omega_0+\vartheta} \frac{\mathrm{d}\omega}{2\pi} \gamma(\omega)\nu(\omega) \Bigg(& n(\omega) L_+^*(\omega) L_-(\omega) + [n(\omega)+1]\, L_-^*(\omega) L_+(\omega) \\ & - \int_{-\infty}^{+\infty} \frac{\mathrm{d}\omega'}{2\pi} \Bigg\{ \Big[\theta(\omega'-\omega)\,(n(\omega)+1) + \theta(-\omega'+\omega) n(\omega) \Big] L_+^*(\omega') L_+(\omega') \\ & \qquad + \big[\theta(-\omega'+\omega)\,(n(\omega)+1) + \theta(\omega'-\omega) n(\omega) \big]\, L_-^*(\omega') L_-(\omega') \Bigg\} \Bigg), \end{aligned} \tag{9.63}$$

where $L_\sigma(\omega)$ describe the quantum jump operators in the frequency space, and $\theta(\omega) = i\mathcal{P}\frac{1}{\omega} + \pi\delta(\omega)$ (where $\mathcal{P}$ denotes the Cauchy principal value) is the Fourier transform of $\theta(t)$ in Eq. (9.60). The terms involving the principal value contribute to the Hamiltonian part of the total Schwinger-Keldysh action of the system $S + S'$. Assuming that the jump operators are quasilocal polynomials of the bosonic field operators of the system, $L_\sigma(\omega)$ transform under $\mathcal{T}_{\beta'}$ as the field operators, i.e.,

$$\mathcal{T}_{\beta'} L_\sigma(\omega) = e^{-\sigma\beta'\omega/2} L_\sigma^*(\omega) \quad \text{and} \quad \mathcal{T}_{\beta'} L_\sigma^*(\omega) = e^{\sigma\beta'\omega/2} L_\sigma(\omega); \tag{9.64}$$

inserting these expressions in Eq. (9.63) one finds that the contour-diagonal terms (i.e., those proportional to $L_\sigma^*(\omega)L_\sigma(\omega)$ with $\sigma = \pm 1$, which include, in particular, the above-mentioned principal value terms) are invariant due to frequency conservation (cf. the discussion in Sec. 9.4.1). On the other hand, for the contribution which is off-diagonal in the Schwinger-Keldysh contour one finds

$$S'_{\mathrm{off-diag}}[\mathcal{T}_{\beta'}\Psi] = -i \int_{\omega_0-\vartheta}^{\omega_0+\vartheta} \frac{\mathrm{d}\omega}{2\pi} \gamma(\omega)\nu(\omega) \Big[n(\omega) e^{\beta'\omega} L_+(\omega) L_-^*(\omega) + (n(\omega)+1)\, e^{-\beta'\omega} L_-(\omega) L_+^*(\omega) \Big]. \tag{9.65}$$

If the value of β' matches the inverse temperature $\beta = 1/T$ of the bath modes, encoded in $n(\omega)$, it is easy to see that these terms are invariant under $\mathcal{T}_\beta$ because $n(\omega)e^{\beta\omega} = n(\omega) + 1$. In summary, one concludes that $S'[\mathcal{T}_\beta\Psi] = S'[\Psi]$ and being also the action S of the system in isolation invariant under $\mathcal{T}_\beta$, the same holds for the total effective action $S + S'$ of the system in contact with the thermal bath.

In order to understand the effect of the Markovian approximation in the driven context on the invariance under $\mathcal{T}_\beta$, let us now consider Eq. (9.63) after this approximation has been done. In particular, in order for these approximations to be valid, we assume that one can choose a "rotating" frame in which the evolution of the system is slow compared to the energy scales ω_0 and ϑ which characterize the bath. This is possible if the system is driven by an external classical field such as a laser, so that the frequency of the drive bridges the gap between the natural time scales of the system and those of the bath. Then, all jump operators in Eq. (9.62) may be evaluated at the same time t, since the integral kernel in Eq. (9.62) (i.e., the product of bath Green's functions $G_\omega^{\sigma\sigma'}$, density of states $\nu(\omega)$ and oscillator strength distribution $\gamma(\omega)$, integrated over the bath bandwidth) differs from zero only within a correlation time $\tau_c \approx 1/\vartheta$, which is assumed to be much shorter than the timescale over which $L_\sigma(t)$ evolves in the rotating frame. Additionally we assume that the spectral density $\nu(\omega)$ of the states of the bath and the corresponding coupling strength $\sqrt{\gamma(\omega)}$ to the system do not vary appreciably within the relevant window $\omega_0 - \vartheta < \omega < \omega_0 + \vartheta$, such that one can set $\gamma(\omega)\nu(\omega) \approx \gamma(\omega_0)\nu(\omega_0)$. As before, the terms in Eq. (9.63) which are diagonal in the contour indices are invariant under $\mathcal{T}_\beta$ (see Eq. (9.64)) also after the Markovian approximation; accordingly, we focus on the off-diagonal terms in Eq. (9.65), which become

$$S'_{\mathrm{off-diag}}[\Psi] = -i\gamma(\omega_0)\nu(\omega_0)\int_{-\infty}^{\infty}\frac{\mathrm{d}\omega}{2\pi}\left[\bar{n}L_+^*(\omega)L_-(\omega) + (\bar{n}+1)\,L_-^*(\omega)L_+(\omega)\right], \tag{9.66}$$

where $\bar{n} = n(\omega_0)$ is the occupation number of the bath modes at frequency ω_0. This makes it clear that ϑ acts as a high-frequency cutoff, whose precise value, under Markovian conditions, does not affect the physics. Applying the transformation $\mathcal{T}_\beta$ to the fields one has

$$S'_{\mathrm{off-diag}}[\mathcal{T}_\beta\Psi] = -i\gamma(\omega_0)\nu(\omega_0)\int_{-\infty}^{\infty}\frac{\mathrm{d}\omega}{2\pi}\left[\bar{n}e^{\beta\omega}L_+(\omega)L_-^*(\omega) + (\bar{n}+1)\,e^{-\beta\omega}L_-(\omega)L_+^*(\omega)\right]. \tag{9.67}$$

In order for $S'_{\mathrm{off-diag}}$ to be invariant under $\mathcal{T}_\beta$, this expression should be equal to $S'_{\mathrm{off-diag}}[\Psi]$ in Eq. (9.66), which requires $\bar{n}e^{\beta\omega} = \bar{n} + 1$ for all values of the frequencies ω within the relevant region $\omega_0 - \vartheta < \omega < \omega_0 + \vartheta$. Clearly this is not possible and therefore the equilibrium symmetry is explicitly broken by the Markovian approximation in the driven context.

9.6.3 System coupled to different baths

A simple way to drive a system out of equilibrium is to bring it in contact with baths at different temperatures and chemical potentials. In this case, a net flux of energy and particles is established across the system, preventing it from thermalizing and, consequently, causing a violation of the symmetry $\mathcal{T}_\beta$. This scenario occurs, e.g., in the context of quantum electronics in a quantum dot connected by tunnel electrodes to two leads, between which a finite voltage difference is maintained. Here, for simplicity, we consider a minimal bosonic counterpart of this system, constituted by a single bosonic mode — described by the fields $\{\psi_\pm, \psi_\pm^*\}$ coupled to two baths of non-interacting harmonic oscillators kept at different temperatures and chemical potentials. We show explicitly that the non-equilibrium nature of this setup is accompanied by a violation of the equilibrium symmetry. The generalization of this argument to a multi-mode system or to a larger number of baths is straightforward.

We consider two baths of non-interacting harmonic oscillators $b_{i,\nu}(t)$, where the label $i = 1, 2$ denotes the bath to which the operator belongs, while ν denotes the corresponding mode with frequency $\omega_{i,\nu}$. Each bath is assumed to be in thermodynamic equilibrium with different inverse temperatures β_1, β_2 and different chemical potentials μ_1, μ_2. The Schwinger-Keldysh action $S_{b,i}$ of each bath takes the same form as in Eq. (9.58). However, in the present case, the distribution functions $n_i(\omega)$ entering the bath Green's functions depend on the chemical potentials μ_i as $n_i(\omega) = 1/(e^{\beta_i(\omega-\mu_i)}-1)$. As in the previous section, the bath is assumed to be coupled linearly to the system variables $L_\pm(t)$ which are quasilocal polynomials of the bosonic fields $\{\psi_\pm, \psi_\pm^*\}$. The dynamics of the system and the baths is then controlled by a functional integral with the total Schwinger-Keldysh action $S + S_{b,1} + S_{b,2} + S_{sb}$, where S is to the action of the system, i.e., the single bosonic mode, and S_{sb} is the system-bath coupling. As in the previous section, an effective dynamics for the system's variables can be obtained by integrating out those of the bath. This yields an effective action

$$S' = -i\int_{-\infty}^{+\infty}\frac{\mathrm{d}\omega}{2\pi}\tilde{J}(\omega)\left(\tilde{n}(\omega)L_+^*(\omega)L_-(\omega) + (\tilde{n}(\omega)+1)\,L_-^*(\omega)L_+(\omega) - \int_{-\infty}^{\infty}\frac{\mathrm{d}\omega'}{2\pi}\Big\{\left[\theta(\omega'-\omega)\,(\tilde{n}(\omega)+1)\right.\right.$$
$$\left.\left.+\theta(-\omega'+\omega)\tilde{n}(\omega)\right]L_+^*(\omega')L_+(\omega') + \left[\theta(-\omega'+\omega)\,(\tilde{n}(\omega)+1) + \theta(\omega'-\omega)\tilde{n}(\omega)\right]L_-^*(\omega')L_-(\omega')\Big\}\right). \tag{9.68}$$

The action S' is formally similar to the one in Eq. (9.63), with the spectral density $\gamma(\omega)\nu(\omega)$ replaced by the sum of the spectral densities of the baths $\tilde{J}(\omega) = J_1(\omega) + J_2(\omega)$, where $J_i(\omega) = \gamma_i(\omega)\nu_i(\omega)$ (with $\nu_i(\omega)$ and $\gamma_i(\omega)$ defined as in Sec. 9.6.2, see after Eq. (9.62)). Analogously, the distribution function $n(\omega)$ of the single bath we considered in Sec. 9.6.2 is replaced by the average of the distribution functions of the two baths $i = 1, 2$ weighted by the relative spectral densities, i.e.,

$$\tilde{n}(\omega) = \frac{J_1(\omega)}{J_1(\omega)+J_2(\omega)}n_1(\omega) + \frac{J_2(\omega)}{J_1(\omega)+J_2(\omega)}n_2(\omega). \tag{9.69}$$

Now, we consider how the effective action (9.68) transforms under the thermal symmetry $\mathcal{T}_\beta$. Since here we are explicitly considering the presence of chemical potentials, we will actually use the generalization of the symmetry $\mathcal{T}_{\beta,\mu}$ in Eq. (9.6). As discussed in Sec. 9.6.2, since $L_\pm, L_\pm^*$ are quasilocal polynomials of the bosonic fields of the system, they transform under $\mathcal{T}_{\beta,\mu}$ as

$$\begin{aligned}\mathcal{T}_{\beta,\mu}L_\sigma(\omega) &= e^{-\sigma\beta(\omega-\mu)/2}L_\sigma^*(\omega),\\ \mathcal{T}_{\beta,\mu}L_\sigma^*(\omega) &= e^{\sigma\beta(\omega-\mu)/2}L_\sigma(\omega).\end{aligned} \tag{9.70}$$

Accordingly, the products $L_\sigma(\omega)L_\sigma^*(\omega)$ are invariant under the symmetry and therefore the contour-diagonal part of S', which contains such terms, is invariant. On the other hand, the part $S'_{\mathrm{off-diag}}$ of S' which is off-diagonal in the Schwinger-Keldysh contour (i.e., the first two terms on the r.h.s. of Eq. (9.68)) is modified as:

$$S'_{\mathrm{off-diag}}[\mathcal{T}_{\beta,\mu}\Psi] = -i\int_{-\infty}^{+\infty}\frac{\mathrm{d}\omega}{2\pi}\tilde{J}(\omega)\left[\tilde{n}(\omega)e^{\beta(\omega-\mu)}L_+(\omega)L_-^*(\omega) + (\tilde{n}(\omega)+1)\,e^{-\beta(\omega-\mu)}L_-(\omega)L_+^*(\omega)\right]. \tag{9.71}$$

Comparing this expression with Eq. (9.68), one readily sees that the invariance of this term under $\mathcal{T}_{\beta,\mu}$ requires $\tilde{n}(\omega)e^{\beta(\omega-\mu)} = \tilde{n}(\omega) + 1$, and therefore $S'_{\mathrm{off-diag}}$ is not invariant under $\mathcal{T}_{\beta,\mu}$, unless the two baths have the same temperature and chemical potential, i.e., $\beta_1 = \beta_2 = \beta$ and $\mu_1 = \mu_2 = \mu$. In this case, one can easily verify from Eq. (9.69) that the average distribution function $\widetilde{n}(\omega)$ is just the Bose-Einstein distribution $\tilde{n}(\omega) = 1/(e^{\beta(\omega-\mu)} - 1)$ and, as a consequence, $\tilde{n}(\omega)e^{\beta(\omega-\mu)} = \tilde{n}(\omega) + 1$.

In conclusion, when the system is driven out of equilibrium by a net flux of energy or particles, induced by a difference between the temperatures or the chemical potentials of the baths, the total action of the system is no longer invariant under $\mathcal{T}_{\beta,\mu}$, as $S'[\mathcal{T}_{\beta,\mu}\Psi] \neq S'[\Psi]$.

9.6.4 Further applications

Among the various possible applications of th symmetry $\mathcal{T}_\beta$, we mention here:

Symmetry-preserving approximations. Properties of interacting many-body systems can usually be obtained only by resorting to certain approximations. Then, while FDRs for correlation and response functions can be established exactly in the absence of interactions, in an approximate inclusion of the latter one has to make sure that the FDRs are not broken. In other words, the approximation should conserve the thermal symmetry. This requirement for classical statistical systems has been implemented in the mode-coupling theory of the glass transition in Ref. [399].

The field-theoretic formalism provides the natural framework for studying the behavior of systems at long wavelengths and low energies by employing renormalization-group methods. In any of these methods, an effective description which is obtained by integrating out fast fluctuations must have the same symmetries as those present at microscopic scales. For example, in the case of the functional renormalization group (for reviews see Refs. [234, 240, 400–402]), this is achieved by choosing an ansatz to approximate the scale-dependent effective action which incorporates these symmetries. In this context, the classical limit of the thermal symmetry discussed here has been used in functional renormalization group studies of model A [244] and model C [403]. The quantum thermal symmetry, instead, is analogously preserved by the ansatz for the effective action chosen in Ref. [404] (in the form of FDT), where the scale-dependent crossover from quantum to classical dynamics is studied. Alternatively, one can devise approximation schemes which are compatible with the equivalent KMS conditions, as discussed in detail in Ref. [373]. Note, however, that in this work the KMS condition in the form of Eq. (9.46) is imposed on the scale-dependent Green's functions (supplemented by the corresponding condition on the vertex functions). On the other hand, the symmetry constraint can directly be applied to the effective action itself, which is the generating functional of vertex functions and contains information on all correlation functions.

Fluctuation relations. Another concrete example of the usefulness of the thermal symmetry is provided by the derivation of transient fluctuation relations [405, 406] for time-dependent particle transport in Ref. [384]. There, the symmetry is generalized in order to account for the presence of a time-dependent counting field which probes the current flowing through the system. This generalized symmetry yields a relation analogous to Eq. (9.46) (however, formulated in terms of the generating functional for correlation and response functions), from which, e.g., a fluctuation relation for the probability distribution of work done on the system and the transmitted charge can be derived.

9.7 Concluding remarks

We demonstrated here that the Schwinger-Keldysh action describing the dynamics of a generic quantum many-body system acquires a certain symmetry $\mathcal{T}_\beta$ if the evolution occurs in thermal equilibrium. To a certain extent, this symmetry was discussed in Ref. [384] in the specific context of fluctuation relations for particle transport. We traced the origin of this symmetry back to the Kubo-Martin-Schwinger (KMS) condition which establishes a relationship between multi-time correlation functions in real and imaginary times of a system in canonical equilibrium at a certain temperature. Fluctuation-dissipation relations are then derived as the Ward-Takahashi identities associated with $\mathcal{T}_\beta$. Remarkably, in the classical limit, this equilibrium symmetry reduces to the one known in classical stochastic systems, where it was derived from the assumption of detailed balance. By comparing with this classical case, important questions on the nature of equilibrium in quantum systems arise. In particular, while microreversibility and detailed balance of the dynamics are deeply connected to the notion of equilibrium in classical stochastic systems, an analogous relationship for quantum systems does not clearly emerge and surely deserves further investigation.

The equilibrium symmetry $\mathcal{T}_\beta$ is expected to play a crucial role in the study of thermalization in quantum systems, in particular when combined with a renormalization-group analysis. In fact, on the one hand, it provides a simple but powerful theoretical tool to assess whether a certain system is able to reproduce thermal equilibrium. This can indeed be accomplished by a direct inspection of the microscopic Schwinger-Keldysh action (or of the effective one generated after integrating out some degrees of freedom, e.g., along a renormalization-group flow) which describes the dynamics of the system, rather than checking, for instance, the validity of the fluctuation-dissipation relations among various correlation functions. On the other hand, the equilibrium symmetry might be useful also in order to investigate or characterize possible departures from equilibrium and, in this respect, it would be interesting to consider the case in which the system evolves in a generalized Gibbs ensemble [31, 61, 62, 68, 95, 96, 109, 389, 390]. Finally, while we focussed here on the case of bosons, the extension of our analysis to different statistics, for instance fermionic and spin systems, represents an interesting issue.

Appendix

9.A Invariance of quadratic dissipative contributions

In order to show explicitly the invariance of S_d in Eq. (9.19) under the transformation $\mathcal{T}_\beta$ in Eq. (9.5), it is convenient to assume that $h(\omega, \mathbf{q})$ as a function of the frequency ω has definite parity and to consider separately the cases of an odd and even function, $h_o(-\omega, \mathbf{q}) = -h_o(\omega, \mathbf{q})$ and $h_e(-\omega, \mathbf{q}) = h_e(\omega, \mathbf{q})$, respectively. The generic case follows straightforwardly by linear combination. We then consider how the actions

$$S_d = i\epsilon \int_{\omega,\mathbf{q}} \Phi_q^\dagger(\omega, \mathbf{q}) \begin{Bmatrix} h_o(\omega, \mathbf{q}) \\ h_e(\omega, \mathbf{q})\sigma_z \end{Bmatrix} (\Phi_c(\omega, \mathbf{q}) + \coth(\beta\omega/2)\Phi_q(\omega, \mathbf{q})) \tag{9.72}$$

— where Φ is introduced in Sec. 9.4.1, see Eq. (9.12) — with a certain β transform under a transformation $\mathcal{T}_{\beta'}$ [see Eq. (9.5)] of the fields, with a generic parameter β'. One finds

$$\begin{aligned} S_d[\mathcal{T}_{\beta'}\Phi] = i\epsilon \int_{\omega,\mathbf{q}} \Big(\sinh(\beta'\omega/2)\Phi_c^\dagger(-\omega, \mathbf{q}) + \cosh(\beta'\omega/2)\Phi_q^\dagger(-\omega, \mathbf{q})\Big) \sigma_x \begin{Bmatrix} h_o(\omega, \mathbf{q}) \\ h_e(\omega, \mathbf{q})\sigma_z \end{Bmatrix} \sigma_x \\ \times \big[\cosh(\beta'\omega/2)\Phi_c(-\omega, \mathbf{q}) - \sinh(\beta'\omega/2)\Phi_q(-\omega, \mathbf{q}) \coth(\beta\omega/2) \big(-\sinh(\beta'\omega/2)\Phi_c(-\omega, \mathbf{q}) + \cosh(\beta'\omega/2)\Phi_q(-\omega, \mathbf{q})\big)\big] . \end{aligned} \tag{9.73}$$

Note that the terms in the second and third lines involving solely the classical field spinor Φ_c cancel each other only if $\beta' = \beta$. Otherwise, terms $\propto \Phi_c^\dagger \Phi_c$ remain, which actually lead to a violation of causality [215]. For $\beta' = \beta$ instead, we obtain

$$\begin{aligned} S_d[\mathcal{T}_\beta\Phi] = -i\epsilon \int_{\omega,\mathbf{q}} \Big(-\sinh(\beta\omega/2)\Phi_c^\dagger(\omega, \mathbf{q}) + \cosh(\beta\omega/2)\Phi_q^\dagger(\omega, \mathbf{q})\Big) \begin{Bmatrix} h_o(\omega, \mathbf{q}) \\ h_e(\omega, \mathbf{q})\sigma_z \end{Bmatrix} \\ \times (\sinh(\beta\omega/2) - \coth(\beta\omega/2)\cosh(\beta\omega/2))\, \Phi_q(\omega, \mathbf{q}). \end{aligned} \tag{9.74}$$

By means of the identity

$$\sinh x - \coth x \cosh x = -1/\sinh x, \tag{9.75}$$

and after some straightforward algebraic manipulations one eventually finds that $S_d[\mathcal{T}_\beta\Phi] = S_d[\Phi]$, i.e., that S_d (with a certain β) is invariant under $\mathcal{T}_\beta$.

9.B Invariance of dissipative vertices

As pointed out in the main text, a first constraint that has to be imposed on the functions $f_{1,2,3}$ appearing in the dissipative vertex in Eq. (9.20) follows from the requirement of causality of the Schwinger-Keldysh action. The latter must vanish when $\psi_+ = \psi_-$ [215], which implies the condition

$$\int_{\omega_1,\ldots,\omega_4} \delta(\omega_1 - \omega_2 + \omega_3 - \omega_4)\psi_+^*(\omega_1)\psi_+(\omega_2)\psi_+^*(\omega_3)\psi_+(\omega_4) \times [f_1(\omega_1,\omega_2,\omega_3,\omega_4) + f_2(\omega_1,\omega_2,\omega_3,\omega_4) + f_3(\omega_1,\omega_2,\omega_3,\omega_4)] = 0. \quad (9.76)$$

Now let us consider Eq. (9.20) with the transformed fields $\mathcal{T}_\beta\Psi_\sigma$, i.e., $S_d[\mathcal{T}_\beta\Psi]$. Requiring it to be equal to $S_d[\Psi]$, we find that the following conditions should be fulfilled:

$$\begin{aligned} &f_1(\omega_1,\omega_2,\omega_3,\omega_4) - f_1(\omega_2,\omega_1,\omega_4,\omega_3) = 0, \\ &f_2(\omega_1,\omega_2,\omega_3,\omega_4) - f_2(\omega_2,\omega_1,\omega_4,\omega_3) = 0, \\ &f_3(\omega_1,\omega_2,\omega_3,\omega_4) - e^{\beta(\omega_1-\omega_2)} f_3(\omega_2,\omega_1,\omega_4,\omega_3) = 0, \end{aligned} \quad (9.77)$$

where we used the conservation of frequencies implied by the δ-function in Eq. (9.20) to simplify the exponent in the last line. Specifically, the necessary conditions are that the expressions on the l.h.s. of these relations should vanish when integrated over frequencies after having been multiplied by the corresponding combinations of fields and factors $f_{1,2,3}$ in Eq. (9.20) and by the δ-function on frequencies. The relations in Eq. (9.77) are, however, sufficient conditions for the equality of $S_d[\mathcal{T}_\beta\Psi]$ and $S_d[\Psi]$.

To begin with we investigate the possible existence of a frequency-independent solution of Eqs. (9.76) and (9.77) for $f_{1,2,3}$; these two equations then imply

$$f_1 = -f_2 = \text{constant} \quad \text{and} \quad f_3 = 0. \quad (9.78)$$

However, this solution can be seen to lack physical relevance for the following reason: any physically sensible dissipative contribution to the Schwinger-Keldysh action compatible with the thermal symmetry can be considered as originating from integrating out a thermal bath which is appropriately coupled to the system. Anticipating the discussion of Sec. 9.6.2, we note that such dissipative contributions always involve terms which are not diagonal in the contour indices (cf. Eq. (9.62)). S_d with $f_{1,2,3}$ given by Eq. (9.78), however, is *not* of this form. In fact, inserting Eq. (9.78) in Eq. (9.20) yields a vertex that is equal to the two-body interaction in Eq. (9.11) apart from an overall factor of i, i.e., such a vertex would originate from an *imaginary* two-body coupling in a Hamiltonian. Clearly, this would violate hermiticity, rendering the Hamiltonian unphysical.

While this demonstrates that — as anticipated in the main text — a frequency-independent number-conserving quartic vertex is not compatible with equilibrium conditions, solutions of Eqs. (9.76) and (9.77) *do* exist with f_i depending on frequency. One particular solution is given by Eq. (9.21) of the main text.

9.C Representation of correlation functions in the Schwinger-Keldysh formalism

Two-time correlation functions. In order to derive the representation of a two-time correlation function in the Schwinger-Keldysh formalism reported in Eq. (9.30), we insert the explicit expressions (9.29) for the Heisenberg operators $A(t_A)$ and $B(t_B)$ in the trace which defines the l.h.s. of Eq. (9.30) according to Eq. (9.28). Then, by introducing an additional and arbitrary time t_f such that $t_i < t_{A,B} < t_f$, and by using the cyclic property of the trace one can write

$$\langle A(t_A)B(t_B)\rangle = \mathrm{tr}\left(e^{-iH\left(t_f-t_B\right)}Be^{-iH(t_B-t_i)}\rho e^{iH(t_A-t_i)}Ae^{iH\left(t_f-t_A\right)}\right). \tag{9.79}$$

The evolution of the density matrix is adjoint to the evolution of Heisenberg operators, i.e., $\rho(t) = e^{-iHt}\rho e^{iHt}$. Thus, the operator $e^{-iH(t-t')}$ ($e^{iH(t-t')}$) acting from the left (right) on the density matrix ρ corresponds to the evolution in time from t' to t. In the correlation function (9.79), the time evolution from t_i to t_f on the left/right of ρ is intercepted by the operator B at time t_B/A at time t_A. In order to convert the r.h.s. of Eq. (9.79) into a path integral, the standard procedure (see, e.g., Refs. [214,215]) to be followed consists in writing the exponentials of the evolution operators as infinite products of infinitesimal and subsequent temporal evolutions (Trotter decomposition), in-between of which one can introduce completeness relations in terms of coherent states carrying the additional label "+" on the left of the density matrix, and a "−" on its right. These coherent states are eventually labeled by a temporal index on the forward (+) and backward (−) branches of the close-time path which characterizes the resulting action. Correspondingly, the operators on the left and on the right of the density matrix (B and A, respectively, in Eq. (9.79)) turn out to be evaluated on the fields (i.e., coherent states) which are defined, respectively, on the forward and backward branches of the closed time path and this yields immediately the equality in Eq. (9.30), where the ordering of the matrix elements A_- and B_+ on its r.h.s. is inconsequential. For the sake of completeness, we note that the expression as a Schwinger-Keldysh functional integral of a two-time function is not unique: in fact, it is straightforward to check that, by rearranging operators in Eq. (9.79), one can equivalently arrive at

$$\langle A(t_A)B(t_B)\rangle = \begin{cases} \langle A_+(t_A)B_+(t_B)\rangle & \text{for } t_A > t_B, \\ \langle A_-(t_A)B_-(t_B)\rangle & \text{for } t_A < t_B. \end{cases} \tag{9.80}$$

However, as discussed below, the choice of Eq. (9.30) naturally lends itself to a generalization to multi-time correlation functions.

Multi-time correlation functions. The functional integral on the r.h.s. of Eq. (9.32) relation can be constructed from a straightforward generalization of Eq. (9.79): after a reshuffling of the operators such that A and B appear respectively on the left and right of the density matrix — as explained above — the temporal evolution can be artificially extended from t_i to t_f and it is intercepted on the l.h.s. of the density matrix by operators $b_1, \ldots, b_M$ at times $t_{B,1}, \ldots, t_{B,M}$ and on the r.h.s. by operators $a_1, \ldots, a_N$ at times $t_{A,1}, \ldots, t_{A,N}$. Again, the resulting expression for the correlation function can be converted directly into a path integral by a Trotter decomposition of the subsequent evolutions and by inserting completeness relations in terms of coherent states carrying the label "+" corresponding

to the forward contour on the l.h.s. of the density matrix and the label "−" for the backward contour on the r.h.s. which eventually leads to Eq. (9.32).

9.D Jacobian of the equilibrium transformation

In order to prove that $|\mathrm{Det}\,\mathcal{J}| = 1$ it is convenient to calculate the Jacobian $\mathcal{J}$ associated with Eq. (9.3) in frequency and momentum space, which reads

$$\mathcal{J}(\omega, \mathbf{q}, \omega', \mathbf{q}') = (2\pi)^d\, \delta^{(d)}(\mathbf{q} + \mathbf{q}') J(\omega, \omega'), \tag{9.81}$$

where

$$J(\omega, \omega') = 2\pi\delta(\omega - \omega') \begin{pmatrix} 0 & e^{\beta\omega/2} & 0 & 0 \\ e^{-\beta\omega/2} & 0 & 0 & 0 \\ 0 & 0 & 0 & e^{\beta\omega/2} \\ 0 & 0 & e^{-\beta\omega/2} & 0 \end{pmatrix}. \tag{9.82}$$

The eigenvectors v_i and eigenvalues λ_i of the frequency-dependent part, i.e., the solutions of the equation

$$\int \frac{\mathrm{d}\omega'}{2\pi} J(\omega, \omega') v_i(\omega') = \lambda_i v_i(\omega), \tag{9.83}$$

are

$$\begin{aligned} v_1(\omega) &= \left(0, 0, -e^{\beta\omega/2}, 1\right)^T, \quad v_2(\omega) = \left(-e^{\beta\omega/2}, 1, 0, 0\right)^T, \\ v_3(\omega) &= \left(0, 0, e^{\beta\omega/2}, 1\right)^T, \qquad v_4(\omega) = \left(e^{-\beta\omega/2}, 1, 0, 0\right)^T, \end{aligned} \tag{9.84}$$

with $\lambda_1 = \lambda_2 = -1$, and $\lambda_3 = \lambda_4 = 1$, so that $\mathrm{Det}\, J = \lambda_1\lambda_2\lambda_3\lambda_4 = 1$. As for the momentum-dependent part of the Jacobian matrix Eq. (9.81), we note that its eigenvectors can be constructed with any function $f(\mathbf{q})$ by taking the even and odd combinations $f(\mathbf{q}) \pm f(-\mathbf{q})$:

$$\int_{\mathbf{q}'} (2\pi)^d\, \delta^{(d)}(\mathbf{q} + \mathbf{q}') \left(f(\mathbf{q}') \pm f(-\mathbf{q}')\right) = \pm \left(f(\mathbf{q}) \pm f(-\mathbf{q})\right). \tag{9.85}$$

Thus the eigenvalues of this part are ± 1, and hence the absolute value of the Jacobian matrix is $|\mathrm{Det}\,\mathcal{J}| = 1$.

Chapter 10

Thermalization and BEC of quantum paraxial light

Abstract

We study the thermalization and the Bose–Einstein condensation of a paraxial, spectrally narrow beam of quantum light propagating in a lossless bulk Kerr medium. The spatiotemporal evolution of the quantum optical field is ruled by a Heisenberg equation analogous to the quantum nonlinear Schrödinger equation of dilute atomic Bose gases. Correspondingly, in the weak-nonlinearity regime, the phase-space density evolves according to the Boltzmann equation. Expressions for the thermalization time and for the temperature and the chemical potential of the eventual Bose–Einstein distribution are found. After discussing experimental issues, we introduce an optical setup allowing the evaporative cooling of a guided beam of light towards Bose–Einstein condensation. This might serve as a novel source of coherent light.

As anticipated in Sec. 6.5 (see also [315,317,318]), in cavityless, propagating, geometry the complex amplitude of the classical optical field is a slowly varying function of space and time which satisfies a nonlinear wave equation formally identical to the Gross–Pitaevskii (GP) equation of dilute Bose–Einstein (BE) condensates [281] after exchanging the roles of the propagation coordinate and of the time parameter. This classical paraxial bulk dynamics may be regarded as the emerging mean-field description of an underlying quantum nonlinear Schrödinger dynamics, as formalized in full generality in Ref. [208].

In a recent experimental study [407], it was provided the first observation of classical-wave condensation using a beam of classical monochromatic light propagating in a nonlinear photorefractive crystal. The mechanism underlying this condensation of classical light finds its origin in the thermalization of the classical optical field [289, 305, 408–416] towards an equilibrium state whose statistics obeys the Rayleigh–Jeans (RJ) thermal law, which corresponds to the classical (high-temperature and/or long-wavelength) limit of the BE distribution.

In this Chapter, we push this research line forward by investigating the very quantum aspects of the thermalization dynamics of the propagating fluid of light. Making use of the fully quantum theory

developed in ref. [208], we discuss the possibility of measuring the Boltzmann tails of the eventual BE distribution, which constitutes the hallmark of the particlelike, quantum, nature of the paraxial beam of light at thermal equilibrium. Inspired by recent advances towards atom-laser devices based on in-waveguide evaporative-cooling schemes [417–420], we finally propose a mechanism leading to a complete BE condensation in the quantum fluid of light. If realized, such a process would offer a novel route to generate spontaneous optical coherence in a novel concept of coherent-light source.

10.1 Quantum formalism

We consider the propagation in the positive-z direction of a paraxial, spectrally narrow beam of light of central angular frequency ω in a bulk, electrically neutral, nonmagnetic, nonabsorbing, nonlinear medium of real-valued intensity-dependent refractive index $n_0 + n_1(\mathbf{r}_\perp, z) + n_2\,|\mathcal{E}|^2$. Here, n_0 is the background refractive index, $n_1[\mathbf{r}_\perp = (x, y), z]$ describes the spatial profile of the refractive index, n_2 quantifies the strength of the —spatially local and instantaneous— Kerr nonlinearity of the medium and $\mathcal{E}$ is the slowly varying [315, 317, 318] envelope of the light wave's electric field $\mathrm{Re}[\mathcal{E}\,\mathrm{e}^{\mathrm{i}(\beta_0 z - \omega t)}]$ of propagation constant $\beta_0 = n_0\,\omega/c$ in the increasing-z direction, where c denotes the vacuum speed of light. For simplicity's sake, we neglect light polarization and we assume that Raman and Brillouin light-scattering processes on phonons in the optical medium occur at a negligible rate.

Following ref. [208], it is possible to map the quantum propagation of the beam of light in the positive-z direction onto a quantum nonlinear Schrödinger evolution of a closed system of many interacting photons in a three-dimensional space spanned by the two-dimensional transverse position vector $\mathbf{r}_\perp$ and by the physical time parameter t. Introducing the time parameter $\tau = \beta_1\,z$ and the three-dimensional position vector $\mathbf{r} = (\mathbf{r}_\perp, \zeta = t/\beta_1 - z)$, where $\beta_1 = \mathrm{d}\beta_0/\mathrm{d}\omega = (n_0 + \omega\,\mathrm{d}n_0/\mathrm{d}\omega)/c$ denotes the inverse of the group velocity of the photons in the medium at ω, the quantum mechanical propagation equation of the light beam may be reformulated in the Heisenberg form $\mathrm{i}\,\hbar\,\partial\hat{\Psi}/\partial\tau = [\hat{\Psi}, \hat{H}]$, where the quantum field operator $\hat{\Psi} = [c\,\varepsilon_0\,n_0\,\beta_1/(2\,\hbar\,\omega)]^{1/2}\,\hat{\mathcal{E}}$ is the second-quantized slowly varying envelope of the electric field, normalized (ε_0 is the vacuum permittivity) in a way to satisfy the usual equal-τ Bose commutation relations $[\hat{\Psi}(\mathbf{r}_1, \tau), \hat{\Psi}^\dagger(\mathbf{r}_2, \tau)] = \delta^{(3)}(\mathbf{r}_1 - \mathbf{r}_2)$ and $[\hat{\Psi}(\mathbf{r}_1, \tau), \hat{\Psi}(\mathbf{r}_2, \tau)] = 0$, and where

$$\hat{H} = \int \mathrm{d}^3 r \left[\frac{\hbar^2}{2\,m_\perp}\,\frac{\partial\hat{\Psi}^\dagger}{\partial\mathbf{r}_\perp}\cdot\frac{\partial\hat{\Psi}}{\partial\mathbf{r}_\perp} + \frac{\hbar^2}{2\,m_\zeta}\,\frac{\partial\hat{\Psi}^\dagger}{\partial\zeta}\,\frac{\partial\hat{\Psi}}{\partial\zeta} + U(\mathbf{r}_\perp, \tau)\,\hat{\Psi}^\dagger\,\hat{\Psi} + \frac{g}{2}\,\hat{\Psi}^\dagger\,\hat{\Psi}^\dagger\,\hat{\Psi}\,\hat{\Psi}\right] \tag{10.1}$$

is the many-body Hamiltonian operator of the system.

In eq. (10.1), $U(\mathbf{r}_\perp, \tau) = -\hbar\,\omega/(c\,\beta_1)\,n_1(\mathbf{r}_\perp, z)$ is the external potential experienced by the photons, due to the spatial variation of the refractive index, and $g = -2\,(\hbar\,\omega)^2/(c^2\,\varepsilon_0\,n_0\,\beta_1^2)\,n_2$ is the strength of the effective photon-photon interactions induced by the Kerr nonlinearity.

Even more importantly, $m_\perp = \hbar\,\beta_0\,\beta_1$ and $m_\zeta = -\hbar\,\beta_1^3/\beta_2$ are the effective masses of the paraxial photons in, respectively, the transverse $\mathbf{r}_\perp$ plane and the ζ direction. In generic media, the values of $m_{\perp,\zeta}$ are typically very different, as they have completely different physical origins: the former originates from paraxial diffraction in the transverse plane while the latter, inversely proportional to the group-velocity-dispersion parameter $\beta_2 = \mathrm{d}\beta_1/\mathrm{d}\omega = (2\,\mathrm{d}n_0/\mathrm{d}\omega + \omega\,\mathrm{d}^2 n_0/\mathrm{d}\omega^2)/c$ of the medium at ω, starts playing a crucial role for nonmonochromatic optical fields having a nontrivial time dependence.

Unless the carrier frequency ω lies in the neighborhood of some optical resonance where dispersion is strong, $m_\perp$ is generally much smaller than m_ζ; as an example, using tabulated data for fused silica [421] around 1.55 μm (1 μm), one obtains a ratio $m_\perp/m_\zeta \simeq 7\times10^{-3}$ ($m_\perp/m_\zeta \simeq -8\times10^{-3}$).

As the Hamiltonian (10.1) is only valid within a limited angular-frequency and wavevector range around (ω,β_0), one has to ensure that photon-photon scattering induces no sizeable photon population outside this paraxial region. Thanks to the conservation of the energy (10.1), a necessary and —unless the chromatic dispersion has an unusually complex shape— sufficient condition is that the two masses $m_{\perp,\zeta}$ have the same sign. The robustness of a coherent photon wave against modulational instabilities imposes further conditions that the longitudinal mass be positive, $m_\zeta > 0$, and the photon-photon interactions be repulsive, $g > 0$; by definition, this amounts to assume that the dielectric is characterized by an anomalous group-velocity dispersion, $\beta_2 < 0$, and a self-defocusing Kerr nonlinearity, $n_2 < 0$ [208].

10.2 Thermalization time

In this section, we provide an analytical estimate of the time $\tau_{\rm th}$ —that is, of the propagation distance $z_{\rm th} = \tau_{\rm th}/\beta_1$ along the Kerr medium— that is necessary for the isolated quantum fluid of light described by the Hamiltonian (10.1) to thermalize. It is worth stressing that the thermalization process is here assumed to occur *via* photon-photon collisions within the fluid only, and not to involve any thermal equilibration with the underlying optical medium, *e.g.*, by photon-phonon scattering or repeated absorption-emission cycles as it was instead the case in the experiment of refs. [289,305].

Assuming for the sake of simplicity that the dielectric is spatially homogeneous, $n_1(\mathbf{r}_\perp,z)=0$, *i.e.*, $U(\mathbf{r}_\perp,\tau)=0$ in eq. (10.1), and that the total interaction energy is small with respect to the total kinetic one in the eventual thermal-equilibrium state, the latter has to be characterized by an occupation number in the plane-wave state of wavevector $\mathbf{k}=[\mathbf{k}_\perp=(k_x,k_y),k_\zeta]$ and energy $E_\mathbf{k}=\hbar^2\,\mathbf{k}_\perp^2/(2\,m_\perp)+\hbar^2\,k_\zeta^2/(2\,m_\zeta)$ of the BE form

$$N_{\rm BE}(E_\mathbf{k},T,\mu)=\left[\exp\left(\frac{E_\mathbf{k}-\mu}{k_{\rm B}\,T}\right)-1\right]^{-1} \tag{10.2}$$

($k_{\rm B}$ is the Boltzmann constant), where T and μ are respectively the temperature and the chemical potential of the thermalized quantum fluid of light. As we have assumed there is no thermal contact with the underlying optical medium, T is not related to the temperature of the latter as in refs. [289, 305], and both T and μ are fully determined as functions of the energy and number densities of the photon fluid entering the medium, as detailed in the next section.

A simple model —based on the quantum nonlinear Schrödinger formalism (10.1)— to investigate the relaxation dynamics of the initial state of the photon fluid, at $\tau=0$ (*i.e.*, $z=0$), towards thermal equilibrium, at $\tau\gtrsim\tau_{\rm th}$ (*i.e.*, $z\gtrsim z_{\rm th}$), is provided by the homogeneous [as $U(\mathbf{r}_\perp,\tau)=0$] Boltzmann kinetic equation [422]

$$\frac{\partial N_\mathbf{k}}{\partial\tau}=\frac{2\,g^2}{\hbar}\int\frac{{\rm d}^3k_2}{(2\pi)^3}\,\frac{{\rm d}^3k_3}{(2\pi)^3}\,\frac{{\rm d}^3k_4}{(2\pi)^3}(2\pi)^3\,\delta^{(3)}(\mathbf{k}+\mathbf{k}_2-\mathbf{k}_3-\mathbf{k}_4)\,\delta(E_\mathbf{k}+E_{\mathbf{k}_2}-E_{\mathbf{k}_3}-E_{\mathbf{k}_4})$$
$$\times\left[(N_\mathbf{k}+1)\,(N_{\mathbf{k}_2}+1)\,N_{\mathbf{k}_3}\,N_{\mathbf{k}_4}-N_\mathbf{k}\,N_{\mathbf{k}_2}\,(N_{\mathbf{k}_3}+1)\,(N_{\mathbf{k}_4}+1)\right] \tag{10.3}$$

for the uniform phase-space density $N_{\mathbf{k}} = N_{\mathbf{k}}(\tau)$ of the paraxial photons occupying the plane-wave state of wavevector $\mathbf{k}$ and energy $E_{\mathbf{k}}$ at the propagation time τ. At long times, *i.e.*, when $\tau \gtrsim \tau_{\rm th}$, the solution $N_{\mathbf{k}}$ of eq. (10.3) approaches the stationary BE distribution (10.2). Equation (10.3) is valid (i) in the absence of condensate and (ii) in the weak-interaction regime. The constraint (i) is satisfied as long as one considers energies and densities yielding noncondensed equilibrium states; otherwise, one has to include the coherent dynamics of the condensate's order parameter in eq. (10.3) [422]. The condition (ii) may be checked *a posteriori* by requiring that, in the eventual thermal state, the total interaction energy is small compared to the total kinetic energy, as already supposed in the second paragraph of the present section.

To estimate the effective relaxation time $\tau_{\rm th}$ towards thermal equilibrium, we are going to mutuate well-known results from the theory of weakly interacting atomic Bose gases. A numerical study [423] demonstrated that the thermalization time $\tau_{\rm th}$ of weakly interacting bosonic atoms not too far from thermal equilibrium is typically of the order of $3/\gamma$, where γ denotes the average collision rate. This means that about three collisions per particle are sufficient to make the system thermalize. This collision rate may be expressed as [281] $\gamma = \rho' \, v' \, \sigma'$, where ρ' denotes the mean number density of the gas, v' is the average norm of the velocity of ideal classical bosons at temperature T and σ' is the low-energy boson-boson-scattering cross section. This expression for γ holds in the case of an isotropic three-dimensional system. In the present optical case, as highlighted in the previous section, the system is characterized by an anisotropic mass tensor. As a result, the above-given formula for γ cannot be applied directly to estimate the time for the quantum fluid of light to relax towards thermal equilibrium.

In order to be able to safely use it, one has to make the kinetic contribution to the Hamiltonian (10.1) isotropic with a common mass m in all the x, y, ζ directions. To do so, we introduce the mass parameter $m = (m_\perp^2 \, m_\zeta)^{1/3}$ —that corresponds to the geometric mean of the paraxial-photon effective masses in the transverse x, y and longitudinal ζ directions— and the rescaled position vector $\mathbf{r}' = [\mathbf{r}'_\perp = (m_\perp/m)^{1/2} \, \mathbf{r}_\perp, \zeta' = (m_\zeta/m)^{1/2} \, \zeta]$. As an inversed rescaling holds in momentum space, one readily verifies that such a transformation preserves the spatial as well as the phase-space densities. In the isotropic $\mathbf{r}'$ space, we are then allowed to use the estimate $\tau_{\rm th} \sim 3/\gamma = 3/(\rho' \, v' \, \sigma')$ for the thermalization time in terms of the mean number density $\rho' = \rho$, the Boltzmann-averaged velocity $v' = \overline{\hbar \, |\mathbf{k}'|/m} = [8 \, k_{\rm B} \, T/(\pi \, m)]^{1/2}$ and the scattering cross section $\sigma' = 8\pi \, a'^2$, where $a' = m \, g'/(4\pi \, \hbar^2)$ is the s-wave scattering length written as a function of the two-body interaction parameter g' in the isotropic $\mathbf{r}'$ space [281]. As our coordinate change preserves both the spatial and the phase-space densities, it is immediate to check that g' is equal to the original photon-photon coupling constant g in the anisotropic $\mathbf{r}$ space, $g' = g$.

Combining the results of the previous paragraph, one eventually gets an explicit formula for the thermalization time $\tau_{\rm th}$,

$$\tau_{\rm th} \sim 3 \left\{ \rho \left[\frac{8 \, k_{\rm B} \, T}{\pi \, (m_\perp^2 \, m_\zeta)^{1/3}} \right]^{1/2} 8\pi \left[\frac{(m_\perp^2 \, m_\zeta)^{1/3} \, g}{4\pi \, \hbar^2} \right]^2 \right\}^{-1}, \tag{10.4}$$

that corresponds to the usual expression of the thermalization time of a three-dimensional weakly interacting atomic Bose gas, with a mass $(m_\perp^2 \, m_\zeta)^{1/3}$ given by the geometric average of the masses in the transverse x, y and longitudinal ζ directions.

10.3 Temperature and chemical potential at thermal equilibrium

As the kinetic-energy density $E_{\rm kin} = \int {\rm d}^3k/(2\pi)^3\, N_{\mathbf{k}}\, E_{\mathbf{k}}$ and the photon number density $\rho = \int {\rm d}^3k/(2\pi)^3\, N_{\mathbf{k}}$ are quantities conserved during the evolution of the quantum fluid of light described by eq. (10.3), the temperature T and the chemical potential μ characterizing the thermal-equilibrium, at $\tau \gtrsim \tau_{\rm th}$, BE distribution (10.2) may be fixed by the initial, at $\tau = 0$, values of $E_{\rm kin}$ and ρ: $E_{\rm kin}(\tau \gtrsim \tau_{\rm th}) = E_{\rm kin}(\tau = 0)$ and $\rho(\tau \gtrsim \tau_{\rm th}) = \rho(\tau = 0)$, where the left-hand sides depend on T and μ and the right-hand sides are functions of the parameters of the incoming electromagnetic field.

In the final equilibrium state ($\tau \gtrsim \tau_{\rm th}$, *i.e.*, $z \gtrsim z_{\rm th}$), using eq. (10.2), one readily gets $E_{\rm kin} = \frac{3}{2}\, k_{\rm B}\, T\, g_{5/2}(f)/(\lambda_\perp^2\, \lambda_\zeta)$ and $\rho = g_{3/2}(f)/(\lambda_\perp^2\, \lambda_\zeta)$, where $f = \exp[\mu/(k_{\rm B}\, T)]$ is the fugacity and $g_\nu(f) = \Gamma^{-1}(\nu) \int_0^\infty {\rm d}u\ u^{\nu-1}/(f^{-1}\, {\rm e}^u - 1)$ refers to the Bose integral, with $\Gamma(\nu)$ the Euler gamma function. These equations are similar to the well-known results of the ideal Bose gas, with the difference that, in the present optical case, there are two different thermal de Broglie wavelengths $\lambda_{\perp,\zeta} = [2\pi\, \hbar^2/(m_{\perp,\zeta}\, k_{\rm B}\, T)]^{1/2}$ due to the anisotropy of the kinetic energy in eq. (10.1). By means of the equation for $E_{\rm kin}$, one finds that $E_{\rm int}/E_{\rm kin} = \frac{1}{3}\, g\, \rho/(k_{\rm B}\, T)\, g_{3/2}(f)/g_{5/2}(f)$, where $E_{\rm int} = g\, \rho^2/2$ is the mean-field interaction-energy density [281] of the fluid of light at equilibrium. Thus, as the Bose integrals $g_{3/2}(f)$ and $g_{5/2}(f)$ are of the same order [$1 \leqslant g_{3/2}(f)/g_{5/2}(f) \leqslant 1.94(7)$ for $0 \leqslant f \leqslant 1$], the weak-interaction condition $E_{\rm int} \ll E_{\rm kin}$ required for eq. (10.3) to be valid reads $g\, \rho \ll k_{\rm B}\, T$, which may be reexpressed in terms of the s-wave scattering length a' in the isotropic $\mathbf{r}'$ space as $\rho\, a'^3 \ll (\rho\, \lambda_\perp^2\, \lambda_\zeta)^{-2}$. Note that this constraint directly implies the usual diluteness condition $\rho\, a'^3 \ll 1$ when one enters the quantum-degeneracy regime, $\rho\, \lambda_\perp^2\, \lambda_\zeta \gg 1$.

We assume that the initial fluid of light ($\tau = 0$), *i.e.*, the incident beam of light ($z = 0$), is characterized by the following Gaussian distribution in real space:

$$\langle \hat\Psi^\dagger(\mathbf{r}, 0)\, \hat\Psi(0, 0)\rangle = \rho_0\, {\rm e}^{-\mathbf{r}_\perp^2/(2\,\ell_\perp^2)}\, {\rm e}^{-\zeta^2/(2\,\ell_\zeta^2)}, \tag{10.5}$$

with finite correlation lengths $\ell_\perp$ and ℓ_ζ in the transverse $\mathbf{r}_\perp$ plane and the longitudinal ζ direction, respectively. In an actual experiment, the input density ρ_0 of the quantum fluid of light is tuned by varying the intensity $\mathcal{I} = \hbar\, \omega\, \rho_0/\beta_1$ of the incoming light beam, the transverse correlation length $\ell_\perp$ may be tuned by processing the input beam through spatial light modulators [407] and the longitudinal correlation length ℓ_ζ may in principle be varied by modifying the coherence time $\beta_1\, \ell_\zeta$ of the incident beam. Note that $\ell_\perp$ must be larger than the wavelength $2\pi/\beta_0$ of the carrier wave to ensure the paraxiality of the beam of light in the medium and $1/(\beta_1\, \ell_\zeta)$ must be smaller than the frequency range within which the quadratic approximation of the dispersion relation of the medium is valid. Fourier transforming eq. (10.5) yields the expression of the initial occupation number $N_{\mathbf{k}}(\tau = 0) = (2\pi)^{3/2}\, \rho_0\, \ell_\perp^2\, \ell_\zeta\, {\rm e}^{-\ell_\perp^2\, \mathbf{k}_\perp^2/2}\, {\rm e}^{-\ell_\zeta^2\, k_\zeta^2/2}$ at $\mathbf{k}$. From this, one obtains, at $\tau = 0$, $E_{\rm kin} = [\hbar^2\, \ell_\perp^{-2}/m_\perp + \hbar^2\, \ell_\zeta^{-2}/(2\, m_\zeta)]\, \rho_0$ and $\rho = \rho_0$.

Making use of the conservation laws $E_{\rm kin}(\tau \gtrsim \tau_{\rm th}) = E_{\rm kin}(\tau = 0)$ and $\rho(\tau \gtrsim \tau_{\rm th}) = \rho(\tau = 0)$, one eventually gets the following 2-by-2 system:

$$\frac{3}{2}\, k_{\rm B}\, T\, \frac{g_{5/2}(f)}{g_{3/2}(f)} = \frac{\hbar^2\, \ell_\perp^{-2}}{m_\perp} + \frac{\hbar^2\, \ell_\zeta^{-2}}{2\, m_\zeta}, \quad \frac{g_{3/2}(f)}{\lambda_\perp^2\, \lambda_\zeta} = \rho_0, \tag{10.6}$$

the resolution of which makes it possible to obtain T and μ in the final thermal-equilibrium state in terms of ρ_0, $\ell_\perp$, ℓ_ζ, $m_\perp$ and m_ζ. Introducing the effective temperatures $T_{\perp,\zeta} = 2\pi\, \hbar^2/(k_{\rm B}\, m_{\perp,\zeta}\, \ell_{\perp,\zeta}^2)$,

the first of eqs. (10.6) may be rewritten as $6\pi\, g_{5/2}(f)/g_{3/2}(f)\, T = 2\, T_\perp + T_\zeta$, which shows that the transverse and longitudinal modes, initially distributed at different temperatures $T_\perp \neq T_\zeta$, eventually equilibrate at the same temperature T.

10.4 Experimental considerations

Reminding the definition of the spatial coordinate ζ, the third component of the paraxial-photon wavevector $\mathbf{k}$ may be expressed as [208,326] $k_\zeta = -\beta_1\, \Delta\omega$, where $\Delta\omega$ is the detuning from the angular frequency ω of the pump. As a result, the measurement of the BE distribution (10.2) as a function of $\mathbf{k} = (\mathbf{k}_\perp, -\beta_1\, \Delta\omega)$ requires a good angular resolution to isolate the light deflected with a transverse wavevector $\mathbf{k}_\perp$ as well as a good spectral resolution to isolate the angular-frequency component of the transmitted light at $\omega \pm \Delta\omega$.

On the other hand, to have access to the large-momentum, Boltzmann, tails of the BE distribution —and so, in turn, to the whole BE distribution as a function of $\mathbf{k}$— at the exit face of the nonlinear dielectric where the fluid of light is imaged, some conditions have to be satisfied.

The inverse of the de Broglie wavelengths $\lambda_\perp$ and λ_ζ being the natural scales of variation of $N_{\rm BE}(E_{\mathbf{k}}, T, \mu)$ as a function of $\mathbf{k}_\perp$ and k_ζ, a first condition for detecting the whole BE distribution in the transmitted beam of light is that $\lambda_\perp$ and λ_ζ must verify the constraints satisfied respectively by $\ell_\perp$ and ℓ_ζ (see the third paragraph of the previous section).

A second, perhaps more challenging, condition concerns the length of the bulk nonlinear medium, which has to be at least of the order of the distance $z_{\rm th} = \tau_{\rm th}/\beta_1$ necessary for the quantum fluid of light to fully relax towards thermal equilibrium. Making use of the analytical result (10.4) and of the first of eqs. (10.6) with the reasonable estimate $g_{5/2}(f) \sim g_{3/2}(f)$ for $0 \leqslant f \leqslant 1$, one finds that $z_{\rm th}$ must behave at a given carrier wave at $(\omega, \beta_0 = n_0\, \omega/c)$ as

$$z_{\rm th} = \frac{K}{|n_2|^2\, \mathcal{I}} \left[\frac{|\beta_2|}{\ell_\perp^{-2} + \beta_0\, |\beta_2|/(2\, \beta_1^2)\, \ell_\zeta^{-2}} \right]^{1/2}, \tag{10.7}$$

where K depends on $\hbar$, c, ε_0, $k_{\rm B}$ and on ω, n_0, β_0. As a most important contribution, it is immediate to see that the stronger the Kerr nonlinearity is, the shorter the thermalization distance $z_{\rm th}$ is. Plugging explicit values into (10.7), we estimate for a light beam of 1.55 μm wavelength, 1 W/μm^2 intensity and initial $\beta_0\, \ell_{\perp,\zeta} = 10$ coherence lengths propagating in bulk silica [$2\, |n_2|/(c\, \varepsilon_0\, n_0) \sim 10^{-20}$ m^2/W] an unreasonably long $z_{\rm th} \sim 10^{13}$ m, *i.e.*, of the order of the estimated radius of the solar system...

While an experiment using such standard bulk nonlinear media looks clearly unfeasable, very promising alternatives are offered by resonant media where photons are strongly mixed with matter excitations. In this way, very strong effective photon-photon interactions may be obtained, *e.g.*, for polaritons in bulk semiconducting materials showing narrow exciton lines such as GaAs or ZnSe [267]. This effect can be further reinforced by many orders of magnitude if the chosen material excitation involves spatially wide (even almost micron-sized) Rydberg states, either in optically dressed atomic gases in the so-called Rydberg-EIT regime [424] or in highest-quality solid-state Cu_2O samples [425]. A further advantage of resonant media is the wide tunability of the optical parameters simply by changing the carrier frequency ω, which is of a great utility to ensure the dynamical stability of the photon fluid.

10.5 Discussion of a recent experiment

In ref. [407], it was reported the experimental observation of the relaxation of a classical, *i.e.*, not quantum, fluid of interacting photons towards a thermal-equilibrium state. A beam of classical monochromatic light, initially prepared in a nonthermal state *via* a suitable tayloring of the incident phase profile, was made to propagate in a photorefractive crystal whose optical nonlinearity was strong enough to make the transverse angular distribution of the beam of light fastly evolve towards a RJ-type, *i.e.*, classical, thermal law. For small enough initial kinetic energies, a marked peak around $\mathbf{k}_\perp = 0$ was observed in the transverse-momentum-$\mathbf{k}_\perp$ distribution, which was interpreted as a signature of the occurrence of a kinetic condensation of classical waves.

In order to fully understand the analogies and the differences with our quantum study, we can start by noting that a key conceptual assumption of the experiment [407] is that the light beam remains perfectly monochromatic all along its propagation across the nonlinear crystal. Under a mean-field approximation and provided no spontaneous temporal modulations such as self-pulsing [208] occur, monochromaticity at all distances is a trivial consequence of the classical GP form of the nonlinear Schrödinger field equation corresponding to the quantum Hamiltonian (10.1).

On the other hand, monochromaticity corresponds within the framework of our quantum theory to having at all propagation times τ a factorized momentum distribution $N_{\mathbf{k}}(\tau) = N_{\mathbf{k}_\perp}(\tau)\, N_{k_\zeta}$, where the transverse-momentum distribution $N_{\mathbf{k}_\perp}(\tau)$ evolves with τ while the longitudinal one N_{k_ζ} remains constant and proportional to the Dirac function $\delta(k_\zeta)$ at all τ's. Monochromaticity at all τ's then requires that no scattering process can change the k_ζ's of the colliding paraxial photons.

Most remarkably, the specific form of the optical nonlinearity of the photorefractive crystal used in the experiment [407] automatically serves this purpose, as its slow response involves the time-t average of the optical intensity and —in many-body terms— corresponds to infinite-range interactions along the ζ axis. As a result, all processes that would generate frequencies different from the incident one are suppressed. Keeping in mind that the population is sharply peaked on the only occupied states with $k_\zeta = 0$, it is then straightforward to see that the kinetics will eventually relax to the classical RJ distribution $N_{\mathrm{RJ}}(E_{\mathbf{k}}, T, \mu) = k_{\mathrm{B}}\, T/(E_{\mathbf{k}} - \mu)$ rather than to the BE one (10.2): because of the δ-shaped factor N_{k_ζ} in the $N_{\mathbf{k}}$'s, all the quantum "$+\,1$" terms in the Boltzmann equation (10.3) are in fact irrelevant, so that the quantum kinetics reduces to a classical one.

The situation is of course completely different if a local and instantaneous nonlinearity is used in an experiment. Within our theory [208], this corresponds to a local interaction in the three-dimensional x, y, ζ space. As a result, wave-mixing processes can mix all the three components of the momentum, therefore allowing for a full three-dimensional thermalization of the photon gas in both its transverse-momentum-$\mathbf{k}_\perp$ distribution and its physical-frequency-$\Delta\omega$ distribution, where $\Delta\omega = -k_\zeta/\beta_1$ is measured from the carrier wave at ω. Given the quantum nature of our model, the final result of this thermalization process will be a BE distribution of the form (10.2), which automatically solves all the ultraviolet black-body catastrophes that infest classical theories such as the one used in ref. [407]. As a final point, it is worth highlighting that thermalization to a quantum distribution is based on the quantum "$+\,1$" terms in the Boltzmann equation and thus does not benefit from the large Bose stimulation factor involved in the thermalization of classical waves. Together with the typically weaker Kerr optical nonlinearity of fast media, this explains why our prediction for z_{th} is dramatically longer than the experimental one of ref. [407].

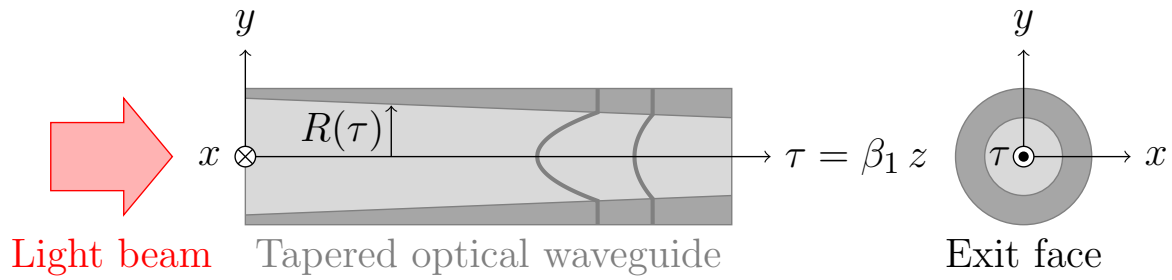

Figure 10.1: Sketch of an optical platform allowing the evaporative cooling of a quantum fluid of light (red) to temperatures below the critical temperature for BE condensation. The core (light gray) of radius $R(\tau)$ and the cladding (dark gray) of the waveguide are designed so that the photons are trapped in an effective harmonic potential (thick gray curves) whose maximum amplitude $\propto R^2(\tau)$ diminishes as the propagation time τ increases. This removes the high-energy photons from the fluid of light, which then cools down.

10.6 Evaporative cooling and BE condensation of a beam of light

An interesting consequence of the above-investigated thermalization process appears when the quantum fluid of light enters the BE-condensed phase. From the theory of the ideal Bose gas [281], the critical line for BE condensation in the (ρ_0, T) plane may be obtained by imposing $f = 1$ in the second of the thermal-state equations (10.6), which yields the usual formula for the BE-condensation critical temperature,

$$T_c = \frac{2\pi\,\hbar^2}{k_B\,(m_\perp^2\,m_\zeta)^{1/3}}\left[\frac{\rho_0}{\zeta(3/2)}\right]^{2/3}, \tag{10.8}$$

in terms of the Riemann zeta function at 3/2, $\zeta(3/2) = g_{3/2}(1) = 2.61(2)$, and the before-introduced geometric mean $m = (m_\perp^2\,m_\zeta)^{1/3}$ of the paraxial-photon effective masses. To realize a BE condensate of light in a bulk geometry, the experimentalist has to choose the rescaled intensity ρ_0 and the correlation lengths $\ell_\perp$ and ℓ_ζ of the incident beam in such a way that the temperature T in the thermal state, solution of eqs. (10.6), is smaller than T_c given by eq. (10.8).

Following the theoretical and experimental investigations [417–420] of the evaporative cooling of an atomic beam propagating in a magnetic trap, a promising way to facilitate BE condensation in the quantum fluid of light consists in progressively making the photon beam evaporate in the transverse $\mathbf{r}_\perp = (x, y)$ directions.

This can be obtained by introducing a time-dependent trapping potential $U(\mathbf{r}_\perp, \tau) \neq 0$ into the Hamiltonian (10.1), for instance of truncated harmonic form $U(\mathbf{r}_\perp, \tau) = \frac{1}{2}\,m_\perp\,\omega_\perp^2\,\mathbf{r}_\perp^2$ for $|\mathbf{r}_\perp| \leqslant R(\tau)$ and $U(\mathbf{r}_\perp, \tau) = \frac{1}{2}\,m_\perp\,\omega_\perp^2\,R^2(\tau)$ for $|\mathbf{r}_\perp| > R(\tau)$, where the radius $R(\tau)$ is a decreasing function of the propagation time τ. Based on the relation $n_1(\mathbf{r}_\perp, z) = -c\,\beta_1/(\hbar\,\omega)\,U(\mathbf{r}_\perp, \tau)$ between the spatial profile of the refractive index and the effective potential in eq. (10.1), this truncated harmonic trap may be realized by means of a conically tapered multimode optical waveguide, as pictorially sketched in fig. 10.1. The core $[|\mathbf{r}_\perp| \leqslant R(\beta_1\,z)]$ is taken to have an inverse-parabolic refractive-index profile, while the cladding $[|\mathbf{r}_\perp| > R(\beta_1\,z)]$ is homogeneous with a refractive index smoothly connecting the one of the core's edge.

As a result of this tapering, the maximum value of the trapping potential decreases as τ increases, so that the large-momentum (or large-energy) tails of the photon distribution are progressively removed. At the same time, the remaining photons keep reequilibrating to lower and lower temperatures under the effect of collisions, until the fluid of light eventually crosses the critical temperature for BE condensation.

Upon the $t \longleftrightarrow z$ mapping, BE condensation from an initially thermal photon gas corresponds to the appearance of spontaneous optical coherence when an initially incoherent beam of light is injected into the nonlinear medium: the long-range order of the BE condensate of light reflects into optical coherence extending for macroscopically long times t and distances x, y. In contrast to trivial angular- and frequency-filtering processes, a key element of our proposal are the collisions between the photons, that allow the fluid of light to reestablish thermal equilibrium at lower and lower temperatures while the most energetic photons keep being removed.

10.7 Concluding remarks

In this Chapter, we have investigated the relaxation dynamics of a paraxial, quasimonochromatic beam of quantum light towards thermal equilibrium in a lossless bulk Kerr medium. Following ref. [208], the propagation of the quantum light field has been mapped onto a quantum nonlinear Schrödinger evolution of a conservative quantum fluid of many interacting bosons. Correspondingly, in the weak-interaction regime, the evolution of the momentum distribution from an arbitrary nonthermal state towards a thermal state with a BE form can be modeled by the Boltzmann kinetic equation, which offers analytical formulas for the thermalization time and for the final temperature and chemical potential in terms of the parameters of the input beam and of the medium.

In addition to extending the concept of classical-light-wave condensation [407] to a fully quantum level and solving well-known ultraviolet pathologies of existing classical theories, our results suggest an intriguing long-term application as a novel source of coherent light: taking inspiration from related advances in atom-laser devices [417–420], we have pointed out a novel in-waveguide evaporative-cooling scheme to obtain spontaneous macroscopic optical coherence from an initially incoherent beam of light. As our proposal does not rely on population-inverted atomic transitions, it holds the promise of being implemented in an arbitrary domain of the electromagnetic spectrum.

Bibliography

[1] A. Maraga, A. Chiocchetta, A. Mitra, and A. Gambassi. *Phys. Rev. E*, 92:042151, 2015.

[2] A Chiocchetta, M. Tavora, A. Gambassi, and A. Mitra. *Phys. Rev. B*, 91:220302, 2015.

[3] A. Chiocchetta, M. Tavora, A. Gambassi, and A. Mitra. *arXiv:1604.04614*, 2016.

[4] A. Chiocchetta, A. Gambassi, S. Diehl, and J. Marino. *arXiv:1606.06272*, 2016.

[5] A. Chiocchetta and I. Carusotto. *Phys. Rev. A*, 90:023633, 2014.

[6] A. Chiocchetta, A. Gambassi, and I. Carusotto. *arXiv:1503.02816*, 2015.

[7] L. M. Sieberer, A. Chiocchetta, A. Gambassi, U. C. Täuber, and S. Diehl. *Phys. Rev. B*, 92:134307, 2015.

[8] A. Chiocchetta, P.-É. Larré, and I. Carusotto. *Europhys. Lett.*, 115:24002, 2016.

[9] A. Polkovnikov, K. Sengupta, A. Silva, and M. Vengalattore. *Rev. Mod. Phys.*, 83:863, 2011.

[10] T. Langen, T. Gasenzer, and J. Schmiedmayer. *J. Stat. Mech.*, 2016:064009, 2016.

[11] S. Inouye, M. R. Andrews, J. Stenger, H. J. Miesner, D. M. Stamper-Kurn, and W. Ketterle. *Nature*, 392:151, 1998.

[12] C. Chin, R. Grimm, P. Julienne, and E. Tiesinga. *Rev. Mod. Phys.*, 82:1225, 2010.

[13] M. Greiner, O. Mandel, T. W. Hansch, and I. Bloch. *Nature*, 419:51, 2002.

[14] T. W. B. Kibble. *J. Phys. A*, 9:1387, 1976.

[15] W. H. Zurek. *Nature*, 317:505, 1985.

[16] W. H. Zurek. *Phys. Rep.*, 276:177, 1996.

[17] G. Lamporesi, S. Donadello, S. Serafini, F. Dalfovo, and G. Ferrari. *Nat. Phys.*, 9:656, 2013.

[18] S. Trotzky, Y-A. Chen, A. Flesch, I. P. McCulloch, U. Schollwock, J. Eisert, and I. Bloch. *Nat. Phys.*, 8:325, 2012.

[19] M. Cheneau, P. Barmettler, D. Poletti, M. Endres, P. Schausz, T. Fukuhara, C. Gross, I. Bloch, C. Kollath, and S. Kuhr. *Nature*, 481:484, 2012.

[20] T. Fukuhara, A. Kantian, M. Endres, M. Cheneau, P. Schausz, S. Hild, D. Bellem, U. Schollwock, T. Giamarchi, C. Gross, I. Bloch, and S. Kuhr. *Nat. Phys.*, 9:235, 2013.

[21] T. Fukuhara, P. Schausz, M. Endres, S. Hild, M. Cheneau, I. Bloch, and C. Gross. *Nature*, 502:76, 2013.

[22] T. Kinoshita, T. Wenger, and D. S. Weiss. *Nature*, 440:900, 2006.

[23] E. H. Lieb and W. Liniger. *Phys. Rev.*, 130:1605, 1963.

[24] E. H. Lieb. *Phys. Rev.*, 130:1616, 1963.

[25] M. Gring, M. Kuhnert, T. Langen, T. Kitagawa, B. Rauer, M. Schreitl, I. Mazets, D. Adu Smith, E. Demler, and J. Schmiedmayer. *Science*, 337:1318, 2012.

[26] T. Langen, M. Gring, M. Kuhnert, B. Rauer, R. Geiger, D. Adu Smith, I. E. Mazets, and J. Schmiedmayer. *Eur. Phys. J. Spec. Top.*, 217:43, 2013.

[27] M. Kuhnert, R. Geiger, T. Langen, M. Gring, B. Rauer, T. Kitagawa, E. Demler, D. Adu Smith, and J. Schmiedmayer. *Phys. Rev. Lett.*, 110:090405, 2013.

[28] D. Adu Smith, M. Gring, T. Langen, M. Kuhnert, B. Rauer, R. Geiger, T. Kitagawa, I. Mazets, E. Demler, and J. Schmiedmayer. *New J. Phys.*, 15:075011, 2013.

[29] T. Langen, S. Erne, R. Geiger, B. Rauer, T. Schweigler, M. Kuhnert, W. Rohringer, I. E. Mazets, T. Gasenzer, and J. Schmiedmayer. *Science*, 348:207, 2015.

[30] R.W. Robinett. *Phys. Rep.*, 392:1, 2004.

[31] T. Barthel and U. Schollwöck. *Phys. Rev. Lett.*, 100:100601, 2008.

[32] C. Gogolin, M. P. Müller, and J. Eisert. *Phys. Rev. Lett.*, 106:040401, 2011.

[33] J. Von Neumann. *Z. Phys.*, 57:30, 1929.

[34] P. Mazur. *Physica*, 43:533, 1969.

[35] A. Peres. *Phys. Rev. A*, 30:504, 1984.

[36] J. M. Deutsch. *Phys. Rev. A*, 43:2046, 1991.

[37] M. Srednicki. *Phys. Rev. E*, 50:888, 1994.

[38] M. Srednicki. *J. Phys. A*, 32:1163, 1999.

[39] L. D'Alessio, Y. Kafri, A. Polkovnikov, and M. Rigol. *Adv. Phys.*, 65:239, 2016.

[40] M. Rigol, V. Dunjko, and M. Olshanii. *Nature*, 452:854, 2008.

[41] L. F. Santos and M. Rigol. *Phys. Rev. E*, 82:031130, 2010.

[42] M. Rigol and L. F. Santos. *Phys. Rev. A*, 82:011604, 2010.

[43] E. Khatami, G. Pupillo, M. Srednicki, and M. Rigol. *Phys. Rev. Lett.*, 111:050403, 2013.

[44] M. Rigol. *Phys. Rev. Lett.*, 103:100403, 2009.

[45] M. Rigol. *Phys. Rev. A*, 80:053607, 2009.

[46] R. Steinigeweg, J. Herbrych, and P. Prelovšek. *Phys. Rev. E*, 87:012118, 2013.

[47] W. Beugeling, R. Moessner, and M. Haque. *Phys. Rev. E*, 89:042112, 2014.

[48] R. Steinigeweg, A. Khodja, H. Niemeyer, C. Gogolin, and J. Gemmer. *Phys. Rev. Lett.*, 112:130403, 2014.

[49] A. Khodja, R. Steinigeweg, and J. Gemmer. *Phys. Rev. E*, 91:012120, 2015.

[50] W. Beugeling, R. Moessner, and M. Haque. *Phys. Rev. E*, 91:012144, 2015.

[51] C. Neuenhahn and F. Marquardt. *Phys. Rev. E*, 85:060101, 2012.

[52] E. Khatami, A. Rigol, M.and Relaño, and A. M. García-García. *Phys. Rev. E*, 85:050102, 2012.

[53] S. Genway, A. F. Ho, and D. K. K. Lee. *Phys. Rev. A*, 86:023609, 2012.

[54] G. Biroli, C. Kollath, and A. M. Läuchli. *Phys. Rev. Lett.*, 105:250401, 2010.

[55] G. Roux. *Phys. Rev. A*, 81:053604, 2010.

[56] S. Sorg, L. Vidmar, L. Pollet, and F. Heidrich-Meisner. *Phys. Rev. A*, 90:033606, 2014.

[57] R. Mondaini, K. R. Fratus, M. Srednicki, and M. Rigol. *Phys. Rev. E*, 93:032104, 2016.

[58] B. Sutherland. *Beautiful models*. World Scientific, Singapore, 2004.

[59] J.-S. Caux and J. Mossel. *J. Stat. Mech.*, 2011:P02023, 2011.

[60] E. A. Yuzbashyan and B. S. Shastry. *J. Stat. Phys.*, 150:704, 2013.

[61] E. T. Jaynes. *Phys. Rev.*, 106:620, 1957.

[62] M. Rigol, V. Dunjko, V. Yurovsky, and M. Olshanii. *Phys. Rev. Lett.*, 98:050405, 2007.

[63] A. C. Cassidy, C. W. Clark, and M. Rigol. *Phys. Rev. Lett.*, 106:140405, 2011.

[64] L. Vidmar and M. Rigol. *J. Stat. Mech.*, 2016:064007, 2016.

[65] M. A. Cazalilla. *Phys. Rev. Lett.*, 97:156403, 2006.

[66] M. Rigol, A. Muramatsu, and M. Olshanii. *Phys. Rev. A*, 74:053616, 2006.

[67] M. Kollar and M. Eckstein. *Phys. Rev. A*, 78:013626, 2008.

[68] A. Iucci and M. A. Cazalilla. *Phys. Rev. A*, 80:063619, 2009.

[69] A. Iucci and M. A. Cazalilla. *New J. Phys.*, 12:055019, 2010.

[70] D. Fioretto and G. Mussardo. *New J. Phys.*, 12:055015, 2010.

[71] P. Calabrese, F. H. L. Essler, and M. Fagotti. *Phys. Rev. Lett.*, 106:227203, 2011.

[72] P. Calabrese, F. H. L. Essler, and M. Fagotti. *J. Stat. Mech.*, 2012:P07022, 2012.

[73] M. A. Cazalilla, A. Iucci, and M.-C. Chung. *Phys. Rev. E*, 85:011133, 2012.

[74] J.-S. Caux and R. M. Konik. *Phys. Rev. Lett.*, 109:175301, 2012.

[75] C. Gramsch and M. Rigol. *Phys. Rev. A*, 86:053615, 2012.

[76] F. H. L. Essler, S. Evangelisti, and M. Fagotti. *Phys. Rev. Lett.*, 109:247206, 2012.

[77] M. Collura, S. Sotiriadis, and P. Calabrese. *Phys. Rev. Lett.*, 110:245301, 2013.

[78] M. Collura, S. Sotiriadis, and P. Calabrese. *J. Stat. Mech.*, 2013:P09025, 2013.

[79] J.-S. Caux and F. H. L. Essler. *Phys. Rev. Lett.*, 110:257203, 2013.

[80] G. Mussardo. *Phys. Rev. Lett.*, 111:100401, 2013.

[81] M. Fagotti. *Phys. Rev. B*, 87:165106, 2013.

[82] M. Fagotti and F. H. L. Essler. *Phys. Rev. B*, 87:245107, 2013.

[83] M. Fagotti, M. Collura, F. H. L. Essler, and P. Calabrese. *Phys. Rev. B*, 89:125101, 2014.

[84] B. Pozsgay. *J. Stat. Mech.*, 2014:P10045, 2014.

[85] T. M. Wright, M. Rigol, M. J. Davis, and K. V. Kheruntsyan. *Phys. Rev. Lett.*, 113:050601, 2014.

[86] S. Sotiriadis and P. Calabrese. *J. Stat. Mech.*, 2014:P07024, 2014.

[87] M. Kormos, M. Collura, and P. Calabrese. *Phys. Rev. A*, 89:013609, 2014.

[88] J. C. Zill, T. M. Wright, K. V. Kheruntsyan, T. Gasenzer, and M. J. Davis. *Phys. Rev. A*, 91:023611, 2015.

[89] J. C. Zill, T. M. Wright, K. V. Kheruntsyan, T. Gasenzer, and M. J. Davis. *New J. Phys.*, 18:045010, 2016.

[90] F. H. L. Essler and M. Fagotti. *J. Stat. Mech.*, 2016:064002, 2016.

[91] J.-S. Caux. *J. Stat. Mech.*, 2016:064006, 2016.

[92] B. Bertini, D. Schuricht, and F. H L Essler. *J. Stat. Mech.*, 2014:P10035, 2014.

[93] M. Fagotti and F. H. L. Essler. *J. Stat. Mech.*, 2013:P07012, 2013.

[94] B. De Nardis, J.and Wouters, M. Brockmann, and J.-S. Caux. *Phys. Rev. A*, 89:033601, 2014.

[95] B. Wouters, J. De Nardis, M. Brockmann, D. Fioretto, M. Rigol, and J.-S. Caux. *Phys. Rev. Lett.*, 113:117202, 2014.

[96] G. Goldstein and N. Andrei. *Phys. Rev. A*, 90:043625, 2014.

[97] E. Ilievski, M. Medenjak, T. Prosen, and L. Zadnik. *J. Stat. Mech.*, 2016:064008, 2016.

[98] E. Ilievski, J. De Nardis, B. Wouters, J.-S. Caux, F. H. L. Essler, and T. Prosen. *Phys. Rev. Lett.*, 115:157201, 2015.

[99] F. H. L. Essler, G. Mussardo, and M. Panfil. *Phys. Rev. A*, 91:051602, 2015.

[100] G. Aarts, G.F. Bonini, and C. Wetterich. *Phys. Rev. D*, 63:025012, 2000.

[101] J. Berges, Sz. Borsányi, and C. Wetterich. *Phys. Rev. Lett.*, 93:142002, 2004.

[102] M. Moeckel and S. Kehrein. *Phys. Rev. Lett.*, 100:175702, 2008.

[103] M. Moeckel and S. Kehrein. *New J. Phys.*, 12:055016, 2010.

[104] A. Rosch, D. Rasch, B. Binz, and M. Vojta. *Phys. Rev. Lett.*, 101:265301, 2008.

[105] M. Kollar, F. A. Wolf, and M. Eckstein. *Phys. Rev. B*, 84:054304, 2011.

[106] J. Marino and A. Silva. *Phys. Rev. B*, 86:060408, 2012.

[107] M. van den Worm, B. C. Sawyer, J. J. Bollinger, and M. Kastner. *New J. Phys.*, 15:083007, 2013.

[108] M. Marcuzzi, J. Marino, A. Gambassi, and A. Silva. *Phys. Rev. Lett.*, 111:197203, 2013.

[109] F. H. L. Essler, S. Kehrein, S. R. Manmana, and N. J. Robinson. *Phys. Rev. B*, 89:165104, 2014.

[110] N. Nessi, A. Iucci, and M. A. Cazalilla. *Phys. Rev. Lett.*, 113:210402, 2014.

[111] M. Fagotti. *J. Stat. Mech.*, 2014:P03016, 2014.

[112] G. P. Brandino, J.-S. Caux, and R. M. Konik. *Phys. Rev. X*, 5:041043, 2015.

[113] B. Bertini and M. Fagotti. *J. Stat. Mech.*, 2015:P07012, 2015.

[114] B. Bertini, F. H. L. Essler, S. Groha, and N. J. Robinson. *Phys. Rev. Lett.*, 115:180601, 2015.

[115] B. Bertini, F. H. L. Essler, S. Groha, and N. J. Robinson. *arXiv:1608.01664*, 2016.

[116] M. Babadi, E. Demler, and M. Knap. *Phys. Rev. X*, 5:041005, 2015.

[117] H.-K. Janssen, B. Schaub, and B. Schmittmann. *Z. Phys. B*, 73:539, 1989.

[118] H.-K. Janssen. In G. Györgyi, I. Kondor, L. Sasvári, and T. Tél, editors, *From Phase Transitions to Chaos, Topics in Modern Statistical Physics*. World Scientific, Singapore, 1992.

[119] P. Calabrese and A. Gambassi. *J. Phys. A: Math. Gen.*, 38:R133, 2005.

[120] M. Henkel, H. Hinrichsen, M. Pleimling, and S. Lübeck. *Non-Equilibrium Phase Transitions: Volume 2: Ageing and Dynamical Scaling Far from Equilibrium*. Springer, 2011.

[121] U. C. Täuber. *Critical Dynamics*. Cambridge University Press, 2014.

[122] B. Schmittmann and R. K. P. Zia. *Statistical Mechanics of Driven Diffusive Systems*. Academic Press, 1995.

[123] M. Doi. *J. Phys. A: Math. Gen.*, 9:1465, 1976.

[124] L Peliti. *J. Phys.*, 46:1469, 1985.

[125] J. Cardy and U. C. Täuber. *Phys. Rev. Lett.*, 77:4780, 1996.

[126] F. Baumann and A. Gambassi. *J. Stat. Mech.*, 2007:P01002, 2007.

[127] S. P. Obukhov. *Phys. A*, 101:145, 1980.

[128] H. Hinrichsen. *Adv. Phys.*, 49:815, 2000.

[129] M. Henkel, H. Hinrichsen, and S. Lübeck. *Non-Equilibrium Phase Transitions: Volume 1: Absorbing Phase Transitions*. Springer, 2008.

[130] H. J. Jensen. *Self-Organized Criticality*. Cambridge University Press, 1998.

[131] M. Kardar, G. Parisi, and Y.-C. Zhang. *Phys. Rev. Lett.*, 56:889, 1986.

[132] I. Corwin. *Random Matrices: Theory Appl.*, 01:1130001, 2012.

[133] V. E. Zakharov, V. S. L'vov, and G. Falkovich. *Kolmogorov Spectra of Turbulence I: Wave Turbulence*. Springer Science & Business Media, 2012.

[134] U. Frisch. *Turbulence. The Legacy of A. N. Kolmogorov*. Cambridge University Press, 1995.

[135] W. F. Vinen. *J. Low Temp. Phys.*, 145:7, 2006.

[136] M. Tsubota. *J. Phys. Soc. Jpn.*, 77:111006, 2008.

[137] C. Scheppach, J. Berges, and T. Gasenzer. *Phys. Rev. A*, 81:033611, 2010.

[138] A. Piñeiro Orioli, K. Boguslavski, and J. Berges. *Phys. Rev. D*, 92:025041, 2015.

[139] J. Berges and D. Sexty. *Phys. Rev. Lett.*, 108:161601, 2012.

[140] T. Gasenzer, B. Nowak, and D. Sexty. *Phys. Lett. B*, 710:500, 2012.

[141] T. Gasenzer, L. McLerran, J. M. Pawlowski, and D. Sexty. *Nucl. Phys. A*, 930:163, 2014.

[142] J. Berges, S. Scheffler, and D. Sexty. *Phys. Lett. B*, 681:362, 2009.

[143] Y. Pomeau and P. Résibois. *Phys. Rep.*, 19:63, 1975.

[144] M. H. Ernst, J. Machta, J. R. Dorfman, and H. van Beijeren. *J. Stat. Phys.*, 34:477, 1984.

[145] J. Lux, J. Müller, A. Mitra, and A. Rosch. *Phys. Rev. A*, 89:053608, 2014.

[146] H. K. Janssen, B. Schaub, and B. Schmittmann. *Z. Phys. B*, 73:539, 1989.

[147] P. Gagel, P. P. Orth, and J. Schmalian. *Phys. Rev. Lett.*, 113:220401, 2014.

[148] P. Gagel, P. P. Orth, and J. Schmalian. *Phys. Rev. B*, 92, 2015.

[149] M. Buchhold and S. Diehl. *Phys. Rev. A*, 92:013603, 2015.

[150] A. J. Bray. *Adv. Phys.*, 43:357, 1994.

[151] L. F. Cugliandolo. *C. R. Phys.*, 16:257, 2015.

[152] G. Biroli. *arXiv:1507.05858*, 2015.

[153] R. A. Barankov, L. S. Levitov, and B. Z. Spivak. *Phys. Rev. Lett.*, 93:160401, 2004.

[154] E. A. Yuzbashyan, B. L. Altshuler, V. B. Kuznetsov, and V. Z. Enolskii. *Phys. Rev. B*, 72:220503, 2005.

[155] R. A. Barankov and L. S. Levitov. *Phys. Rev. Lett.*, 96:230403, 2006.

[156] E. A. Yuzbashyan, O. Tsyplyatyev, and B. L. Altshuler. *Phys. Rev. Lett.*, 96:097005, 2006.

[157] V. Gurarie. *Phys. Rev. Lett.*, 103:075301, 2009.

[158] M. S. Foster, M. Dzero, V. Gurarie, and E. A. Yuzbashyan. *Phys. Rev. B*, 88:104511, 2013.

[159] M. S. Foster, V. Gurarie, M. Dzero, and E. A. Yuzbashyan. *Phys. Rev. Lett.*, 113:076403, 2014.

[160] F. Peronaci, M. Schiró, and M. Capone. *Phys. Rev. Lett.*, 115:257001, 2015.

[161] E. A. Yuzbashyan, M. Dzero, V. Gurarie, and M. S. Foster. *Phys. Rev. A*, 91:033628, 2015.

[162] M. Eckstein, M. Kollar, and P. Werner. *Phys. Rev. Lett.*, 103:056403, 2009.

[163] B. Sciolla and G. Biroli. *Phys. Rev. Lett.*, 105:220401, 2010.

[164] B. Sciolla and G. Biroli. *J. Stat. Mech.*, 2011:P11003, 2011.

[165] M. Schiró and M. Fabrizio. *Phys. Rev. Lett.*, 105:076401, 2010.

[166] M. Schiró and M. Fabrizio. *Phys. Rev. B*, 83:165105, 2011.

[167] N. Tsuji, M. Eckstein, and P. Werner. *Phys. Rev. Lett.*, 110:136404, 2013.

[168] A. Gambassi and P. Calabrese. *Europhys. Lett.*, 95:66007, 2011.

[169] B. Sciolla and G. Biroli. *Phys. Rev. B*, 88:201110, 2013.

[170] A. Chandran, A. Nanduri, S. S. Gubser, and S. L. Sondhi. *Phys. Rev. B*, 88:024306, 2013.

[171] P. Smacchia, M. Knap, E. Demler, and A. Silva. *Phys. Rev. B*, 91:205136, 2015.

[172] A. Maraga, P. Smacchia, and A. Silva. *arXiv:1602.01763*, 2016.

[173] M. Le Bellac. *Quantum and Statistical Field Theory*. Clarendon Press, Oxford, 1991.

[174] P. Calabrese and J. Cardy. *Phys. Rev. Lett.*, 96:136801, 2006.

[175] P. Calabrese and J. Cardy. *J. Stat. Mech.*, 2007:P06008, 2007.

[176] S. Sotiriadis, P. Calabrese, and J. Cardy. *Europhys. Lett.*, 87:20002, 2009.

[177] S. K. Ma. *Modern Theory of Critical Phenomena*. Perseus, 2000.

[178] N. Goldenfeld. *Lectures on Phase Transitions and the Renormalization Group*. Addison-Wesley, 1992.

[179] S. Sachdev. *Quantum Phase Transitions*. Cambridge University Press, 2011.

[180] S. Sotiriadis and J. Cardy. *Phys. Rev. B*, 81:134305, 2010.

[181] R. Kubo. *Rep. Prog. Phys.*, 29:255, 1966.

[182] L. F. Cugliandolo. *J. Phys. A: Math. Theor.*, 44:483001, 2011.

[183] L. Foini, L. F. Cugliandolo, and A. Gambassi. *Phys. Rev. B*, 84:212404, 2011.

[184] A. Mitra and T. Giamarchi. *Phys. Rev. B*, 85:075117, 2012.

[185] L. Foini, L. F. Cugliandolo, and A. Gambassi. *J. Stat. Mech.*, 2012:P09011, 2012.

[186] S. L. Sondhi, S. M. Girvin, J. P. Carini, and D. Shahar. *Rev. Mod. Phys.*, 69:315, 1997.

[187] D. S. Fisher and P. C. Hohenberg. *Phys. Rev. B*, 37:4936, 1988.

[188] M. Marcuzzi and A. Gambassi. *Phys. Rev. B*, 89:134307, 2014.

[189] T. Langen, R. Geiger, M. Kuhnert, B. Rauer, and J. Schmiedmayer. *Nat. Phys.*, 9:640, 2013.

[190] E. M. Stein and G. L. Weiss. *Introduction to Fourier Analysis on Euclidean Spaces*, volume 1. Princeton University Press, 1971.

[191] M. Abramowitz and I. Stegun. *Handbook of Mathematical Functions*. Dover Publications, 1965.

[192] J. Berges and T. Gasenzer. *Phys. Rev. A*, 76:033604, 2007.

[193] A. J. Bray and M. A. Moore. *J. Phys. A*, 10:1927, 1977.

[194] A. J. Bray and M. A. Moore. *Phys. Rev. Lett.*, 38:735, 1977.

[195] J. Zinn-Justin. *Quantum Field Theory and Critical Phenomena*. Oxford Clarendon Press, 1989.

[196] W. H. Press, S. A. Teukolsky, W. T. Vetterling, and B. P. Flannery. *Numerical Recipes in FORTRAN*. Cambridge University Press, 1992.

[197] C. Godrèche and J. M. Luck. *J. Phys. Condens. Matter*, 14:1589, 2002.

[198] T. Kitagawa, A. Imambekov, J. Schmiedmayer, and E. Demler. *New J. Phys.*, 13:073018, 2011.

[199] M. Moeckel and S. Kehrein. *Ann. Phys.*, 324:2146, 2009.

[200] A. Mitra. *Phys. Rev. B*, 87:205109, 2013.

[201] M. Greiner, O. Mandel, T. Esslinger, T. W. Hänsch, and I. Bloch. *Nature*, 415:39, 2002.

[202] S. Trotzky, P. Cheinet, S. Flling, M. Feld, U. Schnorrberger, A. M. Rey, A. Polkovnikov, E. A. Demler, M. D. Lukin, and I. Bloch. *Science*, 319:295, 2008.

[203] W. S. Bakr, J. I. Gillen, A. Peng, S. Folling, and M. Greiner. *Nature*, 462:74, 2009.

[204] W. S. Bakr, A. Peng, M. E. Tai, R. Ma, J. Simon, J. I. Gillen, S. Flling, L. Pollet, and M. Greiner. *Science*, 329:547, 2010.

[205] J. F. Sherson, C. Weitenberg, M. Endres, M. Cheneau, I. Bloch, and S. Kuhr. *Nature*, 467:68, 2010.

[206] M. Endres, M. Cheneau, T. Fukuhara, C. Weitenberg, P. Schau, C. Gross, L. Mazza, M. C. Bauls, L. Pollet, I. Bloch, and S. Kuhr. *Science*, 334:200, 2011.

[207] T. Betz, S. Manz, R. Bücker, T. Berrada, Ch. Koller, G. Kazakov, I. Mazets, H.-P. Stimming, A. Perrin, T. Schumm, and J. Schmiedmayer. *Phys. Rev. Lett.*, 106:020407, 2011.

[208] P.-É. Larré and I. Carusotto. *Phys. Rev. A*, 92:043802, 2015.

[209] J. Berges, A. Rothkopf, and J. Schmidt. *Phys. Rev. Lett.*, 101:041603, 2008.

[210] J. Berges and G. Hoffmeister. *Nuclear Physics B*, 813:383, 2009.

[211] J. Berges and D. Sexty. *Phys. Rev. D*, 83:085004, 2011.

[212] J. Schole, B. Nowak, and T. Gasenzer. *Phys. Rev. A*, 86:013624, 2012.

[213] M. Karl, B. Nowak, and T. Gasenzer. *Phys. Rev. A*, 88:063615, 2013.

[214] A. Altland and B. Simons. *Condensed Matter Field Theory.* Cambridge University Press, 2010.

[215] A. Kamenev. *Field Theory of Non-Equilibrium Systems.* Cambridge University Press, 2011.

[216] E. Calzetta and B. L. Hu. *Phys. Rev. D*, 37:2878, 1988.

[217] T. C. Lubensky and Morton H. Rubin. *Phys. Rev. B*, 11:4533, 1975.

[218] H.W. Diehl and S. Dietrich. *Z. Phys. B*, 42:65, 1981.

[219] A. Mitra and T. Giamarchi. *Phys. Rev. Lett.*, 107:150602, 2011.

[220] A. Mitra. *Phys. Rev. Lett.*, 109:260601, 2012.

[221] K. G. Wilson and J. Kogut. *Phys. Rep.*, 12:75, 1974.

[222] A. Giraud and J. Serreau. *Phys. Rev. Lett.*, 104:230405, 2010.

[223] P. Calabrese, F. H. L. Essler, and M. Fagotti. *J. Stat. Mech.*, 2012:P07016, 2012.

[224] E. Nicklas, M. Karl, M. Höfer, A. Johnson, W. Muessel, H. Strobel, J. Tomkovič, T. Gasenzer, and M. K. Oberthaler. *Phys. Rev. Lett.*, 115:245301, 2015.

[225] J. Berges. *AIP Conf. Proc.*, 739:3, 2004.

[226] J. Berges. *arXiv:1503.02907*, 2015.

[227] M. Tavora and A. Mitra. *Phys. Rev. B*, 88:115144, 2013.

[228] F. J. Wegner and A. Houghton. *Phys. Rev. A*, 8:401, 1973.

[229] H. W. Diehl. *Int. J. Mod. Phys. B*, 11:3503, 1997.

[230] Y. Lemonik. and A. Mitra. *Phys. Rev. B*, 94:024306, 2016.

[231] I. S. Gradshteyn and I. M. Ryzhik. *Table of Integrals, Series, and Products.* Elsevier Academic Press, Amsterdam, 2007.

[232] P. C. Hohenberg and B. I. Halperin. *Rev. Mod. Phys.*, 49:435, 1977.

[233] A. Gambassi. *Eur. Phys. J. B*, 64:379, 2008.

[234] J. Berges, N. Tetradis, and C. Wetterich. *Phys. Rep.*, 363:223, 2002.

[235] P. C. Martin, E. D. Siggia, and H. A. Rose. *Phys. Rev. A*, 8:423, 1973.

[236] H.-K. Janssen. *Z. Phys. B*, 23:377, 1976.

[237] C. De Dominicis. *J. Phys. Colloq.*, 37, 1976.

[238] C. De Dominicis. *Phys. Rev. B*, 18:4913, 1978.

[239] H.-K. Janssen. In C.P. Enz, editor, *Dynamical Critical Phenomena and Related Topics*. Springer, Berlin, Heidelberg, 1979.

[240] B. Delamotte. *Lect. Notes Phys.*, 852:49, 2012.

[241] D.-F. Litim. *Phys. Lett. B*, 486:92, 2000.

[242] C. Wetterich. *Phys. Lett. B*, 301:90, 1993.

[243] D. J. Amit and V. Martin-Mayor. *Field Theory, the Renormalization Group, and Critical Phenomena*. World Scientific, Singapore, 2005.

[244] L. Canet and H. Chaté. *J. Phys. A: Math. Theor.*, 40:1937, 2007.

[245] L. M. Sieberer, S. D. Huber, E. Altman, and S. Diehl. *Phys. Rev. B*, 89:134310, 2014.

[246] L. Canet, H. Chaté, B. Delamotte, I. Dornic, and M. A. Muñoz. *Phys. Rev. Lett.*, 95:100601, 2005.

[247] H.-K. Oerding, K. Janssen. *J. Phys. A: Math. Gen.*, 26:5295, 1993.

[248] H.-K. Oerding, K. Janssen. *J. Phys. A: Math. Gen.*, 26:3369, 1993.

[249] M. Marcuzzi, A. Gambassi, and M. Pleimling. *Europhys. Lett.*, 100:46004, 2012.

[250] M. Marcuzzi, A. Gambassi, and M. Pleimling. *Cond. Matter Phys.*, 17:33603, 2014.

[251] P. Calabrese and A. Gambassi. *Phys. Rev. E*, 66:066101, 2002.

[252] P. Calabrese and A. Gambassi. *Phys. Rev. E*, 65:066120, 2002.

[253] P. Calabrese and A. Gambassi. *J. Stat. Mech.*, 2004:P07013, 2004.

[254] U. Weiss. *Quantum Dissipative Systems*. World Scientific, 1999.

[255] H.-P. Breuer and F. Petruccione. *The Theory of Open Quantum Systems*. Oxford University Press, 2002.

[256] C. Gardiner and P. Zoller. *Quantum Noise*. Springer Science & Business Media, 2004.

[257] T. Halpin-Healy and Y.-C. Zhang. *Physics Reports*, 254:215, 1995.

[258] I. Bloch, J. Dalibard, and W. Zwerger. *Rev. Mod. Phys.*, 80:885, 2008.

[259] M. Lewenstein, A. Sanpera, V. Ahufinger, B. Damski, A. Sen(De), and U. Sen. *Adv. Phys.*, 56:243, 2007.

[260] J. I. Cirac and P. Zoller. *Nat. Phys.*, 8:264, 2012.

[261] J. W. Britton, B. C. Sawyer, A. C. Keith, C. C. J. Wang, J. K. Freericks, H. Uys, M. J. Biercuk, and J. J. Bollinger. *Nature*, 484:489, 2012.

[262] R. Blatt and C. F. Roos. *Nat. Phys.*, 8:277, 2012.

[263] K. Baumann, C. Guerlin, F. Brennecke, and T. Esslinger. *Nature*, 464:1301, 2010.

[264] H. Ritsch, P. Domokos, F. Brennecke, and T. Esslinger. *Rev. Mod. Phys.*, 85:553, 2013.

[265] P. Schausz, M. Cheneau, M. Endres, T. Fukuhara, S. Hild, A. Omran, T. Pohl, C. Gross, S. Kuhr, and I. Bloch. *Nature*, 491:87, 2012.

[266] J. Kasprzak, M. Richard, S. Kundermann, A. Baas, P. Jeambrun, J. M. J. Keeling, F. M. Marchetti, M. H. Szymanska, R. Andre, J. L. Staehli, V. Savona, P. B. Littlewood, B. Deveaud, and L. S. Dang. *Nature*, 443:409, 2006.

[267] I. Carusotto and C. Ciuti. *Rev. Mod. Phys.*, 85:299, 2013.

[268] A. A. Houck, H. E. Türeci, and J. Koch. *Nat. Phys.*, 8:292, 2012.

[269] L. M. Sieberer, M. Buchhold, and S. Diehl. *Rep. Prog. Phys.*, 79:096001, 2016.

[270] W. Lechner and P. Zoller. *Phys. Rev. Lett.*, 111:185306, 2013.

[271] E. Altman, L. M. Sieberer, L. Chen, S. Diehl, and J. Toner. *Phys. Rev. X*, 5:011017, 2015.

[272] F. Piazza and P. Strack. *Phys. Rev. Lett.*, 112:143003, 2014.

[273] J. Keeling, M. J. Bhaseen, and B. D. Simons. *Phys. Rev. Lett.*, 112:143002, 2014.

[274] C. Kollath, A. Sheikhan, S. Wolff, and F. Brennecke. *Phys. Rev. Lett.*, 116:060401, 2016.

[275] J. Raftery, D. Sadri, S. Schmidt, H. E. Türeci, and A. A. Houck. *Phys. Rev. X*, 4:031043, 2014.

[276] M. J. Hartmann, F. G. S. L. Brandão, and M. B. Plenio. *Laser Photonics Rev.*, 2:527, 2008.

[277] E. G. Dalla Torre, E. Demler, T. Giamarchi, and E. Altman. *Nat. Phys.*, 6:806, 2010.

[278] L. M. Sieberer, S. D. Huber, E. Altman, and S. Diehl. *Phys. Rev. Lett.*, 110:195301, 2013.

[279] J. Marino and S. Diehl. *Phys. Rev. Lett.*, 116:070407, 2016.

[280] K. Huang. *Statistical Mechanics*. Wiley, 1987.

[281] L. Pitaevskii and S. Stringari. *Bose Einstein Condensation*. Clarendon Press, Oxford, 2004.

[282] O. Penrose and L. Onsager. *Phys. Rev.*, 104:576, 1956.

[283] J. D. Gunton and M. J. Buckingham. *Phys. Rev.*, 166:152, 1968.

[284] R. Graham and H. Haken. *Z. Phys. A*, 237:31, 1970.

[285] V. DeGiorgio and Marlan O. Scully. *Phys. Rev. A*, 2:1170, 1970.

[286] C. J. Chang-Hasnain. *IEEE J. Sel. Top. Quantum Electron.*, 6:978, 2000.

[287] L. D. A. Lundeberg, G. P. Lousberg, D. L. Boiko, and E. Kapon. *Appl. Phys. Lett.*, 90:021103, 2007.

[288] S. O. Demokritov, V. E. Demidov, O. Dzyapko, G. A. Melkov, A. A. Serga, B. Hillebrands, and A. N. Slavin. *Nature*, 443:430, 2006.

[289] J. Klaers, J. Schmitt, F. Vewinger, and M. Weitz. *Nature*, 468:545, 2010.

[290] H. Deng, H. Haug, and Y. Yamamoto. *Rev. Mod. Phys.*, 82:1489, 2010.

[291] T. Byrnes, N. Y. Kim, and Y. Yamamoto. *Nat. Phys.*, 10:803, 2014.

[292] M. Richard, J. Kasprzak, R. Romestain, R. André, and L. S. Dang. *Phys. Rev. Lett.*, 94:187401, 2005.

[293] M. Richard, J. Kasprzak, R. André, R. Romestain, L. S. Dang, G. Malpuech, and A. Kavokin. *Phys. Rev. B*, 72:201301, 2005.

[294] M. Wouters, I. Carusotto, and C. Ciuti. *Phys. Rev. B*, 77:115340, 2008.

[295] E. Wertz, L. Ferrier, D.D. Solnyshkov, R. Johne, D. Sanvitto, A. Lemaître, I. Sagnes, R. Grousson, A.V. Kavokin, P. Senellart, G. Malpuech, and J. Bloch. *Nat. Phys.*, 6:860, 2010.

[296] M. Wouters and I. Carusotto. *Phys. Rev. B*, 74:245316, 2006.

[297] M. Wouters and I. Carusotto. *Phys. Rev. A*, 76:043807, 2007.

[298] M. H. Szymanska, J. Keeling, and P. B. Littlewood. *Phys. Rev. Lett.*, 96:230602, 2006.

[299] M. Wouters and I. Carusotto. *Phys. Rev. Lett.*, 99:140402, 2007.

[300] D. Bajoni, P. Senellart, A. Lemaître, and J. Bloch. *Phys. Rev. B*, 76:201305, 2007.

[301] J. M. Kosterlitz and D. J. Thouless. *J. Phys. C*, 6:1181, 1973.

[302] P. Minnhagen. *Rev. Mod. Phys.*, 59:1001, 1987.

[303] L. Reatto and G.V. Chester. *Phys. Rev.*, 155:88, 1967.

[304] V. N. Popov. *Theor. Math. Phys.*, 11:565, 1972.

[305] J. Klaers, F. Vewinger, and M. Weitz. *Nat. Phys.*, 6:512, 2010.

[306] B. Fischer and R. Weill. *Opt. Express*, 20:26704, 2012.

[307] A. Mitra, S. Takei, Y. B. Kim, and A. J. Millis. *Phys. Rev. Lett.*, 97:236808, 2006.

[308] S. Diehl, A. Micheli, A. Kantian, B. Kraus, H. P. Büchler, and P. Zoller. *Nat. Phys.*, 4:878, 2008.

[309] S. Diehl, A. Tomadin, A. Micheli, R. Fazio, and P. Zoller. *Phys. Rev. Lett.*, 105:015702, 2010.

[310] E. G. Dalla Torre, E. Demler, T. Giamarchi, and E. Altman. *Phys. Rev. B*, 85:184302, 2012.

[311] E. G. Dalla Torre, S. Diehl, M. D. Lukin, S. Sachdev, and P. Strack. *Phys. Rev. A*, 87:023831, 2013.

[312] A. Chiocchetta and I. Carusotto. *Europhys. Lett.*, 102:67007, 2013.

[313] U. C. Täuber and S. Diehl. *Phys. Rev. X*, 4:021010, 2014.

[314] B. Öztop, M. Bordyuh, Ö. Müstecaplolu, and H. E. Türeci. *New J. Phys.*, 14:085011, 2012.

[315] G. P. Agrawal. *Nonlinear Fiber Optics*. Academic Press, San Diego, 1995.

[316] S. Raghavan and G. P. Agrawal. *Opt. Commun.*, 180:377, 2000.

[317] N. N. Rosanov. *Spatial Hysteresis and Optical Patterns*. Springer, Berlin, 2002.

[318] R. P. Boyd. *Nonlinear Optics*. Academic Press, San Diego, 1992.

[319] M. Vaupel, K. Staliunas, and C. O. Weiss. *Phys. Rev. A*, 54:880, 1996.

[320] W. Wan, S. Jia, and J. W. Fleischer. *Nat. Phys.*, 3:46, 2007.

[321] S. Jia, W. Wan, and J. W. Fleischer. *Phys. Rev. Lett.*, 99:223901, 2007.

[322] W. Wan, S. Muenzel, and J. W. Fleischer. *Phys. Rev. Lett.*, 104:073903, 2010.

[323] W. Wan, D. V. Dylov, C. Barsi, and J. W. Fleischer. *Opt. Lett.*, 35:2819, 2010.

[324] S. Jia, M. Haataja, and J. W Fleischer. *New J. Phys.*, 14:075009, 2012.

[325] D. Vocke, T. Roger, F. Marino, E. M. Wright, I. Carusotto, M. Clerici, and D. Faccio. *Optica*, 2:484, 2015.

[326] P.-É. Larré and I. Carusotto. *Eur. Phys. J. D*, 70:1, 2016.

[327] I. Carusotto and C. Ciuti. *Phys. Rev. B*, 72:125335, 2005.

[328] M. Wouters and V. Savona. *Phys. Rev. B*, 79:165302, 2009.

[329] J. Keeling, F. M. Marchetti, M. H. Szymańska, and P. B. Littlewood. *Semicond. Sci. Technol.*, 22:R1, 2007.

[330] M. Lax. *Phys. Rev.*, 145:110, 1966.

[331] W.L. Louisell. Wiley, New York, 1973.

[332] J. P. Gordon. *Phys. Rev.*, 161:367, 1967.

[333] H. Haken. *Laser Theory*. Springer-Verlag, Berlin, 1984.

[334] P. Kirton and J. Keeling. *Phys. Rev. Lett.*, 111:100404, 2013.

[335] A.-W. de Leeuw, H. T. C. Stoof, and R. A. Duine. *Phys. Rev. A*, 88:033829, 2013.

[336] C. Ciuti and I. Carusotto. *Phys. Rev. A*, 74:033811, 2006.

[337] C. Cohen-Tannoudji, J. Dupont-Roc, and G. Grynberg. *Atom-Photon Interactions*. Wiley-VCH, 2004.

[338] M. O. Scully and M. S. Zubairy. *Quantum Optics*. Cambridge University Press, 1997.

[339] M. Wouters and I. Carusotto. *Phys. Rev. B*, 75:075332, 2007.

[340] M. C. Cross and P. C. Hohenberg. *Rev. Mod. Phys.*, 65:851, 1993.

[341] M. Richard, J. Kasprzak, R. Romestain, R. Andre, and L. S. Dang. *Phys. Rev. Lett.*, 94:187401, 2005.

[342] R. M. Stevenson, V. N. Astratov, M. S. Skolnick, D. M. Whittaker, M. Emam-Ismail, A. I. Tartakovskii, P. G. Savvidis, J. J. Baumberg, and J. S. Roberts. *Phys. Rev. Lett.*, 85:3680, 2000.

[343] Y. Castin and R. Dum. *Phys. Rev. A*, 57:3008, 1998.

[344] D. Sarchi and I. Carusotto. *Phys. Rev. B*, 81:075320, 2010.

[345] A. Le Boité, G. Orso, and C. Ciuti. *Phys. Rev. Lett.*, 110:233601, 2013.

[346] J. Jin, D. Rossini, R. Fazio, M. Leib, and M. J. Hartmann. *Phys. Rev. Lett.*, 110:163605, 2013.

[347] A. Baas, J.-P. Karr, M. Romanelli, A. Bramati, and E. Giacobino. *Phys. Rev. Lett.*, 96:176401, 2006.

[348] G. Roumpos, M. Lohse, W. H. Nitsche, J. Keeling, M. Hanna Szymańska, P. B. Littlewood, A. Löffler, S. Höfling, L. Worschech, A. Forchel, and Y. Yamamoto. *Proc. Natl. Acad. Sci. USA*, 2012.

[349] R. Spano, J. Cuadra, G. Tosi, C. Antón, C. A. Lingg, D. Sanvitto, M. D. Martín, L. Viña, P. R. Eastham, M. van der Poel, and J. M. Hvam. *New J. Phys.*, 14:075018, 2012.

[350] C. W. Gardiner. *Handbook of Stochastic Methods for Physics, Chemistry and the Natural Sciences*. Springer-Verlag, 2004.

[351] Vladimir N. Gladilin, Kai Ji, and Michiel Wouters. *Phys. Rev. A*, 90:023615, 2014.

[352] F. M. Marchetti, J. Keeling, M. H. Szymańska, and P. B. Littlewood. *Phys. Rev. B*, 76:115326, 2007.

[353] T. Byrnes, T. Horikiri, N. Ishida, M. Fraser, and Y. Yamamoto. *Phys. Rev. B*, 85:075130, 2012.

[354] L. A. Lugiato, P. Mandel, and L. M. Narducci. *Phys. Rev. A*, 29:1438, 1984.

[355] M. Lax and W. H. Louisell. *IEEE J. Quant. Electron.*, 3:47, 1967.

[356] M. Lax and H. Yuen. *Phys. Rev.*, 172:362, 1968.

[357] C. Benkert, M. O. Scully, J. Bergou, L. Davidovich, M. Hillery, and M. Orszag. *Phys. Rev. A*, 41:2756, 1990.

[358] H. Haken. *Rev. Mod. Phys.*, 47:67, 1975.

[359] L. I. Plimak, M. K. Olsen, M. Fleischhauer, and M. J. Collett. *Europhys. Lett.*, 56:372, 2001.

[360] A. Polkovnikov. *Phys. Rev. A*, 68:053604, 2003.

[361] K. Vogel and H. Risken. *Phys. Rev. A*, 39:4675, 1989.

[362] M. Wouters and I. Carusotto. *Phys. Rev. Lett.*, 105:020602, 2010.

[363] R. A. Nyman and M. H. Szymańska. *Phys. Rev. A*, 89:033844, 2014.

[364] G.D. Mahan. *Many-particle physics*. Springer Science & Business Media, 2000.

[365] R. Kubo. *J. Phys. Soc. Jpn.*, 12:570, 1957.

[366] P.C. Martin and J. Schwinger. *Phys. Rev.*, 115:1342, 1959.

[367] D.F. Walls and G.J. Milburn. *Quantum optics*. Springer Science & Business Media, 2007.

[368] P. Talkner. *Ann. Phys.*, 167:390, 1986.

[369] G.W. Ford and R.F. O'Connell. *Phys. Rev. Lett.*, 77:798, 1996.

[370] P. Kirton and J. Keeling. *Phys. Rev. A*, 91:033826, 2015.

[371] K.-C. Chou, Z.-B. Su, B.-L. Hao, and L. Yu. *Phys. Rep.*, 118:1, 1985.

[372] E. Wang and U. Heinz. *Phys. Rev. D*, 66:025008, 2002.

[373] S. G. Jakobs, M. Pletyukhov, and H. Schoeller. *J. Phys. A Math. Theor.*, 43:103001, 2010.

[374] A. Messiah. *Quantum Mechanics II*. North-Holland Pubsishing Company, Amsterdam, 1965.

[375] R. Bausch, H. K. Janssen, and H. Wagner. *Z. Phys. B*, 24:113, 1976.

[376] C. Aron, G. Biroli, and L. F. Cugliandolo. *J. Stat. Mech.*, 2010:P11018, 2010.

[377] C. Aron, D. G. Barci, L. F. Cugliandolo, Z. G. Arenas, and G. S. Lozano. *J. Stat. Mech.*, 2016:053207, 2016.

[378] J. Schwinger. *J. Math. Phys.*, 2:407, 1961.

[379] P. M. Bakshi and K. T. Mahanthappa. *J. Math. Phys.*, 4:1, 1963.

[380] P.-M. Bakshi and K. T. Mahanthappa. *J. Math. Phys.*, 4:12, 1963.

[381] K. Mahanthappa. *Phys. Rev.*, 126:329, 1962.

[382] L. V. Keldysh. *Sov. Phys. JETP*, 20:1018, 1965.

[383] H. T. C. Stoof. *J. Low Temp. Phys.*, 114:11, 1999.

[384] A. Altland, A. De Martino, R. Egger, and B. Narozhny. *Phys. Rev. B*, 82:115323, 2010.

[385] A. Kossakowski. *Reports Math. Phys.*, 3:247, 1972.

[386] G. Lindblad. *Commun. Math. Phys.*, 48:119, 1976.

[387] E. M. Lifshitz and L. P. Pitaevskii. *Statistical Physics, Part 2: Theory of the Condensed State.* Pergamon Press, New York, 1980.

[388] R. Folk and G. Moser. *J. Phys. A. Math. Gen.*, 39:R207, 2006.

[389] B. Pozsgay, M. Mestyán, M. A. Werner, M. Kormos, G. Zaránd, and G. Takács. *Phys. Rev. Lett.*, 113:117203, 2014.

[390] M. Mierzejewski, P. Prelovšek, and T. Prosen. *Phys. Rev. Lett.*, 113:020602, 2014.

[391] M.P. A. Fisher, G. Grinstein, and D. S. Fisher. *Phys. Rev. B*, 40:546, 1989.

[392] G. S. Agarwal. *Z. Phys.*, 258:409, 1973.

[393] R. Alicki. *Reports Math. Phys.*, 10:249, 1976.

[394] A. Kossakowski, A. Frigerio, V. Gorini, and M. Verri. *Commun. Math. Phys.*, 57:97, 1977.

[395] A. Frigerio and V. Gorini. *Commun. Math. Phys.*, 93:517, 1984.

[396] W. A. Majewski. *J. Math. Phys.*, 25:614, 1984.

[397] R. Alicki and K. Lendi. *Quantum Dynamical Semigroups and Applications.* Springer, Berlin Heidelberg, 2007.

[398] H. J. Carmichael and D. F. Walls. *Z. Phys. B*, 23:299, 1976.

[399] A. Andreanov, G. Biroli, and A. Lefvre. *J. Stat. Mech.*, 2006:P07008, 2006.

[400] J. M. Pawlowski. *Ann. Phys.*, 322:2831, 2007.

[401] O. J. Rosten. *Phys. Rep.*, 511:177, 2012.

[402] I. Boettcher, J. M. Pawlowski, and S. Diehl. *Nucl. Phys. B (Proc. Suppl.)*, 228:63, 2012.

[403] D. Mesterházy, J. H. Stockemer, L. F. Palhares, and J. Berges. *Phys. Rev. B*, 88:174301, 2013.

[404] D. Mesterházy, J. H. Stockemer, and Y. Tanizaki. *Phys. Rev. D*, 92:076001, 2015.

[405] M. Campisi, P. Hänggi, and P. Talkner. *Rev. Mod. Phys.*, 83:771, 2011.

[406] M. Esposito, U. Harbola, and S. Mukamel. *Rev. Mod. Phys.*, 81:1665, 2009.

[407] C. Sun, S. Jia, C. Barsi, S. Rica, A. Picozzi, and J. W. Fleischer. *Nat .Phys.*, 8:470, 2012.

[408] A. Picozzi. *Opt. Express*, 15:9063, 2007.

[409] Lagrange, S., Jauslin, H. R., and Picozzi, A. *Europhys. Lett.*, 79:64001, 2007.

[410] A. Picozzi. *Opt. Express*, 16:17171, 2008.

[411] A. Picozzi and S. Rica. *Europhys. Lett.*, 84:34004, 2008.

[412] B. Barviau, B. Kibler, S. Coen, and A. Picozzi. *Opt. Lett.*, 33:2833, 2008.

[413] B. Barviau, B. Kibler, A.e Kudlinski, A. Mussot, G. Millot, and A. Picozzi. *Opt. Express*, 17:7392, 2009.

[414] P. Suret, S. Randoux, H. R. Jauslin, and A. Picozzi. *Phys. Rev. Lett.*, 104:054101, 2010.

[415] P. Aschieri, J. Garnier, C. Michel, V. Doya, and A. Picozzi. *Phys. Rev. A*, 83:033838, 2011.

[416] C. Michel, M. Haelterman, P. Suret, S. Randoux, R. Kaiser, and A. Picozzi. *Phys. Rev. A*, 84:033848, 2011.

[417] E. Mandonnet, A. Minguzzi, R. Dum, I. Carusotto, Y. Castin, and J. Dalibard. *Eur. Phys. J. D*, 10:9, 2000.

[418] Y. Castin, R. Dum, E. Mandonnet, A. Minguzzi, and I. Carusotto. *J. Mod. Opt.*, 47:2671, 2000.

[419] T. Lahaye, J. M. Vogels, K. J. Günter, Z. Wang, J. Dalibard, and D. Guéry-Odelin. *Phys. Rev. Lett.*, 93:093003, 2004.

[420] T. Lahaye, Z. Wang, G. Reinaudi, S. P. Rath, J. Dalibard, and D. Guéry-Odelin. *Phys. Rev. A*, 72:033411, 2005.

[421] I. H. Malitson. *J. Opt. Soc. Am.*, 55:1205, 1965.

[422] A. Griffin, T. Nikuni, and E. Zaremba. *Bose-Condensed Gases at Finite Temperatures.* Cambridge University Press, 2009.

[423] H. Wu and C. J. Foot. *J. Phys. B*, 29:L321, 1996.

[424] T. Peyronel, O. Firstenberg, Q.-Y. Liang, S. Hofferberth, A. V. Gorshkov, T. Pohl, M. D. Lukin, and V. Vuletic. *Nature*, 488:57, 2012.

[425] J. I. Jang. *Optoelectronics: Materials and Techniques.* InTech, 2011.